AD_____

Award Number: DAMD17-02-1-0197

TITLE: Targeting of Drugs to ICAM for Treatment of Acute Lung Injury

PRINCIPAL INVESTIGATOR: Vladimir Muzykantov, Ph.D.

CONTRACTING ORGANIZATION: University of Pennsylvania
Philadelphia, PA 19104-6205

REPORT DATE: April 2004

TYPE OF REPORT: Annual

PREPARED FOR: U.S. Army Medical Research and Materiel Command
Fort Detrick, Maryland 21702-5012

REPORT DOCUMENTATION PAGE

Form Approved
OMB No. 074-0188

1. AGENCY USE ONLY (Leave blank)	2. REPORT DATE	3. REPORT TYPE AND DATES COVERED
	April 2004	Annual (11 Mar 2003 - 10 Mar 2004)

4. TITLE AND SUBTITLE

Targeting of Drugs to ICAM for Treatment of Acute Lung Injury

5. FUNDING NUMBERS

DAMD17-02-1-0197

6. AUTHOR(S)

Vladimir Muzykantov, Ph.D.

7. PERFORMING ORGANIZATION NAME(S) AND ADDRESS(ES)

University of Pennsylvania
Philadelphia, PA 19104-6205

E-Mail: muzykant@mail.med.upenn.edu

8. PERFORMING ORGANIZATION REPORT NUMBER

9. SPONSORING / MONITORING AGENCY NAME(S) AND ADDRESS(ES)

U.S. Army Medical Research and Materiel Command
Fort Detrick, Maryland 21702-5012

10. SPONSORING / MONITORING AGENCY REPORT NUMBER

11. SUPPLEMENTARY NOTES

Original contains color plates: ALL DTIC reproductions will be in black and white

12a. DISTRIBUTION / AVAILABILITY STATEMENT

Approved for Public Release; Distribution Unlimited

12b. DISTRIBUTION CODE

13. ABSTRACT (Maximum 200 Words)

In the second year, we characterized intracellular traffic and final destination of anti-CAM conjugates in endothelial cells (EC) and found that CAM-mediated endocytosis initiates an unusually slow vesicular traffic that delivers conjugates to lysosomes several hours after internalization. Further, auxiliary drugs that regulate these processes can be utilized for prolongation of therapeutic duration of internalized conjugates. We characterized a series of in-house models of human ALI (injection of anti-TM/GOX and hyperoxia in mice), studied dynamics and role of EC cell adhesion molecules and leukocytes in these models and developed a new, clinically relevant and reliable model of ALI, based on combined treatment with anti-TM/GOX and hyperoxia. We synthesized anti-CAM/SOD conjugate with proper targeting size (~200 nm), enzymatic activity and affinity to EC and documented that it accumulates in the pulmonary vasculature after intravenous injection, thus satisfying main requirements for subsequent testing in animal models of ALI. In vitro and in vivo fibrinolysis studies have been employed in order to select the optimal candidate fibrinolytic (a novel tPA derivative, Tenektase) for targeting to endothelial CAM. Design and production of optimized affinity carriers for this purpose is in progress.

14. SUBJECT TERMS

Endothelium, immunotargeting, oxidant stress, thrombosis, ICAM-1

15. NUMBER OF PAGES

116

16. PRICE CODE

17. SECURITY CLASSIFICATION OF REPORT	18. SECURITY CLASSIFICATION OF THIS PAGE	19. SECURITY CLASSIFICATION OF ABSTRACT	20. LIMITATION OF ABSTRACT
Unclassified	Unclassified	Unclassified	Unlimited

Table of Contents

Targeting of Drugs to ICAM-1 for Treatment of Acute Lung Injury

A. Introduction. The main goals of the project are to explore, test, optimize and prepare translation into the clinical domain of a new therapeutic strategy for a more effective containment of the Acute Lung Injury (ALI/ARDS). Both oxidative and thrombotic stresses in the pulmonary vasculature are important pathological factors in the development of ALI/ARDS. The proposed strategy is based on the concept that targeted delivery of antioxidant drugs (e.g., antioxidant enzymes, AOE) and anti-thrombotic drugs (e.g., plasminogen activators, PA) to the endothelial cells lining the luminal surface of blood vessels in the lungs would permit more effective and specific therapeutic interventions into developing or ongoing ALI/ARDS. Our results of the first year of grant and related studies in the lab indicate that conjugation of AOE and PA with antibodies to surface endothelial determinants functionally involved in ALI/ARDS, Ig-superfamily Cell Adhesion Molecules ICAM-1 and PECAM-1 (CAMs), can provide such a targeting. In agreement with revised Statement of Work, in the second year we worked on the Specific Aims 1-4, with focus on targeting of diverse AOE (SOD and 1-cysPrx) and novel PA derivatives.

We completed the Specific Aims 1, focusing on characterization of sub-cellular destination of anti-CAM conjugates in endothelial cells. Our main goal was to identify intracellular fate of conjugates internalized via CAM-mediated endocytosis, a novel pathway discovered in the first year of the project. Data shown in Section B1 indicate that conjugates are slowly delivered to lysosomes and that auxiliary drugs can be employed in order to decelerate lysosomal traffic and degradation and thus extend therapeutic window of conjugates.

We practically completed a new Specific Aim 2, which focuses on detailed characterization of animal models of ALI developed in this grant and proposed as test models for estimation of protective effects of our drug delivery systems. By itself, development of adequate and reliable animal models of human ALI syndrome, especially in mice (the species most useful for genetic manipulations) is an important goal in fighting ALI. Characterization of dynamics of cell adhesion molecules and leukocytes in O_2 and GOX-mediated pulmonary oxidant stress (Section B2) provides important, not predictable insights into pathology of these models. Further, development of an original double-hit model of ALI based on combined treatment with GOX and hyperoxia provides a moderate, reproducible, acute oxidant lung injury in mice, an ideal model for testing protective effects of anti-CAM/AOE conjugates.

Our next goal is to develop means for targeted delivery of diverse AOE to endothelial CAMs (Specific Aim 3). Studies in vitro, cell cultures and in animals indicate that SOD can be targeted to endothelial cells and to the pulmonary vasculature and show that SOD conjugate decompose superoxide that promises to alleviate oxidant stress (Section B3). Intracellular delivery of active 1-cysPrx was also achieved. These results provide a solid basis for pursuing the rest of experiments projected for the Specific Aim 3 (including protection evaluation in animal models characterized in the Specific Aim 2) in the third year.

We initiated experiments in the Specific Aim 4, focused on targeting of plasminogen activators to endothelial surface. In order to select the optimal drug for this purpose, we compared several currently available genetic derivatives of plasminogen activators. Our data indicate that in the next year we should concentrate on conjugating Tenektase, as well as urokinase derivatives (Section B4). We also designed a carrier for targeting fibrinolytics to endothelial surface, anti-CAM single chain Fv (scFv). The rest of experiments projected

for Specific Aim 4 will be pursued in the third and fifth year, while the Specific Aim 5 (testing of combined targeting of antioxidants and fibrinolytics) will be pursued in the forth year.

B. Body of the Report (references to our papers included in appendix are in ***bold Italics***).

B.1.Characterization of sub-cellular destination of CAM-targeted conjugates and search for auxiliary pharmacological agents to prolong effects of intracellularly delivered anti-CAM/AOE. Results shown in the first annual report and our recent paper (Muro et al, J.Cell Sci., 2003) clearly demonstrated that endothelial cells (EC) internalize multimeric conjugates directed against CAM (either ICAM-1 or PECAM-1) via a novel endocytotic mechanism, CAM-mediated endocytosis. This result has important implications from the therapeutic standpoint, since the fate of internalized materials is usually dictated by the endocytotic mechanism. For example, phagocytosis and clathrin-mediated endocytosis favor lysosomal targeting, while caveoli-mediated endocytosis favors transcytosis and, in some cases, cytoplasmic delivery. Since CAM-medicated endocytosis is a truly unique and previously unrecognized pathway, one could not predict *a priori* the intracellular destination of the conjugated cargo, its metabolism, fate and duration of activity of anti-CAM conjugates. Therefore, clarification of this final aspect of the Specific Aim 1 was critically important for estimation of prospective therapeutic window of conjugates. We report that this goal is completed, the main findings are and to be published in a new series of our papers and chapters (***Muro et al, AJP Cell; 2003; Muro et al, Bioconjugation Protocols 2004, Chapter 2; Muro et al, Current Vasc. Pharmacol. 2004***). In this section we briefly describe the cardinal findings, please see above papers for illustrations.

To establish a reliable and simple model system for completion of the Specific Aim 1, we first affirmed that HUVEC similarly internalize both anti-CAM/SA/AOE and anti-CAM/FITC-beads conjugates. Using double-staining analysis described in the first annual report and our recent papers (Muro et al, 2003) we confirmed that EC indeed internalize anti-CAM/beads via amiloride-sensitive pathway, CAM-mediated endocytosis.

We utilized this model to characterize intracellular traffic of anti-CAM/beads using labeled antibodies to endosomal and lysosomal markers EEA-1 and LAMP-1. After uptake, conjugates reside in early endosomes for 1-2 h and traffic slowly to lysosomal compartments (2-3 h *vs* less than 15 min for Dextran Red, a marker of fluid phase uptake). Immunostaining for immunoconjugate protein cargo showed its degradation in lysosomes 3 h after uptake. Slow lysosomal traffic fits with the fact that EC normally do not internalize CAM ligands (and thus may lack the effective machinery for their lysosomal trafficking) and emphasizes differences between CAM-mediated *vs* clathrin-mediated endocytosis, which ligands usually rapidly traffic to lysosomes.

Having deciphered the intracellular traffic and pathway of degradation of anti-CAM conjugates, we tested effects of pharmacological agents that might be used to decelerate lysosomal traffic and degradation. We found that chloroquine that inhibits acidification of lysosomes did not alter conjugate trafficking (Fig. 1, below). However, it significantly decelerated degradation, due to buffering vesicular pH towards neutral values, thus inhibiting pH-dependent lysosomal proteases. In contrast, nocodazole, an agent which disrupts microtubules, blocked traffic of anti-PECAM/beads at the level prior to EEA-1 positive endosomal compartment localized on the cellular periphery close to the plasma

membrane, presumably in pre-endosomal vesicles. By virtue of disrupting lysosomal traffic, nocodazole markedly prolonged stability of conjugates inside EC after internalization.

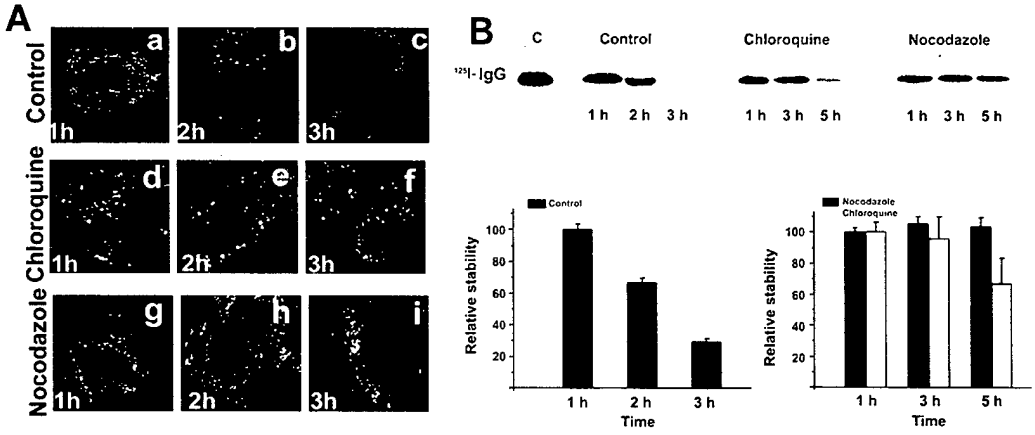

Fig. B.1. Stability of anti-CAM conjugates. (A) Degradation of the anti-CAM was assessed using a TexasRed secondary antibody in permeabilized cells after uptake of anti-CAM/FITC-beads into EC. Yellow: internalized anti-CAM/beads, green: degraded counterpart. In control EC, anti-CAM degrades 3h after uptake. Chloroquine and nocodazole prolong the stability of the conjugates, presumably due to inhibition of lysosomal acidification and trafficking. (B) Radio-autography and densitometric assay of ^{125}I-anti-CAM/beads after uptake by EC. Anti-CAM was considerably degraded 3h after uptake by control HUVEC, while chloroquine or nocodazole markedly prolonged anti-CAM stability, confirming immunofluorescence data. Color version of this figure is available in ***Muro et al, AJP Cell, 2003***.

B.2. Characterization of a novel animal model of human ALI based on pulmonary oxidant stress induced by anti-TM/GOX. Our pilot data shown in the proposal documented that endothelial determinant thrombomodulin (TM) is an excellent candidate target antigen for antibody-directed vascular immunotargeting of the H_2O_2-generating enzyme glucose oxidase (GOX) to the pulmonary endothelial cells (EC), in order to induce EC-specific oxidative lung injury. Indeed, oxidant stress in the lung tissue has been documented by immunostainings for 8-epi-isoprostane (a marker of lipid peroxidation) and nitrotyrosine (a marker of protein oxidative nitration, for example, by peroxinitrate, ONOO). We also detected elevated levels of MDA (malonic di-aldehyde, a cumulative marker of lipid peroxidation) in the lung homogenates obtained from anti-TM/GOX injected mice. Depending of the dose of anti-TM/GOX injected, the severity of pulmonary oxidant stress was so high that 85-95% lethality was observed within 6 h post injection (50-70 ug of anti-TM/GOX per mouse, i.e., 2-2.5 ug/g).

The massive lung injury caused by anti-TMGOX is associated with recruitment of white blood cells (WBC) and especially neutrophils (PMN) to the lungs. WBC recruitment (PMN influx) to the lung was evidenced by MPO evaluation of whole lung homogenates. Moreover, PMN extravasation into the alveolar compartment was revealed. Thus, WBC numbers in the broncho-alveolar lavage fluid (BAL) was 8-fold above over baseline by 24 hours after anti-TM/GOX injection. Our animal experiments performed in the pilot stage of the project also revealed that this model has a potential of combining a specific and "clean" oxidant stress induced in EC solely by hydrogen peroxide with acute pro-thrombotic stress due to inhibition of thrombomodulin. Indeed, we described deposition of fibrin and platelets aggregates in the lungs of mice 4 hours post anti-TM/GOX injection (Christofidou et al, 2002).

These pilot results indicated that lung injury induced by anti-TM/GOX bears several hallmarks of human ALI syndrome: i) an acute oxidant stress in the pulmonary

vasculature; ii) WBC influx in the lungs; iii) pulmonary thrombosis. Therefore, anti-TM/GOX intervention may provide a basis for development of a new animal model of human ALI, a very important goal on its own in the context of the present DOD Program, since currently there is no such a model.

Over the years, a plethora of animal models have been developed for investigation of human ALI. The models employing primary airway insults (e.g., hyperoxia, ozone exposure, intratracheal instillation of hydrochloric acid, bacteria pneumonia, and other), induce local initiation of the lung injury. However, events in the vascular compartment seem to be at least as important as those in the alveolar/airway compartment, in terms of the initiation of many (perhaps, the majority) variants of the syndrome. The models based on the local insults delivered via the airways are thus of relatively limited use for investigation of intravascular initiation of ALI. The models employing intravascular insults (e.g., based on systemic activation of coagulation, complement or leukocytes) arguably possess a higher similarity to variants of human ALI induced by or associated with massive peripheral trauma, or hemorrhage. The realization that distal organ injury may play an important role in the pathogenesis of ALI, paved the way for the development of animal models ALI such as hemorrhage/resuscitation, ischemia/reperfusion of the intestines, kidneys I/R or skeletal muscle, and other. These ALI animal models are characterized by PMN recruitment and increased vascular permeability, however, they suffer from two limitations. First, the extent of induced injury is often relatively mild (with the exception of oleic acid). Second, the pathological events in pulmonary vasculature leading to ALI are not well defined in these models, since pulmonary manifestations and mechanisms are overshadowed by systemic abnormalities.

Based on these considerations, characterization of anti-TM/GOX based models of acute lung injury is of general interest of ALI studies. In addition, a detailed characterization of anti-TM/GOX model was well justified in the frames of the present grant, since it will be employed to test prospective effects of our CAM-targeted drug delivery systems. Therefore, we asked for and have been granted a permission to extend experiments in this model. Originally these animal studies have been projected for the Specific Aim 3, to be completed within the third year. Due to programmatic reasons, we moved this part of the study to the second year. In particular, we wanted to learn main features of the animal model of ALI before we finalize design of the protective conjugates, in order to be able to fine-tune their properties and achieve better effects. This largely extended part of the project, which became a revised Specific Aim 2, is now completed and reported below.

B2.1. Quantitative characterization of pulmonary oxidative stress in mice. One of the goals of this project is to test the protective effect of anti-CAM/AOE targeting in the murine models of pulmonary oxidant stress, anti-TM/GOX and hyperoxia. However, qualitative criteria of lung injury employed in our pilot experiments, such as descriptive tissue morphology and immunostainings for oxidative markers, afford rather relative comparisons between groups. In order to overcome this problem, we have now established additional quantitative parameters of injury inflicted by GOX or hyperoxia in mice, shown in the Table 1 below.

Elevated levels of 8-epi isoprostane (determined by HPLC/MS) and MDA (umol/lung, MDA-586 assay, OxisResearch) in lung homogenates show lipid peroxidation. Protein carbonyls (nm/mg protein) show protein oxidation and myeloperoxidase (MPO) shows

neutrophil sequestration. Elevated levels of protein and WBC in the broncho-alveolar lavage (BAL) show edema and white blood cell (WBC) transmigration. Reduced plasma levels of gelsolin, a marker of acute lung injury, show the severity of cellular destruction (Christofidou, 2002). Measuring these parameters will permit accurate and precise testing of the effects of anti-CAM/AOE conjugates in the Specific Aim 3.

Parameter	Control	Anti-TM/GOX 30 ug	Anti-TM/GOX 60 ug	48 h 100% O_2	72 h 100% O_2
8-epi isoprostane	5.18±0.8	7.21±1.64	19.71±7.22	ND	ND
MDA	4.73±0.42	5.94±0.39	7.84±1.12	6.58±0.03	15.50±0.193
Protein carbonyls	7.5+1.6	ND	ND	15.2+1.8	29.5 (n=1)
MPO	0.23±0.03	0.64±0.04	1.96±0.22	0.56±0.04	0.57±0.09
Lung Wet/Dry ratio	4.23 ±0.1	6.04±0.18	6.67±0.18	4.76±0.06	5.46±0.11
BAL protein	0.14±0.07	0.79±0.71	4.57±1.04	0.928±0.214	4.29±0.54
BAL WBC	58,476±8,901	ND	133,500±45,384	56,838±4,372	72,645±7,958
Plasma gelsolin	373±19	ND	109±18	295±20	110±45

Table 1: Quantitative characterization of oxidant lung injury induced by different doses of anti-TM/GOX or hyperoxia. The data shown as M±SD, n=3-5 (ND: not determined).

B.2.2. Effects of anti-TM/GOX and hyperoxia on expression of Cell Adhesion Molecules (CAM) accessible to blood in the pulmonary endothelium. Of particular interest in the context of this grant was to learn how anti-TM/GOX and hyperoxia alters dynamics of expression of target CAM (Cell Adhesion Molecules) in the pulmonary vasculature and potential effect(s) of blocking WBC interactions with these adhesive determinants in this model. This data will: i) complement described natural history of this pathology and help to understand its molecular and cellular mechanisms; ii) guide fine-tuning of design of anti-CAM conjugates, for example, built-in capacity to block CAM; iii) and provide a basis for interpretation of tentative protective effects of anti-CAM conjugates, projected for testing in the years 3 and 4.

To characterize expression of cell adhesion molecules (CAMs) in the lungs of living mice, we employed a technique of dual radiolabeled Abs described in the previous report developed by the PI previously (Muzykantov et al, 1991). This technique allows quantitative assessment of antigens in the pulmonary vasculature. Importantly, in contrast with tissue immunostainings and analysis of antigens content in tissue homogenates by Western-Blotting that provide no information on accessibility of antigens to circulation, this particular technique reveals only antigens accessible from the bloodstream, i.e., CAM might regulate WBC margination and extravasation. We used ^{125}I-labeled mAbs against P-selectin (BR33.1) and ICAM-1 (YN1) mixed with control non-immune rat ^{131}I-IgG (in order to compensate for CAM-independent component of antibody uptake, such as due to enhanced vascular permeability or binding to Fc-receptor-bearing cells) in Balb C mice. Rat anti-mouse ^{125}I-anti-CAM mAbs, were injected via tail vein 24 hours after injection of anti-TM/GOX conjugate and one hour later mice were sacrificed. Specific pulmonary uptake of ^{125}I-mAb was assessed after subtraction of non-specific ^{131}I-IgG uptake.

Anti-TM/GOX caused 4.9-fold and 2.2-fold elevation of the specific pulmonary uptake of P-selectin and ICAM-1 mAb over control level, respectively. In a new series we found that

anti-PECAM/GOX conjugate that we used in previous studies prior to development of anti-TM/GOX (Christofidou et al, 2001), caused an elevation of the specific pulmonary uptake of ICAM-1 (22% increase over untreated controls) but not P-selectin mAb (3%) after 24 hours after injection. Therefore, anti-TM/GOX injury associated with PMN entry to the alveolar compartment, causes a marked elevation of blood-accessible of P-selectin and ICAM-1 in the lung. In contrast, anti-PECAM/GOX, which is associated with PMN margination but not their extravasation into the airspace (Christofidou et al, 2002), causes a marked elevation of blood-accessible ICAM-1 but not P-selectin in the lung. This result implies that P-selectin and ICAM-1 play significant and likely different roles in oxidant- and leukocyte-mediated lung injury.

To test effects of hyperoxia, mice were placed in a sealed Plexiglas chamber (continuous flow of O_2 at 10 L/min, yielding O_2 concentrations of 80-100% determined by an O_2 analyzer, model 600-ESD; Newark, DE). Under these conditions, animals develop progressive lung injury after 48 hours of exposure and expire by 96 hours. BAL fluid showed increase in protein level indicative of alveolar edema by 4 days (Fig.D3.1). Pathological changes in histological sections manifest by generalized severe vascular congestion and hemorrhagic edema, hyaline membranes and inflammatory infiltrate by 96 h. Our paper describes hyperoxia model in details (Christofidou 2002b).

Injection of ^{125}I-antibodies to P-selectin or CAM mixed with ^{131}I-IgG (a double-label tracing technique accounting for specific and non-specific uptake in lungs developed earlier (Muzykantov 1991)), showed that both anti-TM/GOX and hyperoxia up-regulate expression of surface adhesion molecules in the lungs (Table 2 below).

Lung uptake, %ID	Control	Anti-TM/GOX	24 h O_2	48 h O_2	72 O_2
Control IgG	1.24±0.05	2.69±0.19	1.06±0.13	1.35±0.23	2.65±0.46
P-selectin	1.86±0.06	5.2±1.4	1.84±0.14	2.20±0.15	6.05±0.49
ICAM-1	3.98±0.19	5.93±0.43	3.05±0.13	2.38±0.13	9.44±0.7

Table 2. Oxidant stress augments pulmonary uptake of ^{125}I-labeled antibodies against cell adhesion molecules. Table shows tissue level of Iodine 1 h after IV injection in mice with induced by either injection of anti-TM/GOX (3 h prior the antibodies injection) or exposure in a hyperoxic chamber for indicated period of time. The data shown is M±SEM, n=4-6.

Pathological perturbations (i.e., elevation of CAM-level) in pulmonary endothelial cells EC in anti-TM/GOX treated mice and at early stages of hyperoxia indicate that: a) EC is a prime target of oxidant stress; b) EC injury in hyperoxia may lead to deleterious consequences, e.g., inflammation due to exposure of adhesion molecules; and, c) anti-CAM/AOE targeting likely to be elevated upon hyperoxia.

B.2.3. Effects of blocking of cell adhesion molecules in the models of pulmonary oxidant stress induced by anti-TM/GOX or hyperoxia. In the experiments described above, tracer amounts of isotope-labeled anti-CAM were injected in mice (1-5 ug/animal). In the next series we tested effect of larger doses of blocking CAM antibodies on pulmonary WBC influx and tissue injury in two models of oxidant stress proposed as test systems for drug delivery systems in the present grant: anti-TM/GOX and hyperoxia. The latter model is similar to the anti-TM/GOX model in that it is also: i) oxidant-mediated; ii)

there is EC injury and severe lung injury by 72 hours of 100% O2 exposure; iii) pulmonary sequestration and extravasation into alveoli of activated WBC and PMN.

We used several strategies to test EC CAM involvement in these models, including: i) anti-CAM antibodies and combinations thereof, ii) neutrophil depletion using RB6 antiserum; iii) common L/P-Selectin inhibitor lectin fucoidin (20mg/kg); and, iv) CAM knockout mice. In particular, we employed blocking mAbs against P-selectin, ICAM-1 and PECAM-1 in Balb C mice exposed to 100% O_2 for 72 hours. The mAbs or control IgG (100 ug/mouse) were injected at T=0 and 24 hours of O_2 exposure. Lungs were assessed morphologically, by lung wet/dry ratio and BAL protein accumulation, and BAL WBC/PMN counts. Percent of inhibition of WBC influx was assessed with respect to maximal injury under exposure with no therapeutic intervention.

Either ICAM or PECAM antibodies attenuated pulmonary influx of leukocytes in hyperoxia (28% and 66% inhibition, respectively), while P-selectin antibody or control IgG had no effect (-3% and –4%). Evaluation of injury parameters including wet/dry ratio and protein levels in BAL, however, failed to indicate any significant protection. The study was further expanded using fucoidin, an L- and P-selectin blocker, with similar findings. Furthermore, experiments using PECAM-1, ICAM-1 and P-selectin knockout mice also failed to prevent hyperoxic lung injury. Finally, PMN depletion experiments repeated several times both in Balb C and Black C57 mice to avoid strain specificity, also failed to prevent lung injury at 72 hours in this model. Our data showed that blockade of the inflammatory component, namely suppression of leukocyte influx into the alveoli, or even elimination of neutrophils failed to prevent the development of hyperoxic lung injury.

We also tested role of CAM and PMN in acute pulmonary injury induced by anti-TM/GOX (75 ug/mouse, 90-100 lethality 4-6 h). To our surprise (although attenuated by previous results in hyperoxia model), we found no protective effects of any intervention, whether with anti-CAM antibodies or PMN depletion. We therefore decided to scale-down the anti-TM/GOX dose to sub lethal, injuring in a 24-hour period (35 ug/mouse). BAL proteins in mice challenged with low dose anti-TM/GOX treated with saline or fucoidin were 1.0 vs 1.2 mg/ml respectively, while BAL WBC were 63,000±6,900 versus 58,000±7,000. Therefore, no significant difference was noted. However, mice depleted of PMN, challenged with low dose anti-TM/GOX showed a significant decrease of BAL proteins as compared to non-depleted, challenged controls (0.33 *vs.* 0.51 mg/ml). PECAM knockout mice showed significantly less % BAL PMN (3±1 *vs* 11±7) and BAL WBC (32,686±3,000 *vs.* 48,032±8,683), but no difference in BAL proteins (0.6±0.2 *vs.* 0.5±0.1).

Overall, our data suggested that CAMs, whether endothelial or on leukocytes, play a relatively minor, if any, role in hyperoxia and anti-TM/GOX models of ALI. In fact, we showed that blockade of the inflammatory component, namely suppression of leukocyte influx into the alveoli, or even elimination of neutrophils failed to prevent the development of GOX/TM-induced lung injury. This outcome suggests that PMN play rather limited roles in propagating of acute phase of our models. In retrospect, one can find that this result fits with literature and anecdotal sources citing a controversy on the role of PMN in lung injury in animal models. Currently we reflect on this controversy and contemplate additional studies (perhaps, beyond the frames of this grant) in which to address roles of blood cells, such as involvement in sub-acute or chronic phases, in our murine models of human ALI.

B.2.4. Effect of combined sub-injurious doses of anti-TM/GOX and hyperoxia: a new, more clinically relevant and reliable model of a double-hit ALI. It should be noted that both hyperoxia and anti-TM/GOX models in the way pursued in the literature and in our previous studies, represent somewhat artificial imitation of human ALI syndrome. For example, an extreme severity and acuteness of lung injury and high mortality developed in response to high doses of anti-TM/GOX might mask some relatively minor, yet physiologically important pathological mechanisms of the injury and might overshadow testing of tentative protective effects of drug targeting. In addition, use of high doses enhances probability and influence of systemic side effects of circulating fraction of anti-TM/GOX (that would in turn increase with dose elevation due to saturation of clearing mechanisms).

By these reasons, intermediate or moderate levels of injury induced by lower anti-TM/GOX, more compatible with extent of lung injury in human ALI, would be preferable for the testing of protective interventions. However, the dose dependence curve for anti-TM/GOX is extremely sharp and dose reduction below highly injurious levels leads to high irreproducibility of the data, most likely due to minute variability of the injected dose, size and individual sensitivity of animals. Therefore, in contrast with relatively reproducible acute, severe and lethal outcomes of high doses of anti-TM/GOX (60-70 ug/mouse or >3 ug/g), half animals may show practically no injury, whereas half will display a severe injury and even expire after injection of "borderline" doses (~2.5 ug/g).

On the other hand, exposure of mice to hyperoxia alone induces rather mild, if detectable at all, pulmonary injury within first two days of exposure. Even more importantly, it does not reflect human pathology in the sense that clinically hyperoxia is applied to sick patients (with ongoing pulmonary inflammation, oxidant and thrombotic stresses in cases associated with ALI), not to healthy subjects.

We took seriously these objective downsides of animal models of ALI, projected for testing antioxidant interventions in our study, which resurfaced in our recent studies reported above. In order to overcome these problems, we studied effects of combined treatment of mice with low, sub-injurious doses of anti-TM/GOX (1.0-1.5 ug/g) and hyperoxia, a setting reflecting more adequately clinical hyperoxia treatment of ALI patients with ongoing vascular oxidant stress and inflammation.

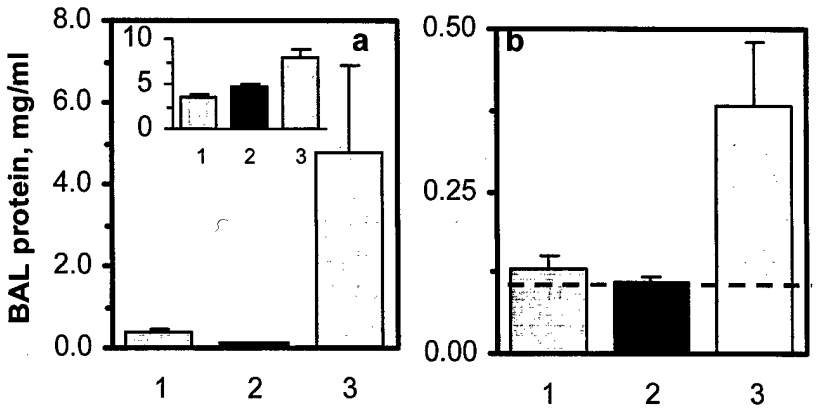

Fig.2. A new model of ALI in mice induced by anti-TM/GOX in hyperoxia. Mice were injected with a sub-toxic 1 ug/g dose of anti-TM/GOX and placed for 4 h in a hyperoxic chamber. Hyperoxia augments lung injury by anti-TM/GOX (A: 100% O_2; B: 80% O_2). BAL protein were measured 4 h post insults: anti-TM/GOX alone (1); hyperoxia alone (2); or anti-TM/GOX and hyperoxia (3). Inset in A shows MDA level in lung tissue homogenates. Dashed line indicates normal level of BAL proteins.

Neither low doses of anti-TM/GOX in room air (1 ug/g), nor 100% O_2 itself caused a significant lung injury in mice within 4 h. In fact, no detectable injury was found in mice exposed to hyperoxia alone for 24 h. In a sharp contrast, combination of anti-TM/GOX and 100% O_2 caused acute severe oxidative lung injury detectable by 5-fold elevation of protein in BAL and doubling of MDA level in the lung tissue homogenates (Fig.2A). The model is highly reproducible and easily tunable by the level of O_2: for example, combined treatment with the same dose of anti-TM/GOX and 80% O_2 produced less severe, but clearly detectable acute lung injury (Fig.2B).

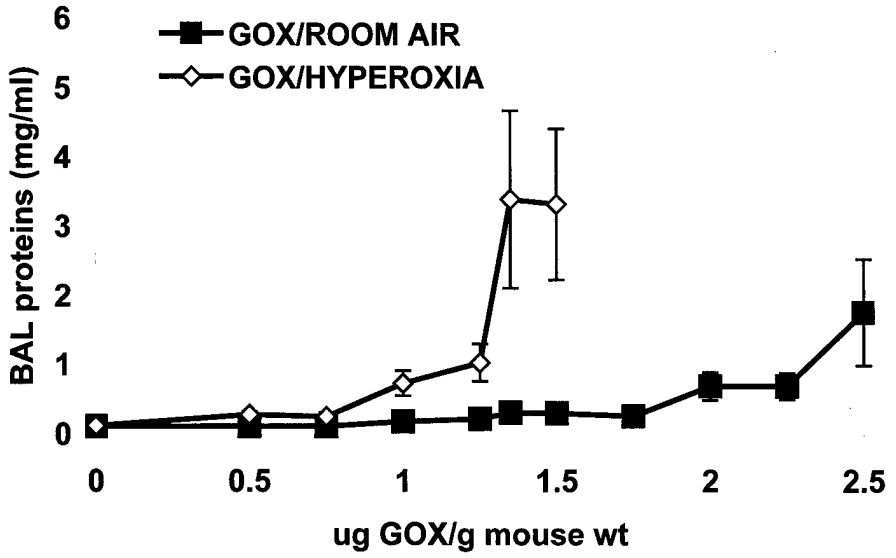

Figure 3 shows detailed comparison of dose-dependence curves for anti-TM/GOX induced injury in room air vs hyperoxia (80% O_2) conditions. One can clearly see that in hyperoxia anti-TM/GOX within the range of 1.0-1.5 ug/g causes a marked, reproducible, yet not overt or lethal pulmonary injury (determined by the level of BAL fluid protein, characterizing lung edema). This reliable, and relatively easily tunable model of acute lung injury, characterized by much lower generalized toxicity (due to reduction of GOX dose), will be utilized in the next year to characterize protective effects of targeting antioxidant enzymes to endothelial CAM.

B.3.Delivery of diverse AOE to endothelial CAMs. Our previous studies were focused mainly on catalase, an enzyme that reduces H_2O_2, an important Reactive Oxygen Species (ROS) involved in ALI. However, other ROS are also play important roles in this pathology. For example, superoxide anion (superoxide), generated by either activated leukocytes or endothelial cells themselves, apparently plays a key role in initiation of the cascades of pro-oxidative reactions, including inactivation of NO, formation of a strong oxidant peroxinitrite (ONOO), formation of H_2O_2 and generation of an extremely strong oxidant, hydroxyl radical in Haber-Weiss reaction. On the other hand, diverse organic peroxides formed in reactions of ONOO and hydroxyl radical with lipids and other biomolecules, ignite chain reactions of lipid peroxidation and directly inactivate proteins and nucleic acids. Figure 1 below illustrates reactions of vascular oxidant stress (VOS, one of the key pathological

mechanisms that underlies ALI) and main antioxidant enzymes, SOD, catalase and 1-cysPrx.

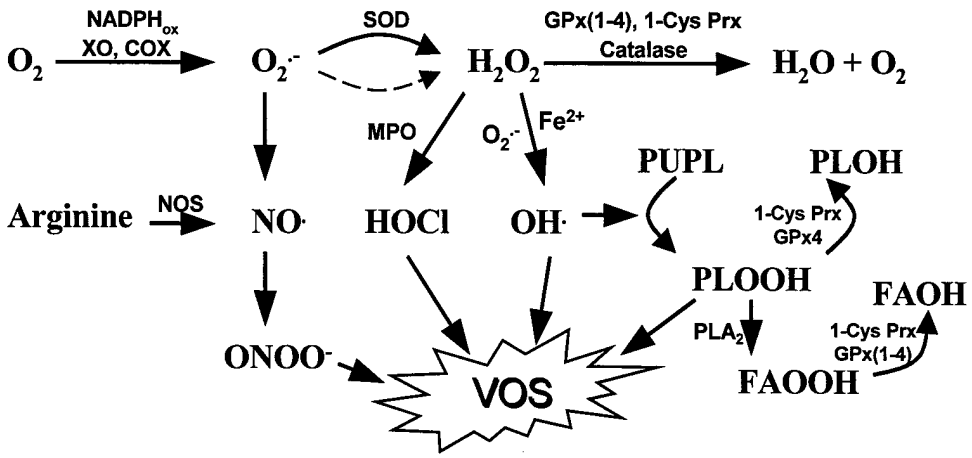

Fig.4. VOS and AOE. SOD prevents inactivation of NO· and generation of $ONOO^-$ by converting $O_2^{\cdot-}$ into H_2O_2 that can form strong oxidants. Catalase, peroxidases and 1-CysPrx reduce H_2O_2 into H_2O. PLOOH (phospholipid hydroperoxides) formed from polyunsaturated phospholipid (PUPL) cause peroxidation of lipids. FAOOH (fatty acid peroxides) excised from cellular membranes by PLA_2 phospholipase A_2 can be reduced into non-toxic hydroxy fatty acid (FAOH) by 1-CysPrx that detoxifies PLOOH into non-toxic PLOH. XO: xanthine oxidase, COX: cyclooxygenase, NOS: nitric oxide synthase, MPO: myeloperoxidase.

Therefore, coordinated delivery of diverse AOE seems to be necessary in order to allow more effective detoxification of diverse ROS and oxidants and thus achieve profound protective effects. Accordingly, in this grant we pursue targeting of SOD (to detoxify superoxide), a novel potent AOE, 1-cysPrx (to detoxify a wide spectrum of organic and inorganic peroxides, see below in Section B.3.4.) and a tandem SOD/catalase, which in theory might permit very effective, coordinated detoxification of both superoxide and H2O2 into water, without excessive formation of harmful intermediates. Sole targeting of catalase, which is viewed mostly as a model system, is pursued elsewhere.

B.3.1. Preparation and characterization of anti-CAM/SOD conjugates. We used streptavidin-biotin cross-linker to produce anti-CAM/SOD conjugates of optimal size (150-250 nm). Firstly, we determined effect of biotinylation on SOD activity and characterized number of biotin residues covalently attached per molecule of SOD, using HABA reagent. Figure 5A (below) shows that biotinylation within biotin to SOD molar ratios 4-8 permits coupling of 1-1.7 biotin residues per SOD molecule with rather modest reduction of enzymatic SOD activity. Further, determined calibration curves for amount of streptavidin that produces anti-CAM/SOD conjugates of the proper size and found that streptavidin forms anti-CAM/SOD conjugates close to 200 nm diameter at a molar ratio 1.25 (Fig. 5B), This size is optimal for targeting and intracellular delivery (Wiewrodt 2002; Muro 2003).

We determined SOD enzymatic activity of the resulting conjugates. Interestingly, we found that SOD activity was reduced sharply after conjugation when a large artificial substrate, a fluorescent substance SOD525 was used (inset in Figure 5B). However, when superoxide anion was used in the testing reaction (detected by reduction of cytochrome C, Cyt C), apparent reduction of SOD activity after conjugation was dramatically less prominent (compare closed and open bars in the inset). We speculate that streptavidin-mediated conjugation of SOD may partially block its active site, which could be more easily revealed by a large substrate. However, superoxide, which is a natural substrate of SOD and tentative ROS target for decomposition by anti-CAM/SOD conjugates, is a small and

relatively easily diffusible molecule and, therefore, enzymatic activity of resulting conjugates is high.

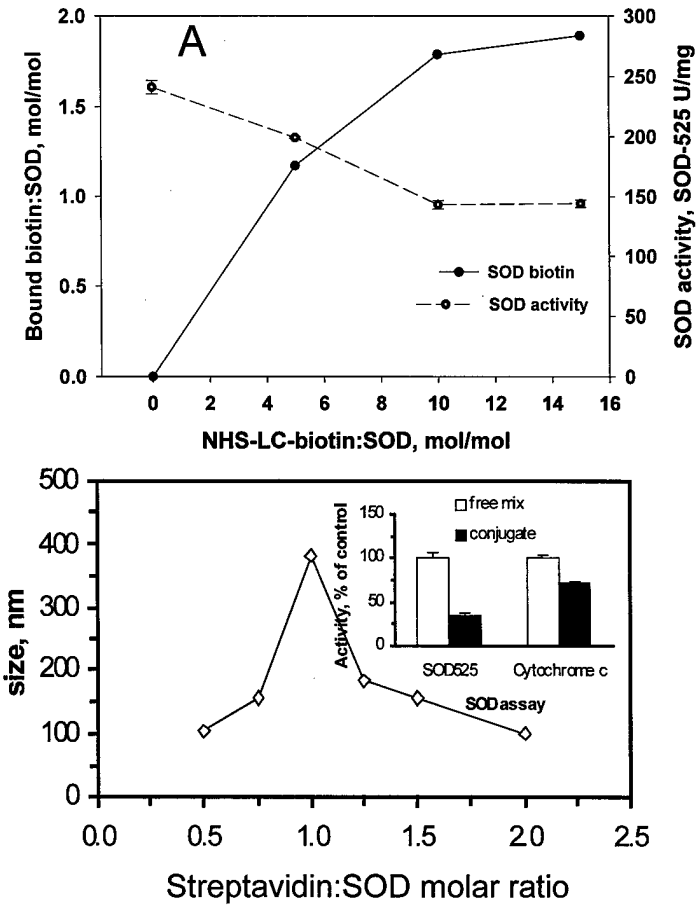

Fig.5. Preparation of anti-CAM/SOD conjugates. Panel A (upper) shows dose dependence of the biotinylation reaction yield and enzymatic activity of biotinylated SOD on the molar excess of biotinylating agent, BHS-LC-biotin. Panel B (bottom) shows mean diameter of anti-CAM/SOD conjugates formed at different molar ratios of cross-linking agent, streptavidin. Size was determined by DLS (dynamic light scattering). For details of conjugation procedure see our recent methodological chapter in Bioconjugation Book (Shuvaev et al, 2004). An inset in the bottom panel shows enzymatic activity of non-conjugated (open bars) and conjugated (closed bars) biotinylated SOD. Activity was determined using a large artificial fluorescent substrate (SOD525) or small, natural SOD substrate, superoxide anion, using color reaction of Cyt C reduction. Note that enzymatic activity of conjugated SOD is higher towards its natural substrate.

B.3.2. Specific binding of anti-CAM/SOD conjugate to endothelial cells. To characterize quantitatively targeting SOD to endothelial cells in vitro and in animals, we synthesized conjugates using procedure described in the previous section, using radiolabeled SOD (^{125}I-SOD). In the first series of targeting experiments, anti-CAM/^{125}I-SOD was incubated with human endothelial cells (HUVEC) or with a cell type routinely used in our studies as a negative control, REN cells (human mesothelioma cells forming an endothelium-like monolayer, yet not expressing endothelium-specific CAMs). Figure 6 (below) demonstrates that anti-CAM/SOD specifically binds to endothelial, but not to control cell type.

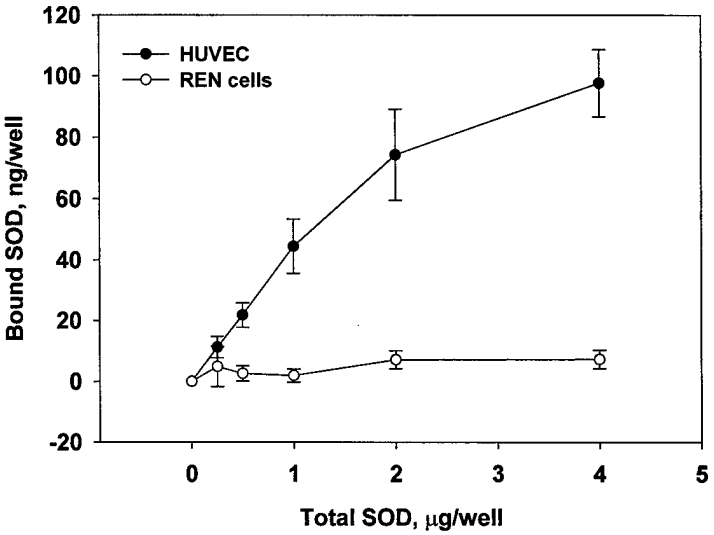

Figure 6. Specific targeting of anti-CAM/SOD to endothelial cells in vitro. Indicated doses of radiolabeled conjugate was incubated with endothelial cells (HUVEC) or control cell type (REN) for 1 h at 37°C. Non-bound conjugate was eliminated and cell-associate radioactivity was determined in a gamma-counter. The data of bound SOD (ng/well) is shown as function of added conjugate, Mean+SD, n=3.

B.3.3. Pharmacokinetics of anti-CAM/SOD in mice and pulmonary targeting of radiolabeled conjugate. We characterized biodistribution of anti-CAM/SOD conjugate containing radiolabeled SOD (i.e., preparation similar to that employed in the previous series in cell cultures) after intravenous injection in intact anesthetized mice. In this series, to control for the specificity of targeting, we utilized a non-immune IgG/SOD counterpart. Fig. 7 below shows results of this critically important animal study.

As described in more detail animal protocol for the grant, we calculated several parameters of the conjugates biodistribution in organs. Firstly, % of injected dose per gram of tissue (%ID), shows total distribution of the conjugates in the main organs and blood. As one can see, non-immune control IgG/SOD shows higher uptake in liver and spleen (most likely due to relatively non-specific recognition of Fc-fragments by resident macrophages in reticuloendothelial system organs), whereas anti-CAM/SOD shows much higher uptake in the lung due to specific binding to endothelium and lower blood level, likely due to partial depletion of circulating pool by endothelial binding (Fig.7A).

Calculation of %ID per gram permits comparisons of uptake in different organs and evaluates tissue selectivity of an antibody uptake. Without normalization per weight, uptake in large organs (liver) may look extremely large when compared with that in a relatively smaller organ (e.g., lung or heart). This parameter reveals that IgG/SOD has the highest tropism to spleen, whereas anti-CAM/SOD has highest tropism to the lung (Fig.7B).

The ratio between %ID/g in an organ of interest and that in blood gives Localization Ratio, LR. This parameter compensates for a difference in blood level of circulating antibodies (e.g., due to different rate of renal or hepatic clearance or uptake by targets), helps to account for the level of non-specific IgG in an organ and allows a more objective comparison of targeting between different carriers. Compensation for faster blood clearance of anti-CAM/SOD shows that pulmonary LR was the highest for anti-CAM/SOD

and achieved 10 one hour post injection (Fig. 7C), level compatible to other lung targeting systems described in our previous studies.

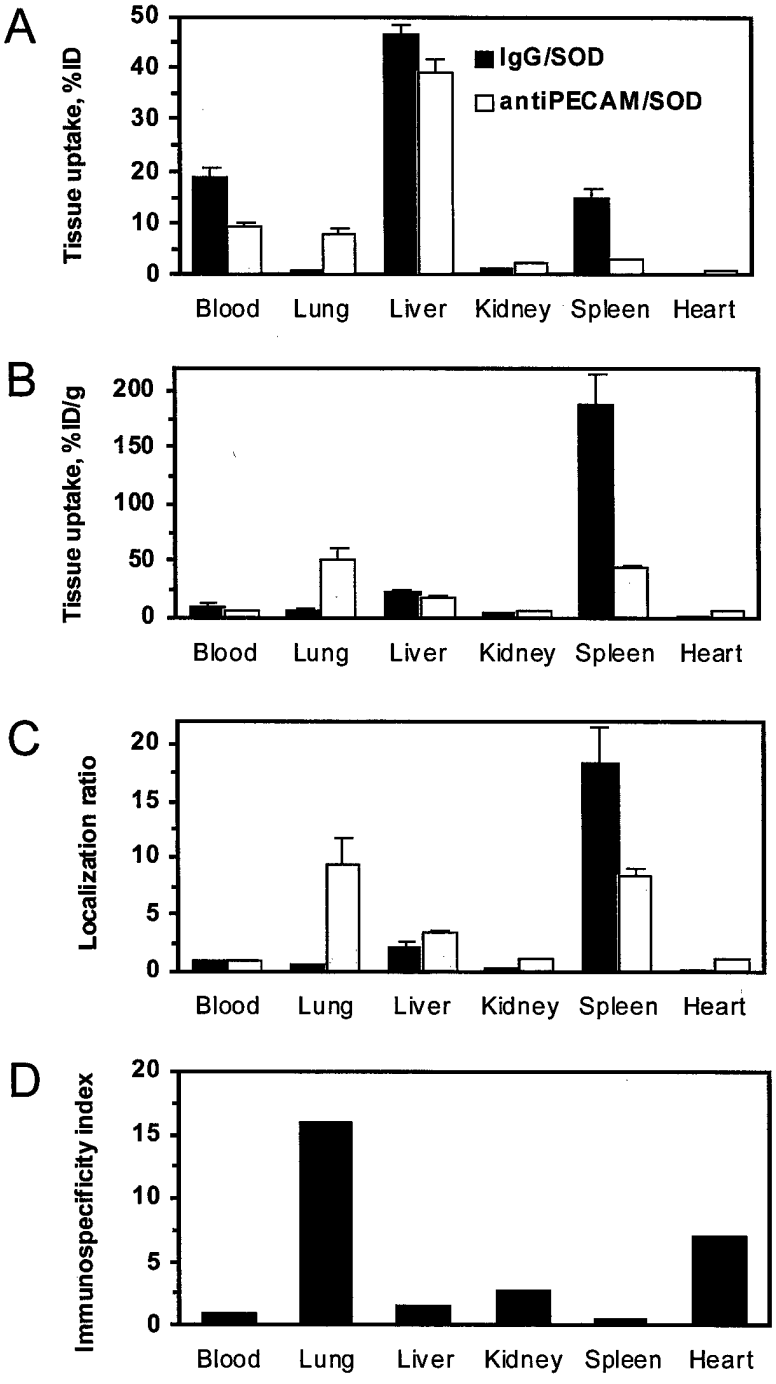

Figure 7. Pulmonary targeting of anti-CAM/SOD. A tracer amount of the conjugates (1-3 ug per animal) was used in this study. Animals were sacrificed 1 hour after IV injection of conjugates, organs obtained, rinsed by a buffer, blotted and radioactivity determined in a gamma-counter.

Finally, the ratio between levels of an antibody and control IgG (the Immunospecificity Index, ISI, that can be calculated using LR) shows the specificity of an antibody uptake comparing with non-targeted IgG. ISI shows that anti-CAM/SOD has 15-times higher tropism to pulmonary vasculature than IgG/SOD counterpart (Fig.7D).

B.3.5. Cellular delivery of 1-CysPrx, a novel potent AOE. Phospholipid hydroperoxides (PLOOH) generated by ROS damage membranes. Excision of the oxidized fatty acid moiety by a phospholipase followed by re-acylation of residual lysophospholipid helps to restore membrane integrity. However, 1-Cys-Peroxiredoxin (1-CysPrx) directly reducing PLOOH to non-toxic hydroxy derivatives (e.g., PLOH) affords even more effective protection (***Manevich 2002***). 1-CysPrx is a 26 kD cytosolic protein with a sole redox-active cysteine using GSH as a reducing co-factor, a unique member of a superfamily of non-seleno-peroxidases which usually have two redox-active cysteines using as a co-factor thioredoxin.

1-CysPrx antisense augments oxidative stress in cells, while its overexpression in cells enhances their ability to reduce H_2O_2 and organic peroxides (e.g., tBOOH), enhancing their resistance to oxidative stress, lipid peroxidation, apoptosis and toxicity induced by H_2O_2, tBOOH and $^{\bullet}OH$ (***Manevich, 2002***). Animal studies implicate endogenous 1-CysPrx in protection against pulmonary oxidative stress. 1-CysPrx reduces a wide range of peroxides and has a unique concomitant phospholipase activity. Reduction of H_2O_2 or t-BOOH and protection against lipid peroxidation in the membranes via reduction of membrane-associated PLOOH to PLOH derivatives followed by restoration of membrane function due to phospholipase activity are likely components of the unique antioxidant mechanism of 1-CysPrx (***Manevich 2002***).

In collaboration with Dr. Aron Fisher, a pioneer in 1-cysPrx studies, we obtained a pure recombinant rat 1-CysPrx protein demonstrating high purity and enzymatic activity (Fig. 8), sufficient to synthesize and test anti-PECAM/1-CysPrx conjugates.

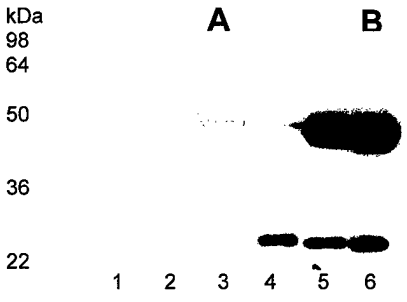

Fig.8 Characterization of recombinant rat 1-cys peroxiredoxin (Prx) expressed in E.coli. Electrophoretic (A) and Western blot (B) analysis of the protein after initial separation on DEAE-Sepharose (lanes 1 and 4) and final purification on CM-Sepharose (lanes 2, 3, 5 and 6) shows monomers and dimers of 1-cysPrx. 1-Palmitoyl-2-linonenoyl hydroperoxide-sn-glycero-3-phosphocholine was used as a substrate in NADPH/GR-coupled assay for purified 1-cysPrx activity that was estimated as 3.5 μmol/mg/min.

We tested delivery of purified 1-cysPrx to model target cells (H441 cells, which lack natural 1-cysPrx and, therefore, represent an ideal culture for testing effects of transfection, transduction or delivery of this protein). Figure 9 shows binding of purified 1-cysPrx loaded in FITC-labeled liposomes (Pro-Ject liposomes, Pierce) to cells in culture. Western blotting of the cellular lysates using anti-1-cysPrx mAb 17 (Fig.9 F) identifies localization of the delivered enzyme. Furthermore, analysis of NADPH-dependent enzymatic reduction of a lipid peroxide substrate (1-palmitoyl-2-(13-hydroperoxy)-linolenoyl-sn-glycero-3-phosphocholine) revealed significant 1-cysPrx activity (2.8 umol/mg protein/min) in the cell

lysates of cells incubated with 1-cysPrx liposomes, but not in the control cells, indicating presence of active 1-cysPrx inside the cells.

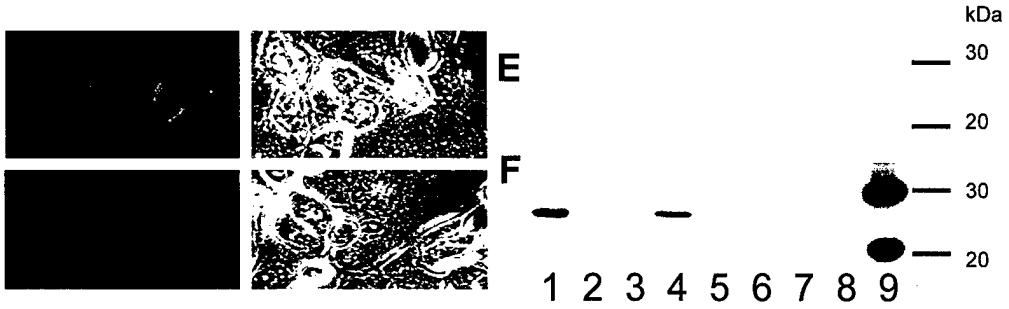

Fig. 9. Intracellular delivery of recombinant 1-CysPrx. A and B: cell-associated fluorescence and phase contrast of the cells incubated with 1-CysPrx loaded into FITC-labeled liposomes, C and D: control cells. E: staining of PAGE of pure 1-CysPrx (1), a reference protein (2), supernatants from control cells shown in D (3) and from the cells incubated with 1-CysPrx loaded liposomes, shown in B (4), soluble fraction of cell lysates of control cells (5) and cells incubated with 1-CysPrx loaded liposomes (6), insoluble fraction of cell lysates of these cells (7,8) and molecular weight standards (9). F: immunoreactive band of 1-CysPrx (detected by a mAb #17) was revealed in the medium of the cells incubated with 1-CysPrx liposomes (4) and in a soluble fraction of cell lysates (6).

B4. Delivery of fibrinolytics to endothelial CAMs: selection of optimal drugs and carriers. Our initial efforts in pilot studies and in the first year of the project prior to revision of the SOW were focused on tissue-type plasminogen activator, tPA, as a prototype fibrinolytic agent for targeting to endothelial CAM for alleviation of thrombotic burden in the pulmonary vasculature in ALI/ARDS (***Murciano 2003***). However, individual plasminogen activators have quite different profile in terms of fibrinolytic activity, resistance to plasma inhibitors, rate of elimination from the bloodstream, penetration into haemostatic clots and side effects in the tissues. In order to select the best candidate for this specific application, we compared side-by-side several currently available plasminogen activators including wild-type tPA, its molecular derivatives obtained by gene engineering (Retavase and Tenektase) and urokinase.

Firstly, we compared enzymatic activities of these specific proteases using a small chromogenic substrate, Chromogen. Its cleavage in active site of plasminogen activators (generating a color) imitates plasminogen cleavage without any confounding effects. This was necessary since these plasminogen activators come from different sources, which express their fibrinolytic activity in different units and often do not provide absolute amount of protein in their preparations.

Having equalized enzymatic activities of these four proteases, we compared rates of dissolution of pure fibrin clots containing plasminogen by equally enzymatically potent doses of plasminogen activators. We found that in this model system free of effects of plasma inhibitors, all four plasminogen activators produce equally effective, 100% fibrinolysis with similar kinetics.

However, when we tested dissolution of clots formed from human plasma (e.g., containing plasma inhibitors), we found that only Tenektase produces fibrinolysis that was similar to that of pure fibrin clot. Other fibrinolytics showed markedly lower extent of fibrinolysis, due

to inhibition by plasma inhibitors. This experiment revealed the following order of resistance to plasma inhibitors: Tenektase>tPA>>Retavase>urokinase.

In the next pilot series, we injected these plasminogen activators in mice and took samples of blood at 10 and 60 min post injection. Clots formed from blood were allowed to dissolve at 37oC (background level of spontaneous dissolution of blood clots under these conditions did not exceed 10% by 2-3 hours incubation at 37oC). We found that blood clots formed 10 min post injection tPA, Retavase or Tenektase display similar extent of acceleration of fibrinolysis, whereas injection of urokinase did not cause significant acceleration of fibrinolysis. However, only blood clots formed from blood taken 60 min after injection of Tenektase displayed marked acceleration and augmentation of fibrinolysis, while blood obtained 60 min after injection of either tPA or Retavase showed no enhanced fibrinolytic activity. Our pilot study using radiolabeled tPA and Tenektase revealed that the latter circulates for markedly longer time.

Therefore, these pilot data obtained *in vitro* and *in vivo* indicate that Tenektase, which is resistant to plasma inhibitor and retains its fibrinolytic activity for a prolonged time in the bloodstream, is optimal plasminogen activator derivative for targeting to CAM.

B.4.2. Design of anti-CAM single-chain antigen-binding fragment, anti-PECAM scFv. In order to provide thromboprophylaxis in ALI, we proposed to deliver fibrinolytics to endothelial CAM. Importantly, endothelial cells normally poorly internalize monomolecular ligands of these cell adhesion molecules. Therefore, a monomolecular anti-CAM conjugate would reside for a relatively prolonged time on the luminal surface of endothelial cells, an ideal strategic position for its fibrinolytic effects. Methods for conjugating with antibodies include chemical covalent coupling (e.g., using bi-functional cross-linking agents, such as SPDP) and non-covalent coupling (e.g., via streptavidin-biotin or cross-linking antibodies). However, these conventional methods for conjugation suffer serious downsides. From a general, technical standpoint, a large-scale production of standard protein conjugates using chemical means is almost impossible. More specifically, it is very difficult to obtain pure monomolecular conjugates. However, conjugates containing polyvalent anti-CAM will undergo internalization and disappear from the lumen, hence lost therapeutic effect.

Creation of genetically engineered fusion proteins, which combine a specific target-binding site of the affinity moiety (single chain antigen-binding fragment, or scFv) and fibrinolytics might help to solve most, if not all these problems. This strategy, from the general technological standpoint, represents the most advanced approach permitting production of large amounts of standard, QQ-amenable, stable recombinant products with reasonable shelf-lives. In addition to these technological advantages, utilization of fusion proteins helps to solve some side effects associated with parts of antibody which are not important from the standpoint of delivery of anti-thrombotic effect(s), but can cause side effects (e.g., Fc-fragment of antibodies). Finally, fusion proteins represent exact copies of an encoded recombinant monomeric protein, which solves intrinsic problems associated with poor control of size and valency of heterogeneous chemical polymer conjugates. Therefore, fusion proteins will represent the most useful candidate formulations for targeted vascular delivery of in clinical practice.

Based on this rationale, we teamed up with Dr. Claudia Gottstein (University of Cologne, Germany) to design and produce anti-CAM scFv. Due to cellular characteristics of rat

myeloma cells and splenocytes obtained from immunized rats, hybridoma producing monoclonal antibody directed against murine PECAM (mAb 390) is more amenable to molecular engineering than corresponding anti-ICAM counterpart. However, our recent data obtained in cell cultures and in animals clearly documented that antibody conjugates directed to PECAM-1 or ICAM-1 can be relatively universally and easily exchanged for the purpose of targeting AOE and fibrinolytics to endothelial cells (Muro 2003; Murciano 2003). Therefore, we utilized mAb 390 hybridoma to produce anti-CAM scFv.

The variable regions of all heavy and light chains of interest from cDNA isolated from mAb 390 hybridoma cells have been cloned and sequenced. This step (cloning and sequencing) has been repeated to rule out that we accidentally pick up a PCR-caused mutation. There were two different heavy chains (which is unusual) and two different light chains (that's normal). Upon more detailed analysis of the sequences (testing whether the right number of amino acids is present, whether the cysteins are in the right places, whether there are stop codons or frame-shifts, etc) only one heavy chain and one light chain fulfilled all necessary criteria. Using specific primers the scFv have been assembled (the attachment shows the corresponding gel), produced and purified. To test its antigen-binding capacity, we used FACS analysis in HUVEC. Figure 10 (below) shows that scFv produced from anti-PECAM mAb 390 binds to endothelial cells and displays a high affinity, similar to mAb 390.

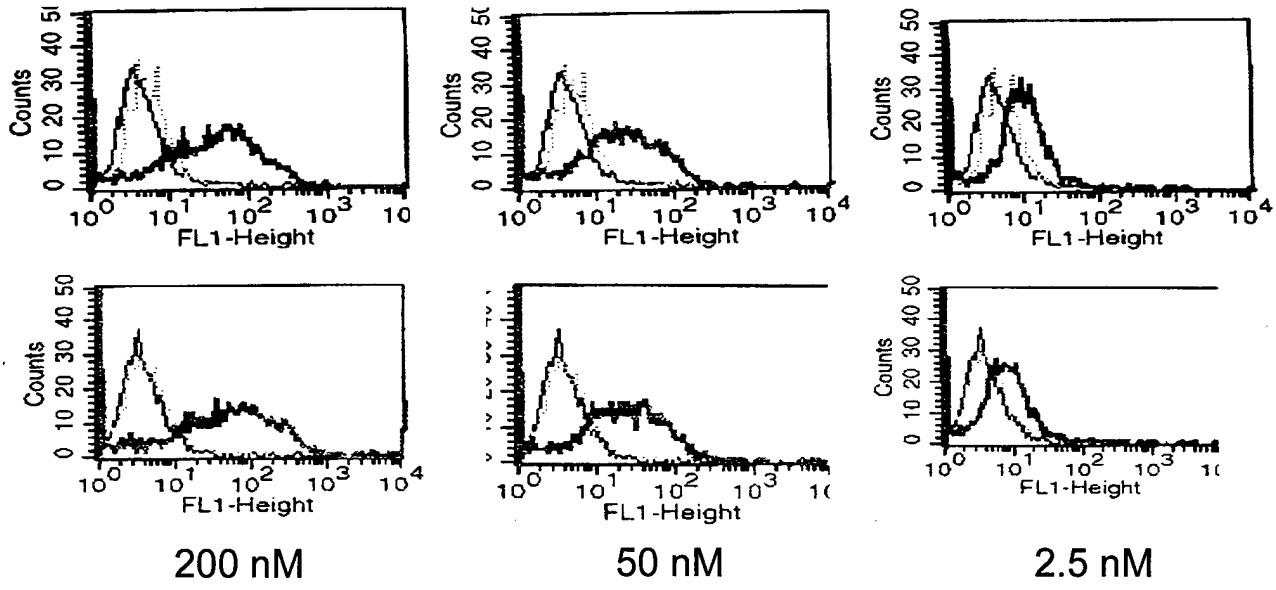

Figure 10. FACS analysis of anti-PECAM scFv binding to EC. Left peaks show staining secondary antibody control without anti-PECAM. Right (high fluorescence, red) peaks show binding of anti-PECAM to cells. Comparison of upper (whole IgG) and lower (scFv) panels shows almost identical binding down to the low nano-molar range, at which point the whole anti-PECAM shows slightly higher binding to EC.

PECAM and ICAM antibodies have a good safety profile in animals. However, use of scFv fragments, inducing minimal, if any, side effects and immune reactions are preferable for clinical studies. Therefore, production of scFv enables us to translate endothelial targeting means from IgG and Fab-fragments to clinically more useful targeting strategies.

C. Key Research Accomplishments. In the second year, the experiments have been mostly focused on the aspects of ALI oxidant stress and targeting antioxidant enzymes for ALI treatment, with relatively minor experimentation on targeting of plasminogen activators. Our new results indicate that anti-CAM conjugates can serve for intracellular targeting of antioxidant enzymes to endothelial interior and their effects can be tested in new animal models of ALI, developed and characterized in this project. We report the following key research results achieved in course of pursuing the Specific Aim 2 (completed) and, at lesser extent, the Specific Aims 1 (completed), 3 (significantly advanced) and 4 (initiated).

- The intracellular traffic, destination and metabolism of internalized anti-CAM conjugates have been characterized.
- Effects of auxiliary pharmacological agents chloroquine and nocodazole on the rate of intracellular degradation of anti-CAM conjugates in endothelial cells has been tested and remarkable deceleration of degradation has been demonstrated.
- Multifaceted parameters characterizing quantitatively pulmonary injury in mice models of anti-TM/GOX and hyperoxia injury have been measured. Use of these parameters will permit accurate and precise characterization of protective effects of CAM targeting in animals.
- Dynamics of expression of blood-accessible cell adhesion molecules and uptake of leukocytes in the pulmonary vasculature were quantitatively characterized in mice models of anti-TM/GOX and hyperoxia lung injury.
- A novel, clinically relevant and reliable model of acute moderate oxidant injury in the lungs based on combined anti-TM/GOX and hyperoxia treatment has been developed.
- Conjugation of SOD to anti-CAM producing enzymatically active conjugates of proper size (200 nm) has been designed and excelled.
- Specific binding of radiolabeled anti-CAM/SOD conjugate to endothelial cells has been verified.
- Specific accumulation of this conjugate in the pulmonary vasculature after IV injection in mice has been demonstrated.
- The optimal plasminogen activator (Tenektase) for anti-CAM targeting has been identified, based on in vitro and in vivo fibrinolytic performance.
- The optimal delivery moiety for targeting of plasminogen activators to CAM, single chain anti-CAM scFv 390 has been designed and produced.

D. Reportable Outcomes

We organized this section in a way that permits to maintain confluence of reported publications (which may partially overlap between the grant years, such as "in press in year 1" vs "published in year 2"), yet avoid double reporting of the results. In order to achieve this goal, we start with *publications reported in the previous years of the grant in Italics,* followed by an extra-space and a list of publications within the current funding year.

D.1. Full-size publications (papers in which the PI is senior author):*

1. S.Muro, R.Wiewrodt, A.Thomas, L.Koniaris, S.Albelda, ***V.Muzykantov***** and M.Koval (2003) A novel endocytic pathway induced by clustering endothelial ICAM-1 or PECAM-1. J Cell Sci. 2003;116(Pt 8):1599-1609*

2. ***V.Muzykantov*** *(2003) Targeting pulmonary endothelium. in: "Biomedical Aspects of Drug Targeting",* ***Vladimir Muzykantov*** *and Vladimir Torchilin*, Eds., *Kluwer Academic Publishers, Boston-Dodrecht-London, pages 129-148*

3. J.C.Murciano, S.Muro, L.Koniaris, M.Christofidou-Solomidou, D.Harshaw, S.Albelda, D.Granger, D.Cines and **V.R.Muzykantov*** (2003) ICAM-directed vascular immunotargeting of anti-thrombotic agents to the endothelial luminal surface. *Blood*, 101:3977-1984
4. S.Muro, X.Cui, C.Gajewski, **V.Muzykantov*** and M.Koval (2003) Slow intracellular trafficking of catalase nanoparticles targeted to ICAM-1 protects endothelial cells from oxidative stress. *Am.J.Physiol., Cell Physiol.*, 285(5):C1339-47.
5. V.Shuvaev, T.Dziubla, R.Wiewrodt, and **V.Muzykantov*** (2004) Streptavidin-biotin cross-linking of therapeutic enzymes with carrier antibodies: nanoconjugates for protection against endothelial oxidative stress. In: "*Bioconjugation Strategies*", C.Niemeyer, Ed., Humana Press (in press)
6. S.Muro, **V.Muzykantov*** and J.Murciano (2004) Characterization of endothelial internalization and targeting of antibody-enzyme conjugates in cell cultures and in laboratory animals". In: "*Bioconjugation Strategies*", C.Niemeyer, Ed., Humana Press (in press)
7. S.Muro, M.Koval and **V.Muzykantov*** (2004) Endothelial endocytic pathways: gates for vascular drug delivery. *Current Vascular Pharmacology*, in press

D.2. Published presentations at international and national scientific conferences.

1. *S.Muro, A.Thomas,* ***V.Muzykantov****, M.Koval (2002) PKc-mediated endocytosis of conjugates targeted to ICAM-1. Abstracts of Experimental Biology 2002 Meeting, New Orleans, LA, April 20-24, 2002 (A.382.12) FASEB J., 2002, 16(4), p A439*
2. *A.Scherpereel, J.C.Murciano, R.Wiewerodt, S.Kennel,* ***V.Muzykantov****, M.Christofidou-Solomidou (2002) Glucose oxidase vascular immunotargeting to pulmonary endothelium enhances luminal expression of ICAM-1 and P-selectin in the lung. Abstracts of Experimental Biology 2002 Meeting, New Orleans, LA, April 20-24, 2002 (A.382.13) FASEB J., 2002, 16(4), p A439*
3. *S. Muro, M.Koval, A.Thomas and* ***V.Muzykantov*** *(2002) Affinity carriers targeted ICAM-1: trafficking into endothelial cells. Abstracts of American Thoracic Society International Conference, Atlanta, GA, May 17-22, 2002; Am.J.Resp.Crit.Care Med., 2002; 165 (4):A101*
4. *A.Thomas, T.Sweitzer, R.Wiewrodt, S.Muro, M.Koval and* ***V.Muzykantov*** *(2002) Size-dependent intracellular targeting of immunoconjugates directed against endothelial surface adhesion molecules. Abstracts of XIV World Congress of Pharmacology, San Francisco, CA July 7-12, 2002; Pharmacologist, 2002, 44, #2 (suppl. 1), 61.2*
5. *S.Muro, T.Sweitzer, R.Wiewrodt, L.Koniaris, A.Thomas, S.Albelda, M.Koval and* ***V.Muzykantov*** *(2002) Kinetics of intracellular immunotargeting to endothelium via adhesion molecules. Ibid, 61.3*
6. ***V.Muzykantov*** *(2002) Catalase immunotargeting: protection against oxidative stress in the pulmonary vasculature. Abstr. Int.Symposium "Reactive Oxygen*

and Nitrogen Species", St.Petersburg-Kizhi, Russia, 8-12 July, 2002, Palma Press, Moscow, p.58

7. M.Christofidou, S.Muro, J.Murciano, M.Barry, A.Thomas, V.Shuvaev, S.Albelda, D.Cines and **V.R.Muzykantov** (2003) Targeting endothelial surface adhesion molecules. Abstr. Symposium of Vector Targeting, Cold Spring Harbor, NY, March 20-22, 2003, page 19)
8. M.Christofidou, A.Scherpereel, A.Boyen, E.Arguiri, V.Shuvaev, S.Kennel and **V.Muzykantov** (2003) Hyperoxia potentiates oxidative injury in murine lungs induced by glucose oxidase targeted to thrombomodulin. Abstr., Experimental Biology Meeting, San Diego, CA, April 11-15, 2003; FASEB J., 2003; 17(4) part I, page A247
9. S.Muro, X.Cui, C.Gajewski, M.Koval, **V.Muzykantov** (2003) Pharmacological Modulation of Intracellular Trafficking and Lysosomal Degradation Prolongs the Anti-oxidant Effect of Catalase Conjugates Delivered into Endothelial Cells via ICAM-1. Abstr. 11th Intern.Symp. Recent Advances in Drug Delivery Systems, Salt Lake City, UT, March 3-6, 2003 (#014)
10. M.Christofidou-Solomiudou, B.Kozower, A.Scherpereel, T.Szeitzer,, S.Muro, R.Wiewrodt, V.Shuvaev, A.Thomas, M.Koval, A.Patterson, S.Albelda and **V.Muzykantov**. Targeting of antioxidants to adhesion molecules (2003) Inflammation Research, 52, Suppl.2, p.S81 (Abstracts of 6th World Congress on Inflammation, Vancouver, Canada, August 2-6, 2003)
11. E.Berk, **V.Muzykantov** and S.Muro (2003) Binding and uptake of anti-ICAM-1 coated nanoparticles by flow-adapted endothelial cells. Abstr. 9th Annual Respiration Research Retreat of the University of Pennsylvania, Sugarloaf Conference Center, Philadelphia, OA, June 20, 2003, #9
12. M.Christofidou-Solomidou, A.Scherpereel, A.Bohen, E.Arguiri, V.Shuvaev, S.Kennel, **V.Muzykantov** (2003) Hyperoxia potentiates oxidative injury in murine lungs induced by glucose oxidase targeted to thrombomodulin. *Ibid*, #16
13. S.Muro, C.Gajewsky, M.Koval, **V.Muzykantov** (2003) Slow intracellular degradation of ICAM-1 or PECAM-1 targeted catalase nanoparticles protects endothelial cells from oxidative stress. *Ibid*, #49
14. V.Shuvaev, S.Tliba, T.Dziubla, **V.Muzykantov** (2003) Combined immunoconjugate delivery of CuZnSOD and catalase to human endothelial cells and their protection against oxidative stress. *Ibid*, #55

D. 3. Unpublished presentations at scientific conferences and invited seminars.
Dr. V.Muzykantov presented the results of this project in the following invited lectures:

05/24/02 *Invited Speaker, ATS International Conference, Atlanta, GA:*
"Targeting antioxidant enzymes to the pulmonary vasculature"

07/10/02 *Invited Speaker, International Symposium "Reactive Oxygen Species", St.Petersburg, Russia,*
"Intracellular delivery of catalase to endothelium"

09/31/02 *University of Cologne, Germany*
"Delivery of therapeutics to the pulmonary vasculature"

10/01/02 *University of Mainz, Germany*

"Targeting endothelial cell adhesion molecules"

10/03/02 *Urbino University, Italy*
"Novel strategies for vascular delivery of anti-thrombotic agents"

12/16/02 *Centocor, Radnor, PA*
"Perspectives for translation of the vascular immunotargeting into the clinical domain"

02/24/03 *Harvard University/MGH, Department of Radiology*
"Targeting of enzymes to surface adhesion molecules"

03/05/03 Invited Speaker, International Symposium of Controlled Release and Advanced Drug Delivery Systems, Salt Lake City, Utah: "Vascular Immunotargeting of Antioxidant Enzymes to Endothelial Cells"

04/04/03 Department of Pharmacogenetics, Pittsburgh University, PA: "Delivery of antioxidants to pulmonary endothelium".

06/24/03 Department of Cardiology, Emory University School of Medicine, Atlanta, GA: "Targeting antioxidant enzymes via cell adhesion molecules"

07/30/03 Department of Pharmaceutical Sciences, University of Nebraska, Omaha: "Molecular design of drug delivery systems for targeting endothelium".

08/10/03 Invited Speaker, 6th World Congress on Inflammation (International Association Inflammation Societies Congress, IAIS), August 2-6th, Vancouver, Canada: "Targeting endothelial cell adhesion molecules"

09/12/03 Keynote Speaker, 4th Annual Colloqium "Cellular and Molecular Biomechanics", University of Virginia, Charlottesville, VA: "New horizons in targeting endothelial cell adhesion molecules"

10/02/03 Cardio-Pulmonary Research Institute, Winthrop University Hospital, SUNY at Stony Brook School of Medicine, Mineola, NY: "Novel strategies for protection against oxidant pulmonary stress".

11/21/03 Department Molecular Cardiology, Cleveland Clinic Foundation, Cleveland, OH: "Drug targeting to endothelial cells"

01/21/04 Invited Discussant, Transatlantic Airway Conference "Gene and Drug Therapies of Airway Diseases", Lucerne, Switzerland

D.4. Graduate Students Training

Mr. Rudy Fuentes, a Graduate Student of the University of Pennsylvania Pharmacology Graduate Group, completed 2003 fall semester rotation training in the Muzykantov's lab. Mr. Fuentes studied effects of biotinylation and conjugation with anti-CAM on biochemical properties of SOD.

Ms. Anu Thomas, a Graduate Student of the Philadelphia University of Science, enlisted for her Ph.D. Thesis experimental studies in Muzykantov's lab since fall semester of 2004. Ms. Thomas studies mechanisms of internalization of anti-CAM conjugates in endothelial cells.

D.5. Special Honors and Recognition by the Scientific Community.

1. Dr. Muzykantov has been invited to the **Gordon Research Conference** "Oxygen Radicals in Biology" (Ventura, CA, February 8-13, 2004) to give a talk: "Targeting antioxidant enzymes to vascular endothelium". Traditionally, talks at GRC (that is regarded as the highest-level scientific forum) are not published in order to permit unlimited sharing of fresh research data with peers.

2. Dr. Muzykantov organized and chaired a Symposium on Targeted Drug Delivery at 6th World Congress on Inflammation (International Association Inflammation Societies Congress, IAIS), August 2-6th, Vancouver, Canada

3. Dr. Muzykantov has been invited as a Keynote Speaker to 4th Annual Colloqium "Cellular and Molecular Biomechanics", University of Virginia, Charlottesville, VA (September 12th, 2003).

E. Conclusions.

We have characterized intracellular traffic, final destination, metabolism and duration of anti-CAM conjugates internalized by endothelial cells.

Further, we found that use of auxiliary drugs, which in a controlled fashion alter intracellular traffic or lysosomal degradation, markedly prolongs duration and activity of internalized anti-CAM conjugates.

We have characterized proposed animal models of acute oxidant pulmonary injury (treatment of mice with anti-TM/GOX or exposure to hyperoxia) using quantitative analysis of several specific (tissue oxidation, leukocyte influx) and general (lung edema, surrogate markers) parameters of lung injury. Use of these measurements will allow accurate and precise characterization of tentative protective effects of anti-CAM targeting of AOE and fibrinolytics.

We also characterized expression of cell adhesion molecules on the luminal surface of pulmonary vascular cells in mice treated with anti-TM/GOX or exposed to hyperoxia, thus documenting yet one more parameter of lung pro-inflammatory changes in the proposed models of human ALI.

We studied role of neutrophils in these animal models of human ALI by blocking interactions of blood leukocytes with these cell adhesion molecules and neutrophils elimination. We found that PMN efflux into the pulmonary vasculature and lung tissue provides only little, if any, augmentation of the injury.

Using a combined treatment of mice with sub-toxic levels of anti-TM/GOX and hyperoxia, we developed a new, reliable and testable model of acute pulmonary oxidant stress, highly relevant to human ALI.

We designed and produced anti-CAM/SOD conjugate of a proper targeting size, enzymatic activity and affinity to endothelial cells, which accumulates in the pulmonary vasculature after intravenous injection in mice.

Using in vitro and in vivo studies of fibrinolysis of plasma clots, we have selected a candidate fibrinolytic agent (Tenektase) that displayed optimal profile for targeting to pulmonary endothelium.

In order to produce monomolecular conjugates of fibrinolytics for surface targeting, we have designed and obtained a high-affinity anti-CAM scFv, which will also provide an ideal basis for subsequent translation into the clinical domain.

The general conclusion is that the achieved research progress: i) corresponds to the SOW and research plan projected for first two years of the grant; ii) indicates the feasibility of the studies projected for years 3 and 4; and, iii) further supports high probability of general success of the proposed project.

G. References. In this section we provide exclusively references to the published studies from our group. Other publications pertinent to this report can be found in the original grant and attached appendix items.

1. S.Muro, R.Wiewrodt, A.Thomas, L.Koniaris, S.Albelda, **V.Muzykantov*** and M.Koval (2003) A novel endocytic pathway induced by clustering endothelial ICAM-1 or PECAM-1. J Cell Sci. 2003 Apr 15;116(Pt 8):1599-1609
2. R.Wiewrodt, A.Thomas, L.Cipelletti, M.Christofidou-Solomidou, D.Weitz, S.I.Feinstein, D.Schaffer, S.M.Albelda, M.Koval and **V.Muzykantov*** (2002) Size-dependent immunotargeting of cargo materials into endothelial cells. *Blood*, 99: 912-922.
3. A.Scherpereel, J.C.Murciano, R.Wiewerodt, S.Kennel, **V.Muzykantov**, M.Christofidou-Solomidou (2002) Glucose oxidase vascular immunotargeting to pulmonary endothelium enhances luminal expression of ICAM-1 and P-selectin in the lung. Abstracts of Experimental Biology 2002 Meeting, New Orleans, LA, April 20-24, 2002 (A.382.13) FASEB J., 2002, 16(4), p A439
4. S. Muro, M.Koval, A.Thomas and **V.Muzykantov** (2002) Affinity carriers targeted ICAM-1: trafficking into endothelial cells. Abstracts of American Thoracic Society International Conference, Atlanta, GA, May 17-22, 2002; Am.J.Resp.Crit.Care Med., 2002; 165 (4):A101
5. J.C.Murciano, S.Muro, L.Koniaris, M.Christofidou-Solomidou, D.Harshaw, S.Albelda, D.Granger, D.Cines and **V.R.Muzykantov*** (2003) ICAM-directed vascular immunotargeting of anti-thrombotic agents to the endothelial luminal surface. *Blood*, 101:3977-1984
6. S.Muro, X.Cui, C.Gajewski, **V.Muzykantov*** and M.Koval (2003) Slow intracellular trafficking of catalase nanoparticles targeted to ICAM-1 protects endothelial cells from oxidative stress. *Am.J.Physiol., Cell Physiol.*, 285(5):C1339-47.
7. V.Shuvaev, T.Dziubla, R.Wiewrodt, and **V.Muzykantov*** (2004) Streptavidin-biotin cross-linking of therapeutic enzymes with carrier antibodies: nanoconjugates for protection against endothelial oxidative stress. In: "*Bioconjugation Strategies*", C.Niemeyer, Ed., Humana Press (in press)
8. S.Muro, **V.Muzykantov*** and J.Murciano (2004) Characterization of endothelial internalization and targeting of antibody-enzyme conjugates in cell cultures and in laboratory animals". In: "*Bioconjugation Strategies*", C.Niemeyer, Ed., Humana Press (in press)
9. S.Muro, M.Koval and **V.Muzykantov*** (2004) Endothelial endocytic pathways: gates for vascular drug delivery. *Current Vascular Pharmacology*, in press

Appendices
Attached are:

1. J.C.Murciano, S.Muro, L.Koniaris, M.Christofidou-Solomidou, D.Harshaw, S.Albelda, D.Granger, D.Cines and **V.R.Muzykantov*** (2003) ICAM-directed vascular immunotargeting of anti-thrombotic agents to the endothelial luminal surface. *Blood*, 101:3977-1984
2. S.Muro, X.Cui, C.Gajewski, **V.Muzykantov*** and M.Koval (2003) Slow intracellular trafficking of catalase nanoparticles targeted to ICAM-1 protects endothelial cells from oxidative stress. *Am.J.Physiol., Cell Physiol.*, 285(5):C1339-47.
3. V.Shuvaev, T.Dziubla, R.Wiewrodt, and **V.Muzykantov*** (2004) Streptavidin-biotin cross-linking of therapeutic enzymes with carrier antibodies: nanoconjugates for protection against endothelial oxidative stress. In: "*Bioconjugation Strategies*", C.Niemeyer, Ed., Humana Press (in press)
4. S.Muro, **V.Muzykantov*** and J.Murciano (2004) Characterization of endothelial internalization and targeting of antibody-enzyme conjugates in cell cultures and in laboratory animals". In: "*Bioconjugation Strategies*", C.Niemeyer, Ed., Humana Press (in press)
5. S.Muro, M.Koval and **V.Muzykantov*** (2004) Endothelial endocytic pathways: gates for vascular drug delivery. *Current Vascular Pharmacology*, in press
6. M.Christofidou, S.Muro, J.Murciano, M.Barry, A.Thomas, V.Shuvaev, S.Albelda, D.Cines and **V.R.Muzykantov** (2003) Targeting endothelial surface adhesion molecules. Abstr. Symposium of Vector Targeting, Cold Spring Harbor, NY, March 20-22, 2003, page 19)
7. M.Christofidou, A.Scherpereel, A.Boyen, E.Arguiri, V.Shuvaev, S.Kennel and **V.Muzykantov** (2003) Hyperoxia potentiates oxidative injury in murine lungs induced by glucose oxidase targeted to thrombomodulin. Abstr., Experimental Biology Meeting, San Diego, CA, April 11-15, 2003; FASEB J., 2003; 17(4) part I, page A247
8. S.Muro, X.Cui, C.Gajewski, M.Koval, **V.Muzykantov** (2003) Pharmacological Modulation of Intracellular Trafficking and Lysosomal Degradation Prolongs the Anti-oxidant Effect of Catalase Conjugates Delivered into Endothelial Cells via ICAM-1. Abstr. 11th Intern.Symp. Recent Advances in Drug Delivery Systems, Salt Lake City, UT, March 3-6, 2003 (#014)
9. M.Christofidou-Solomiudou, B.Kozower, A.Scherpereel, T.Szeitzer,, S.Muro, R.Wiewrodt, V.Shuvaev, A.Thomas, M.Koval, A.Patterson, S.Albelda and **V.Muzykantov**. Targeting of antioxidants to adhesion molecules (2003) Inflammation Research, 52, Suppl.2, p.S81 (Abstracts of 6th World Congress on Inflammation, Vancouver, Canada, August 2-6, 2003)
10. E.Berk, **V.Muzykantov** and S.Muro (2003) Binding and uptake of anti-ICAM-1 coated nanoparticles by flow-adapted endothelial cells. Abstr. 9th Annual Respiration Research Retreat of the University of Pennsylvania, Sugarloaf Conference Center, Philadelphia, OA, June 20, 2003, #9

11. M.Christofidou-Solomidou, A.Scherpereel, A.Bohen, E.Arguiri, V.Shuvaev, S.Kennel, **V.Muzykantov** (2003) Hyperoxia potentiates oxidative injury in murine lungs induced by glucose oxidase targeted to thrombomodulin. *Ibid*, #16
12. S.Muro, C.Gajewsky, M.Koval, **V.Muzykantov** (2003) Slow intracellular degradation of ICAM-1 or PECAM-1 targeted catalase nanoparticles protects endothelial cells from oxidative stress. *Ibid*, #49
13. V.Shuvaev, S.Tliba, T.Dziubla, **V.Muzykantov** (2003) Combined immunoconjugate delivery of CuZnSOD and catalase to human endothelial cells and their protection against oxidative stress. *Ibid*, #55

ICAM-directed vascular immunotargeting of antithrombotic agents to the endothelial luminal surface

Juan-Carlos Murciano, Silvia Muro, Lauren Koniaris, Melpo Christofidou-Solomidou, David W. Harshaw, Steven M. Albelda, D. Neil Granger, Douglas B. Cines, and Vladimir R. Muzykantov

Drug targeting to a highly expressed, noninternalizable determinant up-regulated on the perturbed endothelium may help to manage inflammation and thrombosis. We tested whether inter-cellular adhesion molecule-1 (ICAM-1) targeting is suitable to deliver antithrombotic drugs to the pulmonary vascular lumen. ICAM-1 antibodies bind to the surface of endothelial cells in culture, in perfused lungs, and in vivo. Proinflammatory cytokines enhance anti-ICAM binding to the endothelium without inducing internalization. ^{125}I-labeled anti-ICAM and a reporter enzyme (β-Gal) conjugated to anti-ICAM bind to endothelium and accumulate in the lungs after intravenous administration in rats and mice. Anti-ICAM is seen to localize predominantly on the luminal surface of the pulmonary endothelium by electron microscopy. We studied the pharmacological effect of ICAM-directed targeting of tissue-type plasminogen activator (tPA). Anti-ICAM/tPA, but not control IgG/tPA, conjugate accumulates in the rat lungs, where it exerts plasminogen activator activity and dissolves fibrin microemboli. Therefore, ICAM may serve as a target for drug delivery to endothelium, for example, for pulmonary thromboprophylaxis. Enhanced drug delivery to sites of inflammation and the potential anti-inflammatory effect of blocking ICAM-1 may enhance the benefit of this targeting strategy. (Blood. 2003;101:3977-3984)

Introduction

Thrombosis and inflammation are often intertwined processes that contribute to cardiovascular morbidity and mortality. In many cases, the pulmonary vasculature is the major site of vascular inflammation and thrombosis, and considerable efforts have been expended to develop strategies to target drugs to this site. Yet current methods to manage inflammation-related thrombosis remain suboptimal.[1-3] For example, targeting fibrin and activated platelets promotes the delivery of antithrombotic agents to existing blood clots, for example, in coronary vessels.[4,5] However, targeting components of preformed clots has afforded only modest improvements in experimental models, likely due to limited penetration,[6] and such clot-targeting strategies are unlikely to be useful for thromboprophylaxis.

Targeted delivery of antithrombotic drugs to the vascular lumen, including those involved by inflammation, prior to clot formation may permit thromboprophylaxis in patients with a high propensity for thrombosis. Theoretically, overexpression of certain antithrombotic proteins by vascular endothelial cells themselves would help to achieve this goal.[7-9] However, gene therapies currently are not suitable to manage acute conditions.[10]

Immunotargeting of therapeutic proteins may provide a complementary strategy suitable for more immediate interventions. Antibodies to diverse determinants are being explored as affinity carriers for drug targeting to endothelium.[11-15] A poorly internalizable, high-density, and stably exposed determinant on the endothelial surface, up-regulated and functionally involved in vascular thrombosis and inflammation, would provide an ideal target for antithrombotic proteins. Previous data indirectly suggest that inter-cellular adhesion molecule-1 (ICAM) may provide such a target to deliver anti-inflammatory and, perhaps, antithrombotic agents.[16-20] However, neither the endothelial internalization of ICAM antibodies (anti-ICAM) nor the tissue distribution, localization, activity, and effects of ICAM-targeted therapeutics have been characterized.

In this work we studied ICAM-directed immunotargeting to endothelium in cell cultures, perfused lungs, and animals, and found that (1) anti-ICAM is not internalized efficiently by the endothelium, (2) cytokine up-regulation of ICAM expression augments surface targeting, but not internalization, of anti-ICAM, (3) anti-ICAM can be used to produce either internalizable (100-200 nm diameter) or noninternalizable (approximately 1 μm) conjugates, and (4) ICAM targeting delivers active tPA to the pulmonary vascular lumen and facilitates intravascular fibrinolysis.

Materials and methods

The materials used were $Na^{125}I$ and $Na^{131}I$ from Perkin-Elmer (Boston, MA), iodogen, streptavidin (SA), and 6-biotinylaminocaproic acid N-hydroxysuccinimide ester from Pierce (Rockford, IL), human recombinant tPA from Genentech (San Francisco, CA), β-galactosidase-streptavidin

From the Institute of Environmental Medicine, Department of Pharmacology, Department of Medicine, Department of Pathology and Laboratory Medicine, University of Pennsylvania, Philadelphia, PA; and the Department of Physiology, Louisiana State University, Shreveport, LA.

Submitted September 18, 2002; accepted January 7, 2003. Prepublished online as *Blood* First Edition Paper, January 16, 2003; DOI 10.1182/blood-2002-09-2853.

Supported by NIH SCOR in Acute Lung Injury (NHLBI HL 60290, Project 4, NHLBI RO1 HL/GM 71175-01) and a Department of Defense Grant (PR 012262) to V.R.M., grants HL60169 and R03 TW01468 to D.B.C., a fellowship from the Spanish Ministry of Education and Science (MEC) to J.-C.M., and Fundación Ramón Areces (Spain) (S.M.). M.C.-S. was supported in part by the American Heart Association.

Presented in part as posters at the American Thoracic Society (ATS) Meeting, May 5-10, 2000, Toronto, ON, Canada.

Reprints: Vladimir Muzykantov, Institute for Environmental Medicine, University of Pennsylvania, School of Medicine, 1 John Morgan Building, Philadelphia, PA 19104-6068; e-mail: muzykant@mail.med.upenn.edu.

The publication costs of this article were defrayed in part by page charge payment. Therefore, and solely to indicate this fact, this article is hereby marked "advertisement" in accordance with 18 U.S.C. section 1734.

conjugate (SA-β-Gal) from Sigma (St Louis, MO), chromogenic tPA substrate, Spectrozyme tPA, a kind gift from American Diagnostica (Greenwich, CT), and fluorescein-labeled transferrin or SA from Molecular Probes (Eugene, OR). Monoclonal (IgG) antibodies were mAb R6.5,[21] mAb 1A29,[22] and mAb YN1[23] against human, rat, and murine ICAM-1; mAb 9B9 against human and rat angiotensin-converting enzyme (ACE)[24]; and mAb 1009 and mAb 311 against human and murine thrombomodulin, TM.[11] Antibodies against IgG (fluorescent-labeled or gold-conjugated) were from Jackson Immunoresearch (West Grove, PA) and Amersham (Piscataway, NJ).

Conjugation and size determination

Antibodies, IgG, and tissue-type plasminogen activator (tPA) were biotinylated and radiolabeled using Iodogen without loss of activity, as described.[25] The number of biotin residues per molecule of protein was determined by Immunopure-HABA assay (Pierce) as per manufacturer instructions. Biotinylated tPA or β-Gal was coupled to biotinylated antibodies using streptavidin cross-linking following a 3-step procedure described in detail previously.[25-27] The size of the resulting conjugates was determined by dynamic light scattering, as described.[25-27] The conjugates are designated hereafter as anti-ICAM/β-Gal and IgG/β-Gal or anti-ICAM/tPA and IgG/tPA.

Cell culture experiments

Surface binding and intracellular uptake of ^{125}I-labeled antibodies were measured in cultures of human umbilical vein endothelial cells (HUVECs, from Clonetics) and a human mesothelioma cell line expressing ICAM-1 (REN cells) as described previously for anti–platelet-endothelial cell adhesion molecule (PECAM).[28] Control and tumor necrosis factor α (TNFα)–challenged cells were incubated for 1 hour at either 4°C or 37°C with ^{125}I–anti-ICAM, ^{125}I–anti-ACE, ^{125}I–anti-TM, or ^{125}I–control IgG. After washing, surface-bound antibodies were eluted with glycine, while internalized antibodies were measured in the cell lysates.

Suspended control or TNFα-treated HUVEC and REN cells were incubated with 30 μg/mL anti-ICAM or anti-TM for 1 hour at 4°C, washed, counterstained with fluorescein isothiocyanate (FITC)–labeled goat anti–mouse IgG (30 minutes at 4°C), resuspended in phosphate-buffered saline (PBS), and analyzed by fluorescence-activated cell-sorter scanner (FACS).

Cellular localization of anti-ICAM was visualized using immunofluorescence at magnification × 60 or × 40. TNFα-treated cells were incubated with 10 μg/mL anti-ICAM for 1 hour at either 4°C or 37°C in 1% bovine serum albumin (BSA)–containing medium. After washing and fixation, the surface-associated anti-ICAM was stained with Texas Red–labeled goat anti–mouse IgG. Thereafter, internalized anti-ICAM was counterstained in permeabilized cells using FITC-labeled goat anti–mouse IgG. Fluorescein-labeled transferrin was used as a control for internalizable ligand in parallel wells. In separate experiments, rat pulmonary microvascular endothelial cells (RPMVECs) were incubated with anti-ICAM/SA–Texas Red conjugates of different sizes (100-200 nm or approximately 1 μm) for 1 hour at 37°C. After cell fixation, surface-bound conjugates were counterstained with an FITC-labeled goat anti–mouse IgG.

Experiments in isolated perfused rat lungs (IPL)

Lungs were isolated from anesthetized male 170-200 g Sprague-Dawley rats following protocols approved by the University of Pennsylvania Institutional Animal Care and Use Committee (IACUC) and were ventilated and perfused for 1 hour at 37°C or 4°C with Krebs ringer buffer (KRB)–BSA buffer containing ^{125}I-labeled antibodies (1 μg, unless indicated otherwise), followed by nonrecirculating perfusion with KRB-BSA, as described.[29,30] In separate experiments, 100 μg nonradiolabeled, biotinylated anti-ICAM or anti-ACE was perfused for 1 hour at 37°C. ^{125}I-labeled streptavidin (^{125}I-SA) was added to the perfusate immediately after washing the unbound antibody or after an additional 60 minutes of nonrecycling perfusion to measure surface-accessible b–anti-ICAM.

^{125}I–anti-ICAM biodistribution in rats

Anesthetized rats and mice were killed 1 hour after a tail-vein injection of a mixture of ^{125}I–anti-ICAM and ^{131}I-IgG (10 μg each), and the radioactivity in blood and major organs (washed with saline, blotted dry, and weighed) was measured to calculate the parameters of targeting: percent of injected dose per organ (%ID) or per gram (%ID/g), organ-to-blood ratio (localization ratio, LR), and immunospecificity index (ISI) (see Murciano et al[29] and Danilov et al[31] for details).

Biodistribution and tissue localization of anti-ICAM and anti-ICAM/β-Gal conjugates in animals

The tissue localization of enzymatically active anti-ICAM/β-Gal 1 hour after the tail-vein injection of 100 μg conjugate in BALB/c mice was visualized by histological analysis of X-Gal staining in the tissues, as described previously for anti-PECAM/β-Gal conjugate.[26] In a similar experiment, lungs were processed for electron microscopy and developed using a gold-conjugated secondary antibody, as described.[26]

Characterization of tPA activity in lung tissue

Anti-ICAM/tPA conjugate or control preparations (IgG/tPA and tPA) were perfused in IPL for 1 hour; unbound materials were eliminated by a 5-minute nonrecycling perfusion. In one series, lungs were perfused with 3 μg ^{125}I-labeled tPA conjugated to either anti-ICAM or IgG, and the radioactivity was measured. In the next series, aliquots of lung homogenates obtained after perfusion of 100 μg of unlabeled tPA conjugates were added to ^{125}I-labeled fibrin clots, formed as described previously,[30] and the release of ^{125}Iodine into the supernatant at 37°C was measured. In the next series, 750 μL of a 0.4 mM/L solution of a chromogenic tPA substrate was infused into the lung via the pulmonary artery for 20 minutes, and the optical density at 405 nm in the outflow perfusate was measured. In the last series, a suspension of ^{125}I-labeled fibrin microemboli (^{125}I-ME, 3-10 micron diameter), prepared as described previously,[32] was infused into the common pulmonary artery after perfusion with either anti-ICAM/tPA or IgG/tPA. ^{125}I-ME lodge and degrade slowly in intact isolated perfused rat lungs.[30] The lungs were perfused for 1 hour with buffer containing 20% plasma as a source of plasminogen, and the residual radioactivity in the lungs was measured.

Statistics

A *t* test or a one-way analysis of variance (ANOVA) (SigmaStat 2.0) was used to determine statistically significant differences ($P < .05$) between groups. Post hoc testing was performed with Fisher Least Square difference test. Data are shown as mean ± SEM unless otherwise stated.

Results

Endothelial cells internalize anti-ICAM inefficiently

^{125}I–anti-ICAM, but not control IgG, bound specifically to unstimulated endothelial cells (HUVECs) (Figure 1A). Eighty-five percent of the ^{125}I–anti-ICAM bound to cells at 37°C was eluted by glycine one hour later, compared with 90%-95% bound at 4°C (not shown).

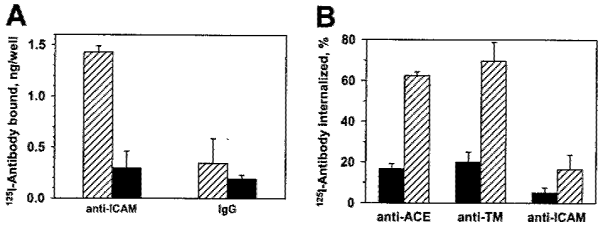

Figure 1. Resting endothelial cells bind but do not internalize ^{125}I–anti-ICAM. (A) HUVECs were incubated with ^{125}I–anti-ICAM or ^{125}I-IgG (1 hour, 37°C), and radioactivity was determined in the surface fraction (glycine elution, ▨) and in the cell lysates (■). (B) Percent of internalization of ^{125}I-labeled antibodies against ACE, TM, and ICAM-1 by HUVECs at either 4°C (■) or 37°C (▨). The data are expressed as means ± SD (n = 3).

Consistent with this, approximately 10% of bound anti-ICAM was internalized by 60 minutes at 37°C versus approximately 60% of ^{125}I–anti-ACE and ^{125}I–anti-TM (Figure 1B). Therefore, resting endothelial cells internalize anti-ICAM inefficiently, leaving approximately 90% of the antibody on the cell surface.

Anti-ICAM uptake in the perfused rat lungs (IPL)

We then asked whether anti-ICAM was handled similarly by intact vascular endothelium under flow. Rat IPLs were perfused with ^{125}I–anti-ICAM or control ^{125}I-IgG in a blood-free buffer. ^{125}I–anti-ICAM bound specifically to the lungs (Figure 2A), reaching saturation at approximately 10 μg per gram of tissue. Scatchard analysis (inset) revealed that rat lungs contain approximately 5×10^{13} anti-ICAM binding sites per gram (approximately 1.5-2.5×10^5 binding sites per endothelial cell).

We then examined the internalization of anti-ICAM and anti-ACE in IPL. Pulmonary uptake of ^{125}I–anti-ACE was markedly lower at 6°C than at 37°C, likely due to inhibition of the energy-dependent uptake of antibody. In contrast, practically the same uptake of ^{125}I–anti-ICAM was seen at 6°C and at 37°C (Figure 2B). This result reflects minor, if any, contribution of an energy-dependent internalization pathway for anti-ICAM in IPL.

The IPL setting permits sequential perfusion of ^{125}I-SA immediately or 1 hour after biotinylated antibodies, to test the accessibility of endothelium-bound antibodies to the circulation. Binding of ^{125}I-SA in the lungs was reduced by 70% when biotinylated anti-ACE was allowed to remain in the vasculature for 1 hour at 37°C, indicating antibody disappearance from the lumen. In contrast, binding of ^{125}I-SA after perfusion of biotinylated anti-ICAM did not diminish with time, indicating that the endothelium-bound anti-ICAM remains accessible from the lumen at 37°C (Figure 2C). Therefore, pulmonary endothelium under flow conditions avidly binds but internalizes anti-ICAM poorly.

TNFα stimulates anti-ICAM binding, but not internalization

TNFα augmented anti-ICAM binding to HUVECs but inhibited anti-TM binding, while REN cells, which do not express thrombomodulin, bound anti-ICAM constitutively at a relatively high level that was augmented further by TNFα (FACS analysis, Figure 3A).

FACS results were confirmed by ^{125}Iodine tracing studies using HUVEC monolayers. TNFα markedly augmented binding of ^{125}I–anti-ICAM but not control ^{125}I-IgG (Figure 3B). However, the intracellular uptake of ^{125}I–anti-ICAM by TNFα-stimulated cells after a 1-hour incubation at 37°C was equivalent in HUVEC

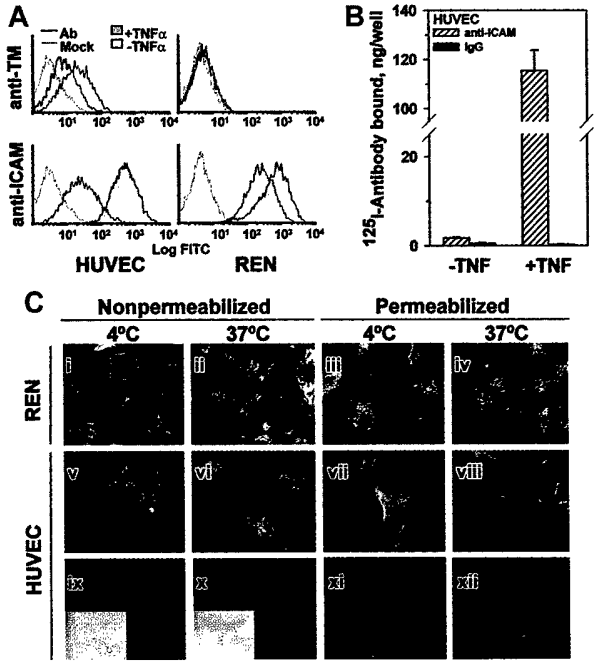

Figure 3. TNFα increases anti-ICAM binding but not internalization by endothelial and mesothelioma cells. (A) FACS analysis using anti-ICAM and anti-TM. TNFα suppresses expression of thrombomodulin (TM, upper panels) by HUVECs and stimulates that of ICAM-1 (lower panels) by HUVEC and REN cells. Dashed line: antibody-free medium; resting (open histogram) or TNFα-challenged (shaded histogram) cells. (B) ^{125}I–anti-ICAM binding to resting and TNFα-treated HUVEC monolayer. The data are shown as means ± SD, n = 4. (C) Fluorescent micrographs (× 60) of TNFα-stimulated cells incubated with anti-ICAM. The cells were incubated at 4°C or 37°C with anti-ICAM (panels i-viii), antibody-free medium (ix, x) or transferrin (xi, xii). After washing and fixation the cells were sequentially stained with Texas Red secondary antibody, permeabilized, and counterstained with FITC-labeled secondary antibody (yellow, surface-bound anti-ICAM; green, internalized anti-ICAM). On the left, the nonpermeabilized cells were stained with both Texas Red and FITC-labeled antibodies (positive control for surface staining, yellow color). Green color corresponds to the intracellular staining (see panels xi and xii showing staining of HUVECs incubated with fluorescein-labeled transferrin). Insets of subpanels ix and x show phase contrast images in controls. Original magnification, × 60; insets minimized to ⅓ of original size.

(11.6% ± 0.7%) and REN cells (10.1% ± 2.7%); background levels at 4°C were 5.1% ± 0.8% and 3.2% ± 0.6%, respectively.

These radiotracer data showing minimal (no more than 10%) internalization of anti-ICAM by cytokine-stimulated cells were confirmed by immunofluorescence microscopy. Figure 3C shows typical images of TNFα-stimulated HUVEC and REN cells

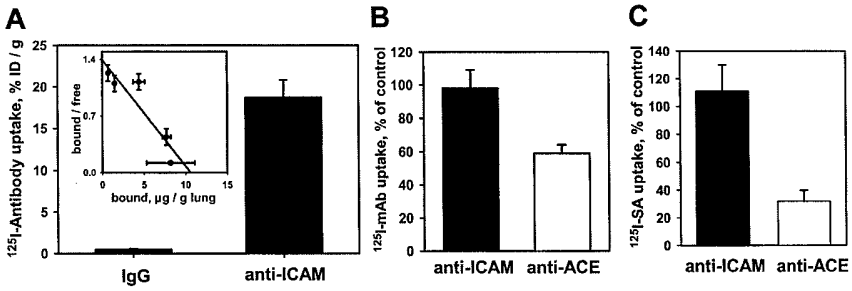

Figure 2. ^{125}I–anti-ICAM accumulates without internalization in the isolated rat lungs. (A) Accumulation of ^{125}I–anti-ICAM or ^{125}I-IgG perfused for 1 hour at 37°C. Inset shows a Scatchard analysis of ^{125}I–anti-ICAM binding. (B) Temperature dependence of anti-ICAM uptake (■) and anti-ACE uptake (□) in the lungs. At 4°C, the pulmonary uptake of ^{125}I–anti-ACE is inhibited, whereas the uptake of ^{125}I–anti-ICAM is not affected (uptake at 4°C is shown as percent of the 100% control value attained at 37°C). (C) Disappearance of anti-ICAM (■) and anti-ACE (□) from the luminal surface in the lungs perfused at 37°C. After accumulation in the lungs, biotin–anti-ICAM, but not biotin–anti-ACE, is accessible to the blood for a prolonged time. ^{125}I-streptavidin (^{125}I-SA) was perfused in the lungs either immediately after biotinylated antibody accumulation or after 60 minutes of additional perfusion at 37°C with antibody-free buffer. Data of ^{125}I-SA uptake after 60 minutes delay are shown as percent of that observed immediately after biotinylated antibody accumulation (100% level). All data are shown as means ± SEM; n = 4.

incubated with anti-ICAM for 1 hour at either 4°C or 37°C and stained before or after permeabilization with Texas Red and FITC-labeled secondary antibody. The staining of intact and permeabilized cells was essentially identical, showing predominantly dual (yellow) labeling of the surface-bound anti-ICAM both at 4°C and 37°C, with no appreciable green staining (representing internalized anti-ICAM). As a control, the intracellular staining of HUVECs incubated with internalizable fluorescein-labeled transferrin was evident at 37°C but not at 4°C (Figure 3Bxi-xii). Therefore, TNFα markedly up-regulates anti-ICAM binding to endothelial and mesothelial cells, but does not augment anti-ICAM internalization.

Biodistribution of radiolabeled anti-ICAM in vivo

^{125}I–anti-ICAM, but not ^{131}I-IgG, accumulated in the lungs after intravenous injection in rats (Figure 4) and in mice (not shown). Significant uptake also was seen in the liver and spleen, but anti-ICAM uptake per gram of tissue was always greatest in the lungs. Pulmonary uptake of anti-ICAM was 20%-30% lower after intra-arterial injection (not shown).

We analyzed the specificity of anti-ICAM targeting to pulmonary tissue. In rats, the pulmonary uptake of ^{125}I–anti-ICAM was approximately 17% ID/g (Figure 4A), an immunospecificity index ($ISI_{\%ID/g}$, ratio of %ID/g of anti-ICAM to that of IgG) of approximately 25, 10-fold higher than that in the liver and spleen (Figure 4B). The blood level of anti-ICAM was lower than that of control IgG, likely due to depletion of the circulating pool. The anti-ICAM pulmonary localization ratio (LR, tissue-to-blood ratio) was approximately 50 (Figure 4C), while the IgG LR was approximately 0.2. Therefore, the pulmonary ISI_{LR} calculated using anti-ICAM and IgG LR, thereby correcting for the blood level, was approximately 250 (Figure 4D).

Effects of proinflammatory challenges on anti-ICAM targeting

Endotoxin facilitated pulmonary uptake of ^{125}I–anti-ICAM, likely due to up-regulation of endothelial ICAM in response to cytokines. In rats, lipopolysaccharide (LPS) caused a 30% increase in the pulmonary uptake of ^{125}I–anti-ICAM (Figure 5), with a concomitant reduction in the blood level (pulmonary LR almost doubled from 50 to 85). In contrast, LPS suppressed pulmonary uptake of ^{125}I–anti-ACE in rats by 50% (pulmonary LR reduced from 14 to 7). Therefore, anti-ICAM targeting in LPS-treated rats was 10 times more robust than that of anti-ACE (LR 85 vs 7). Pulmonary targeting of ^{125}I–anti-ICAM was stably enhanced at 5 and 24 hours after LPS injection (LR 77 and 85). A similar elevation of

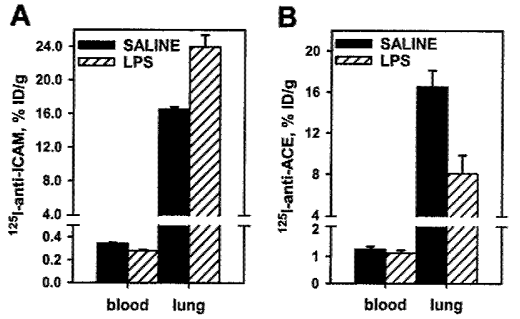

Figure 5. Endotoxin enhances ^{125}I–anti-ICAM pulmonary targeting. ^{125}I–anti-ICAM (left panel) or ^{125}I–anti-ACE (right panel) was injected in control rats (black bars) or after intraperitoneal injection of LPS (hatched bars). Lung and blood level of ^{125}I was determined 1 hour later. Data are presented as means ± SEM, n = 4.

^{125}I–anti-ICAM pulmonary targeting was seen in LPS-treated mice (not shown). The ^{125}I–anti-ICAM pulmonary uptake was doubled in mice exposed to 98% O_2 atmosphere, in contrast with a 50% decrease in the ^{125}I–anti-TM uptake (not shown). Therefore, proinflammatory factors suppress anti-ACE and anti-TM but augment anti-ICAM targeting.

Visualization of ICAM-directed vascular immunotargeting in animals

We visualized the pulmonary localization of anti-ICAM in mice by electron microscopy. Specific binding of the secondary gold-labeled antibody was evident in lungs harvested 4 hours after anti-ICAM injection (Figure 6A). Semiquantitative analysis after anti-ICAM injection revealed 16 ± 3 endothelium-associated particles/field versus 3 ± 1 particles/field associated with alveolar epithelium and interstitium (M ± SEM, 10 fields). Anti-ICAM was primarily localized along the luminal surface of the endothelium (arrows in Figure 6Ai). Noteworthy, we did not see endocytic vacuoles containing gold particles, the hallmark of endothelial uptake of internalizable conjugates in the lungs.[26]

To test whether anti-ICAM delivers an active enzyme cargo to endothelium, we conjugated a reporter enzyme, β-galactosidase, with anti-ICAM or control IgG. Figure 6B shows the results of X-Gal staining of the organs 1 hour after injection of either anti-ICAM/β-Gal or IgG/β-Gal conjugate in mice. After IgG/β-Gal injection (Figure 6Bv-viii), β-Gal activity was seen in the peripheral zone of the splenic follicles, the known site of Fc-receptor mediated uptake of immunoconjugates.[26,33] The splenic follicles also were stained by anti-ICAM/β-Gal (Figure 6Bi), as

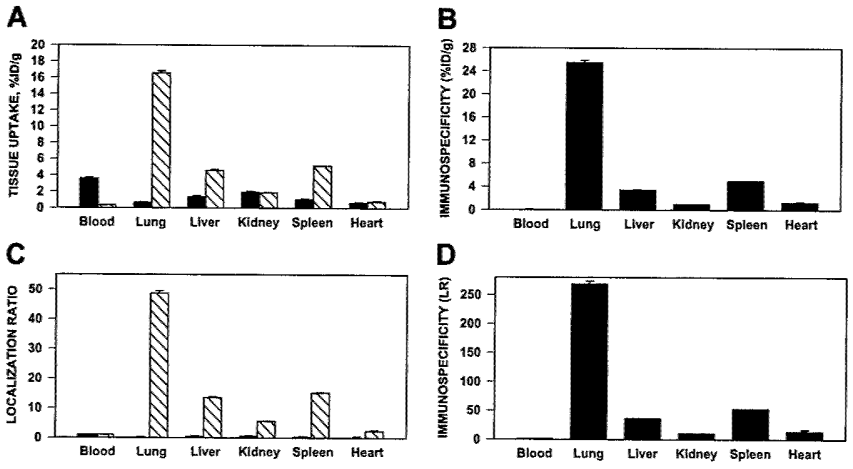

Figure 4. Pulmonary targeting of ^{125}I–anti-ICAM in rats. Biodistribution of ^{125}I–anti-ICAM (▨) or ^{131}I-IgG (■) 1 hour after intravenous injection in anesthetized rats. The data are shown as means ± SEM, n = 4. (A) Absolute values of the uptake in organs expressed as percent of injected dose per gram. (B) Immunospecificity index ($ISI_{\%ID/g}$), calculated as ratio of anti-ICAM to IgG %ID/g. (C) Localization ratio (LR) calculated as ratio of %ID/g in an organ to that in blood. (D) ISI_{LR} calculated as ratio of anti-ICAM LR to IgG LR.

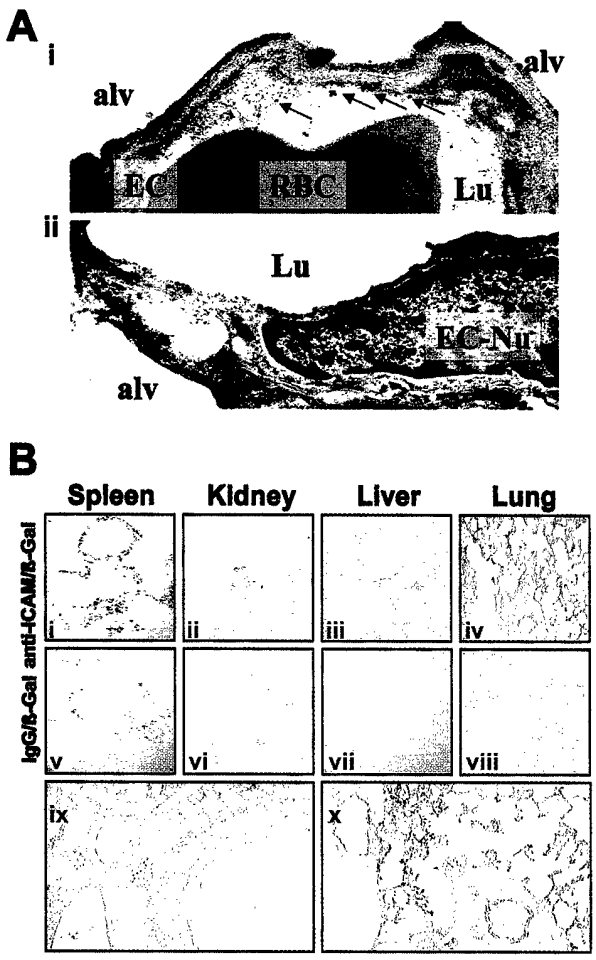

Figure 6. Localization of anti-ICAM and anti-ICAM/β-Gal in the pulmonary vasculature after injection in mice. (A) Immunogold electron microscopy of the lungs harvested 4 hours after intravenous injection of 100 μg anti-ICAM (i) or control IgG (ii). Arrows show endothelium-associated gold particles. RBC indicates red blood cells in a capillary lumen; Lu, vascular lumen; Alv, alveolar compartment; EC, endothelial cell; EC-Nu, endothelial cell nucleus. (B) Targeting of an active β-Gal conjugate was visualized 1 hour after injection in mice, using standard X-Gal chromogenic substrate staining protocol. Distribution of anti-ICAM/β-Gal (panels i-iv) and control IgG/β-Gal (panels v-viii). Detailed view of anti-ICAM/β-Gal in the lungs (panels ix and x). Original magnifications: Ai, × 70 000; Aii, × 60 000; Bi-Bviii, × 10; Bix-Bx, × 20.

were the renal glomeruli (Figure 6Bii), the known site of β-Gal elimination.[26,33]

However, injection of anti-ICAM/β-Gal, but not IgG/β-Gal, delivered β-Gal activity to the lungs (compare Figure 6Biv with Figure 6Bviii). Anti-ICAM/β-Gal was concentrated in the alveolar capillaries and in the lumen of larger vessels; no β-Gal activity was seen in subendothelial layers of blood vessels, interstitium, or airways (Figure 6Bix-x).

Effect of anti-ICAM conjugate size on endothelial internalization

Streptavidin was cross-linked to biotinylated anti-ICAM and biotinylated tPA at varying molar ratios of reactants, as previously studied with other proteins.[25-27] Analysis using dynamic light scattering analysis showed that conjugates ranging in size from 100 nm to several microns were generated, depending on the molar ratio between SA and biotinylated anti-ICAM (Figure 7A). Double staining of fluorescent-labeled anti-ICAM conjugates revealed that rat microvascular endothelial cells internalized those anti-ICAM conjugates having a diameter of 100-200 nm but did not internalize large conjugates around 1 μm (Figure 7B). In fact, after a 1-hour incubation at 37°C, the large, 1-2 micron double-labeled anti-ICAM conjugates (the preparation that corresponds to the peak farthest to the right in Figure 7A) decorated the entire cell surface (Figure 7C). Control IgG conjugates did not bind to endothelium irrespective of size and did not accumulate in the isolated rat lungs (not shown).

ICAM-directed targeting of tPA to the pulmonary vasculature

We then tested whether anti-ICAM would target an antithrombotic drug to sites of inflammation susceptible to thrombosis. To do so, we prepared large (approximately 1 μm), poorly internalizable anti-ICAM/^{125}I-tPA and IgG/^{125}I-tPA conjugates. One hour after intravenous injection, 7% of the injected anti-ICAM/^{125}I-tPA had accumulated in the rat lungs, compared with less than 0.3% for IgG/^{125}I-tPA (Figure 8A), a pulmonary $ISI_{\%ID/g}$ of 25 (Figure 8B). The blood level of anti-ICAM/^{125}I-tPA showed a corresponding decrease compared to IgG/^{125}I-tPA. Therefore, the pulmonary LR of anti-ICAM/^{125}I-tPA exceeded 20 (Figure 8C), with a calculated ISI_{LR} of approximately 80 (Figure 8D). Anti-ICAM/^{125}I-tPA was retained in the lungs for at least several hours after injection (not shown). Similar results were obtained in mice (not shown).

Anti-ICAM/tPA bound to the pulmonary endothelium surface retains plasminogen activity and dissolves intravascular clots

To test whether anti-ICAM can be used to deliver enzymatically active tPA to the endothelial lumen, we perfused anti-ICAM/tPA or

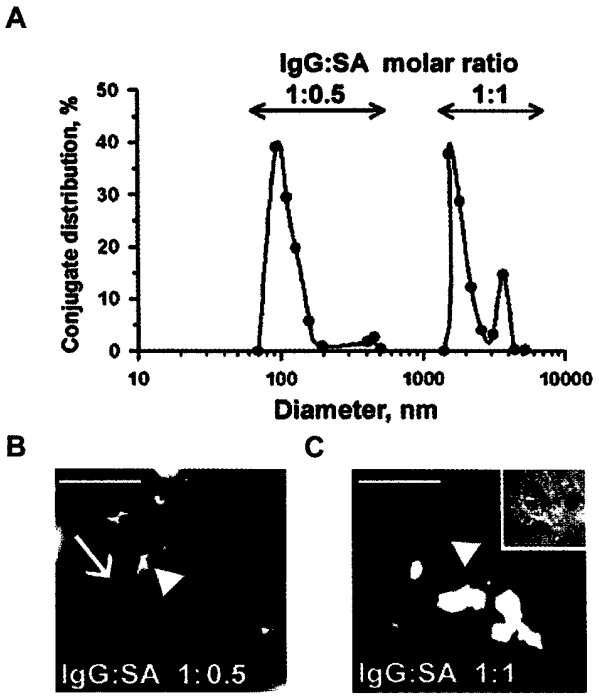

Figure 7. Size of anti-ICAM conjugates modifies their uptake by endothelial cells. (A) DLS analysis of size distribution of the conjugates prepared at molar ratio between biotinylated anti-ICAM and streptavidin of 1:0.5 (left peak) or 1:1 (right peak). (B-C) RPMVECs were incubated for 1 hour at 37°C with anti-ICAM conjugates containing rhodamine-labeled streptavidin with mean diameters of 100-200 nm (panel B) or larger than 1 μm (panel C). The surface-bound fraction of the conjugate was double-labeled using an FITC-labeled secondary antibody. Red color (arrows) denotes internalized conjugates; yellow color (arrowheads) denotes the noninternalizable, larger conjugates. White bars in panels B and C correspond to 5 μm size. Panel C inset shows the contrast phase micrograph (× 40) minimized to ⅛ the original size.

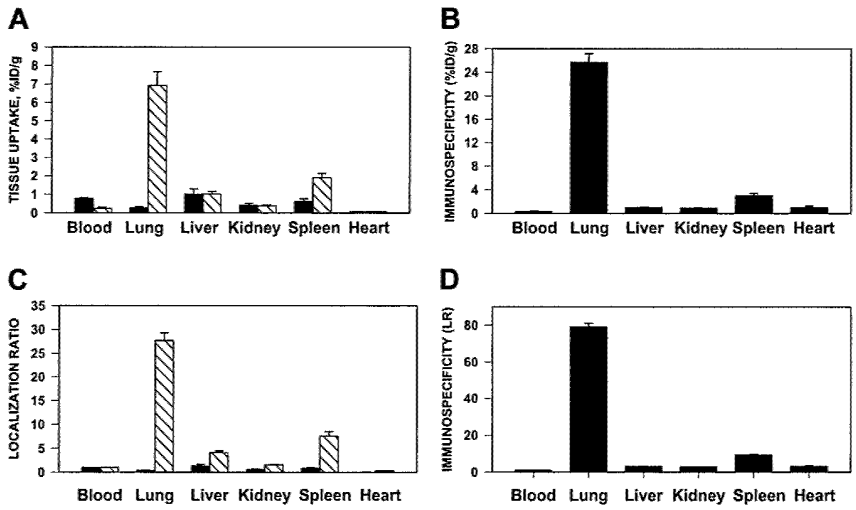

Figure 8. Pulmonary targeting of ^{125}I-tPA conjugated with anti-ICAM in rats. Biodistribution of ^{125}I-tPA conjugated to anti-ICAM IgG (▨) or control IgG (■) 1 hour after intravenous injection in anesthetized rats. The data are shown as means ± SEM, n = 4. (A) Absolute values of the uptake in organs expressed as percent of injected dose per gram. (B) Immunospecificity index ($ISI_{\%ID/g}$), calculated as ratio of anti-ICAM to IgG %ID/g. (C) Localization ratio (LR) calculated as ratio of %ID/g in an organ to that in blood. (D) ISI_{LR} calculated as ratio of anti-ICAM LR to IgG LR.

IgG/tPA in IPL. In all experiments, the vasculature was washed free of unbound conjugates prior to measuring tPA uptake and activity. Anti-ICAM but not the control IgG carriage led to pulmonary accumulation of ^{125}I-tPA (Figure 9A).

Aliquots of lung homogenates obtained after perfusion of anti-ICAM/tPA or IgG/tPA were then incubated with ^{125}I-fibrin clots at 37°C in vitro. Homogenates of lungs perfused with anti-ICAM/tPA caused 10-fold more fibrinolysis, measured by release of ^{125}I, than lungs perfused with IgG/tPA (Figure 9B).

We then infused a chromogenic tPA substrate into IPL. Enzymatic conversion of the substrate leading to appearance of a colored product was detected in the perfusate outflow of lungs preperfused with anti-ICAM/tPA but not those preperfused with IgG/tPA (Figure 9C). Therefore, the anti-ICAM/tPA associated with the luminal surface of the pulmonary endothelium retains its enzymatic activity.

Accessibility to a small synthetic substrate (mol wt < 500 D) does not prove that the anti-ICAM/tPA is accessible to convert its protein substrate, plasminogen. To examine this issue, a suspension of ^{125}I-microemboli was infused into the pulmonary artery 1 hour after perfusion with either anti-ICAM/tPA or IgG/tPA. The radioactivity in the lungs was determined 1 hour later as a measure of residual unlysed fibrin clots. Lungs preperfused with anti-ICAM/tPA practically completely dissolved the radiolabeled fibrin clots, whereas fibrinolysis in the lungs perfused with IgG/tPA did not differ significantly from the basal level measured in control lungs (Figure 9D). Therefore, anti-ICAM/tPA accumulates in the lungs, resides in enzymatically active form on the luminal endothelial surface, and thereby markedly facilitates fibrinolysis in the pulmonary vasculature.

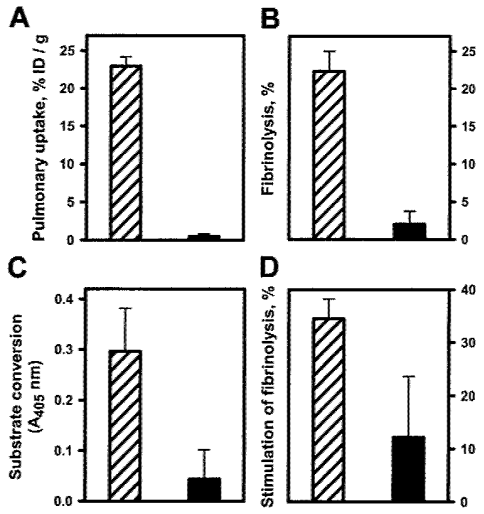

Figure 9. Anti-ICAM/tPA accumulated in pulmonary vasculature facilitates fibrinolysis. Isolated rat lungs were perfused with anti-ICAM/tPA (▨) or IgG/tPA (■) for 30 minutes at 37°C and washed free of unbound conjugates (5 minutes of noncirculating perfusion with a buffer). (A) Pulmonary uptake of ^{125}I-tPA conjugated to either anti-ICAM or control IgG. (B) Fibrinolysis of fibrin clots by aliquots of lung homogenates obtained after perfusion. (C) Conversion of chromogenic tPA substrate perfused after the conjugates. (D) Dissolution of radiolabeled fibrin emboli lodged in the pulmonary vasculature after perfusion of the conjugates. The data are shown as means ± SEM, n = 4.

Discussion

Drug targeting and concurrent blocking of a noninternalized highly expressed pro-inflammatory determinant expressed on the endothelial lumen that is stably up-regulated in the perturbed vasculature may provide a specific and powerful approach for treatment and prophylaxis of vascular inflammation and thrombosis. Our data indicate that ICAM-1 (CD54) fulfills the criteria of an "ideal" target for this specific goal and that anti-ICAM may be used for vascular immunotargeting of antithrombotic drugs.

Static human endothelial cells cultured under sterile conditions constitutively express relatively modest levels of ICAM-1 (Figure 1). However, the level of expression is much higher in vivo,[34] and anti-ICAM binds to the resting endothelium in intact animals.[20,34] Diverse cell types express ICAM-1, but the largest fraction directly accessible to the bloodstream is exposed on the endothelial surface.[34] This fact explains anti-ICAM targeting in vascularized organs (Figures 2 and 4) and confinement of the targeted cargoes to the vascular lumen (Figures 2, 6, and 9).

The pulmonary vasculature is the first major capillary network encountered by intravenously injected antibodies, contains roughly one-third of the endothelium in the body, is exposed to the entire cardiac output of venous blood, and, therefore, comprises the preferred target for affinity carriers recognizing pan-endothelial determinants.[28,31] Importantly, pulmonary uptake of anti-ICAM and anti-ICAM conjugates is not due to a nonspecific binding or mechanical retention in the vasculature, as control IgG counterparts neither bound to HUVECs nor accumulated in the lungs. In fact, the immunospecificity of the anti-ICAM and anti-ICAM/tPA conjugate pulmonary accumulation in normal rats approaches

values of 250 and 50, respectively (Figures 4 and 8). Analysis of the quantitative binding data obtained in rat lungs (Figure 2) indicates that binding of approximately 5-50 mg anti-ICAM can be expected in the human pulmonary vasculature. Thus, anti-ICAM carriers are likely to provide robust and preferential targeting to the pulmonary endothelium in intact animals, matching the characteristics of the best candidate carriers tested to date, including antibodies directed against PECAM, ACE, and a caveoli-associated antigen gp90.[15,24,28,31,33]

Certain pathological conditions suppress targeting to other constitutive endothelial determinants, such as thrombomodulin and ACE.[18,35,36] For example, endotoxin inhibits anti-ACE targeting in rats by 50% (Figure 5). In contrast, cytokines, oxidants, abnormal shear stress, and thrombin[37] are all known to enhance endothelial ICAM-1 expression[34,38] and augment anti-ICAM vascular targeting in vivo.[16,20] Up-regulation of endothelial ICAM-1 expression by thrombin[37] also makes it a preferred candidate for delivering antithrombotic agents. Our data extend these observations and reveal that (1) cytokine stimulation does not augment anti-ICAM internalization (Figure 3) and (2) pulmonary targeting of anti-ICAM is stably augmented in models of proinflammatory challenge in vivo (eg, Figure 5). This feature distinguishes targeting ICAM from targeting selectins, which are only transiently exposed on the perturbed endothelium.[39]

Antibodies and conjugates may unintentionally suppress important functions of endothelial proteins with potentially deleterious consequences (eg, thrombosis), making them less suitable for the therapeutic targeting.[40] ICAM-1, a counter-receptor for leukocyte integrins, supports cell adhesion on endothelium.[34,41] Because anti-ICAM suppresses inflammation by blocking leukocyte adhesion,[34,38,41-44] drug targeting to endothelial ICAM-1 is unlikely to have unintended deleterious effects on the host and, indeed, may provide secondary therapeutic benefits against inflammation, thrombosis, and oxidative stress. This feature of anti-ICAM conjugates deserves additional investigation.

Published studies on anti-ICAM internalization have yielded inconsistent results: epithelial and blood cells have been reported to internalize ICAM ligands in vitro,[45,46] but fragmentary data in other cell types showed the opposite outcome.[47,48] Our studies in cell culture, perfused rat lungs, and in animals show that endothelial cells internalize ICAM antibodies poorly (Figures 1, 2, 3, and 6). Thus, ICAM seems to be well suited for drug targeting to the luminal surface. This feature distinguishes ICAM from other similarly prevalent endothelial determinants, all of which are rapidly internalized, including thrombomodulin and ACE (Figures 1 and 2), selectins,[47-50] and caveoli-associated antigens.[15] A monoclonal antibody against gp85 antigen accumulates in the rat lungs and is not internalized and therefore can be used for surface targeting in this species,[29] but the identity, function, and regulation of its human counterpart are not known.

The uptake of anti-ICAM conjugates is modified by their size: endothelium internalizes conjugates with a mean diameter of 100-200 nm, but not anti-ICAM conjugates larger than 1 μm (Figure 7). This result indicates that anti-ICAM follows the paradigm observed previously with antibodies directed against another noninternalizable determinant, PECAM-1.[26-28] Conjugate size can be readily and stably modulated by varying the molar ratios of the reactants, as measured by dynamic light scattering (Figure 7). In theory, therefore, anti-ICAM represents a carrier that can be modified to facilitate drug delivery to either the endothelial surface (using monomolecular conjugates or conjugates larger than 500 nm) or to the intracellular compartment (using 100-300 nm conjugates). The anti-ICAM/tPA conjugates used in the present study were around 1 μm in size, which exceeds the effective internalizable size. Clearly, anti-ICAM/tPA bound along the cell surface retains enzymatic activity in the pulmonary vascular lumen and augments intravascular fibrinolysis (Figure 9).

This result serves as a proof-of-principle that ICAM represents a suitable target to deliver antithrombotic agents to the endothelial lumen. Although anti-ICAM/tPA conjugate itself may represent a useful agent, we anticipate that the strategy can be further optimized by generation of a monomolecular noninternalizable anti-ICAM/tPA fusion protein.

To our knowledge this is the first study showing that fibrinolytic agents can be used in a prophylactic mode to protect vital vascular beds, including those in the lungs. Patients are at high risk to develop pulmonary emboli after trauma: (1) when extensive proximal deep venous thrombi are present; (2) after recent pulmonary emboli; (3) in the setting serious respiratory compromise due to diverse cardiopulmonary disease; or (4) when the risk of bleeding after systemic anticoagulation is prohibitive.[1,2] Our data suggest that targeted delivery of antithrombotic agents to the pulmonary endothelium itself may be a suitable alternative in some of these settings, although additional studies will be needed to establish the duration and extent of fibrinolytic activity that is delivered.

In summary, ICAM possesses a number of highly desirable characteristics as a target for antithrombotic and anti-inflammatory drug delivery. Anti-ICAM targeting may allow a spectrum of novel therapeutic approaches, for example, a strategy to facilitate the antithrombotic potential of the pulmonary vasculature in patients at high risk to develop acute lung injury (ALI/ARDS) and thromboembolism. Future studies in larger animals will define potential therapeutic applicability and limitations of this strategy.

Acknowledgments

The authors appreciate the gift of anti-ACE from Dr S. Danilov (University of Illinois in Chicago) and anti-TM from Drs C. Esmon (Oklahoma Medial Research Foundation) and S. Kennel (National Oakridge Laboratory).

References

1. Bergqvist D, Agnelli G, Cohen AT, et al. Duration of prophylaxis against venous thromboembolism with enoxaparin after surgery for cancer. N Engl J Med. 2002;346:975-980.
2. Decousus H, Leizorovicz A, Parent F, et al. A clinical trial of vena caval filters in the prevention of pulmonary embolism in patients with proximal deep-vein thrombosis: Prevention du Risque d'Embolie Pulmonaire par Interruption Cave Study Group. N Engl J Med. 1998;338:409-415.
3. Lang IM, Marsh JJ, Olman MA, Moser KM, Loskutoff DJ, Schleef RR. Expression of type 1 plasminogen activator inhibitor in chronic pulmonary thromboemboli. Circulation. 1994;89:2715-2721.
4. Holvoet P, Dewerchin M, Stassen JM, et al. Thrombolytic profiles of clot-targeted plasminogen activators: parameters determining potency and initial and maximal rates. Circulation. 1993; 87:1007-1016.
5. Runge MS, Harker LA, Bode C, et al. Enhanced thrombolytic and antithrombotic potency of a fibrin-targeted plasminogen activator in baboons. Circulation. 1996;94:1412-1422.
6. Sakharov DV, Rijken DC. Superficial accumulation of plasminogen during plasma clot lysis. Circulation. 1995;92:1883-1890.
7. Muller DW, Gordon D, San H, et al. Catheter-mediated pulmonary vascular gene transfer and expression. Circ Res. 1994;75:1039-1049.
8. Dichek DA, Anderson J, Kelly AB, Hanson SR, Harker LA. Enhanced in vivo antithrombotic effects of endothelial cells expressing recombinant

plasminogen activators transduced with retroviral vectors. Circulation. 1996;93:301-309.

9. Waugh JM, Kattash M, Li J, et al. Gene therapy to promote thromboresistance: local overexpression of tissue plasminogen activator to prevent arterial thrombosis in an in vivo rabbit model. Proc Natl Acad Sci U S A. 1999;96:1065-1070.
10. Carmeliet P, Stassen JM, Van Vlaenderen I, Meidell RS, Collen D, Gerard RD. Adenovirus-mediated transfer of tissue-type plasminogen activator augments thrombolysis in tissue-type plasminogen activator-deficient and plasminogen activator inhibitor-1-overexpressing mice. Blood. 1997;90: 1527-1534.
11. Kennel SJ, Lee R, Bultman S, Kabalka G. Rat monoclonal antibody distribution in mice: an epitope inside the lung vascular space mediates very efficient localization. Int J Rad Appl Instrum B. 1990;17:193-200.
12. Keelan ET, Harrison AA, Chapman PT, Binns RM, Peters AM, Haskard DO. Imaging vascular endothelial activation: an approach using radiolabeled monoclonal antibodies against the endothelial cell adhesion molecule E-selectin. J Nucl Med. 1994;35:276-281.
13. Harari OA, Wickham TJ, Stocker CJ, et al. Targeting an adenoviral gene vector to cytokine-activated vascular endothelium via E-selectin. Gene Ther. 1999;6:801-807.
14. Lindner JR, Song J, Christiansen J, Klibanov AL, Xu F, Ley K. Ultrasound assessment of inflammation and renal tissue injury with microbubbles targeted to P-selectin. Circulation. 2001;104:2107-2112.
15. McIntosh DP, Tan XY, Oh P, Schnitzer JE. Targeting endothelium and its dynamic caveolae for tissue-specific transcytosis in vivo: a pathway to overcome cell barriers to drug and gene delivery. Proc Natl Acad Sci U S A. 2002;99:1996-2001.
16. Panes J, Perry MA, Anderson DC, et al. Regional differences in constitutive and induced ICAM-1 expression in vivo. Am J Physiol. 1995;269: H1955-H1964.
17. Bloemen PG, Henricks PA, van Bloois L, et al. Adhesion molecules: a new target for immunoliposome-mediated drug delivery. FEBS Lett. 1995;357:140-144.
18. Atochina EN, Balyasnikova IV, Danilov SM, Granger DN, Fisher AB, Muzykantov VR. Immunotargeting of catalase to ACE or ICAM-1 protects perfused rat lungs against oxidative stress. Am J Physiol. 1998;275:L806-L817.
19. Weiner RE, Sasso DE, Gionfriddo MA, et al. Early detection of bleomycin-induced lung injury in rat using indium-111-labeled antibody directed against intercellular adhesion molecule-1 [published erratum appears in J Nucl Med. 1998;39: 869]. J Nucl Med. 1998;39:723-728.
20. Villanueva FS, Jankowski RJ, Klibanov S, et al. Microbubbles targeted to intercellular adhesion molecule-1 bind to activated coronary artery endothelial cells. Circulation. 1998;98:1-5.
21. Marlin SD, Springer TA. Purified intercellular adhesion molecule-1 (ICAM-1) is a ligand for lymphocyte function-associated antigen 1 (LFA-1). Cell. 1987;51:813-819.
22. Christensen PJ, Kim S, Simon RH, Toews GB, Paine R. Differentiation-related expression of ICAM-1 by rat alveolar epithelial cells. Am J Resp Cell Mol Biol. 1993;8:9-15.
23. Jevnikar AM, Wuthrich RP, Takei F, et al. Differing regulation and function of ICAM-1 and class II antigens on renal tubular cells. Kidney Int. 1990; 38:417-425.
24. Danilov SM, Muzykantov VR, Martynov AV, et al. Lung is the target organ for a monoclonal antibody to angiotensin-converting enzyme. Lab Invest. 1991;64:118-124.
25. Muzykantov VR, Barnathan ES, Atochina EN, Kuo A, Danilov SM, Fisher AB. Targeting of antibody-conjugated plasminogen activators to the pulmonary vasculature. J Pharmacol Exp Ther. 1996;279:1026-1034.
26. Scherpereel A, Wiewrodt R, Christofidou-Solomidou M, et al. Cell-selective intracellular delivery of a foreign enzyme to endothelium in vivo using vascular immunotargeting. FASEB J. 2001;15: 416-426.
27. Wiewrodt R, Thomas AP, Cipelletti L, et al. Size-dependent intracellular immunotargeting of therapeutic cargoes into endothelial cells. Blood. 2002; 99:912-922.
28. Muzykantov VR, Christofidou-Solomidou M, Balyasnikova I, et al. Streptavidin facilitates internalization and pulmonary targeting of an anti-endothelial cell antibody (platelet-endothelial cell adhesion molecule 1): a strategy for vascular immunotargeting of drugs. Proc Natl Acad Sci U S A. 1999;96:2379-2384.
29. Murciano JC, Harshaw DW, Ghitescu L, Danilov SM, Muzykantov VR. Vascular immunotargeting to endothelial surface in a specific macrodomain in alveolar capillaries. Am J Resp Crit Care Med. 2001;164:1295-1302.
30. Murciano JC, Harshaw D, Neschis DG, et al. Platelets inhibit the lysis of pulmonary microemboli. Am J Physiol Lung Cell Mol Physiol. 2002; 282:L529-L539.
31. Danilov SM, Gavrilyuk VD, Franke FE, et al. Lung uptake of antibodies to endothelial antigens: key determinants of vascular immunotargeting. Am J Physiol Lung Cell Mol Physiol. 2001;280:L1335-L1347.
32. Bdeir K, Murciano JC, Tomaszewski J, et al. Urokinase mediates fibrinolysis in the pulmonary microvasculature. Blood. 2000;96:1820-1826.
33. Scherpereel A, Rome JJ, Wiewrodt R, et al. Platelet-endothelial cell adhesion molecule-1-directed immunotargeting to cardiopulmonary vasculature. J Pharmacol Exp Ther. 2002;300: 777-786.
34. Dustin ML, Rothlein R, Bhan AK, Dinarello CA, Springer TA. Induction by IL 1 and interferon-gamma: tissue distribution, biochemistry, and function of a natural adherence molecule (ICAM-1). J Immunol. 1986;137:245-254.
35. Atochina EN, Hiemisch HH, Muzykantov VR, Danilov SM. Systemic administration of platelet-activating factor in rat reduces specific pulmonary uptake of circulating monoclonal antibody to angiotensin-converting enzyme. Lung. 1992;170: 349-358.
36. Moore KL, Esmon CT, Esmon NL. Tumor necrosis factor leads to the internalization and degradation of thrombomodulin from the surface of bovine aortic endothelial cells in culture. Blood. 1989;73:159-165.
37. Kaplanski G, Marin V, Fabrigoule M, et al. Thrombin-activated human endothelial cells support monocyte adhesion in vitro following expression of intercellular adhesion molecule-1 (ICAM-1; CD54) and vascular cell adhesion molecule-1 (VCAM-1; CD106). Blood. 1998;92:1259-1267.
38. Kumasaka T, Quinlan WM, Doyle NA, et al. Role of the intercellular adhesion molecule-1(ICAM-1) in endotoxin-induced pneumonia evaluated using ICAM-1 antisense oligonucleotides, anti-ICAM-1 monoclonal antibodies, and ICAM-1 mutant mice. J Clin Invest. 1996;97:2362-2369.
39. Fries JW, Williams AJ, Atkins RC, Newman W, Lipscomb MF, Collins T. Expression of VCAM-1 and E-selectin in an in vivo model of endothelial activation. Am J Pathol. 1993;143:725-737.
40. Christofidou-Solomidou M, Kennel S, Scherpereel A, et al. Vascular immunotargeting of glucose oxidase to the endothelial antigens induces distinct forms of oxidant acute lung injury: targeting to thrombomodulin, but not to PECAM-1, causes pulmonary thrombosis and neutrophil transmigration. Am J Pathol. 2002;160:1155-1169.
41. Diamond MS, Staunton DE, de Fougerolles AR, et al. ICAM-1 (CD54): a counter-receptor for Mac-1 (CD11b/CD18). J Cell Biol. 1990;111: 3129-3139.
42. DeMeester SR, Molinari MA, Shiraishi T, et al. Attenuation of rat lung isograft reperfusion injury with a combination of anti-ICAM-1 and anti-beta2 integrin monoclonal antibodies. Transplantation. 1996;62:1477-1485.
43. Broide DH, Humber D, Sullivan S, Sriramarao P. Inhibition of eosinophil rolling and recruitment in P-selectin- and intracellular adhesion molecule-1-deficient mice. Blood. 1998;91:2847-2856.
44. Broide DH, Sullivan S, Gifford T, Sriramarao P. Inhibition of pulmonary eosinophilia in P-selectin- and ICAM-1-deficient mice. Am J Respir Cell Mol Biol. 1998;18:218-225.
45. Mastrobattista E, Storm G, van Bloois L, et al. Cellular uptake of liposomes targeted to intercellular adhesion molecule-1 (ICAM-1) on bronchial epithelial cells. Biochim Biophys Acta. 1999;1419: 353-363.
46. Gursoy RN, Siahaan TJ. Binding and internalization of an ICAM-1 peptide by the surface receptors of T cells. J Pept Res. 1999;53:414-421.
47. Almenar-Queralt A, Duperray A, Miles LA, Felez J, Altieri DC. Apical topography and modulation of ICAM-1 expression on activated endothelium. Am J Pathol. 1995;147:1278-1288.
48. von Asmuth EJ, Smeets EF, Ginsel LA, Onderwater JJ, Leeuwenberg JF, Buurman WA. Evidence for endocytosis of E-selectin in human endothelial cells. Eur J Immunol. 1992;22:2519-2526.
49. Kuijpers TW, Raleigh M, Kavanagh T, et al. Cytokine-activated endothelial cells internalize E-selectin into a lysosomal compartment of vesiculotubular shape: a tubulin-driven process. J Immunol. 1994;152:5060-5069.
50. Spragg DD, Alford DR, Greferath R, et al. Immunotargeting of liposomes to activated vascular endothelial cells: a strategy for site-selective delivery in the cardiovascular system. Proc Natl Acad Sci U S A. 1997;94:8795-8800.

Am J Physiol Cell Physiol 285: C1339–C1347, 2003.
First published July 23, 2003; 10.1152/ajpcell.00099.2003.

Slow intracellular trafficking of catalase nanoparticles targeted to ICAM-1 protects endothelial cells from oxidative stress

Silvia Muro,[1] Xiumin Cui,[1] Christine Gajewski,[1] Juan-Carlos Murciano,[1,2] Vladimir R. Muzykantov,[1,2] and Michael Koval[1,3]

[1]*Institute for Environmental Medicine and Departments of* [2]*Pharmacology and* [3]*Physiology, University of Pennsylvania School of Medicine, Philadelphia, Pennsylvania 19104*

Submitted 14 March 2003; accepted in final form 14 July 2003

Muro, Silvia, Xiumin Cui, Christine Gajewski, Juan-Carlos Murciano, Vladimir R. Muzykantov, and Michael Koval. Slow intracellular trafficking of catalase nanoparticles targeted to ICAM-1 protects endothelial cells from oxidative stress. *Am J Physiol Cell Physiol* 285: C1339–C1347, 2003. First published July 23, 2003; 10.1152/ajpcell.00099.2003.—Nanotechnologies promise new means for drug delivery. ICAM-1 is a good target for vascular immunotargeting of nanoparticles to the perturbed endothelium, although endothelial cells do not internalize monomeric anti-ICAM-1 antibodies. However, coupling ICAM-1 antibodies to nanoparticles creates multivalent ligands that enter cells via an amiloride-sensitive endocytic pathway that does not require clathrin or caveolin. Fluorescence microscopy revealed that internalized anti-ICAM nanoparticles are retained in a stable form in early endosomes for an unusually long time (1–2 h) and subsequently were degraded following slow transport to lysosomes. Inhibition of lysosome acidification by chloroquine delayed degradation without affecting anti-ICAM trafficking. Also, the microtubule disrupting agent nocodazole delayed degradation by inhibiting anti-ICAM nanoparticle trafficking to lysosomes. Addition of catalase to create anti-ICAM nanoparticles with antioxidant activity did not affect the mechanisms of nanoparticle uptake or trafficking. Intracellular anti-ICAM/catalase nanoparticles were active, because endothelial cells were resistant to H_2O_2-induced oxidative injury for 1–2 h after nanoparticle uptake. Chloroquine and nocodazole increased the duration of antioxidant protection by decreasing the extent of anti-ICAM/catalase degradation. Therefore, the unique trafficking pathway followed by internalized anti-ICAM nanoparticles seems well suited for targeted delivery of therapeutic enzymes to endothelial cells and may provide a basis for treatment of acute vascular oxidative stress.

drug delivery; endocytosis; microtubules; lysosomes

NANOTECHNOLOGIES offer the opportunity for the design of novel carriers for more effective, specific, and safe drug delivery (4, 24). For example, impressive advances have been achieved in synthesis of nanoparticles with controlled rates of drug release (8, 30, 41, 44). Specific affinity for targets and favorable subcellular addressing are some parameters that are critically important for optimizing the therapeutic potential of nanoparticles as drug delivery vehicles (2, 4, 20, 39).

The vascular endothelium is a prime target for drug delivery. Endothelial cells represent a barrier for drug delivery from the bloodstream to target tissues (42). Conversely, the endothelium is involved in diverse pathological processes including inflammation, oxidative stress, and thrombosis and, therefore, itself represents an important drug delivery target (17, 48, 50). One particularly good target for drug delivery to perturbed endothelial cells is intercellular adhesion molecule-1 (ICAM-1) (3, 51, 52), a plasma membrane protein that is upregulated and functionally involved in inflammation and thrombosis (11, 14, 23, 38). However, ICAM-1 and another Ig superfamily cell adhesion molecule, platelet endothelial cell adhesion molecule-1 (PECAM-1), are not readily internalized by endothelial cells (33, 37, 53).

Nevertheless, despite the inability of these cell adhesion molecules (CAM) to act as receptors to mediate endocytosis of monomeric antibodies, endothelial cells internalize multimeric anti-PECAM nanoparticles and anti-ICAM nanoparticles <300 nm in diameter (34, 37, 53). Importantly, internalization of these anti-CAM nanoparticles is distinct from clathrin- and caveolin-mediated endocytosis. Instead, anti-CAM nanoparticle uptake depends on signaling induced by CAM clustering and represents a unique actin-dependent process requiring activation of protein kinase C, Src kinase, and Rho kinase (CAM-mediated endocytosis) (34). Furthermore, anti-CAM nanoparticles enable vascular delivery of diverse active and reporter cargoes in vivo to pulmonary and cardiac endothelium (1, 9, 33, 37, 47). However, little is known about the intracellular trafficking and fate of anti-CAM nanoparticles. This is a critical component in the design of drug carriers, given that delivery to the appropriate cellular compartment can increase therapeutic efficacy.

Address for reprint requests and other correspondence: V. R. Muzykantov (drug delivery and vascular immunotargeting), Univ. of Pennsylvania School of Medicine, Institute for Environmental Medicine, 1 John Morgan/6068, 3620 Hamilton Walk, Philadelphia, PA 19104 (E-mail: muzykant@mail.med.upenn.edu); or M. Koval (cell biology and endocytosis), Univ. of Pennsylvania School of Medicine, Dept. of Physiology, B-400 Richards Bldg./6085, 3700 Hamilton Walk, Philadelphia, PA 19104 (E-mail: mkoval@mail.med.upenn.edu).

The costs of publication of this article were defrayed in part by the payment of page charges. The article must therefore be hereby marked "*advertisement*" in accordance with 18 U.S.C. Section 1734 solely to indicate this fact.

Here we examine the intracellular trafficking, activity, and fate of anti-ICAM nanoparticles in endothelial cells. The antioxidant activity of anti-ICAM nanoparticles loaded with catalase, an H_2O_2-degrading enzyme potentially useful for antioxidant protection in the cardiovascular system (35, 36), was also tested. Our data show that *1*) the kinetics of anti-ICAM nanoparticle trafficking to lysosomes are remarkably slow; *2*) nanoparticle degradation by endothelial cells can be further delayed by auxiliary pharmacological agents; and *3*) anti-ICAM/catalase nanoparticles permit effective protection against oxidative stress for several hours after internalization. These results indicate that internalization via ICAM-1 permits nanoparticles to be retained in intracellular compartments where they can avoid degradation for a relatively prolonged time. This feature of ICAM targeting and CAM-mediated endocytosis suggests that drug carriers may be designed to be retained in a protected early endocytic compartment with the potential to enhance their therapeutic effects.

METHODS

Antibodies and reagents. Mouse anti-human ICAM-1 (antibody R6.5) was affinity purified from the hybridoma HB-9580 (ATCC, Manassas, VA) (33, 34). Polyclonal antibodies to catalase, human early endosome antigen-1 (EEA-1), or lysosome-associated membrane protein-1 (LAMP-1) were from Calbiochem (La Jolla, CA), Affinity BioReagents (Golden, CO), and BD Biosciences/PharminGen (Franklin Lakes, NJ), respectively. Secondary fluorescent antibodies were from Jackson ImmunoResearch (West Grove, PA) and Molecular Probes (Eugene, OR). Fluoresbrite YG microspheres, which are polystyrene latex microspheres 100 nm in diameter containing a fluorochrome compatible with FITC fluorescence, were from Polysciences (Warrington, PA). Unless otherwise stated, all other reagents were from Sigma (St. Louis, MO).

Preparation of anti-ICAM nanoparticles. Nanoparticles were prepared as described previously (34) by coating on fluorescently labeled latex microspheres with either anti-ICAM-1 alone (anti-ICAM nanoparticles) or anti-ICAM-1 and biotinylated catalase (biotin-catalase) at a 1:0.5 molar ratio (anti-ICAM/catalase nanoparticles). The final effective diameter of resulting nanoparticles was determined by dynamic light scattering (53). In each case, these protocols yielded preparations with diameter ranging from 100 to 300 nm.

Cell culture. Human umbilical vein endothelial cells (HUVEC), pooled from several donors, were from Clonetics (San Diego, CA). The cells were cultured in M199 medium (GIBCO BRL, Grand Island, NY) supplemented with 15% heat-inactivated fetal bovine serum, 2 mM glutamine, 15 μg/ml endothelial cell growth supplement, 100 μg/ml heparin, 100 U/ml penicillin, and 100 μg/ml streptomycin. The cells were maintained at 37°C, 5% CO_2, and 95% relative humidity. When seeded for experiments, HUVEC between *passages 4* and *5* were cultured onto 12-mm^2 gelatin-coated coverslips in 24-well plates and then activated by overnight incubation with TNF-α.

Internalization, trafficking, and stability of anti-ICAM nanoparticles. TNF-α-activated confluent HUVEC were incubated at 4°C for 30 min with FITC-labeled anti-ICAM or anti-ICAM/catalase nanoparticles to enable binding to the cell surface. The cells were then washed, warmed to 37°C for varying amounts of time, cooled to 4°C, and washed, and the cells were fixed with 2% paraformaldehyde at room temperature (RT) for 15 min. Intracellular delivery of catalase was confirmed by labeling permeabilized cells with rabbit anti-catalase followed by Alexa Fluor 350-conjugated goat anti-rabbit IgG. Also, to preferentially label nanoparticles bound to the cell surface, nonpermeabilized cells were treated with Texas red-conjugated goat anti-mouse IgG (to label anti-ICAM-1). The samples were analyzed with an Olympus IX70 fluorescence microscope using ×10 or ×40 PlanApo objectives and filters optimized for FITC, Texas red, and Alexa Fluor 350 fluorescence. Images were obtained with a Hamamatsu Orca-1 charge-coupled device camera and analyzed using ImagePro 3.0 software. With this approach, internalized nanoparticles were imaged as single-labeled green particles and surface-bound nanoparticles were double-labeled in yellow. Merged micrographs were scored automatically by image analysis to obtain the percentage of cell-associated particles that were internalized. Images of cells from two to five independent determinations were combined to form the average percentage of internalized particles, where *n* reflects the total number of cells averaged for a given value. To examine the effect of inhibitors on nanoparticle uptake, TNF-α-activated HUVEC were pretreated at 37°C for 30 min in the presence of 3 mM amiloride, 50 μM monodansyl cadaverine (MDC), or 1 μg/ml filipin before incubation with nanoparticles.

To identify compartments containing internalized particles, TNF-α-activated HUVEC were incubated with nanoparticles as described above. After surface labeling of nonpermeabilized cells, the cells were permeabilized with a 15-min incubation with 0.2% Triton X-100 at RT, washed, and further labeled with polyclonal rabbit anti-human EEA-1 followed by Texas red-goat anti-rabbit IgG or with phycoerythrin-labeled rabbit anti-human LAMP-1. To determine the intracellular stability of anti-ICAM or anti-ICAM/catalase nanoparticles, internalized particles were counterstained with either Texas red-goat anti-mouse IgG (to recognize nondegraded anti-ICAM-1) or rabbit anti-catalase followed by Texas red-goat anti-rabbit IgG. Alternatively, cells were incubated with nanoparticles prepared with either ^{125}I-labeled anti-ICAM or biotin-catalase for varying amounts of time. The cells were then harvested, and proteins were resolved by SDS-PAGE and transferred to polyvinylidene difluoride. Degradation of ^{125}I-anti-ICAM-1 was determined by densitometric analysis of autoradiograms, and intact biotin-catalase was analyzed using an avidin-horseradish peroxidase (HRP) blot. Lanes were normalized to total cell protein, which was loaded in the range of 10–20 μg/lane. When indicated, cells were pretreated with either 20 μM nocodazole or 300 μM chloroquine before incubation with nanoparticles. To measure kinetics of fluid-phase endocytic delivery to lysosomes, cells were incubated for varying amounts of time at 37°C with 2 mg/ml amine-fixable 10-kDa Texas red-dextran (Molecular Probes) and then fixed with 2% paraformaldehyde and counterstained with FITC-conjugated rabbit anti-human LAMP-1.

Antioxidant effect of anti-ICAM/catalase nanoparticles. The antioxidant effect of anti-ICAM/catalase nanoparticles was tested at different periods of time after their internalization within control HUVEC or cells treated with either 20 μM nocodazole or 300 μM chloroquine. The cells containing either internalized control anti-ICAM nanoparticles or anti-ICAM/catalase nanoparticles were incubated for 15 min at RT with 5 mM H_2O_2 in Phenol red-free RPMI. The cells were washed after H_2O_2 treatment, incubated with 0.1 μM calcein-AM and 1 μM ethidium (Live/Dead kit; Molecular Probes) for 15 min at 37°C, and finally scored to determine the percentage of surviving (calcein positive/ethidium nega-

tive) cells. Unless stated otherwise, the data were calculated as means ± SE, where statistical significance was determined by Student's *t*-test.

RESULTS

Anti-ICAM nanoparticles, with a size range between 100 and 300 nm in diameter, are internalized by endothelial cells through a unique endocytic pathway, CAM-mediated endocytosis (34). Therefore, these nanoparticles have the potential to provide intracellular delivery of therapeutics for the treatment of pathologically altered endothelium. Given this, we analyzed the intracellular trafficking and fate of anti-ICAM nanoparticles. Internalization of anti-ICAM nanoparticles by HUVEC was temperature dependent. Cells were incubated with anti-ICAM nanoparticles for 1 h at either 4 or 37°C and then fixed and incubated with Alexa Fluor 350-goat anti-mouse IgG to double label nanoparticles remaining on the cell surface. As shown in Fig. 1, HUVEC incubated at 4°C showed green/blue double-labeled nanoparticles retained on the cell surface. In contrast, cells incubated at 37°C showed little, if any, blue labeling, indicating near complete anti-ICAM nanoparticle internalization. For trafficking studies described below, we routinely counterstained cells using this approach to identify noninternalized nanoparticles. Typically, there was little, if any, blue nanoparticle labeling in these experiments, suggesting that there was near complete internalization of anti-ICAM nanoparticles in the colocalization experiments described.

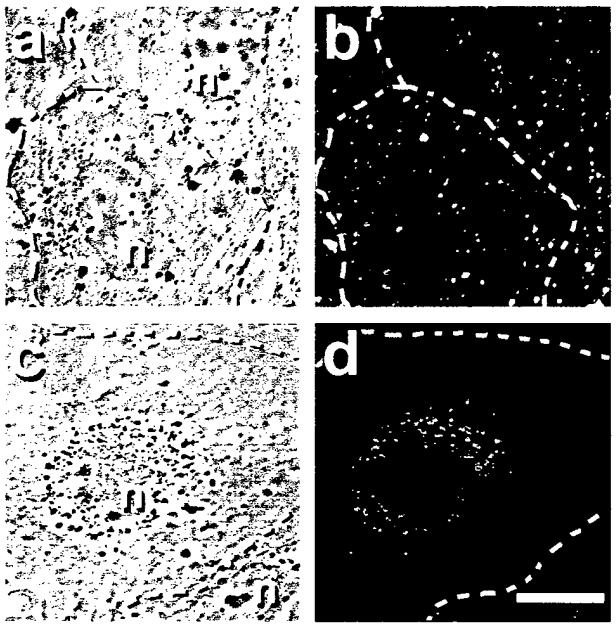

Fig. 1. Temperature dependence of anti-intercellular adhesion molecule (ICAM) nanoparticle uptake. Human umbilical vein endothelial cells (HUVEC) were incubated for 30 min at 4°C with green fluorescent anti-ICAM nanoparticles to permit binding. Cells were washed, incubated at 4°C (*a* and *b*) or 37°C (*c* and *d*) for 1 h, and fixed, and then surface-bound anti-ICAM nanoparticles were counterstained with goat anti-mouse IgG conjugated to blue Alexa Fluor 350. Phase-contrast images are shown in *a* and *c*, where n indicates the position of the nucleus and dashed lines denote regions of the plasma membrane in contact with adjacent cells. Immunofluorescence images show extensive blue labeling of anti-ICAM nanoparticles when cells were incubated at 4°C (*b*), consistent with a lack of internalization at this temperature. In contrast, after 37°C incubation (*d*), there was little, if any, blue colocalization, confirming that virtually all cell-associated anti-ICAM nanoparticles were internalized after incubation for 1 h at 37°C. Bar, 10 μm.

As shown in Fig. 2, *A* and *B*, internalized anti-ICAM nanoparticles partially colocalized with EEA-1-positive endosomes in the perinuclear region 1 h after internalization by HUVEC. With time at 37°C the nanoparticles redistributed from EEA-1-positive endosomes to LAMP-1-positive lysosomal compartments. The lysosomal trafficking of anti-ICAM nanoparticles was remarkably slow compared with that of the fluid phase marker Texas red-dextran, which HUVEC trafficked to LAMP-1-positive vesicles after a 15-min incubation (Fig. 2*Bd*).

Because trafficking of anti-ICAM nanoparticles to lysosomes was slow, we examined degradation of anti-ICAM nanoparticles using a qualitative immunofluorescence assay (Fig. 3*A*). Anti-ICAM nanoparticles internalized by HUVEC lost immunoreactivity after a 2- to 3-h incubation at 37°C, a rate of degradation consistent with the slow rate of delivery to lysosomes. This was confirmed directly by examining the degradation of ^{125}I-anti-ICAM by HUVEC, where ~30% of the HUVEC associated anti-ICAM remained intact after a 3-h incubation (Fig. 3*E*). These data suggest that degradation of anti-ICAM nanoparticles, which occurred at an unusually slow rate, takes place after delivery to lysosomes.

Therefore, we determined whether pharmacological agents that interfere with lysosome activity could inhibit nanoparticle degradation. Pretreatment of HUVEC with either chloroquine or nocodazole before incubation with anti-ICAM nanoparticles inhibited anti-ICAM degradation (Fig. 3). The mechanism of action for these agents was distinct. Pretreatment of HUVEC with the weak base chloroquine did not affect trafficking of anti-ICAM nanoparticles from early endosomes to lysosomes (Fig. 4, *A* and *B*) but markedly prolonged their stability (Fig. 3*F*), consistent with decreased lysosome acidification in the presence of chloroquine and suggesting that that anti-ICAM nanoparticles were degraded by acidic proteolytic enzymes. Comparable results were obtained by using bafilomycin to inhibit lysosome acidification (Muro S, Muzykantov VR, and Koval M, unpublished observations).

In contrast, nocodazole pretreatment blocked anti-ICAM nanoparticle trafficking by HUVEC to lysosomes by disrupting the microtubule network of the cell (46, 49). Previously, we found that nocodazole did not inhibit nanoparticle uptake (34). Instead, for nocodazole-treated cells, anti-ICAM nanoparticles were internalized and scattered throughout the cell periphery instead of distributing to the perinuclear area. Consistent with blocking anti-ICAM nanoparticle trafficking to lysosomes (Fig. 5*B*), nocodazole markedly decelerated degradation of anti-ICAM nanoparticles (Fig. 3*F*). Also,

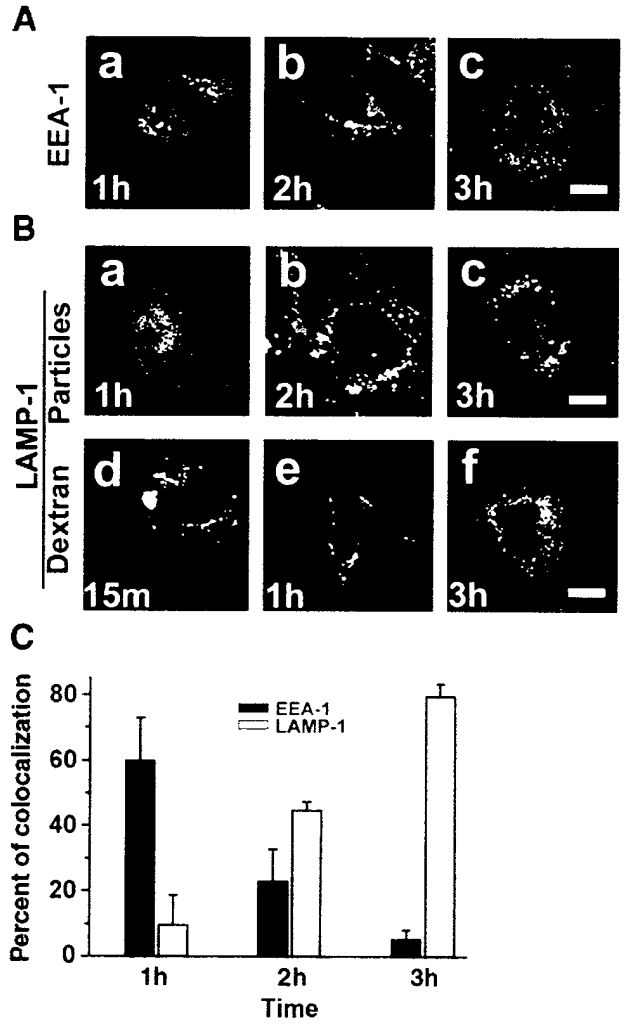

Fig. 2. Slow lysosomal trafficking anti-ICAM nanoparticles. *A*: HUVEC were incubated for 30 min at 4°C with green fluorescent anti-ICAM nanoparticles to permit binding. Cells were washed and then incubated at 37°C for 1 (*a*), 2 (*b*), or 3 h (*c*) to allow nanoparticle internalization and trafficking. Cells were fixed, surface-bound anti-ICAM nanoparticles were counterstained with goat anti-mouse IgG conjugated to blue Alexa Fluor 350, the cells were permeabilized, and early endosomes were stained with rabbit anti-early endosome antigen-1 (EEA-1) and Texas red-goat anti-rabbit IgG. Cells showed little, if any, blue fluorescence, confirming that virtually all cell-associated anti-ICAM nanoparticles were internalized under these conditions (compare with Fig. 1*b*). Yellow color in *a* and *b* reflects anti-ICAM nanoparticles localized to early endosomes. *B*: HUVEC were incubated with fluorescent anti-ICAM nanoparticles as in *A*, except that lysosomes were labeled with Texas red-conjugated rabbit anti-lysosome-associated membrane protein-1 (LAMP-1) (*a–c*). To measure fluid-phase trafficking to lysosomes, HUVEC were incubated with FITC-conjugated dextran for 15 min (*d*), 1 h (*e*), or 3 h (*f*) before fixation and immunolabeling with Texas red anti-LAMP-1. Yellow color reflects anti-ICAM nanoparticles or FITC-dextran localized to lysosomes. Bars, 10 μm. *C*: the extent of colocalization of anti-ICAM nanoparticles and EEA-1 or LAMP-1 was quantified by image analysis and plotted as a function of incubation time. Data are means ± SD and represent %colocalization for n = 20–25 cells.

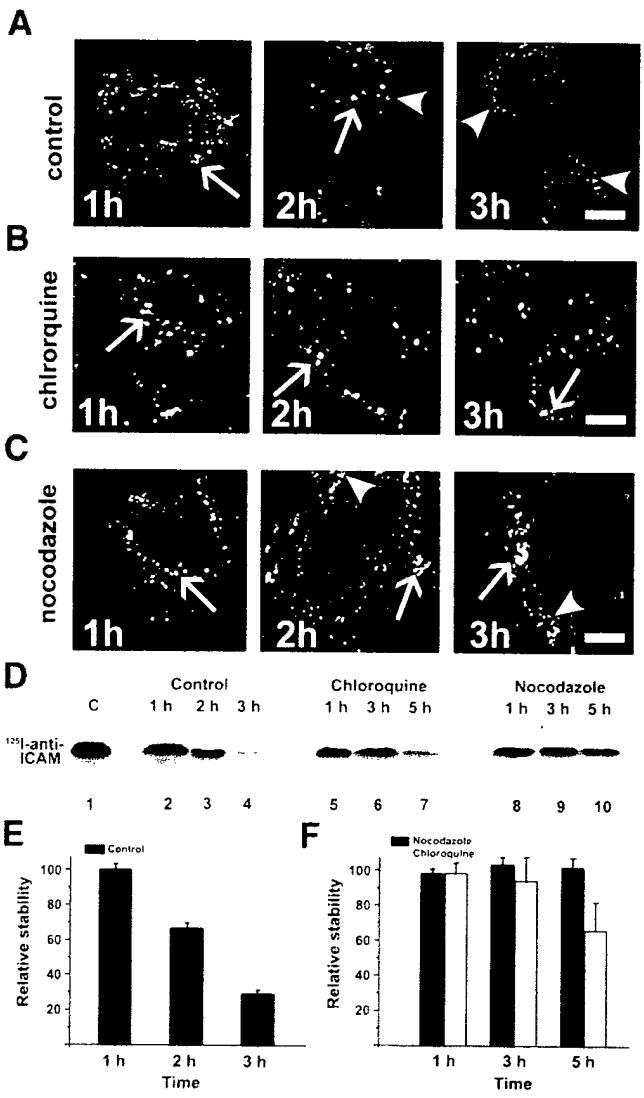

Fig. 3. Stability of internalized anti-ICAM nanoparticles. HUVEC were either untreated (*A*) or preincubated for 30 min at 37°C in the presence of either 300 μM chloroquine (*B*) or 20 μM nocodazole (*C*) before incubation with anti-ICAM nanoparticles. Stability of intracellular anti-ICAM-1 was tested by incubating cells with anti-ICAM nanoparticles as described in Fig. 2 and then immunolabeling permeabilized cells with Texas red-goat anti-mouse IgG, which binds nondegraded anti-ICAM-1 to produce yellow double-labeled particles (arrows). Arrowheads denote green nanoparticles, which did not bind Texas red-goat anti-mouse IgG, suggesting that anti-ICAM was degraded. Bars, 10 μm. *D*: cells were either untreated (*lanes 2–4*) or treated with chloroquine (*lanes 5–7*) or nocodazole (*lanes 8–10*) as described above and then incubated with anti-ICAM nanoparticles containing ^{125}I-labeled IgG for varying amounts of time. Cells were harvested, proteins were resolved by SDS-PAGE, and the amount of cell-associated ^{125}I-IgG was determined by densitometric analysis of autoradiograms (*E*, controls; *F*, nocodazole and chloroquine). *Lane 1* contained ^{125}I-anti-ICAM nanoparticles loaded directly onto the gel; other lanes were loaded with equal amounts of total cell protein. Densitometric values are means ± SD (n = 3) normalized to values obtained for the corresponding 1 h time point.

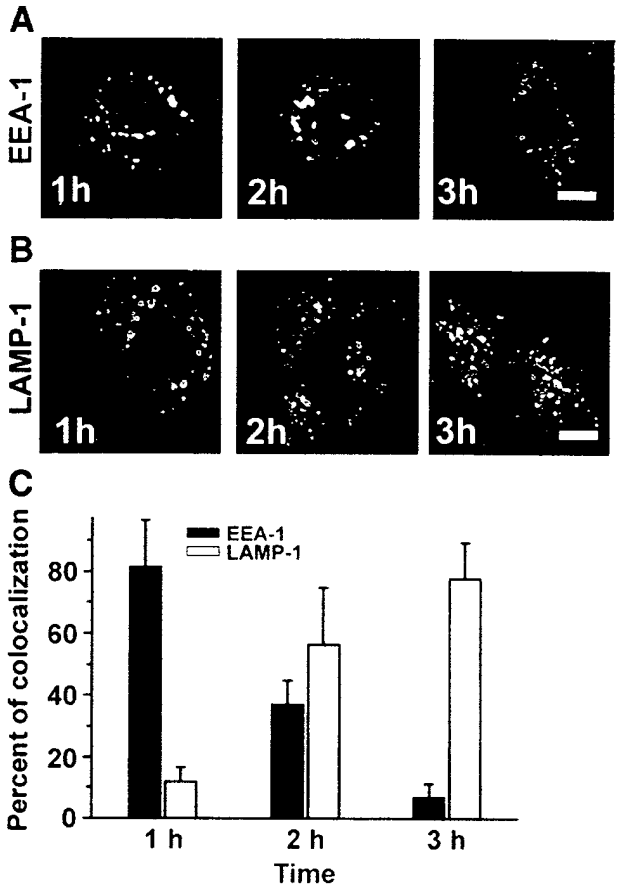

Fig. 4. Chloroquine did not inhibit anti-ICAM nanoparticle transport to lysosomes. HUVEC were treated as described in Fig. 2, except that cells were preincubated for 30 min at 37°C in the presence of 300 μM chloroquine before incubation with anti-ICAM nanoparticles and immunolabeling for surface nanoparticles (blue), EEA-1 (*A*), or LAMP-1 (*B*). Cells showed little, if any, blue fluorescence, confirming that virtually all cell-associated anti-ICAM nanoparticles were internalized under these conditions (compare with Fig. 1*b*). Yellow color reflects localization of anti-ICAM nanoparticles to early endosomes (*A*) or lysosomes (*B*). Bars, 10 μm. *C*: the extent of colocalization of anti-ICAM nanoparticles and EEA-1 or LAMP-1 was quantified by image analysis and plotted as a function of incubation time. Data are means ± SD and represent %colocalization for n = 10–12 cells.

nocodazole-treated cells showed little, if any, colocalization of internalized anti-ICAM nanoparticles with EEA-1 (Fig. 5*A*), suggesting that microtubules may be required for nanoparticle trafficking to EEA-1-positive early endosomes as well as to late endocytic compartments.

These findings imply that anti-ICAM nanoparticles could deliver a drug into endothelial cells that might be transiently stable for several hours and that could be further stabilized by using auxiliary agents that inhibit lysosomal traffic and/or degradation, features that make anti-ICAM nanoparticles good candidates for antioxidant delivery. To test this, we prepared anti-ICAM nanoparticles carrying catalase, a classic antioxidant enzyme that protects cells from H_2O_2 generated during oxidative stress (35). Anti-ICAM/catalase nanoparticles were internalized by HUVEC (Fig. 6*A*). Neither MDC nor filipin significantly inhibited internalization of anti-ICAM/catalase nanoparticles (14 ± 2 and 23 ± 3% inhibition of control levels of internalization, respectively; n = 10–15 cells from 2 independent experiments), showing that neither clathrin- nor caveolin-mediated endocytic pathways are responsible for internalization. However, the uptake was significantly inhibited by amiloride (Fig. 6, *B* and *C*; 40 ± 3% inhibition of control level of internalization; n = 10–15 cells from 2 independent experiments), consistent with internalization of anti-ICAM/catalase nanoparticles by CAM-mediated endocytosis (34).

Internalized anti-ICAM/catalase nanoparticles were transported to lysosomes (Fig. 7*A*), where degradation occurred (Fig. 7*B*). Both trafficking and degradation kinetics were slow (3 h) and similar to that observed for

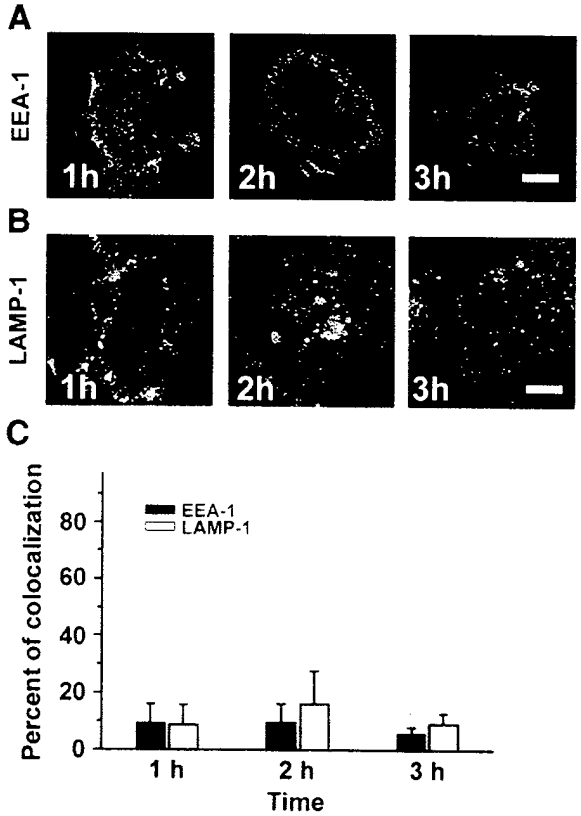

Fig. 5. Nocodazole inhibited trafficking of anti-ICAM nanoparticles to lysosomes. HUVEC were labeled as described in Fig. 2, except that cells were preincubated for 30 min at 37°C in the presence of 20 μM nocodazole before to incubation with anti-ICAM nanoparticles and immunolabeling surface nanoparticles (blue), EEA-1 (*A*), or LAMP-1 (*B*). Cells showed little, if any, blue fluorescence, confirming that virtually all cell-associated anti-ICAM nanoparticles were internalized under these conditions (compare with Fig. 1*b*). Yellow color reflects localization of anti-ICAM nanoparticles in early endosomes (*A*) or lysosomes (*B*). Bars, 10 μm. *C*: the extent of colocalization of anti-ICAM nanoparticles and EEA-1 or LAMP-1 was quantified by image analysis and plotted as a function of incubation time. Data are means ± SD and represent %colocalization for n = 15–18 cells.

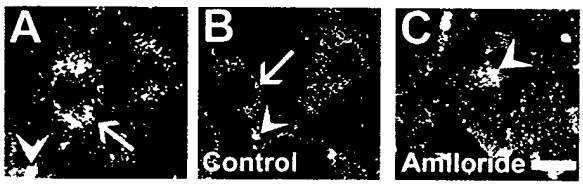

Fig. 6. Intracellular delivery of catalase nanoparticles by ICAM-mediated internalization. *A*: HUVEC were incubated for 1 h at 37°C with green fluorescent anti-ICAM/catalase nanoparticles. Cells were washed, fixed, and counterstained with Texas red-goat anti-mouse IgG. Cells were then permeabilized and stained using rabbit anti-catalase and blue Alexa Fluor 350-goat anti-rabbit IgG. Internalized nanoparticles containing catalase show a blue-green color (arrow), and surface-bound triple-labeled nanoparticles appear white (arrowhead). The internalization of anti-ICAM/catalase nanoparticles was tested in control HUVEC (*B*) or cells treated with 3 mM amiloride (*C*), where surface-bound particles were counterstained with Texas red-goat anti-mouse IgG without cell permeabilization. Internalized anti-ICAM/catalase nanoparticles were single labeled green (arrow), and nanoparticles at the cell surface were double-labeled yellow (arrowhead). Bar, 10 μm.

control anti-ICAM nanoparticles. Also, the kinetics for biotin-catalase degradation, as assessed by HRP-avidin blot (Fig. 7*D*), were comparable to the kinetics for anti-ICAM degradation (Fig. 3*E*). These data are consistent with the notion that the catalase cargo did not affect the mechanism of uptake, traffic, and degradation of anti-ICAM nanoparticles.

To test the antioxidant capacity of catalase delivered within the cells by anti-ICAM nanoparticles, HUVEC were incubated after internalization of anti-ICAM/catalase nanoparticles at 37°C for varying amounts of time and then subsequently exposed to 5 mM H_2O_2 for 15 min. Cells pretreated with unloaded anti-ICAM nanoparticles showed significant H_2O_2-mediated toxicity; only ~60% of the cells survived 15 min after H_2O_2 shock (Fig. 8, *Ad–Af* and *B*). In contrast, anti-ICAM/catalase nanoparticle-treated cells were resistant to H_2O_2 (>90% cell survival; Fig. 8, *Ag*, *Ah*, and *B*), indicating that catalase nanoparticles delivered inside the cells had a protective effect. The protective effect of anti-ICAM/catalase nanoparticles diminished 3 h after internalization, consistent with the kinetics of lysosomal trafficking and degradation of these nanoparticles (Fig. 8*Ai*).

To determine whether auxiliary pharmacological agents prolong the therapeutic effect of anti-ICAM/catalase nanoparticles, HUVEC were pretreated with either chloroquine or nocodazole. Both agents markedly prolonged the duration of antioxidant protective effect of anti-ICAM/catalase nanoparticles (Fig. 8*C*) and inhibited catalase degradation (Fig. 7 *E*). In particular, nocodazole enabled internalized catalase to remain active for at least 5 h after internalization, which doubled the duration of the antioxidant activity of anti-ICAM/catalase nanoparticles.

DISCUSSION

The present data demonstrate that functionally active, catalase-carrying anti-ICAM nanoparticles are internalized by endothelial cells using CAM-mediated endocytosis and were retained in an early endosomal compartment for an unusually long period of time (1–2 h). Anti-ICAM nanoparticles were ultimately delivered to lysosomes after 2–3 h, where they were degraded and inactivated. By comparison, ligands internalized

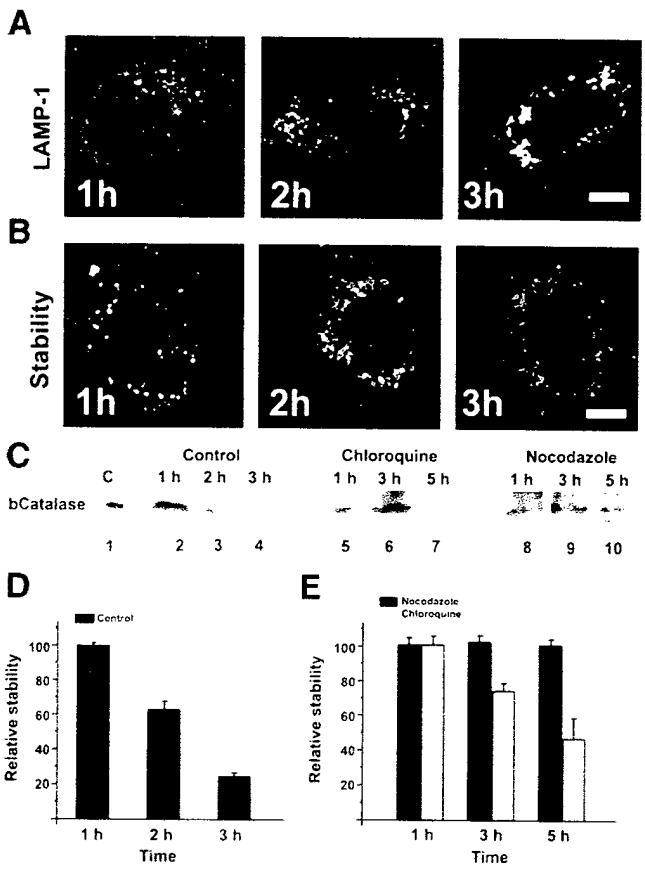

Fig. 7. Slow lysosomal trafficking and degradation of internalized anti-ICAM/catalase nanoparticles. *A*: HUVEC were incubated with Texas red-dextran to label lysosomes and then incubated with anti-ICAM/catalase nanoparticles for 30 min at 4°C, washed, and incubated at 37°C for different periods of time to permit internalization. Surface-bound particles were counterstained with blue Alexa Fluor 350-goat anti-mouse IgG. Cells showed little, if any, blue fluorescence, confirming that virtually all cell-associated anti-ICAM/catalase nanoparticles were internalized under these conditions (compare with Fig. 1*b*). Yellow color reflects localization of green fluorescent nanoparticles to Texas red-labeled lysosomes. *B*: surface-bound particles were counterstained with blue Alexa Fluor 350-goat anti-mouse IgG, and then the stability of intracellular anti-ICAM/catalase nanoparticles was tested by immunolabeling permeabilized cells with rabbit anti-catalase and Texas red-goat anti-rabbit IgG, as described in Fig. 3. Bars, 10 μm. *C*: cells were either untreated (*lanes 2–4*) or treated with chloroquine (*lanes 5–7*) or nocodazole (*lanes 8–10*) as described above and incubated with anti-ICAM nanoparticles containing biotinylated catalase for varying amounts of time. Cells were harvested, proteins were resolved by SDS-PAGE and transferred to membranes, and the amount of cell-associated biotinylated catalase was determined by densitometric analysis of horseradish peroxidase (HRP)-avidin blots (*D*, controls; *E*, nocodazole and chloroquine). *Lane 1* contains biotinylated catalase nanoparticles loaded directly onto the gel; other lanes were loaded with equal amounts of cell protein. Densitometric values are means ± SD (n = 3) normalized to values obtained for the corresponding 1 h time point.

via other pathways including clathrin-mediated or fluid-phase endocytosis and phagocytosis are delivered to lysosomes within minutes (6, 21, 31). The slow kinetics of anti-ICAM nanoparticle trafficking to lysosomes proved advantageous for the intracellular targeting of catalase, which had prolonged antioxidant protective activity due to the prolonged (1–2 h) residence time in a nondegrading early endosomal compartment. Furthermore, catalase activity was extended when cells were treated with pharmacological agents that delayed proteolysis by decreasing lysosome acidification or nanoparticle delivery to lysosomes.

The multivalent nature of anti-ICAM nanoparticles is likely to contribute to the delay in trafficking to lysosomes. Consistent with this, Marsh et al. (27) found that oligomerized transferrin was retained in an early endocytic compartment, where it was resistant to degradation. Furthermore, oligomerized transferrin ultimately was recycled to the plasma membrane, consistent with the trafficking of natural transferrin. This is in contrast to our results, where anti-ICAM-1 nanoparticles were ultimately transported to lysosomes. Thus, although the multivalent nature of the ligands affects the kinetics of transport through endocytic compartments, the destination of internalized multivalent ligands appears to depend more on the receptor, rather than on ligand valency.

The intracellular trafficking of internalized ligands is influenced by receptor determinants (6, 31). However, Ig superfamily CAM, such as ICAM-1 and PECAM-1, are not typically thought of as endocytic receptors. In fact, monomeric anti-ICAM-1 and anti-PECAM-1 are poorly internalized by endothelial cells (33, 37, 53). Nevertheless, endothelial cells internalize multivalent anti-ICAM and anti-PECAM nanoparticles in the size range of 100–300 nm in diameter through CAM-mediated endocytosis, an endocytic mechanism that is distinct from clathrin- and caveolin-mediated endocytosis, phagocytosis, and macropinocytosis (34, 53). Given this, the trafficking of internalized anti-CAM nanoparticles could not be predicted on the basis of known properties of ICAM-1 or PECAM-1 trafficking. Nonetheless, it seems plausible that internalization by CAM-mediated endocytosis may be critical for targeting and retention of anti-CAM nanoparticles to an early endosomal compartment.

Both in vitro and in vivo results suggest that CAM-mediated internalization may have the potential to be useful for the specific intracellular immunotargeting of nanoparticles (33, 34, 53). Although agents such as catalase can be active when bound to the endothelial cell surface, internalization offers several advantages. For instance, receptor shedding has the potential to decrease the efficacy of anti-ICAM/catalase complexes by releasing them from the cell surface. Consistent

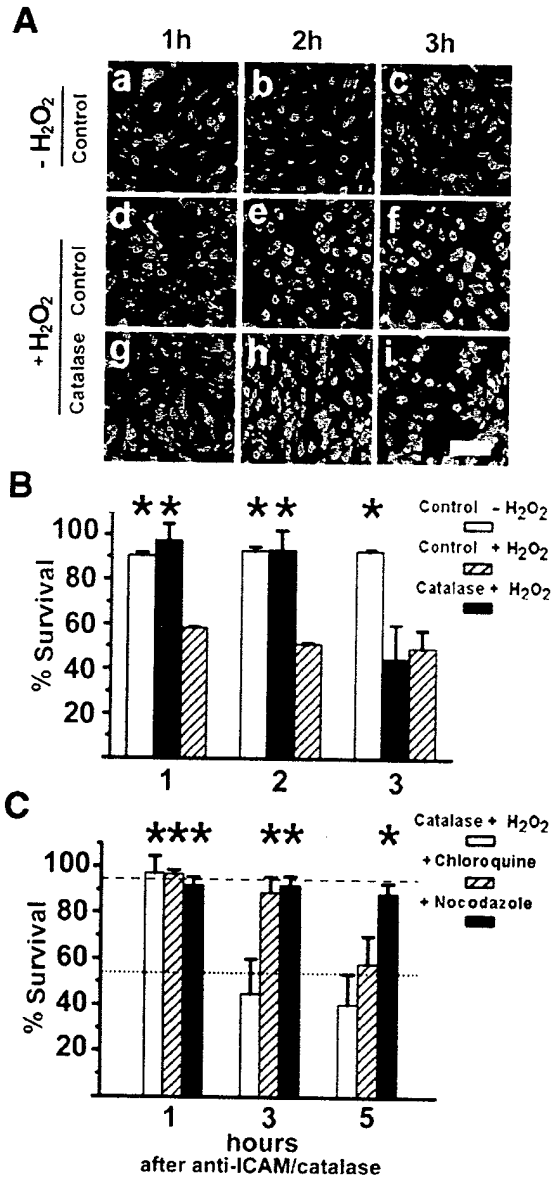

Fig. 8. Prolonged antioxidant protection by intracellular delivery of anti-ICAM/catalase nanoparticles. *A*: HUVEC were incubated with either control anti-ICAM nanoparticles (*a–f*) or anti-ICAM/catalase nanoparticles (*g–i*) for 30 min at 4°C and then incubated at 37°C for 1 (*a*, *d*, *g*), 2 (*b*, *e*, *h*), or 3 h (*c*, *f*, *i*). Cells were washed and then mock-treated (*a–c*) or treated with 5 mM H_2O_2 for 15 min at room temperature (*d–i*). Cell viability was then assessed using the Live/Dead assay, which reveals live, intact cells as calcein positive/ethidium negative (green) and dead cells as calcein negative/ethidium positive (red). Bar, 50 μm. *B*: cell viability was quantified by fluorescence microscopy from at least 500 cells per condition. Data are means ± SE and represent the percentage of survival. Cells treated with anti-ICAM/catalase nanoparticles (catalase + H_2O_2) were resistant to H_2O_2 damage, compared with untreated cells (control + H_2O_2). *C*: HUVEC were pretreated with either 300 μM chloroquine or 20 μM nocodazole and then incubated with anti-ICAM/catalase nanoparticles, and protection to H_2O_2 injury was analyzed as described above. Cells pretreated with nocodazole or chloroquine had prolonged resistance to H_2O_2 damage, compared with control H_2O_2-treated cells that received catalase nanoparticles alone (catalase + H_2O_2). Dashed line shows the mean value for %survival of cells that were not exposed to H_2O_2; dotted line shows the mean value for %survival of cells treated with unloaded anti-ICAM nanoparticles and H_2O_2. *$P < 0.05$ compared with H_2O_2-exposed cells that were not treated with anti-ICAM/catalase nanoparticles.

with this possibility, dimeric ICAM-1 was found to be shed into the pleural space in response to inflammation (29). Also, because internalized catalase will have access to intracellular oxidants diffusing from all directions, internalized catalase has the potential to be more effective than catalase localized to the cell surface. The ability to target catalase to specific intracellular compartments also has the additional potential for intercepting oxidants near sites of generation or sites sensitive to damage (such as nuclear DNA).

The trafficking of anti-ICAM/catalase nanoparticles underscores the notion that the fate of therapeutic cargoes should and can be modulated to optimize drug delivery strategies. For example, fast endosomal traffic and escape are critical for activity of immunotoxins (45). Conversely, targeting drugs to parasitophorous vacuoles or lysosomes is preferable for antiparasitic and certain types of enzyme replacement therapies (15, 25, 55), and nuclear delivery is necessary for gene therapies (7, 19, 40). Furthermore, ligands targeted to antigens involved in caveolin-mediated endocytosis have the potential to be transcytosed by endothelial cells via a pathway that eludes lysosomes and has the potential to circumvent the endothelial barrier (28, 43).

ICAM-1 represents a particularly attractive target for targeting antioxidant enzymes because it is upregulated by stressed endothelial cells and is functionally involved in vascular oxidative stress, ischemia-reperfusion injury, and inflammation (12, 13, 18, 32). Intracellular delivery of antioxidants may permit effective interception and detoxification of reactive oxygen species produced inside endothelial cells and diffusing through the plasma membrane from released activated leukocytes (16, 26, 54). Also, anti-ICAM nanoparticles may also have the capacity to occupy ICAM-1 at the cell surface and thus block leukocyte adhesion to endothelial cells, which could provide a secondary anti-inflammatory benefit (5, 10, 11, 23).

Catalase delivered by anti-ICAM nanoparticles afforded antioxidant protection for over 2 h after internalization (Fig. 7). In fact, this time frame for antioxidant protection is consistent with animal studies showing that anti-CAM/catalase nanoparticles protect the lung from acute oxidative injury during transplantation (22). Here, we found that this therapeutic time window can be further extended by the use of auxiliary drugs, which either inhibit pH-dependent lysosomal proteolysis or prevent microtubule-dependent lysosomal trafficking. This raises the possibility that pharmacological agents already approved for clinical use (e.g., chloroquine) can be used in combination with anti-CAM nanoparticles to improve the in vivo efficacy of nanoparticle-based drug delivery vehicles, an approach with the potential to enhance therapeutic interventions in acute pathological conditions associated with vascular oxidative stress, including acute lung injury, hyperoxia, and ischemia-reperfusion injury.

We thank Samira Tliba and Dr. Vladimir Shuvaev for technical assistance and advice.

DISCLOSURES

This work was supported by National Institutes of Health (NIH) Specialized Center of Research in Acute Lung Injury Grant HL-60290, Project 4 (to V. R. Muzykantov); NIH Grants HL/GM-71175-01 (to V. R. Muzykantov), GM-61012 (to M. Koval), and P01-HL-19737-26, Project 3 (M. Koval); and Department of Defense Grant PR 012262 (to V. R. Muzykantov). S. Muro was supported by a fellowship from Fundación Ramón Areces (Spain).

REFERENCES

1. **Atochina EN, Balyasnikova IV, Danilov SM, Granger DN, Fisher AB, and Muzykantov VR.** Immunotargeting of catalase to ACE or ICAM-1 protects perfused rat lungs against oxidative stress. *Am J Physiol Lung Cell Mol Physiol* 275: L806–L817, 1998.
2. **Blackwell JE, Dagia NM, Dickerson JB, Berg EL, and Goetz DJ.** Ligand coated nanosphere adhesion to E- and P-selectin under static and flow conditions. *Ann Biomed Eng* 29: 523–533, 2001.
3. **Bloemen PG, Henricks PA, van Bloois L, van den Tweel MC, Bloem AC, Nijkamp FP, Crommelin DJ, and Storm G.** Adhesion molecules: a new target for immunoliposome-mediated drug delivery. *FEBS Lett* 357: 140–144, 1995.
4. **Brigger I, Dubernet C, and Couvreur P.** Nanoparticles in cancer therapy and diagnosis. *Adv Drug Deliv Rev* 54: 631–651, 2002.
5. **Broide DH, Humber D, Sullivan S, and Sriramarao P.** Inhibition of eosinophil rolling and recruitment in P-selectin- and intracellular adhesion molecule-1-deficient mice. *Blood* 91: 2847–2856, 1998.
6. **Caron E and Hall A.** Phagocytosis. In: *Endocytosis*, edited by Marsh M. Oxford, UK: Oxford University Press, 2001, p. 58–77.
7. **Chan CK and Jans DA.** Using nuclear targeting signals to enhance non-viral gene transfer. *Immunol Cell Biol* 80: 119–130, 2002.
8. **Chorny M, Fishbein I, Danenberg HD, and Golomb G.** Study of the drug release mechanism from tyrphostin AG-1295-loaded nanospheres by in situ and external sink methods. *J Control Release* 83: 401, 2002.
9. **Christofidou-Solomidou M, Pietra GG, Solomides CC, Arguiris E, Harshaw D, Fitzgerald GA, Albelda SM, and Muzykantov VR.** Immunotargeting of glucose oxidase to endothelium in vivo causes oxidative vascular injury in the lungs. *Am J Physiol Lung Cell Mol Physiol* 278: L794–L805, 2000.
10. **DeMeester SR, Molinari MA, Shiraishi T, Okabayashi K, Manchester JK, Wick MR, Cooper JD, and Patterson GA.** Attenuation of rat lung isograft reperfusion injury with a combination of anti-ICAM-1 and anti-beta2 integrin monoclonal antibodies. *Transplantation* 62: 1477–1485, 1996.
11. **Diamond MS, Staunton DE, de Fougerolles AR, Stacker SA, Garcia-Aguilar J, Hibbs ML, and Springer TA.** ICAM-1 (CD54): a counter-receptor for Mac-1 (CD11b/CD18). *J Cell Biol* 111: 3129–3139, 1990.
12. **Diamond MS, Staunton DE, Marlin SD, and Springer TA.** Binding of the integrin Mac-1 (CD11b/CD18) to the third immunoglobulin-like domain of ICAM-1 (CD54) and its regulation by glycosylation. *Cell* 65: 961–971, 1991.
13. **Doerschuk CM, Quinlan WM, Doyle NA, Bullard DC, Vestweber D, Jones ML, Takei F, Ward PA, and Beaudet AL.** The role of P-selectin and ICAM-1 in acute lung injury as determined using blocking antibodies and mutant mice. *J Immunol* 157: 4609–4614, 1996.
14. **Dustin ML, Rothlein R, Bhan AK, Dinarello CA, and Springer TA.** Induction by IL 1 and interferon-gamma: tissue distribution, biochemistry, and function of a natural adherence molecule (ICAM-1). *J Immunol* 137: 245–254, 1986.
15. **Eng CM, Banikazemi M, Gordon RE, Goldman M, Phelps R, Kim L, Gass A, Winston J, Dikman S, Fallon JT, Brodie S, Stacy CB, Mehta D, Parsons R, Norton K, O'Callaghan M, and Desnick RJ.** A phase 1/2 clinical trial of enzyme replacement in fabry disease: pharmacokinetic, substrate clearance, and safety studies. *Am J Hum Genet* 68: 711–722, 2001.

16. **Fisher AB, Al-Mehdi AB, and Muzykantov V.** Activation of endothelial NADPH oxidase as the source of a reactive oxygen species in lung ischemia. *Chest* 116: 25S–26S, 1999.
17. **Heffner JE and Repine JE.** Pulmonary strategies of antioxidant defense. *Am Rev Respir Dis* 140: 531–554, 1989.
18. **Hubbard AK and Rothlein R.** Intercellular adhesion molecule-1 (ICAM-1) expression and cell signaling cascades. *Free Radic Biol Med* 28: 1379–1386, 2000.
19. **Johnson-Saliba M and Jans DA.** Gene therapy: optimising DNA delivery to the nucleus. *Curr Drug Targets* 2: 371–399, 2001.
20. **Kim CK and Lim SJ.** Recent progress in drug delivery systems for anticancer agents. *Arch Pharm Res* 25: 229–239, 2002.
21. **Koval M, Preiter K, Adles C, Stahl PD, and Steinberg TH.** Size of IgG-opsonized particles determines macrophage response during internalization. *Exp Cell Res* 242: 265–273, 1998.
22. **Kozower BD, Christofidou-Solomidou M, Sweitzer TD, Muro S, Buerk DG, Solomides CC, Albelda SM, Patterson GA, and Muzykantov VR.** Immunotargeting of catalase to the pulmonary endothelium alleviates oxidative stress and reduces acute lung transplantation injury. *Nat Biotechnol* 21: 392–398, 2003.
23. **Kumasaka T, Quinlan WM, Doyle NA, Condon TP, Sligh J, Takei F, Beaudet A, Bennett CF, and Doerschuk CM.** Role of the intercellular adhesion molecule-1(ICAM-1) in endotoxin-induced pneumonia evaluated using ICAM-1 antisense oligonucleotides, anti-ICAM-1 monoclonal antibodies, and ICAM-1 mutant mice. *J Clin Invest* 97: 2362–2369, 1996.
24. **Langer R.** Drug delivery. Drugs on target. *Science* 293: 58–59, 2001.
25. **Lin L and Lobel P.** Production and characterization of recombinant human CLN2 protein for enzyme-replacement therapy in late infantile neuronal ceroid lipofuscinosis. *Biochem J* 357: 49–55, 2001.
26. **Lum H and Roebuck KA.** Oxidant stress and endothelial cell dysfunction. *Am J Physiol Cell Physiol* 280: C719–C741, 2001.
27. **Marsh EW, Leopold PL, Jones NL, and Maxfield FR.** Oligomerized transferrin receptors are selectively retained by a lumenal sorting signal in a long-lived endocytic recycling compartment. *J Cell Biol* 129: 1509–1522, 1995.
28. **McIntosh DP, Tan XY, Oh P, and Schnitzer JE.** Targeting endothelium and its dynamic caveolae for tissue-specific transcytosis in vivo: a pathway to overcome cell barriers to drug and gene delivery. *Proc Natl Acad Sci USA* 99: 1996–2001, 2002.
29. **Melis M, Pace E, Siena L, Spatafora M, Tipa A, Profita M, Bonanno A, Vignola AM, Bonsignore G, Mody CH, and Gjomarkaj M.** Biologically active intercellular adhesion molecule-1 is shed as dimers by a regulated mechanism in the inflamed pleural space. *Am J Respir Crit Care Med* 167: 1131–1138, 2003.
30. **Mu L and Feng SS.** A novel controlled release formulation for the anticancer drug paclitaxel (Taxol): PLGA nanoparticles containing vitamin E TPGS. *J Control Release* 86: 33–48, 2003.
31. **Mukherjee S, Ghosh RN, and Maxfield FR.** Endocytosis. *Physiol Rev* 77: 759–803, 1997.
32. **Mulligan MS, Vaporciyan AA, Miyasaka M, Tamatani T, and Ward PA.** Tumor necrosis factor alpha regulates in vivo intrapulmonary expression of ICAM-1. *Am J Pathol* 142: 1739–1749, 1993.
33. **Murciano JC, Muro S, Koniaris L, Christofidou-Solomidou M, Harshaw DW, Albelda SM, Granger DN, Cines DB, and Muzykantov VR.** ICAM-directed vascular immunotargeting of anti-thrombotic agents to the endothelial surface. *Blood* 101: 3977–3984, 2003.
34. **Muro S, Wiewrodt R, Thomas AP, Koniaris L, Albelda SM, Muzykantov VR, and Koval M.** A novel endocytic pathway induced by clustering endothelial ICAM-1 or PECAM-1. *J Cell Sci* 116: 1599–1609, 2003.
35. **Muzykantov VR.** Delivery of antioxidant enzyme proteins to the lung. *Antioxid Redox Signal* 3: 39–62, 2001.
36. **Muzykantov VR.** Targeting of superoxide dismutase and catalase to vascular endothelium. *J Control Release* 71: 1–21, 2001.
37. **Muzykantov VR, Christofidou-Solomidou M, Balyasnikova I, Harshaw DW, Schultz L, Fisher AB, and Albelda SM.** Streptavidin facilitates internalization and pulmonary targeting of an anti-endothelial cell antibody (platelet-endothelial cell adhesion molecule 1): a strategy for vascular immunotargeting of drugs. *Proc Natl Acad Sci USA* 96: 2379–2384, 1999.
38. **Panes J, Perry MA, Anderson DC, Manning A, Leone B, Cepinskas G, Rosenbloom CL, Miyasaka M, Kvietys PR, and Granger DN.** Regional differences in constitutive and induced ICAM-1 expression in vivo. *Am J Physiol Heart Circ Physiol* 269: H1955–H1964, 1995.
39. **Panyam J, Zhou WZ, Prabha S, Sahoo SK, and Labhasetwar V.** Rapid endo-lysosomal escape of poly(DL-lactide-co-glycolide) nanoparticles: implications for drug and gene delivery. *FASEB J* 16: 1217–1226, 2002.
40. **Pauly DF, Fraites TJ, Toma C, Bayes HS, Huie ML, Hirschhorn R, Plotz PH, Raben N, Kessler PD, and Byrne BJ.** Intercellular transfer of the virally derived precursor form of acid alpha-glucosidase corrects the enzyme deficiency in inherited cardioskeletal myopathy Pompe disease. *Hum Gene Ther* 12: 527–538, 2001.
41. **Polakovic M, Gorner T, Gref R, and Dellacherie E.** Lidocaine loaded biodegradable nanospheres. II. Modelling of drug release. *J Control Release* 60: 169–177, 1999.
42. **Poznansky MJ and Juliano RL.** Biological approaches to the controlled delivery of drugs: a critical review. *Pharmacol Rev* 36: 277–336, 1984.
43. **Predescu D, Predescu S, McQuistan T, and Palade GE.** Transcytosis of alpha1-acidic glycoprotein in the continuous microvascular endothelium. *Proc Natl Acad Sci USA* 95: 6175–6180, 1998.
44. **Prokop A, Kozlov E, Newman GW, and Newman MJ.** Water-based nanoparticulate polymeric system for protein delivery: permeability control and vaccine application. *Biotechnol Bioeng* 78: 459–466, 2002.
45. **Raso V.** Immunotargeting intracellular compartments. *Anal Biochem* 222: 297–304, 1994.
46. **Scheel J, Matteoni R, Ludwig T, Hoflack B, and Kreis TE.** Microtubule depolymerization inhibits transport of cathepsin D from the Golgi apparatus to lysosomes. *J Cell Sci* 96: 711–720, 1990.
47. **Scherpereel A, Wiewrodt R, Christofidou-Solomidou M, Gervais R, Murciano JC, Albelda SM, and Muzykantov VR.** Cell-selective intracellular delivery of a foreign enzyme to endothelium in vivo using vascular immunotargeting. *FASEB J* 15: 416–426, 2001.
48. **Springer TA.** Adhesion receptors of the immune system. *Nature* 346: 425–434, 1990.
49. **Swanson J, Burke E, and Silverstein SC.** Tubular lysosomes accompany stimulated pinocytosis in macrophages. *J Cell Biol* 104: 1217–1222, 1987.
50. **Varani J and Ward PA.** Mechanisms of endothelial cell injury in acute inflammation. *Shock* 2: 311–319, 1994.
51. **Villanueva FS, Jankowski RJ, Klibanov S, Pina ML, Alber SM, Watkins SC, Brandenburger GH, and Wagner WR.** Microbubbles targeted to intercellular adhesion molecule-1 bind to activated coronary artery endothelial cells. *Circulation* 98: 1–5, 1998.
52. **Weiner RE, Sasso DE, Gionfriddo MA, Syrbu SI, Smilowitz HM, Vento J, and Thrall RS.** Early detection of bleomycin-induced lung injury in rat using indium-111-labeled antibody directed against intercellular adhesion molecule-1. *J Nucl Med* 39: 723–728, 1998.
53. **Wiewrodt R, Thomas AP, Cipelletti L, Christofidou-Solomidou M, Weitz DA, Feinstein SI, Schaffer D, Albelda SM, Koval M, and Muzykantov VR.** Size-dependent intracellular immunotargeting of therapeutic cargoes into endothelial cells. *Blood* 99: 912–922, 2002.
54. **Wolin MS, Gupte SA, and Oeckler RA.** Superoxide in the vascular system. *J Vasc Res* 39: 191–207, 2002.
55. **Yayon A, Cabantchik ZI, and Ginsburg H.** Identification of the acidic compartment of *Plasmodium falciparum*-infected human erythrocytes as the target of the antimalarial drug chloroquine. *EMBO J* 3: 2695–2700, 1984.

Job: Niemeyer (098-0)
Chapter: 01/Muzykantov
Template: MiMB Box 9/Template/Rev 02.03
Pub. Date: July 1, 2004
Compositor: CC
Date: February 4, 2004
Revision: 1st Pass

1

Streptavidin–Biotin Crosslinking of Therapeutic Enzymes With Carrier Antibodies

Nanoconjugates for Protection Against Endothelial Oxidative Stress

Vladimir V. Shuvaev, Thomas Dziubla, Rainer Wiewrodt, and Vladimir R. Muzykantov

Summary

The streptavidin–biotin system may be used to synthesize immunoconjugates for targeted delivery of drugs, including therapeutic enzymes. The size of antibody–enzyme conjugates, which is controlled by the extent of biotinylation and molar ratio between the conjugate components, represents an important parameter that in some cases dictates subcellular addressing of drugs. This chapter describes the methodology of formation and characterization of polymeric immunoconjugates in the nanoscale range. A theoretical model of streptavidin conjugation based on general principles of polymer chemistry is considered. Factors that influence size and functional characterization of resulting polymer conjugates, as well as advantages and limitations of this approach, are described in detail. The protocols describe the formation of immunoconjugates possessing an antioxidant enzyme, catalase, directed to endothelial cells by anti-platelet endothelial cell adhesion molecule antibodies. However because of the modular nature of the streptavidin–biotin crosslinker system, the techniques herein can be easily adapted for the preparation of nanoscale immunoconjugates delivering other protein drugs to diverse cellular antigens.

Key Words: Immunoconjugates; vascular immunotargeting; polymerization; nanoscale carrier; catalase; streptavidin; biotin; dynamic light scattering; drug delivery.

1. Introduction

Targeted drug delivery, as attained by conjugating therapeutic enzymes with affinity carrier antibodies, promises a significant improvement over the current therapeutic means and, therefore, has remained the focus of intense research for several decades. For example, endothelial cells lining the luminal surface

From: *Methods in Molecular Biology, vol. 283: Bioconjugation Protocols: Strategies and Methods*
Edited by: C. M. Niemeyer © Humana Press Inc., Totowa, NJ

Job: Niemeyer (098-0)
Chapter: 01/Muzykantov
Template: MIB5x9/Template/Rev-02.03
Pub. Date: Jul 12 2004
Compositor: CC
Date: February 4, 2004
Revision: 1st Pass

of the vasculature represent an important target for delivery of antithrombotic, anti-inflammatory, antioxidant agents and genetic materials. Cell adhesion molecules (e.g., platelet endothelial cell adhesion molecule [PECAM] and intercellular adhesion molecule [ICAM]) represent very attractive endothelial determinants for vascular immunotargeting, for example, in the context of inflammation. Some drugs require intracellular uptake. Recent studies revealed that although endothelial cells do not internalize monomeric antibodies against PECAM and ICAM, one can facilitate intracellular delivery of therapeutic cargoes by controlling size of the anti-PECAM and anti-ICAM immunoconjugates in the nanoscale range *(1–3)*.

The biotin–streptavidin system can be used to synthesize nanoscale therapeutic immunoconjugates, providing an interesting alternative to other commonly pursued intravenous drug targeting strategies, such as liposomes and polymeric nanocarriers *(4–7)*. These immunoconjugates are typically characterized by (1) their high drug incorporation efficiency, (2) high drug to carrier ratio, (3) a wide tunable range of particles sizes with the same or similar composition, and (4) a relatively rigid and biodegradable structure. In optimal conditions, the degree of drug inclusion is so high that the level of free drug becomes negligible and a separation step may often be omitted. Several reporter and therapeutic enzymes conjugated with anti-PECAM and anti-ICAM have been successfully delivered in therapeutic levels to pulmonary endothelium *(1,2,8–11)*.

This chapter describes the methodology and detail protocols for the generation of nanoscale immunoconjugates using the polymeric form of the streptavidin–biotin system in addition to methods to control their size and shows examples of targeted delivery of an antioxidant therapeutic enzyme, catalase, to vascular endothelium in cell culture.

The distinguishing feature of the streptavidin–biotin system is the extraordinary affinity ($K_d = 10^{-15}$ *M*) of this noncovalent interaction. It may be compared only with systems involving liganded metal ions either as partial covalent bonds or chelates. This extremely specific almost irreversible reaction is widely used in biology and medicine *(12)*. If a biotin derivative is covalently linked to proteins, these biotinylated proteins will bind to streptavidin and form a conjugate. These conjugates can be categorized into two types depending on protein biotinylation level: oligomeric and polymeric conjugates. Oligomeric conjugates, which are readily used in many labeling techniques, occur when the protein contains less than two biotin residues per protein (**Fig. 1A**). However, when the average biotinylation level of the proteins (e.g., biotinylated antibody and enzyme) is equal to or exceeds 2, polymer structures can be formed (**Fig. 1B** and **C**). Because the linkage occurs through the paired coupling of

Fig. 1

Job: Niemeyer (098-0)
Chapter: 01/Muzykantov
Template: Mi[illegible]
Pub. Date: Ju[illegible]
Compositor: CC
Date: February 4, 2004
Revision: 1st Pass

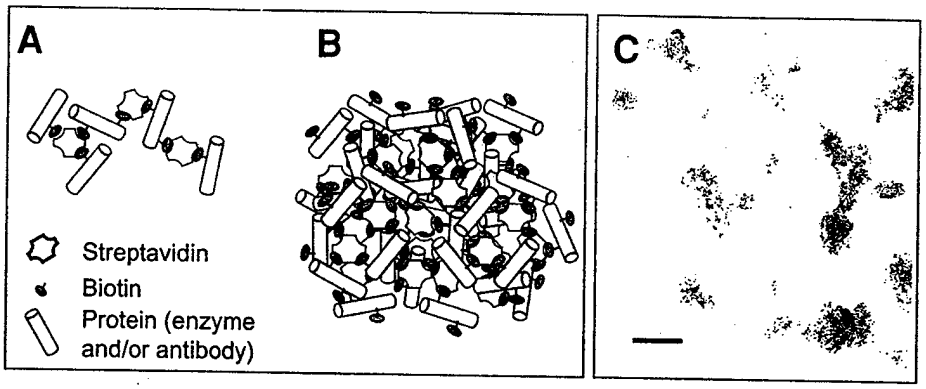

Fig. 1. Scheme of protein conjugation with streptavidin–biotin system. Proteins with less than 2 biotin/molecule form an oligomeric structure (**A**). Higher biotinylated proteins can switch polymerization reactions in the presence of streptavidin as a crosslinker with formation of polymeric structure (**B**). Polymer size depends on reactive conditions, probably a result of the high rate of streptavidin–biotin reaction and formation of internal core inaccessible for free copolymers. (**c**) Electron micrograph of negatively stained immunoconjugates. Conjugates were placed on grids precoated with thin carbon films, and negative staining was performed with uranyl acetate. Images were taken from representative areas at an original magnification of ×50,000 and enlarged to ×440,000. Scale bar = 100 nm.

specific subunits isolated on separate molecular species, it is convenient to relate these conjugates to the classic step (condensation) polymerization chemistry *(13)*. In this circumstance, the modified Carathor's equation applies to this reaction scheme.

$$X_n = \frac{1 + r}{1 + r - frp}$$

where X_n is the average number of monomer residues (both streptavidin and protein) per conjugate, r is the ratio of streptavidin molecules to protein molecules, f is the number of proteins that can bind to streptavidin, and p is the extent of reaction (number of available linkage sites that are actually linked). From this equation, it is noted that polymerization occurs only when the denominator approaches zero. Hence, it is possible to approximately know *a priori* what protein:streptavidin ratio, r, will provide the maximum conjugate size for a given biotinylation level. Also, because of the high sensitivity of the extent of reaction on X_n, small changes in polymerization procedures can have a large impact upon the final size of the conjugate.

Job: Niemeyer (098-0)
Chapter: 01/Muzykantov
Template: MiMB/Box9/Template/Rev.02.03
Pub. Date: Jul 1 2004
Compositor: CC
Date: February 4, 2004
Revision: 1st Pass

2. Materials

2.1. Equipment

1. Dynamic light scattering apparatus 90Plus Particle Sizer (Brookhaven Instruments Corp., NY) or similar apparatus.
2. UV-VIS spectrophotometer.
3. Microplate reader.
4. Gamma-counter.
5. Fluorescent microscope.

Au: Please provide city for Brookhaven Instruments, Corp.

2.2. Reagents and Proteins

1. Succinimidyl-6-(biotinamido) hexanoate (NHS-LC-Biotin; Pierce, Rockford, IL).
2. 2-(4'-hydroxyazobenzene) benzoic acid (HABA; Pierce).
3. o-Phenylenediamine (OPD, in tablets of 60 mg; Sigma, St. Louis, MO).
4. $Na^{51}CrO_4$ (Perkin Elmer, Boston, MA).
5. Dimethylformamide (DMF).
6. Hydrogen peroxide (H_2O_2).
7. Glycerol.
8. Catalase from bovine liver (Calbiochem, CA).
9. Streptavidin from *Streptomyces avidinii* (Calbiochem).
10. Avidin (Pierce).
11. Horseradish peroxidase (HRP).
12. Monoclonal anti-PECAM antibody (clone 62 was generously provided by Dr. Nakada; Centocor).
13. Mouse IgG (Calbiochem).

Au: Please provide city for Calbiochem. Please provide city and state/country for Centocor.

2.3. Buffers, Media, and Cells

1. Phosphate-buffered saline (PBS): 0.1 *M* sodium phosphate, 0.15 *M* sodium chloride, pH 7.2.
2. HABA stock solution: 10 m*M* HABA in 10 m*M* NaOH. Add 24.2 mg to 10 mL of 10 m*M* NaOH. The solution may be stored at 4°C.
3. HABA/avidin working solution: dissolve 10 mg of avidin in 19.4 mL PBS and add 600 µL of 10 m*M* HABA stock solution.
4. Cell culture medium: M199 medium (Gibco, Grand Island, NY), 10% fetal calf serum (Gibco) supplemented with 100 µg/mL heparin (Sigma), 2 m*M* L-glutamine (Gibco), 15 µg/mL endothelial cell growth supplement (Upstate, Lake Placid, NY), 100 U/mL penicillin, and 100 µg/mL streptomycin.
5. RPMI 1640 medium without phenol red (Gibco).
6. Human umbilical vein endothelial cells (HUVEC; Clonetics, San Diego, CA).

3. Methods

3.1. Biotinylation of IgG Antibodies and Catalase

1. Dissolve IgG (anti-PECAM antibody or any other mouse IgG) and catalase in 0.1 *M* PBS to concentrations of 3.5 and 5.0 mg/mL, respectively. Considering

that molecular masses of IgG and catalase are 150 and 240 kDa, respectively, their molar concentrations are 23.3 μ*M* and 20.8 μ*M*, respectively.

2. Prepare fresh 0.1 *M* NHS-LC-biotin in DMF, that is, dissolve 4.5 mg NHS-LC-biotin in 100 μL of anhydrous DMF. Keep solutions of proteins and NHS-LC-biotin on ice.
3. Add appropriate volume of 0.1 *M* NHS-LC-biotin to protein solution to have 5-, 10-, and 15-fold biotin:protein molar excess using following equation:

$$V_{NHS-Biotin} = kV_{protein}\left(\frac{C_{protein}}{C_{NHS-Biotin}}\right)$$

where $V_{NHS\text{-}biotin}$ and $V_{protein}$ are the volumes of NHS-LC-biotin and protein (antibody or catalase), respectively in μL; $C_{NHS\text{-}biotin}$ and $C_{protein}$ are the molar concentrations of NHS-LC-biotin and protein (antibody or catalase), respectively in m*M*; k is molar excess of biotin label. Thus, add 1.2, 2.3, and 3.5 μL of 0.1 *M* NHS-LC-biotin to 1 mL of antibody solution and 1.0, 2.1, and 3.1 μL of 0.1 *M* NHS-LC-biotin to 1 mL of catalase solution. Vortex the samples.

4. Incubate the samples on ice for 2 h.
5. Remove unbound biotin derivatives by dialysis against 1.0 L of PBS with three changes.
6. Measure protein concentration in catalase and antibody preparations by A_{280} absorbance using following coefficients: A(0.1%) 1.04 for catalase and 1.7 for IgG. Bradford assay (Bio-Rad) or other protein assays may be used as well.
7. Split antibody preparation in Eppendorf tubes 100 μL/tube and store at –80°C (or –20°C) because IgG at 4°C can easily aggregate and even partial aggregation of IgG may significantly affect further conjugation. Catalase may be stored in PBS at 4°C during several months without significant loss of its activity.

3.2. Estimation of Protein Biotinylation Level

1. Add 450 μL of HABA/avidin working solution into plastic spectrophotometric cuvet and measure absorbance at 500 nm A°. Add 50 μL of sample, mix it in cuvet and measure A'_{500}. Biotin competes with HABA for same binding sites on avidin and releases HABA in free solution that in turn decreases the absorbance of the dye. Because the reaction may require 2–5 min to be complete, check the absorbance several times and take into calculation only the value after absorbance was stabilized for at least 15 s.
2. Calculate molar concentration of biotin using following equation:

$$[biotin, \mu M] = \frac{(D' \times A^{\circ} - A') \times D'' \times 10^6}{\varepsilon_{HABA}}$$

where D' is dilution coefficient for HABA/avidin working solution D' = 0.9; D' is dilution coefficient of the sample D" = 50 μL/500 μL = 10;
10^6 is a coefficient to express biotin concentration in μ*M*; ε_{HABA} is molar extinction coefficient of HABA bound to avidin at 500 nm that equals 34000 AU × $M^{-1}cm^{-1}$.

Job: Niemeyer (098-0)
Chapter: 01/Muzykantov
Template: MiMB/Style9/Template/Rev 02.03
Pub. Date: Jul 1 2004
Compositor: CC
Date: February 4, 2004
Revision: 1st Pass

Considering all known parameters the equation may be easily transformed into a simple formula:

$$[biotin, \mu M] = (0.9 \times A^{\circ} - A') \times 294$$

3. Calculate protein biotinylation using following equation:

$$\text{Protein Biotinylation} = \frac{[biotin, \mu M]}{[Protein, \mu M]}$$

3.3. Conjugation

Immunoconjugates may be prepared by a one-step or two-step procedure. In both cases, the molar ratio between biotinylated protein that should be specifically delivered (i.e., catalase) and biotinylated antibody that targets specific antigen on cell surface (i.e., anti-PECAM) is kept constant. As a rule, the catalase:anti-PECAM ratio is 1:1 mol/mol. In contrast, an optimal concentration of streptavidin (with respect to the desired conjugation size) varies and should be determined for each preparation of biotinylated ligands. In the one-step procedure, biotinylated proteins (enzyme and antibody) are premixed and then streptavidin is added to conjugate them. In two-step procedure, biotinylated enzyme is first conjugated with streptavidin and then antibody is added to form the larger secondary conjugate.

3.3.1. One-Step Procedure

3.3.1.1. Streptavidin Titration

1. Prepare 110 µL of catalase/antibody mixture with the molar ratio 1:1 in PBS. For that, mix 58 µL of 5.0 mg/mL catalase and 52 µL of 3.5 mg/mL anti-PECAM. All components for conjugation are to be kept on ice.
2. Split the mixture into 5 aliquots of 20 µL each in 1.5-mL transparent Eppendorf tubes.
3. Add 10.0 mg/mL streptavidin solution in PBS to have final molar ratio streptavidin:(catalase + antibody) 0.5, 1.0, 1.5, 2.0, and 2.5 (i.e., add 1.3, 2.6, 4.0, 5.3, and 6.6 µL of streptavidin, respectively). The conjugation should be performed while vortexing. Continuous and regular mixing is critical for correct conjugation.
4. Measure the mean effective diameter of the obtained conjugates by dynamic light scattering (DLS). Add 180 µL of PBS to each conjugate sample, mix it well, and transfer the diluted sample into NMR tube for the analysis on DLS apparatus 90Plus Particle Sizer. Count rate should be from 100 kcps to 1 Mcps. Run the sample for at least 3 min and determine effective diameter (*see* **Note 7**).
5. Plot the effective diameter of conjugates as a function of streptavidin/(catalase + antibody) molar ratio. Make additional points if necessary. The standard streptavidin titration curve is bell shaped, similar to the classical antigen–anti-

Au: Please cite all Notes in the text (sequentially).

Job: Niemeyer (098-0)
Chapter: 01/Muzykantov
Template: MiMB/6x9/Template/Rev-02.03
Pub. Date: Jul 1 2004
Compositor: CC
Date: February 4, 2004
Revision: 1st Pass

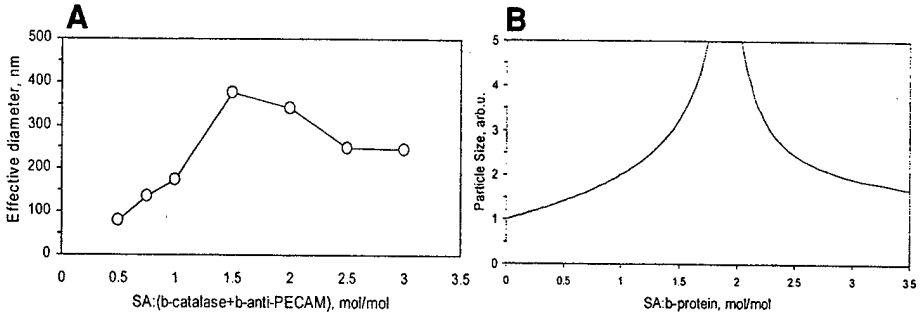

Fig. 2. Titration of biotinylated proteins (catalase and anti-PECAM antibody) with streptavidin. **A,** Catalase was mixed with antibody, and streptavidin was added as a bulk to conjugate both proteins. Size was measured by DLS. **B,** Modeling of conjugation reaction. Parametric addition of Carathor's equation with streptavidin as the limiting reagent (streptavidin:protein <1.0) and protein as the limiting reagent (streptavidin:protein >1). The extent of reaction was selected such that these two equations converged to a maximum value. Degree of polymerization was related to particle size through the r^2 relationship of conjugate molecular weight to radius of gyration.

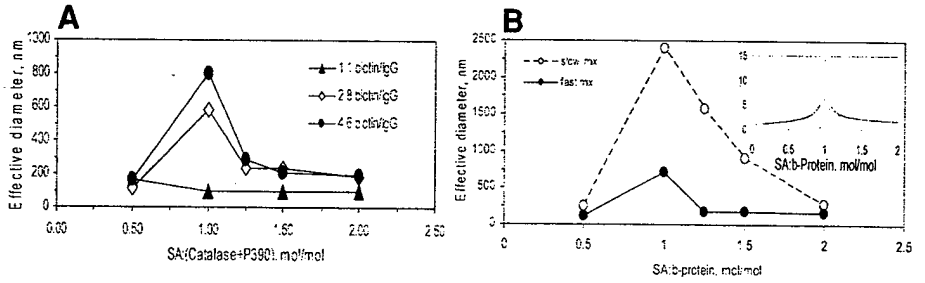

Fig. 3. Effects of biotinylation level and mixing conditions on size of immunoconjugate. (**A**) Catalase at a level of biotinylation of 12 biotin/tetramer was mixed with antibody of indicated biotinylation at a molar ratio 1:1. Streptavidin was added as a bulk. (**B**) The rate of streptavidin addition affects the size of conjugate. Streptavidin was added as a bulk (closed circles) or at slow rate of about 5 μL/min. Insert shows theoretical modeling of this effect. An increase in the extent of reaction results in an increase in the maximum of the titration curve. It is hypothesized that by adding reactants slowing, the likelihood of steric shielding of binding sites is reduced. This results in an overall increase in the extent of reaction and the conjugate size.

body precipitation titration curves. Higher biotinylated component(s) produces larger conjugates (*see* **Subheading 3.5.1.** as well as **Figs. 2A** and **3A** for examples).

Job: Niemeyer (098-0)
Chapter: 01/Muzykantov
Template: MiMB Box 9/Template/Rev 02.03
Pub. Date: Jul 1 2004
Compositor: CC
Date: February 4, 2004
Revision: 1st Pass

3.3.1.2. Preparation of Conjugate Stock

1. Chose optimal streptavidin:(catalase + antibody) molar ratio that gives you the required size of conjugate (*see* **Subheading 3.3.1.1., step 5**).
2. Prepare 100 μL of catalase + antibody mixture with the molar ratio 1:1 in PBS. Mix 53 μL of 5.0 mg/mL catalase and 47 μL of 3.5 mg/mL anti-PECAM.
3. Calculate the volume of 10 mg/mL streptavidin that should be added to reach a specific molar ratio. For example, if you found that the optimal molar ratio is 2, add 26.4 μL of 10.0 mg/mL streptavidin.
4. Add 5 μL of the conjugate preparation to 195 μL of PBS. Transfer the diluted sample into NMR tube and measure the effective diameter of obtained conjugates by DLS. Upscaling may change the size of conjugate. If this occurs, then adjustment in volume of streptavidin should be done to correct optimal streptavidin:protein molar ratio.

3.3.2. Two-Step Procedure

3.3.2.1. Titration by Streptavidin

1. Transfer 10.6-μL aliquots of 5.0 mg/mL biotinylated catalase into five 0.5-mL Eppendorf tubes.
2. In the first conjugation step, add 1.3, 2.6, 4.0, 5.3, and 6.6 μL of 10 mg/mL streptavidin per tube. Addition of streptavidin solution should be as fast as possible while the sample is at constant vortexing. Keep vortexing for several seconds after streptavidin was added. Spin it down briefly.
3. Incubate 5 min on ice.
4. In the second conjugation step, add 9.4 μL of 3.5 mg/mL anti-PECAM to all five samples in a similar way as in first conjugation step. Final streptavidin:(catalase + antibody) molar ratios are 0.5, 1.0, 1.5, 2.0, and 2.5, respectively.
5. Measure the effective diameter of obtained conjugates by DLS (*see* **Subheading 3.3.1.1., step 4,** and **Note 7** for details).
6. Plot the effective diameter of conjugates as a function of streptavidin:(catalase + antibody) molar ratio. Make additional points if necessary. Higher biotinylated component(s) produces larger conjugates (*see* **Subheading 3.5.1.**, for example).

3.3.2.2. Preparation of Conjugate Stock

1. Chose optimal streptavidin:(catalase + antibody) molar ratio that gives you required size of the conjugate (*see* plot obtained in **Subheading 3.3.2.1., step 6**).
2. Transfer 53 μL of 5.0 mg/mL biotinylated catalase into 1.5-mL transparent Eppendorf tubes.
3. In the first conjugation step, add specified quantity of streptavidin. For example, if you found that the final streptavidin:(catalase + antibody) molar ratio has to be 2, add 26.4 μL of 10 mg/mL streptavidin. Addition of streptavidin solution should be as fast as possible while the sample is at constant vortexing. Keep vortexing for several seconds after streptavidin was added, spin it down and incubate sample during 5 min on ice.

Job: Niemeyer (098-0)
Chapter: 01/Muzykantov
Template: MiMB_Bv9/Template/Rev.02.03
Pub. Date: Ju[illegible]
Compositor: CC
Date: February 4, 2004
Revision: 1st Pass

4. In the second conjugation step, add 47 μL of 3.5 mg/mL anti-PECAM to primary conjugate in a similar way as in first conjugation step.
5. Mix 5 μL of the final conjugate preparation with 195 μL of PBS. Transfer the diluted sample into NMR tube and measure an effective diameter of obtained conjugates by DLS. Upscaling may slightly change the size of conjugate compared with results of streptavidin titration using small volumes. In this case adjustment in volume of streptavidin should be done to correct optimal streptavidin:protein molar ratio.

3.3.3. Storage of Conjugate

Because conjugates tend to aggregate, keeping them at 4°C for longer than several hours is not recommended. Freezing is also not recommended for the same reason of material aggregation after thawing. To store conjugate for further use, add glycerol to 50% and keep the preparation at –20°C. Under these conditions, no significant changes in conjugate size, catalase enzymatic activity, and antibody binding occur for at least 1 wk.

3.4. Characterization of Conjugates In Vitro

To be therapeutically functional, immunoconjugates should preserve both its activities: enzymatic activity of catalase and antibody binding to cell antigen. Because the conjugation process may affect both protein components, functional activity of the conjugates must be tested in vitro before more expensive and challenging in vivo studies. For example, protection assay against H_2O_2-induced injury of endothelial cell culture reveals functional activity of the catalase conjugate.

3.4.1. Catalase Activity

1. Prepare 10X stock solution of assay buffer: 50 m*M* sodium phosphate, pH 7.0.
2. Prepare working solution: dilute 75 μL of 3% H_2O_2 in 10 mL 1X assay buffer.
3. Take 1 mL of working solution and add catalase (as free enzyme or conjugate) to final concentration of 0.1–1.0 μg of catalase/mL.
4. Place the sample immediately in a quartz cuvet into UV-VIS spectrophotometer and follow the kinetics of H_2O_2 degradation at 242 nm.
5. Measure the slope of the curve ΔA/min using initial linear fragment and calculate catalase activity as follows:

$$\text{Catalase activity, U/mg} = 23.0(\Delta A/\text{min})/\text{mg of catalase}$$

3.4.2. Protection Against Hydrogen Peroxide Cytotoxicity

1. Pretreat a 24-well plate with 0.5 mL/well of 1% gelatin for 1 h, remove the solution ,and allow it to dry out for 1 h. Plate HUVEC (4th passage) in the plate at a cell density of 50,000–100,000 cell/well in cell culture medium. Grow cells for

Job: Niemeyer (098-0)
Chapter: 01/Muzykantov
Template: MiMB5x9/Template/Rev.02.03
Pub. Date: Jul 1 2004
Compositor: CC
Date: February 4, 2004
Revision: 1st Pass

3–4 d until confluent culture. One day before the experiment, replace the medium with a fresh one containing 200,000 cpm/mL of [^{51}Cr] as $Na^{51}CrO_4$.

2. The next day, wash out free [^{51}Cr] with fresh cell culture medium and add 0.25 mL/well of catalase/anti-PECAM immunoconjugates (*see* **Subheading 3.3.1.2.**) diluted with the medium at a concentration of 5–10 μg of catalase/well. Incubate cells for 1 h at 37°C. Wash out unbound conjugates first with fresh cell culture medium and then with phenol red-free RPMI medium.
3. Induce oxidative stress by addition of 5 m*M* H_2O_2 in RPMI (i.e., 257 μl/50 mL of RPMI) and incubate cells at 37°C for 5 h.
4. Place an aliquot of 20 μL of supernatant into 96-well low-binding plate at 0, 15, 30, 45, and 60 min for the H_2O_2 degradation assay. In the meantime, prepare calibration curve by placing 0, 5, 10, 15, and 20 μL of 5 m*M* H_2O_2 in duplicates and adjust the volume with RPMI.
5. For the H_2O_2 degradation assay, prepare fresh OPD/HRP working solution: dissolve one 60-mg tablet of OPD in 17.5 mL of PBS on rotating platform or orbital shaker and add 100 μL of 1 mg/mL HRP. Add 180 μL of OPD/HRP working solution to sample-containing wells on 96-well plate. Incubate the plate on ELISA shaker for 15 min. Stop the reaction by addition of 50 μL/well of 50% H_2SO_4. Read the absorbance in microplate reader at 490 nm. Calculate the H_2O_2 concentration in the samples using calibration curve.
6. To detect of [^{51}Cr] release, after a 5-h incubation take 100 μL of cell culture supernatant into tubes for gamma-counter. Pool the rest of supernatant and cell lysate with 0.5 mL of 1% Triton X-100, 1.0 *M* NaOH. Measure radioactivity in the samples and calculate the % of released [^{51}Cr].

3.5. Results

3.5.1. Conjugate Preparation

Catalase was biotinylated to a level of 3.25 biotin/catalase monomer (or approx 12–13 biotin/catalase tetramer) and monoclonal anti-PECAM antibody was biotinylated to 3.5 biotin/IgG. Both proteins were mixed at a molar ratio 1:1, and streptavidin was added to form conjugates. The titration curve of the conjugation is shown in **Fig. 2A** as a dependence of conjugate effective diameter determined by DLS on molar ratio streptavidin:biotinylated proteins. The curve demonstrates a continuous increase of the conjugate size at relative excess of biotinylated proteins (**Fig. 2A**, right shoulder of the curve). The maximum is reached at equimolar ratio between accessible biotin-binding sites on streptavidin and available biotins on proteins. Thus the position of the maximum will depend on effective number and flexibility of biotins on the proteins, size and structure of the proteins and mixing conditions. Further increase of streptavidin concentration results in relative excess of streptavidin and decreasing of conjugate size (**Fig 2A**, left shoulder). Noteworthy, the left shoulder has a plateau supposedly because the reaction between biotin and streptavidin is so fast that a rate of mixing of two these components is always a limiting step.

Au/PE: Comp was instructed to place Figs. 2 and 3 at the end of Subheading 3.3.1.1., step 5. before figures were actually mentioned in text. Is this okay?

Job: Niemeyer (098-0)
Chapter: 01/Muzykantov
Template: MiMB Rev.9/Template/Rev.02.03
Pub. Date: Jul 1 2004
Compositor: CC
Date: February 4, 2004
Revision: 1st Pass

Au: Please define SA if possible.

Based upon the Carathor's equation, the relative concentration of the two reagents (SA and biotinylated protein) is one of the key determinants in the ultimate number of proteins per conjugate. As such, by varying the ratio of streptavidin to biotinylated protein, it is theoretically possible to control the size of particle. If we use the average biotinylation of catalase and antibody at a converging extent of reaction, a theoretical titration curve with a maximum at 1.95 streptavidin:proteins molar ratio is obtained (**Fig. 2B**). This is very close to the actual maximum obtained in experiment (compare with **Fig. 2A**). Deviations from theory are most likely the result of the presence of proteins with two distinct biotinylation levels (i.e., catalase and antibody). Also, the extent of reaction is dependent upon size of conjugate, which is not considered in the model presented. Although this model is limiting in its ability to account for varying accessible functionality with extent of reaction, it still demonstrates the sensitivity of size on reaction conditions.

The size of resulting conjugate depends on biotinylation level of protein(s). Biotinylated catalase was mixed with antibody biotinylated at different extents (**Fig. 3A**). Higher biotinylated antibody formed larger conjugates. The rate of streptavidin addition is another important parameter that affects the size of conjugate. Slow addition of streptavidin leads to increased size of forming conjugates compared to instant mixing (**Fig. 3B**). This dependence of particle size on mixing conditions can also be accounted for by the extent of reaction in the Carathor's. Because the reaction rate proceeds nearly instantaneously, mixing conditions will greatly affect the extent of reaction. As such, experiment agrees well with theory that the increase in reaction mixing results in a decrease in extent of reaction, and therefore results in smaller maximum particle sizes (**Fig. 3B**, insert).

3.5.2. Conjugate Characterization

We prepared catalase/anti-PECAM immunoconjugates for further characterization. The conjugates were analyzed by high-performance liquid chromatography gel filtration. We could detect only trace amounts of free catalase in conjugate preparation, whereas practically all streptavidin and antibody were apparently included in conjugates (**Fig. 4A**). Thus use of the conjugates does not require additional step of conjugate separation from free component. Conjugation only slightly decreased activity of catalase. Its activity in the conjugate was measured to be 80% of initial catalase activity in free solution. Furthermore, the binding of the conjugates was visualized by immunofluorescence microscopy using fluorescein isothiocyanate-labeled antimouse IgG antibody. The conjugates readily bound to cultured human endothelial cells (**Fig. 4B**). Interestingly, they are mostly localized on cell-cell borders in accordance to PECAM distribution in confluent culture (*14*).

Fig. 4

Job: Niemeyer (098-0)
Chapter: 01/Muzykantov
Template: Mi[illegible]
Pub. Date: Ju[illegible]
Compositor: CC
Date: February 4, 2004
Revision: 1st Pass

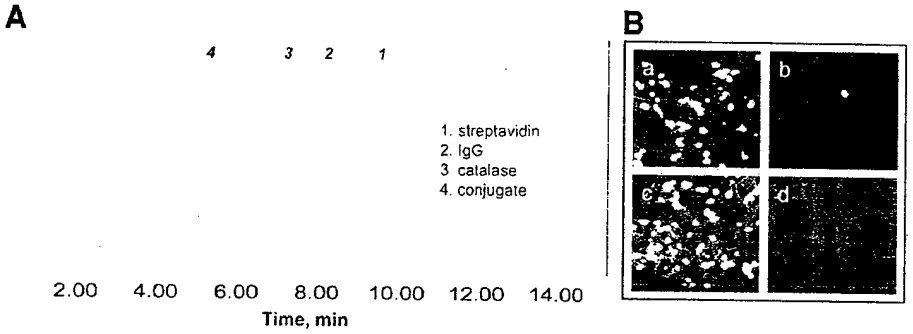

Fig. 4. Characterization of immunoconjugates. (**A**) High-performance liquid chromatography analysis of catalase/anti-PECAM immunoconjugates on SW-300 gel-filtration column (Waters, MA). The conjugation was performed by the one-step procedure. The immunoconjugate and its individual components were injected in phosphate buffer. Normalized chromatograms are shown. (**B**) Binding of the immunoconjugates to HUVECs. Catalase/anti-PECAM (a and c) or catalase/nonimmune IgG (b and d) 300-nm immunoconjugates at a concentration of 5 μg of catalase/well were incubated with confluent cell culture. Cells were fixed without (a and b) or with (c and d) after permeabilization and conjugates were stained using fluorescein isothiocyanate-labeled anti mouse IgG. Samples were analyzed by fluorescence microscopy.

The conjugates were used for protecting endothelial cells against oxidative stress (**Fig. 5**). HUVECs were preincubated with catalase/anti-PECAM antibody at different doses of catalase (0.1–5.0 μg of catalase/well as indicated) and protective properties of the bound conjugates were analyzed by H_2O_2 degradation assay, [^{51}Cr] release, and visually by phase-contrast microscopy. Enzymatic activity of the bound conjugates estimated by H_2O_2 degradation assay showed dose-dependent response up to 5 μg of catalase/well (**Fig. 5A**). However, only doses of 1.0 and 5.0 μg of catalase/well were protective as detected by [^{51}Cr] release (**Fig. 5B**). Phase-contrast microscopy also demonstrated that those doses protected cells against oxidative stress compared to cells untreated with the conjugates (**Fig. 5 C**). Fig. 5

4. Notes

4.1. Biotinylation

1. It is important to remember that biotinylation depends on initial concentration of protein. The level of biotinylation is increased at a higher concentration of protein even at same NHS-LC-biotin:protein molar ratio.

Job: Niemeyer (098-0)
Chapter: 01/Muzykantov
Template: MiMB/x9/Template/Rev-02-03
Pub. Date: Jul 1 2004
Compositor: CC
Date: February 4, 2004
Revision: 1st Pass

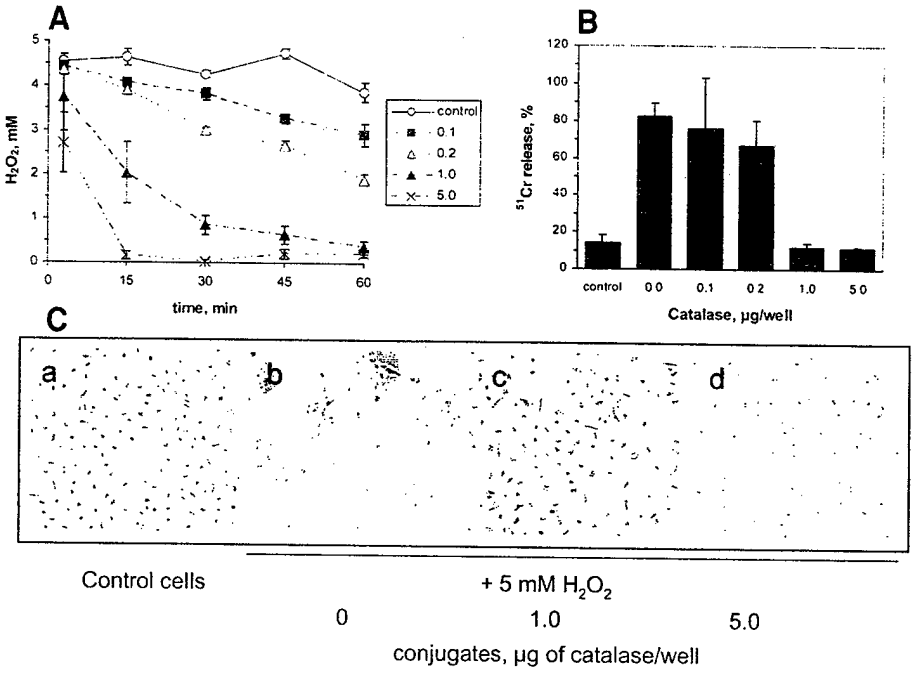

Fig. 5. Cell protection against H_2O_2-induced oxidative stress by catalase/anti-PECAM immunoconjugates. Cells were treated with the immunoconjugates as described in **Subheading 3.4.2.** at several concentrations. (**A**) Degradation of H_2O_2 by bound catalase-containing conjugates. Initial concentrations of immunoconjugates used for cell treatment are indicated in micrograms of catalase/well. (**B**) Cell death as a result of severe oxidative stress was analyzed by release of [^{51}Cr]. Cells were incubated with 5 m*M* H_2O_2 for 5 h. Release of [^{51}Cr] in control cells shows level of passive diffusion whereas practically complete [^{51}Cr] release in the absence of immunoconjugates demonstrates significant cell death (**C**).

2. Biotinylation efficiency and its effects on protein activities vary significantly from protein to protein. In case of catalase, biotinylation does not change the catalytic activity at up to a level of 4–5 biotin/catalase monomer.

4.2. Estimation of Protein Biotinylation Level

3. HABA is not readily soluble in 10 m*M* NaOH and requires 10–20 min of intense vortexing.
4. HABA will change its color from yellow to amber because the dye instantly interacts with avidin. HABA/avidin working solution may be stored during 2–4 wk at 4°C. Absorbance of the solution at 500 nm should be 0.9–1.3 AU (we

recommend to adjust it to 0.95–1.05 AU with HABA appropriately diluted in PBS to keep constant concentration of HABA).

5. Absorbance of working solution after addition of biotin should be no less than 0.35–0.4. Otherwise the sample of biotinylated protein will have to be diluted.

4.3. Conjugation

6. A number of factors are important in conjugation and may affect a size of particles:a.
   a. Streptavidin:protein ratio is the most important parameter. A titration curve is required for each new preparation of biotinylated catalase or antibody.
   b. The optimal biotinylation level should be estimated experimentally for every protein. To produce 150- to 400-nm conjugates, proteins have to be biotinylated to a level of 3–4 biotin/catalase monomer or IgG. Under-biotinylated protein may form too small particles and does not reach desired size. It may be rebiotinylated. Overbiotinylated protein will form precipitates and titration curve does not show a visible maximum. Such proteins cannot be used for conjugation.
   c. Reaction between streptavidin and biotin is so fast that mixing conditions are able to change size of formed conjugates. Instant addition of streptavidin is recommended because it is easier to control. However, you can prepare larger conjugates if you inject streptavidin slower. It can be useful tool for preparation conjugates of different size and essentially same composition.
   d. Although we usually look on the left shoulder of the titration curve to find the optimal condition for conjugation, it is possible to use right steep shoulder as well. An advantage of using the right shoulder is that streptavidin may be added in several steps with control of the conjugate size after each step.
7. DLS is an attractive technique in measuring conjugate size because this is an absolute method that does not require preliminary calibration or standards. It is fast, reliable, direct technique and the easiest method to measure particles sizes in the 20- to 1000-nm range. However, DLS is based on the principle of light scattering of moving objects that implies specific limitations on preparation of sample and its reading. There are a number of important issues that should always be taken into consideration to obtain meaningful values. First of all, it is important to possess a rudimentary knowledge of the theory to effectively use the machine. Briefly, at a moment in time, particles in solution will scatter light with a particular intensity at a set angle (at 90° in case of 90Plus Particle Sizer). If we wait for some time (Δt) and then check the scattering intensity, the intensity will change as a result in the change of particle orientation. If Δt is very small, then the intensity will not change very much, because the particles have not had enough time to move around in solution. However, as Δt increases, the chances of the intensity being the same (autocorrelating) will decrease dramatically. This dependence of intensity autocorrelation on time is directly related to the ability of particles to randomly move. If we assume the particles move according to the rules of Brownian motion, we can obtain equations that describe the speed of

Au: This section is a little different from manuscript hardcopy.

Job: Niemeyer (098-0)
Chapter: 01/Muzykantov
Template: MiMB5x9/Template/Rev.02.03
Pub. Date: Jul 2004
Compositor: CC
Date: February 4, 2004
Revision: 1st Pass

particle motion as a function of particle size. Hence, we can relate the decay in the autocorrelation directly to particle size. When the assumptions built into the math equations are accurate, then the DLS provides a rapid reliable means of measurement. In practical circumstances, the following points should be kept in mind when analyzing data:

a. Monitor the count rate to insure that samples are not too dilute or too concentrated for calculations (100 kcps to 1 Mcps). If the count rate is too small, then random fluctuations (e.g., dust particles) will impose very large error in the readings, and very long measurement times will be necessary to average out these occurrences. However, if concentration is too large, then particle–particle interactions become significant, and the Brownian motion is no longer valid.

b. Check at least four different fitting functions to verify particle size. To account for particle size distributions, the autocorrelator can impose different distribution functions to calculate a size and dispersity (linear, quadratic, and so on). Particle sizes calculated from each of these functions should agree seemingly well with each other. If they do not, or if dispersities are rather large (>0.2), then keep in mind that measured particle sizes are not guaranteed.

c. A simple way to evaluate homogeneity in the sample is by monitoring the shape of the decay curve at the point where the autocorrelation goes to zero. If this curve is smooth, and drops down to zero, then particles are nicely dispersed. If the curve is other than exponential and does not go to zero, particle sizes are very high and not well distributed. Typically we consider a reading is good when the autocorrelation curve is linear for 2 logs, which is rare for conjugates larger than 300–400 nm.

8. Appropriate storage of conjugates may be critical for experiments that have to be performed at a different time or location. In this case, the major obstacle is the general tendency of immunoconjugates to aggregate with time. We found that aggregation of conjugates can be slowed down or prevented by increasing viscosity of the solution. Good results were obtained by storage of conjugates in 30% or 50% at –20°C. Under these conditions, 30% glycerol was enough to slow down aggregation for 1–2 d. However, longer incubation revealed some aggregation. Storage in 50% glycerol apparently completely prevents aggregation, as size of conjugates was stable for at least 1 yr (**Fig. 6**). Protective and enzymatic activities of catalase/anti-PECAM conjugates were practically intact after at least 1 wk. It is important to remember that glycerol affects DLS reading by changing the viscosity of solution. Thus, effects of storage in glycerol should always be compared vs. freshly prepared samples in the same concentration of glycerol.

Fig. 6

Acknowledgments

We thank Drs. Thomas Sweitzer, Arnaud Scherpereel, and Ms. Anu P. Thomas for critically important contributions to the previous studies, which provided experimental background for development of the protocols outlined in

Job: Niemeyer (098-0)
Chapter: 01/Muzykantov
Template: MiMB_v9/Template/Rev_02_03
Pub. Date: Jul 1 2004
Compositor: CC
Date: February 4, 2004
Revision: 1st Pass

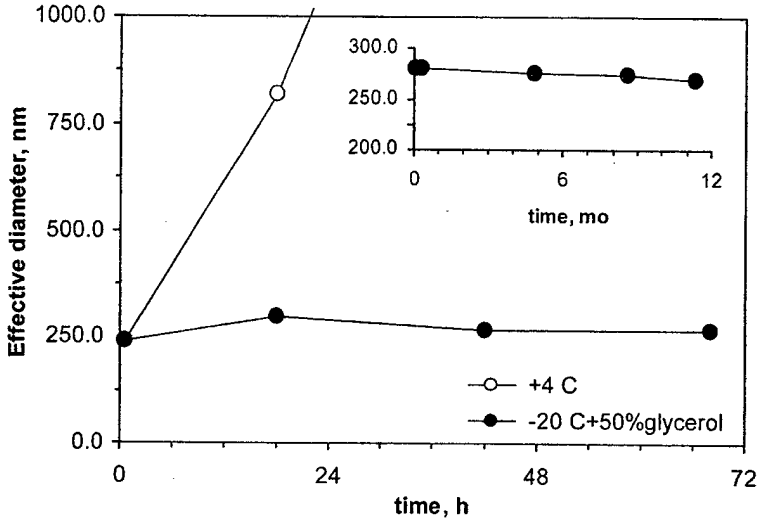

Fig. 6. Effects of viscosity on conjugate aggregation. Storage of conjugate at +4°C in PBS results in significant aggregation and imminent precipitation of immunoconjugate (open circles) whereas 50% glycerol at –20°C prevents their change in size for both short-term (closed circles) and long-term storage (insert).

this chapter. This work was supported by NIH SCOR in Acute Lung Injury (NHLBI HL 60290, Project 4), NHLBI RO1 HL/GM 71175-01, and the Department of Defense Grant (PR 012262) to VRM.

References

1. Muzykantov, V. R., Christofidou-Solomidou, M., Balyasnikova, I., Harshaw, D. W., Schultz, L., Fisher, A. B., et al. (1999) Streptavidin facilitates internalization and pulmonary targeting of an anti-endothelial cell antibody (platelet-endothelial cell adhesion molecule 1): a strategy for vascular immunotargeting of drugs. *Proc. Natl. Acad. Sci. USA* **96,** 2379–2384.
2. Wiewrodt, R., Thomas, A. P., Cipelletti, L., Christofidou-Solomidou, M., Weitz, D. A., Feinstein, S. I., et al. (2002) Size-dependent intracellular immunotargeting of therapeutic cargoes into endothelial cells. *Blood* **99,** 912–922.
3. Muro, S., Wiewrodt, R., Thomas, A., Koniaris, L., Albelda, S. M., Muzykantov, V. R., et al. (2003) A novel endocytic pathway induced by clustering endothelial ICAM-1 or PECAM-1. *J. Cell Sci.* **116,** 1599–1609.
4. Lasic, D. D. (1998) Novel applications of liposomes. *Trends Biotechnol.* **16,** 307–321.
5. Panyam, J. and Labhasetwar, V. (2003) Biodegradable nanoparticles for drug and gene delivery to cells and tissue. *Adv. Drug Deliv. Rev.* **55,** 329–347.

Job: Niemeyer (098-0)
Chapter: 01/Muzykantov
Template: MiMB5x9/Template/Rev.02.03
Pub. Date: Jul 1 2004
Compositor: CC
Date: February 4, 2004
Revision: 1st Pass

6. Muzykantov, V. R. (1997) Conjugation of catalase to a carrier antibody via a streptavidin-biotin cross-linker. *Biotechnol. Appl. Biochem.* **26,** 103–109.
7. Muzykantov, V. R. (2001) Delivery of antioxidant enzyme proteins to the lung. *Antioxid. Redox. Signal.* **3,** 39–62.
8. Atochina, E. N., Balyasnikova, I. V., Danilov, S. M., Granger, D. N., Fisher, A. B., and Muzykantov, V. R. (1998) Immunotargeting of catalase to ACE or ICAM-1 protects perfused rat lungs against oxidative stress. *Am. J. Physiol.* **275,** L806–L817.
9. Sweitzer, T. D., Thomas, A. P., Wiewrodt, R., Nakada, M. T., Branco, F., and Muzykantov, V. R. (2003) PECAM-directed immunotargeting of catalase: specific, rapid and transient protection against hydrogen peroxide. *Free Radic. Biol. Med.* **34,** 1035–1046.
10. Murciano, J. C., Muro, S., Koniaris, L., Christofidou-Solomidou, M., Harshaw, D. W., Albelda, S. M., et al. (2003) ICAM-directed vascular immunotargeting of anti-thrombotic agents to the endothelial luminal surface. *Blood*, **101,** 3977–3984..
11. Kozower, B. D., Christofidou-Solomidou, M., Sweitzer, T. D., Muro, S., Buerk, D. G., Solomides, C. C., et al. (2003) Immunotargeting of catalase to the pulmonary endothelium alleviates oxidative stress and reduces acute lung transplantation injury. *Nat. Biotechnol.* **21,** 392–398.
12. Wilchek, M. and Bayer, E. A., eds. (1990) *Avidin-Biotin Technology*. Academic Press, Inc., San Diego, CA.
13. Odian, G. (1991) *Principles of Polymerization*. John Wiley and Sons, Inc., New York, NY.
14. Osawa, M., Masuda, M., Kusano, K., and Fujiwara, K. (2002) Evidence for a role of platelet endothelial cell adhesion molecule-1 in endothelial cell mechanosignal transduction: is it a mechanoresponsive molecule? *J. Cell Biol.* **158,** 773–785.

Job: Niemeyer (098-0)
Chapter: 02/Muro
Template: MiMB/Template/Rev.02.03
Pub. Date: July 2004
Compositor: CC
Date: February 4, 2004
Revision: 1st Pass

2

Characterization of Endothelial Internalization and Targeting of Antibody–Enzyme Conjugates in Cell Cultures and in Laboratory Animals

Silvia Muro, Vladimir R. Muzykantov, and Juan-Carlos Murciano

Summary

Streptavidin–biotin conjugates of enzymes with carrier antibodies provide a versatile means for targeting selected cellular populations in cell cultures and in vivo. Both specific delivery to cells and proper subcellular addressing of enzyme cargoes are important parameters of targeting. This chapter describes methodologies for evaluating the binding and internalization of labeled conjugates directed to endothelial surface adhesion molecules in cell cultures using anti-intercellular adhesion molecule/catalase or anti-platelet endothelial cell adhesion molecule/catalase conjugates as examples. It also describes protocols for characterization of biodistribution and pulmonary targeting of radiolabeled conjugates in rats using anti-intercellular adhesion molecule/tPA conjugates as an example. The experimental procedures, results, and notes provided may help in investigations of vascular immunotargeting of reporter, experimental, diagnostic, or therapeutic enzymes to endothelial and, perhaps, other cell types, both in vitro and in vivo.

Key Words: Endothelium; cell adhesion molecules; catalase; plasminogen activators; lung targeting.

1. Introduction

Au: Has the correct chapter number been added here?

Streptavidin crosslinking of reporter and therapeutic enzymes with antibodies to endothelial cell adhesion molecules provides nanoscale conjugates useful for experimental and, perhaps, diagnostic or therapeutic vascular immunotargeting (*see* Chapter 1 and **refs. *1–3***). Binding and appropriate subcellular addressing of antibody–enzyme conjugates to and/or into the target cells are key components for optimal design of drug-delivery systems. The size of the conjugates is an important parameter that determines the rate of intracellular uptake and, perhaps, subcellular trafficking of the conjugates ***(4,5)***.

From: *Methods in Molecular Biology, vol. 283: Bioconjugation Protocols: Strategies and Methods*
Edited by: C. M. Niemeyer © Humana Press Inc., Totowa, NJ

Job: Niemeyer (098-0)
Chapter: 02/Muro
Template: MIMB 5x8/Template/Rev-02-03
Pub. Date: July 1, 2004
Compositor: CC
Date: February 4, 2004
Revision: 1st Pass

This chapter outlines basic experimental protocols useful in the characterization of these relevant conjugates parameters. The first part (**Subheading 3.1.**) describes protocols for cell culture experiments that use fluorescent and radioisotope labeling as means to trace binding, internalization, and fate of anti-platelet endothelial cell adhesion molecule (PECAM)/catalase and anti-intercellular adhesion molecule (ICAM)/catalase conjugates. The second part (**Subheading 3.2.**) describes protocols for in vivo experiments in intact anesthetized rats using anti-ICAM/tissue-type plasminogen activator (tPA) conjugate labeled with radioisotopes. Thus, particular immunoconjugates described in this chapter are potentially useful for vascular targeting of either antioxidant (e.g., catalase to detoxify H_2O_2, ref. *6*) or antithrombotic enzymes (e.g., tPA to dissolve fibrin, ref. *3*). However, because of the modular nature of the conjugation and labeling procedures used, the described protocols can be used for the characterization of endothelial targeting and uptake of diverse reporter and therapeutic enzyme cargoes conjugated with a variety of carrier antibodies *(7)*. Furthermore, cell culture protocols given here for endothelial cells can be applied to other cell types of interest.

2. Materials

2.1. Equipment

1. Gamma counter.
2. Fluorescence microscope equipped with 40× or 60× magnification objectives; filters compatible with fluorescein isothiocyanate (FITC; green), Texas Red (red), and UV or Alexa Fluor 350 (blue) fluorescence; digital camera; and image analysis software (ImagePro).

2.2. Reagents, Proteins, and Antibodies

1. Standard phosphate buffer, PBS, (NaH_2PO_4 20 m*M*, 150 m*M* NaCl, pH 7.4).
2. Glycine solution (50 m*M* glycine, 100 m*M* NaCl, pH 2.5) is used for elution of conjugates or antibodies from its interaction with their antigen expressed in the cells.
3. Lysis buffer (PBS containing 2% Triton X-100) is used to lyse cells and differentiate the internalized from the surface retained fractions of conjugates or antibodies.
4. PBS enriched with 5% bovine serum albumin (PBS-BSA) is used to increase the protein content in the analysis of free iodine label released from damaged proteins.
5. PBS enriched in 10% fetal bovine serum (PBS-FBS) is used to block the unspecific binding of conjugates or antibodies to the cells while providing the cell necessary nutrients.
6. Antibodies: human anti-ICAM-1 (mAb R6.5) or rat anti-ICAM-1 (mAb 1A29); human anti-PECAM-1 (mAb 62); and goat anti-mouse IgG conjugated to FITC, Texas Red or Alexa Fluor 35

Job: Niemeyer (098-0)
Chapter: 02/Muro
Template: MiMB/5x9/Template/Rev.02.03
Pub. Date: Jul 2004
Compositor: CC
Date: February 4, 2004
Revision: 1st Pass

7. Other reagents: Concentrated (100% w/v) trichloroacetic acid solution (TCA); goat serum; FITC-labeled streptavidin; tPA; catalase; paraformaldehyde; mowiol; [^{125}]iodine.

2.3. Immunoconjugates

^{125}I-labeled and nonlabeled immunoconjugates synthesized and characterized by dynamic light scattering as described in Chapter 1, where radioisotope is coupled to the cargo enzyme, not the carrier antibody, were used. In some cases, anti-ICAM/catalase conjugates based on FITC-labeled polymer were used *(4,5)*.

2.4. Cells and Media

1. Human umbilical vein endothelial cells (HUVECs, Clonetics).
2. Endothelial cell growth medium (*see* Chapter 1 for details on medium composition) free of antibiotics.

3. Methods

3.1. Characterization of Immunoconjugates in Cell Culture

3.1.1. Quantitative Tracing of Radiolabeled Conjugates in HUVECs

1. Seed the cells in 24-well plates. Cultivate to confluence (approx 48 h) in the appropriate medium. Replace by fresh antibiotic-free medium 24 h before the experiment.
2. Wash cells twice by warm (37°C) culture medium. Add 0.5 μg to 1 μg of conjugate per well (i.e., specific activity 0.03 μCi/μg to 0.1 μCi/μg) in 0.5 mL of medium supplemented with 10% FBS. Incubate cells for 1–2 h at 37°C in the presence of the immunoconjugates.
3. Wash cells three times by medium to remove nonbound conjugates. Incubate cells with a glycine solution (15 min, room temperature [RT]) to elute noninternalized immunoconjugates bound to the cell surface. Using a gamma-counter, determine radioactivity in glycine-eluted fraction (*see* **Note 5**).
4. Wash cells three times by medium and incubate them for 15 min at RT with 0.5 mL of lysis buffer. Add 0.1 mL of the obtained cell lysates to 0.5 mL of PBS-BSA and sequentially add 0.2 mL of TCA and incubate 20 min at RT to precipitate proteins. Centrifuge TCA–lysate mixture (3000 rpm, 10 min) and determine radioactivity in pellet and supernatant fractions.
5. Determine protein concentration in a fraction of cell lysates to normalize radioactivity values in samples per gram of total cell protein. Relative and absolute binding, internalization, and/or degradation of the immunoconjugates can be calculated as follows:

$$\text{Total binding} = \frac{\text{cpm in glycine fraction} + \text{cpm in lysate pellet fraction} + \text{cpm in lysate supernatant fraction}}{\text{specific activity (cpm/ng of conjugate)}}$$

Au: Please supply centrifugation speed in gravity (g) throughout.

Au/Ed: This "(15 min, room temperature [RT])" is different from manuscript hardcopy.

Job: Niemeyer (098-0)
Chapter: 02/Muro
Template: MiMB5x9/Template/Rev.02.03
Pub. Date: Jul 1 2004
Compositor: CC
Date: February 4, 2004
Revision: 1st Pass

$$\text{Internalization percentage (if applicable)} = 100 \times \frac{\text{cpm in lysate fraction}}{\text{cpm in lysate fraction} + \text{cpm in glycine-eluted fraction}}$$

$$\text{Total internalization (if applicable)} = \frac{\text{cpm in lysate fraction}}{\text{specific activity (cpm/ng of conjugate)}}$$

$$\text{Degradation percentage} = 100 \times \frac{\text{cpm in supernatant fraction}}{\text{cpm in glycine} + \text{cpm in lysate supernatant} + \text{cpm in lysate pellet fractions}}$$

$$\text{Total degradation} = \frac{\text{cpm supernatant fraction}}{\text{specific activity (cpm/ng of conjugate)}}$$

3.1.2. SubCellular Detection of Immunoconjugates by Immunofluorescence

3.1.2.1. Binding of Immunoconjugates to Target Cells

1. Seed the cells onto 12-mm^2 glass coverslips coated with 1% gelatin in 24-well plates. Allow cells to grow for 48 h to confluence. Replace medium by fresh antibiotic-free medium 24 h before the experiment. Incubate cells for 5 min at 4°C before the experiment. Wash cells twice and replace by medium containing 10% FBS and a conjugate (1–1.5 μg of per well). Incubate cells for 30 min at 4°C to permit binding.
2. Wash cells three times with cold medium to eliminate nonbound conjugates. Fix cell by a cold solution 2% paraformaldehyde in PBS (15 min).
3. Wash cells three times with PBS and stain surface-bound conjugates by incubating fixed cells for 30 min at RT with a 4 μg/mL solution of Texas Red-labeled goat anti-mouse IgG in PBS-FBS (alternatively, use fluorescently labeled antibodies against the enzyme cargo). Wash cells three times with PBS.
4. Mount cell-containing coverslips on glass microscope slides using mowiol and incubate overnight at RT to allow the mounting media to polymerize. Observe samples by fluorescence microscopy using 40× or 60× objectives. Compare images of fluorescence and phase-contrast fields to confirm location of the immunoconjugate to the cell surface.

3.1.2.2. Internalization of Immunoconjugates Into Target Cells

1. Seed and grow cells to confluence as described in **Subheading 3.1.2.1.**
2. Wash cells twice with 37°C prewarmed medium and add immunoconjugate and incubate with cells for 1 h at 37°C to permit binding and internalization. Fix cells and stain surface-bound conjugates as described in **Subheading 3.1.2.1.**
3. Wash cells three times with PBS and permeabilize them by 15-min incubation with a cold solution 0.2% Triton X-100 in PBS. Stain internalized conjugates by incubating permeabilized cells with FITC-labeled goat anti-mouse IgG (4 μg/mL in PBS serum).
4. Wash cells and mount coverslips on microscope slides as described in **Subheading 3.1.2.1.**

Job: Niemeyer (098-0)
Chapter: 02/Muro
Template: MiMB_x9/Template/Rev-02.03
Pub. Date: Jul 1 2004
Compositor: CC
Date: February 4, 2004
Revision: 1st Pass

5. Take images using filters compatible with Texas Red (red) and FITC (green) in a fluorescence microscope (40× or 60× objective) and merge them. Surface-bound conjugates will appear yellow (double-labeled), whereas internalized conjugates will be single-labeled in green. Imaging software can be programmed to quantify relative conjugate internalization, following the formula:

$$\text{Internalization percentage} = 100 \times \frac{(\text{number of green conjugates} - \text{number of red conjugates})}{\text{number of green conjugates}}$$

3.1.2.3. Fate of Intracellularly Delivered Immunoconjugates

1. For this type of experiments, use fluorescently labeled conjugates (i.e., based on FITC-labeled nondegradable polymer beads; *see* **Note 4**) prepared as previously described in detail ***(4,5)***. First, incubate cells in the presence of conjugates at 4°C to permit binding to the cell surface. Then, wash nonbound immunoconjugates with cold medium, add FBS-supplemented medium, and incubate cells for the time period of interest at 37°C to permit endocytosis and intracellular trafficking of the immunoconjugates previously bound to the cell surface.
2. Wash and fix cells as in **Subheading 3.1.2.1.** followed by staining of the noninternalized conjugates for 30 min at RT with a solution 4 μg/mL goat anti-mouse IgG (i.e., labeled with Alexa Fluor 350) in PBS serum.
3. Wash the preparations three times with PBS and permeabilize cells for 15 min with a cold solution 0.2 % Triton X-100 in PBS. Incubate permeabilized cells with a solution 4 μg/mL goat anti-mouse IgG (i.e., labeled with Texas Red) in PBS serum.
4. Wash cells and mount coverslips on microscope slides as described in **Subheading 3.1.2.1.**

Inspect in a fluorescence microscope using filters compatible with FITC (green), Alexa Fluor 350 (blue), and Texas Red (red) and merge images. Immunoconjugates bound to the cell surface will appear triple-labeled as white. Nondegraded internalized conjugates will appear as double-labeled in yellow, whereas internalized counterparts with degraded protein component will be single-labeled as green.

3.2. Characterization of Immunoconjugates In Vivo

3.2.1. Biodistribution of Radiolabeled Conjugates After Intravenous Administration

1. Anesthetize rats (Sprague–Dawley) weighing 250 g using an intraperitoneal injection of 300 μL of Nembutal solution (70 mg/kg of body weight) and wait 5 min until animals are fully anesthetized (i.e., they do not react to their legs being squeezed with forceps).
2. Inject ^{125}I-labeled conjugates (approx 1–5 μg of the conjugate, 100,000–300,000 cpm per animal) via a tail vein in 0.2 mL of PBS using an insulin syringe with a

Job: Niemeyer (098-0)
Chapter: 02/Muro
Template: MiMB Book9/Template/Rev 02.03
Pub. Date: Jul 1 2004
Compositor: CC
Date: February 4, 2004
Revision: 1st Pass

27.5-gage needle. Warming up the tail by using hot water makes the vein more visible and easy to inject.

3. 1 h after injection, sacrifice anesthetized animals by dissection of the descending aorta, collect 1 mL of blood from the peritoneal cavity, and place it in a heparin-containing tube. Excise internal organs, including lung, liver, kidney, spleen, and heart; rinse in saline; blot in filter paper; weigh; and analyze for radioactivity in a gamma-counter.
4. Use radiotracing data to calculate the following parameters of conjugates behavior in vivo (for more information, *see* **refs. *3***, ***8***, and ***9***):
   A. Percent of injected dose (%ID) characterizes total uptake in a given organ and thus it shows biodistribution and effectiveness of the immunoconjugate targeting. However, this parameter does not take into account organ sizes; thus, uptake in the liver (approx 10 g in a rat) might appear far greater than the uptake in smaller organs (e.g., lung, ~1 g).
   B. To evaluate tissue selectivity of the uptake (and compare the data obtained in different animal species, as well as different organ sizes), calculate %ID per gram (%ID/g).
   C. The ratio between %ID/g in an organ of interest and that in blood gives the localization ratio (LR) that compensates for a difference in the blood level of circulating conjugates and allows comparison of targeting between different carriers, which may have different rates of blood clearance.
   D. By dividing the LR of a specific antibody conjugate in an organ by that of the control IgG counterpart, calculate the immunospecificity index ($ISI = LR_{mAb}/LR_{IgG}$), the ratio between the tissue uptake of immune and nonimmune counterparts normalized to their blood level). ISI is the most objective parameter of the targeting specificity.

3.3. Results

3.3.1. Characterization of Immunoconjugates in Cell Culture

3.3.1.1. Analysis of Binding and Fate of Radiolabeled Conjugates

Site-specific binding and degradation of the conjugates by cells was determined by measuring ^{125}I in fractions of glycine elution, TCA pellet, and supernatant of cell lysates obtained from HUVECs incubated with anti-PECAM/^{125}I-catalase and IgG/^{125}I-catalase conjugates as described in **Subheading 3.1.1.** The sum of the recovered ^{125}I shows total amount of catalase associated with cells and reveals the specificity of binding of anti-PECAM conjugates, using as negative control nonspecific IgG conjugates (**Fig. 1A**). A relatively minor fraction of ^{125}I was found in the supernatant after TCA precipitation of cell lysates, indicating that catalase undergoes very modest degradation within 1 h of incubation at 37°C in endothelial cells (**Fig. 1B**).

Fig. 1

Job: Niemeyer (098-0)
Chapter: 02/Muro
Template: MiMB/Template/Rev.02.03
Pub. Date: Jul 12 2004
Compositor: CC
Date: February 4, 2004
Revision: 1st Pass

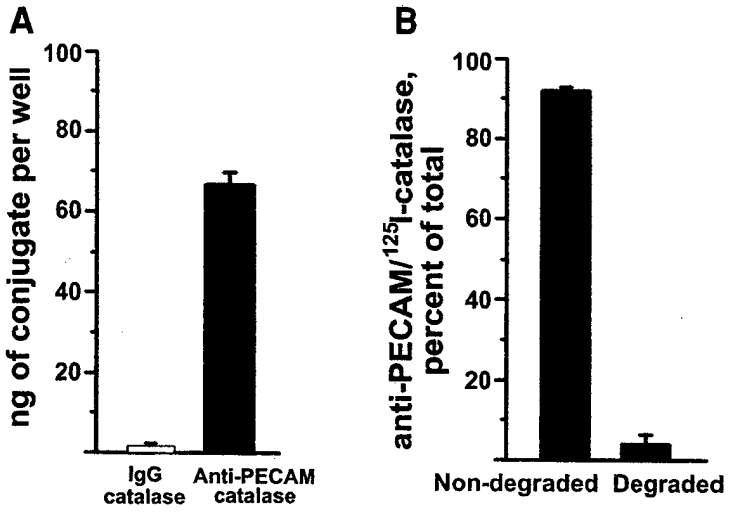

Fig. 1. Quantitative analysis of binding and degradation of radiolabeled anti-PECAM/catalase conjugates in HUVECs. HUVECs were incubated for 90 min at 37°C with anti-PECAM/^{125}I-catalase or control IgG counterpart conjugates, washed, and lysed to determine the TCA-soluble fraction of cell-bound radioactivity. The absolute amount of conjugate in the different fractions is calculated based on its specific activity as described in **Subheading 3.1.1.**

3.3.1.2. Imaging of Binding, Internalization, and Fate of Immunoconjugates by Immunofluorescence

Fig. 2

Figure 2 shows that anti-PECAM/catalase but not IgG/catalase conjugates bind to HUVECs at 4°C, thus confirming the data obtained with ^{125}I tracing (*see* **Fig. 1**). Comparison of fluorescence and phase-contrast images indicates that anti-PECAM/catalase conjugates are located in the cell periphery, consistent with the predominant expression of PECAM-1 to the cell borders.

Moreover, in cells incubated for 1 h at 37°C with anti-PECAM/catalase conjugates, only a fraction of the conjugate was labeled before permeabilization by Texas Red-labeled secondary antibody, whereas FITC-labeled secondary antibody applied after permeabilization reveals abundant immunostaining

Fig. 3

(**Fig. 3A**). Single FITC-labeled (green) internalized conjugates are localized in the perinuclear region of the cell, whereas noninternalized double-labeled (yellow) conjugates tend to localize to the cell periphery. Semiquantitative analysis of double-labeled and single-labeled images shows that endothelial cells internalize 50% of cell-bound anti-PECAM/catalase conjugates.

Job: Niemeyer (098-0)
Chapter: 02/Muro
Template: MiMB/Books/Template/Rev-02.03
Pub. Date: July 2004
Compositor: CC
Date: February 4, 2004
Revision: 1st Pass

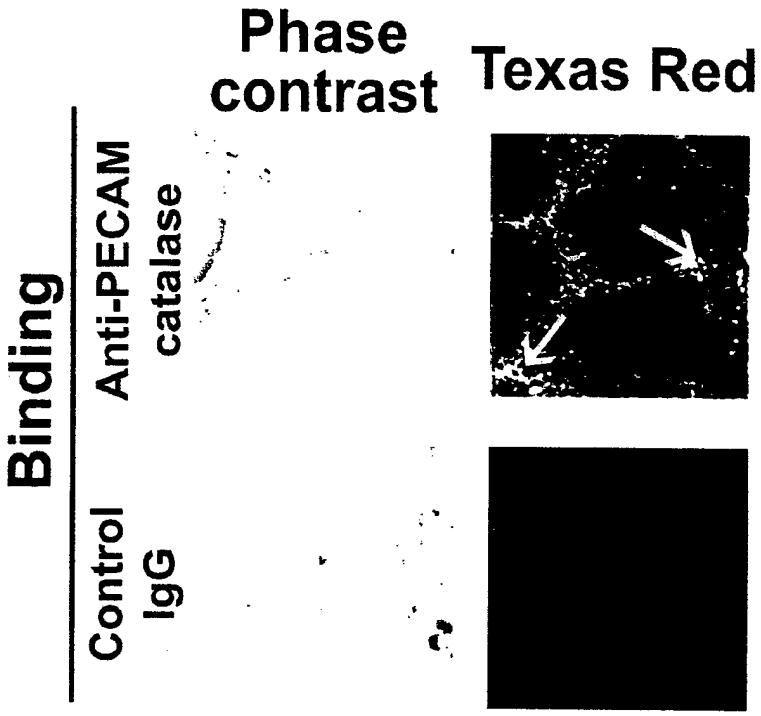

Fig. 2. Fluorescent detection of binding of anti-ICAM/catalase conjugates to HUVECs. HUVECs were incubated for 30 min at 4°C with anti-PECAM/catalase or nonspecific IgG conjugates, washed, fixed, and surface-bound anti-PECAM was stained with Texas Red goat anti-mouse IgG. The samples were analyzed by phase contrast and fluorescence microscopy. The arrows show conjugates bound to the cell surface.

To visualize and estimate degradation of internalized cargoes by fluorescence microscopy, one can retreat to use fluorescently-labeled conjugates, for example, based on FITC-labeled synthetic nanobeads used as carriers for both targeting antibodies and enzyme cargoes *(4,5)*. The advantage of this carrier is that it permits direct tracing of the conjugates in cellular compartments, including lysosomes. FITC-labeled regular immunoconjugates can also be used for this purpose, (e.g., conjugates containing FITC–streptavidin; *see* **Note 4**). A pulse-chase incubation (initial incubation 30 min at 4°C followed by removal of nonbound conjugates and incubation at 37°C), permits one to separate phases of binding, internalization, and intracellular trafficking. After internalization and fixation, surface-bound particles are counterstained using goat anti-mouse IgG conjugated to Alexa Fluor 350, followed by cell permeabilization and

Job: Niemeyer (098-0)
Chapter: 02/Muro
Template: MilBB_6x9/Template/Rev 02.03
Pub. Date: Jul 1 2004
Compositor: CC
Date: February 4, 2004
Revision: 1st Pass

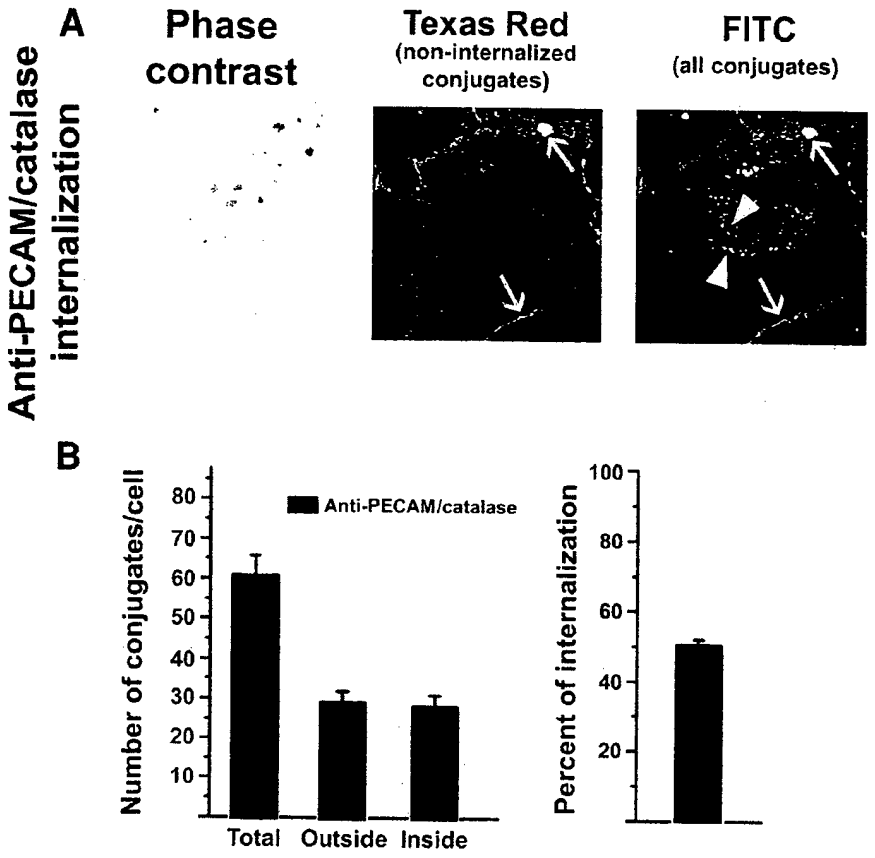

Fig. 3. Fluorescence microscopy of the uptake of anti-PECAM/catalase conjugates by HUVECs. HUVECs were incubated for 1 h at 37°C in the presence of anti-PECAM/catalase conjugates, washed, fixed, and noninternalized conjugates were stained with Texas Red-labeled goat anti-mouse IgG, followed by cell permeabilization and staining with FITC-labeled goat anti-mouse IgG. **A,** The arrows show double-labeled conjugates on the cell surface. The arrowheads show single FITC-labeled conjugates, internalized within the cell. **B,** Quantification of the experiment described above, expressed as mean and standard error (n = 10 fields, from two independent experiments).

Fig. 4

incubation with Texas Red-labeled goat anti-mouse IgG. This staining method (**Fig. 4**) distinguishes surface-bound (triple-stained, white), as well as internalized nondegraded (double-stained, yellow) and degraded conjugates (single stained, green). The results of the particular experiment shown in **Figure 4** indicate that conjugates are stable within the cell for 1–2 h and degrade 3 h after internalization.

Job: Niemeyer (098-0)
Chapter: 02/Muro
Template: MiMB/5x9/Template/Rev.02.03
Pub. Date: Jul 2004
Compositor: CC
Date: February 4, 2004
Revision: 1st Pass

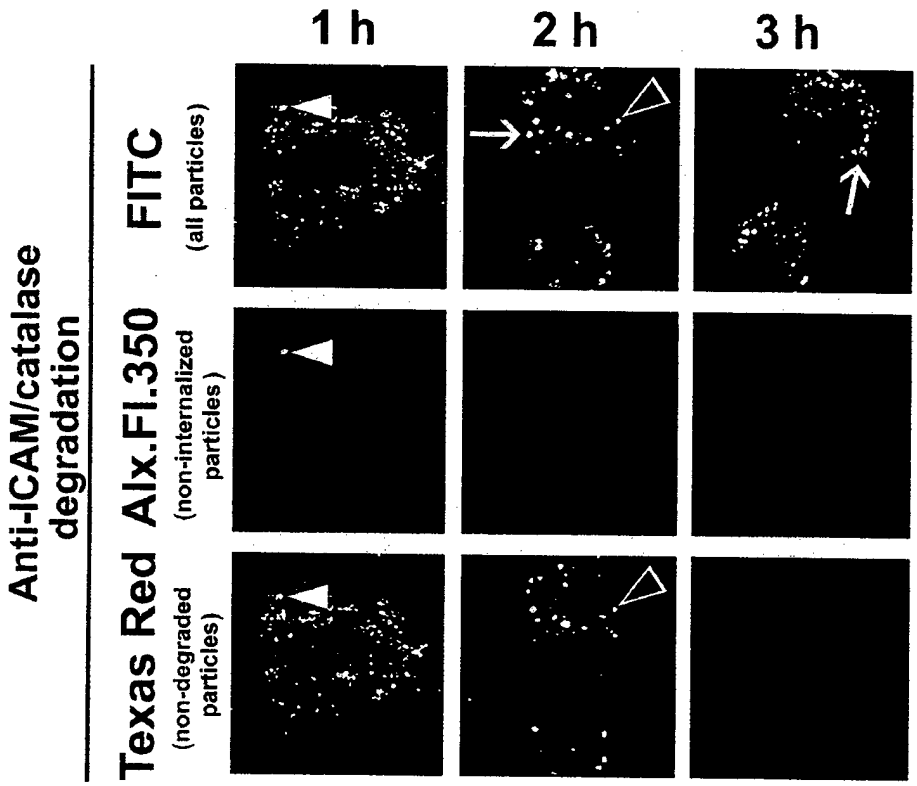

Fig. 4. Imaging of the stability of anti-ICAM/catalase nanoparticles internalized in HUVECs. HUVECs were incubated for 30 min at 4°C in the presence of FITC-labeled anti-ICAM/catalase nanoparticles to permit binding of these to the surface antigen. Then, nonbound particles were washed and the cells were incubated either for 1 h, 2 h, or 3 h at 37°C, to permit internalization and intracellular trafficking of the anti-ICAM/catalase particles. After cell fixation, noninternalized particles were stained with Alexa Fluor 350 goat anti-mouse IgG. Thereafter, the cells were permeabilized and incubated with Texas Red goat anti-mouse IgG. The samples were analyzed by fluorescence microscopy. Closed arrowheads show a triple FITC+Alexa Fluor 350+Texas Red-labeled particle, located to the cell surface. Open arrowheads show a double FITC+Texas Red-labeled particle, which indicates that the targeting antibody was not degraded after internalization within the cell. The arrow shows single FITC-labeled particles, indicating that the targeting antibody in the internalized particles has been degraded.

Job: Niemeyer (098-0)
Chapter: 02/Muro
Template: MiMB/Template/Rev.02.03
Pub. Date: July 2004
Compositor: CC
Date: February 4, 2004
Revision: 1st Pass

3.3.2. Characterization of Immunoconjugates In Vivo

3.3.2.1. Biodistribution and Pulmonary Targeting of tPA Conjugated With Anti-ICAM

Experiments with tPA conjugated with an ICAM-1 monoclonal antibody illustrate analysis of vascular immunotargeting in vivo. **Figure 5A** shows comparison of biodistribution of radiolabeled anti-ICAM/^{125}I-tPA conjugate and its components, either ^{125}I-anti-ICAM or ^{125}I-tPA, 1 h after intravenous injection in rats. Anti-ICAM and anti-ICAM/tPA conjugate display preferential uptake in the pulmonary vasculature and significant uptake in hepatic and splenic vasculature. These highly vascularized organs (especially lungs that possess about 30% of endothelial surface in the body) represent privileged targets in agreement with the fact that ICAM is constitutively expressed on the endothelial surface ***(10)***. Nonconjugated tPA shows no pulmonary targeting; in fact, its extremely rapid clearance (its half-life in rats is around 1–5 min; **ref. *11***) leads to disappearance of the tracer from blood and major organs within 1 h after injection.

Fig. 5

3.3.2.2. Comparison of Biodistribution Attained Using Different Injection Routes

High levels of pulmonary uptake of conjugates directed against pan-endothelial determinants, such as ICAM-1, might be to the result of several reasons: (1) an extremely extended endothelial surface in the alveolar capillaries; (2) the fact that lung receives 100% of the heart blood output; or (3) the phenomenon of first-pass blood after intravenous injection. **Figure 5B** shows that injection of anti-ICAM/tPA conjugate via the left ventricle, which obviates the first pass in the lungs, produces less effective pulmonary targeting, suggesting that indeed first-pass phenomenon contributes to the pulmonary targeting. However, a high level of pulmonary uptake after left ventricle administration confirms the specificity of anti-ICAM conjugates targeting in vivo.

3.3.2.3. Evaluation of the Targeting Specificity of Immunoconjugates

Fig. 6

Figure 6 illustrates the analysis of immunoconjugates biodistribution and targeting in rats 1 h after intravenous injection. A comparison of %ID/g in organs reveals that anti-ICAM/tPA conjugate but not IgG/tPA counterpart accumulates in the pulmonary vasculature. However, the blood level of anti-ICAM/tPA is lower than that of the nonimmune IgG/tPA counterpart, likely because of depletion of circulating blood pool by endothelial binding. The LR that compensates for differences in blood level reveals very high selectivity of anti-ICAM/tPA uptake in highly vascularized organs including liver (LR close to 3), spleen (LR exceeds 7), and especially lungs (LR close to 30). Calculation

Job: Niemeyer (098-0)
Chapter: 02/Muro
Template: MiBB5x9/Template/Rev-02-03
Pub. Date: Jul 1 2004
Compositor: CC
Date: February 4, 2004
Revision: 1st Pass

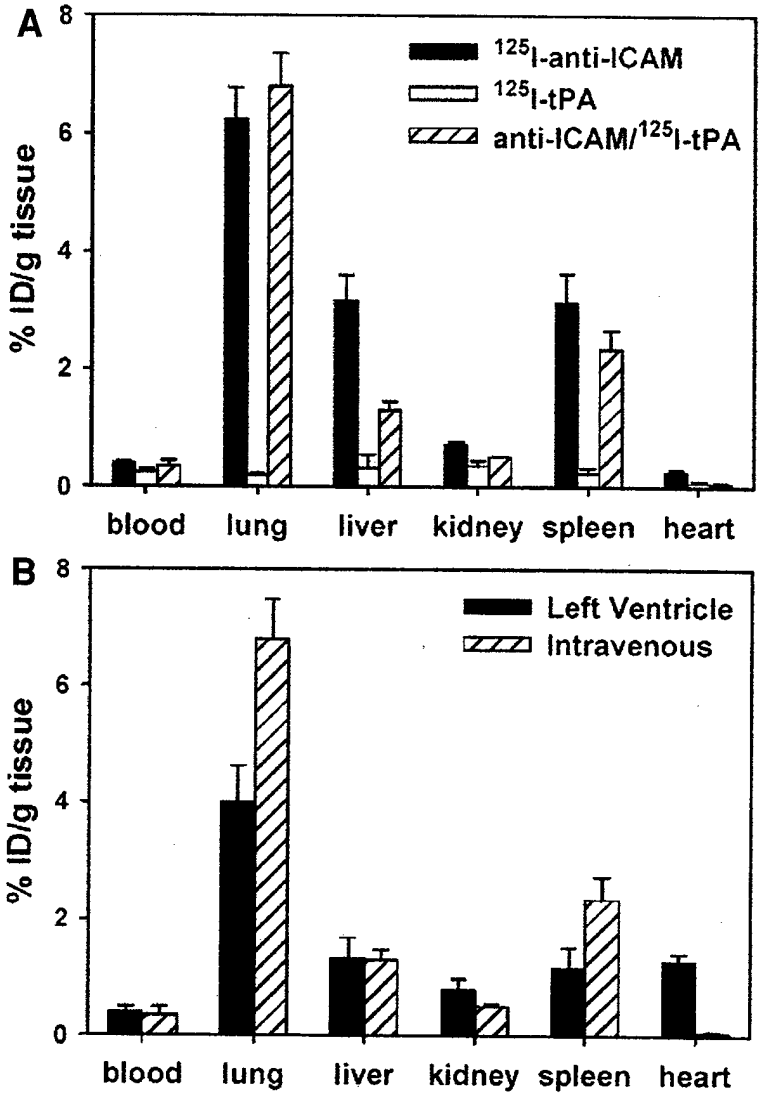

Fig. 5. Biodistribution of immunoconjugates and free components in vivo. Tracer amounts of radiolabeled proteins (approx 1 μg of radioactive material per sample) were injected intravascularly in anesthetized rats. After 1 h animals were sacrificed and blood and organs extracted and analyzed for radioactivity. **A,** ^{125}I-anti-ICAM (black bars) or anti-ICAM/125I-tPA (hatched bars), but not free ^{125}I-tPA (white bars) accumulate in the lung, liver, and spleen after intravenous injection. **B,** Comparison of biodistribution of anti-ICAM/^{125}I-tPA after injections via the tail vein (hatched bars) or the left ventricle (black bars). Data are presented as mean ± SD, n = 4–9 animals per determination.

Job: Niemeyer (098-0)
Chapter: 02/Muro
Template: Mi[illegible]
Pub. Date: Ju[illegible]
Compositor: CC
Date: February 4, 2004
Revision: 1st Pass

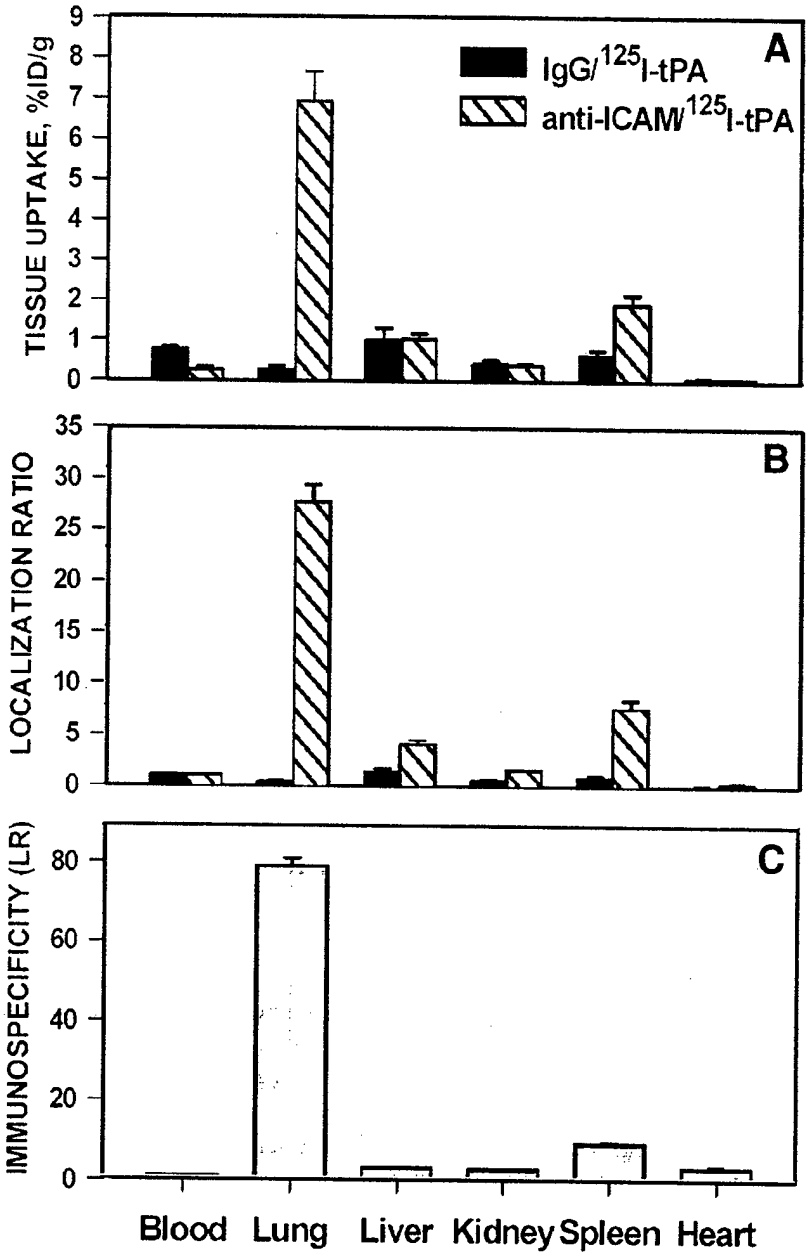

Fig. 6. Analysis of anti-ICAM/tPA biodistribution in vivo. Radioactivity in organs was analyzed 1 h after intravenous injection anti-ICAM/^{125}I-tPA (hatched bars) or control nonspecific IgG/^{125}I-tPA (black bars). The data (mean ± SD, n = 4–9) is presented as: (**A**) % ID/g of tissue; (**B**) LR; and (**C**) ISI. Adapted from **ref. 3**.

Job: Niemeyer (098-0)
Chapter: 02/Muro
Template: MiMB_6x9_Template/Rev-02-03
Pub. Date: Jul 1 2004
Compositor: CC
Date: February 4, 2004
Revision: 1st Pass

of ISI reveals that anti-ICAM/tPA accumulates in the lungs almost 100 times higher than IgG/tPA counterpart, thus confirming high specificity of targeting.

Au: Please cite all notes (sequentially) in the text.

4. Notes

1. Uptake and trafficking of immunoconjugates within the target cells can be studied by tracing the antibody carrier, the enzymatic cargo, or both moieties. The protocols described in **Subheadings 3.1.2.1., 3.1.2.2.**, and **3.1.2.3.** trace antibody moieties using secondary antibodies against murine IgG. The same protocols can be used to trace enzyme cargo, for example, using an antibody to catalase. Moreover, conjugates directly labeled with a fluorescent probe, such as the ones based on fluorescent-labeled nanobeads or streptavidin crosslinker, are optimal because they can be visualized without additional staining. There are some specific factors that may require adjustment and optimization of the described protocols to be applied to particular conjugates and target cells of interest. Some general considerations are given below.
2. Many cell types do not adhere well to glass surfaces. Coating coverslips with a proadhesive protein (i.e., fibronectin, vitronectin, collagen) before cell seeding helps to solve this problem. A 1-h incubation with 1% gelatin solution in PBS followed by a 1-h incubation to dry coverslips up is a generic choice. The density of seeding of each cell type must be adjusted to reach confluence within the first 48 h after seeding to avoid repeated division cycles that can lead to detachment. For example, optimal density for HUVEC is 7×10^4 cell per 24 wells when seeded 48 h before the experiment. Moreover, cells tend to detach from any substrate at 4°C; thus, cold incubation should be minimal to permit binding of the conjugates. To avoid excessive detachment, pour washing medium gently and slowly on the well wall rather than directly on the cells. Glycine elution of membrane-bound conjugates may also provoke cell detachment and incubation time must be minimal (do not exceed 15 min). Inspect cell morphology and monolayer integrity by phase contrast microscopy and terminate "high risk" exposures at the first signs of cell retraction, rounding or detachment.
3. Fixation of cells with 2% paraformaldehyde solution (10–15 min) is generally used when preparing samples for immunofluorescence, but the concentration must be optimized and can be lowed to 0.5 % to 1% if necessary to avoid disruption of the plasma membrane and partial cell permeabilization. In addition, the concentrations and incubation times of labeled antibodies given above are arbitrary and should be adjusted for particular preparations. To block nonspecific binding of labeled antibodies, preincubate fixed cells with a solution 10–20% serum of a corresponding animal species before immunostaining. To reduce nonspecific binding of the immunoconjugates (e.g., to control cells that do not express a target antigen), use incubation media containing 2–4% BSA.
4. Adjust settings for acquisition and processing of fluorescence images to optimize visualization. For instance, in the case that fluorescent signal was low, rational increase of the exposure time or brightness post-acquisition can be performed, although preserving the specificity of the signal and the legitimacy of the image.

Job: Niemeyer (098-0)
Chapter: 02/Muro
Template: MiBB5x9/Template/Rev-02-03
Pub. Date: Jul 2004
Compositor: CC
Date: February 4, 2004
Revision: 1st Pass

This approach helps to colocalize fluorescent signals obtained from different objects when labeled with fluorescent probes at different intensity, such as staining of a highly fluorescent FITC-labeled conjugate using secondary antibody that is relatively poorly labeled with Texas Red. Merging the images taken under similar acquisition parameters will show FITC signal masking Texas Red on the same object, not permitting visualization of a real double-labeled object and, therefore, leading to misinterpretation of the result. In addition, the choice of the fluorescent probes to reveal colocalizing objects should be made such that colors resulting from merged images permit an easy interpretation of the results. For instance, colocalization of green and red results in yellow and the three colors can be readily interpreted. However, colocalization of green and blue results in a light, bluish shade, not clearly distinguishable from the two parental colors.

5. Finally, the data on internalization and degradation of the radiolabeled conjugates should be analyzed and interpreted cautiously. For instance, multimeric conjugates can bind to cells with such high avidity that resulting large antibody/antigen clusters are difficult to disrupt by glycine elution, providing false-positive internalization result. Visualization of the uptake using double-fluorescence based techniques permits to circumvent this artifact.

Acknowledgments

The authors thank Drs. Michael Koval and Steven Albelda for contributions to the previous studies, which provided experimental background for the development of the protocols outlined in this chapter. This work was supported by NIH SCOR in Acute Lung Injury (NHLBI HL 60290, Project 4), NHLBI RO1 HL/GM 71175–01, and the Department of Defense Grant (PR 012262) to VRM.

References

1. Muzykantov, V. R., Christofidou-Solomidou, M., Balyasnikova, I., Harshaw, D. W., Schultz, L., Fisher, A. B., et al. (1999) Streptavidin facilitates internalization and pulmonary targeting of an anti-endothelial cell antibody (platelet-endothelial cell adhesion molecule 1): a strategy for vascular immunotargeting of drugs. *Proc. Natl. Acad. Sci. USA* **96,** 2379–2384.
2. Scherpereel, A., Wiewrodt, R., Christofidou-Solomidou, M., Gervais, R., Murciano, J. C., Albelda, S. M., et al. (2001) Cell-selective intracellular delivery of a foreign enzyme to endothelium in vivo using vascular immunotargeting. *FASEB J.* **15,** 416–426.
3. Murciano, J. C., Muro, S., Koniaris, L., Christofidou-Solomidou, M., Harshaw, D. W., Albelda, S. M., et al. (2003) ICAM-directed vascular immunotargeting of antithrombotic agents to the endothelial luminal surface. *Blood* **101,** 3977–3984.
4. Wiewrodt, R., Thomas, A. P., Cipelletti, L., Christofidou-Solomidou, M., Weitz, D. A., Feinstein, S. I., et al. (2002) Size-dependent intracellular immunotargeting of therapeutic cargoes into endothelial cells. *Blood* **99,** 912–922.

5. Muro, S., Wiewrodt, R., Thomas, A., Koniaris, L., Albelda, S. M., Muzykantov, V. R., et al. (2003) A novel endocytic pathway induced by clustering endothelial ICAM-1 or PECAM-1. *J. Cell Sci.* **116,** 1599–1609.
6. Kozower, B. D., Christofidou-Solomidou, M., Sweitzer, T. D., Muro, S., Buerk, D. G., Solomides, C. C., et al. (2003) Immunotargeting of catalase to the pulmonary endothelium alleviates oxidative stress and reduces acute lung transplantation injury. *Nat. Biotechnol.* **21,** 392–398.
7. Muzykantov, V. R., Atochina, E. N., Ischiropoulos, H., Danilov, S. M., and Fisher, A. B. (1996) Immunotargeting of antioxidant enzyme to the pulmonary endothelium. *Proc. Natl. Acad. Sci. USA* **93,** 5213–5218.
8. Danilov, S. M., Gavrilyuk, V. D., Franke, F. E., Pauls, K., Harshaw, D. W., et al. (2001) Lung uptake of antibodies to endothelial antigens: key determinants of vascular immunotargeting. *Am. J. Physiol. Lung Cell Mol. Physiol.* **280,** L1335–L1347.
9. Murciano, J. C., Harshaw, D., Neschis, D. G., Koniaris, L., Bdeir, K., Medinilla, S., et al. (2002) Platelets inhibit the lysis of pulmonary microemboli. *Am. J. Physiol. Lung Cell Mol. Physiol.* **282,** L529–L539.
10. Panes, J., Perry, M. A., Anderson, D. C., Manning, A., Leone, B., Cepinskas, G., et al. (1995) Regional differences in constitutive and induced ICAM-1 expression in vivo. *Am. J. Physiol.* **269,** H1955–H1964.
11. Kuiper, J., Otter, M., Rijken, D. C., and van Berkel, T. J. (1988) Characterization of the interaction in vivo of tissue-type plasminogen activator with liver cells. *J. Biol. Chem.* **263,** 18,220–18,224.

Endothelial Endocytic Pathways: Gates for Vascular Drug Delivery

Silvia Muro[1], Michael Koval[2] and Vladimir Muzykantov[1,3,*]

FINAL

[1]*Institute for Environmental Medicine, Departments of* [2]*Physiology and* [3]*Pharmacology, University of Pennsylvania, School of Medicine, 1 John Morgan Building, 3620 Hamilton Walk, Philadelphia, PA 19104-6068, USA*

Abstract: Vascular endothelium plays strategic roles in many drug delivery paradigms, both as an important therapeutic target itself and as a barrier for reaching tissues beyond the vascular wall. Diverse means are being developed to improve vascular drug delivery including stealth liposomes and polymer carriers. Affinity carriers including antibodies or peptides that specifically bind to endothelial surface determinants, either constitutive or pathological, enhance targeting of drugs to endothelial cells (EC) in diverse vascular areas. In many cases, binding to endothelial surface determinants facilitates internalization of the drug/carrier complex. There are several main endocytic pathways in EC, including clathrin- and caveoli-mediated endocytosis, phagocytosis and macropinocytosis (these two are less characteristic of generic EC) and the recently described Cell Adhesion Molecule (CAM)-mediated endocytosis. The latter may be of interest for intracellular drug delivery to EC involved in inflammation or thrombosis. The metabolism and effects of internalized drugs largely depend on the routes of intracellular trafficking, which may lead to degrading lysosomal compartments or other organelles, recycling to the plasma membrane or transcytosis to the basal surface of endothelium. The latter route, characteristic of caveoli-mediated endocytosis, may serve for trans-endothelial drug delivery. Pericellular trafficking, which can be enhanced under pathological conditions or by auxiliary agents, represents an alternative for transcytosis. Endothelial surface determinants involved in endocytosis, mechanisms of the latter and trafficking pathways, as well as specific characteristics of EC in different vascular areas, are discussed in detail in the context of modern paradigms of vascular drug delivery.

Keywords: Drug delivery, Vascular endothelium, Endocytosis, Transcytosis, Paracellular transport, Intracellular trafficking.

1. INTRODUCTION. VASCULAR ENDOTHELIUM: A BARRIER AND TARGET FOR DRUG DELIVERY

The inner surface of blood vessels is lined with endothelial cells (EC) strategically positioned to control vascular physiology. EC control numerous vital functions and represent an extremely important target and barrier for drug delivery.

For instance, numerous vasoactive factors secreted by EC and including (yet most likely not limited to) NO, prostacyclin and endothelium-derived hyperpolarizing factor (EDHF), suppress contractility of the vascular smooth muscle cells and therefore control vascular tone [1, 2].

EC help to control thrombosis [1]. For example, in concert with plasma protein C, endothelial transmembrane glycoprotein thrombomodulin converts thrombin into an anti-coagulant enzyme [3]. Among other anti-thrombotic factors, EC secrete NO and prostacyclin, which suppress platelet aggregation, as well as urokinase and tissue type plasminogen activators that dissolve blood clots *via* generation of the fibrin-degrading protease plasmin.

The endothelium is also involved in inflammation, a process that is often intertwined with thrombosis [4, 5]. Under normal circumstances, EC provide very limited, if any, support for activities of pro-inflammatory cells (e.g., white blood cells, WBC). However, pathological mediators, including cytokines, reactive oxygen species (ROS), growth factors and abnormal shear stress, induce endothelial secretion of chemoattractants and exposure of adhesion molecules leading to leukocyte attraction, adhesion and transmigration [6-9].

Furthermore, EC play an important role in normal and pathological vascular redox mechanisms [10]. They produce ROS (superoxide anion O_2^- and H_2O_2) *via* enzymatic pathways that can be further activated by pathological mediators [11]. ROS apparently play an important role in cellular signaling. However, ROS overproduction by EC or by activated WBC leads to vascular oxidant stress, inactivation of NO by O_2^-, lipid peroxidation and tissue injury [12].

EC function is modulated by exposure to dynamic environmental factors such as blood flow shear stress, aggressive inflammatory cells and compounds in the circulation, including lipids, proteases, oxidants and xenobiotics. Disruption of normal endothelial function can exacerbate the pathology of a number of diseases including atherosclerosis, hypertension, thrombosis, diabetes, acute lung injury and sepsis. Improper EC function can also lead to defects in angiogenesis, which in turn, could either inhibit vascularization during wound repair resulting in tissue necrosis or cause inappropriate blood vessel formation, which can lead to tumor vascularization. Therefore, EC

*Address correspondence to this author at the IFEM, University of Pennsylvania Medical Center, 1 John Morgan Building, 3620 Hamilton Walk, Philadelphia, PA 19104-6068, USA; Tel: 215-898-9823; Fax: 215-898-0868; E-mail: muzykant@mail.med.upenn.edu

1570-1611/04 $45.00+.00

represent an important potential target for delivery of therapeutic agents including, but not limited to, antioxidants to protect against oxidative stress, anticoagulants and fibrinolytics to manage thrombotic stress, NO donors to reduce vessel tone and blood pressure, and anti-inflammatory agents to suppress vascular inflammation.

The total surface area of vascular endothelium in the human body approaches the size of a tennis court (~ 240 m^2), making it a large and highly accessible target for drugs circulating in the bloodstream. Most therapeutic agents, however, have no specific affinity to this target. Therefore, only a small fraction of injected drugs produces a therapeutic effect in endothelium, whereas the major fraction is handled as a waste product, or worse, produces deleterious side effects. Furthermore, binding to target cells is necessary, but not sufficient, for effective action of many drugs, which require internalization and proper sub-cellular addressing. Thus, it is a key issue in the design of drug delivery vehicles to create carriers that are targeted to EC and also are trafficked by the target cells to destinations where they can have maximal efficacy. Recognizing this problem, more and more groups are focusing their research efforts on the design of novel strategies for targeted delivery of therapeutics to EC [13-26].

With other layers of the blood vessel wall, the endothelium forms a barrier for delivery of drugs to extravascular targets, such as tumors, brain and myocardium. Understanding the mechanisms involved in trans-cellular and pericellular endothelial transport may permit more effective delivery of these drugs. Among other parameters, endothelial uptake and transcytosis depend on the size of a transported agent. Barrier function of endothelium is especially restrictive for large therapeutic molecules (e.g., proteins or genetic materials) and drug delivery systems that employ carrier nanoparticles, liposomes, or high molecular mass polymers.

Therefore, the endothelium is an extremely important tissue in the context of vascular drug delivery, either as a target itself for therapeutic interventions by a delivered drug or as a barrier on route to peripheral tissues [27, 28]. Targeted delivery of drugs to endothelium and control of their internalization, sub-cellular addressing and transendothelial transport are critically important components for the rational design of safe, effective and specific therapies. The goal of this article is to review these issues in the context of drug delivery systems designed for targeting of drugs to and beyond EC.

2. A BRIEF OVERVIEW OF VASCULAR DRUG DELIVERY SYSTEMS

Most known drugs lack specific binding and uptake by target organs. On the other hand, many drugs undergo rapid inactivation in the body by aggressive components of blood and special cellular detoxifying systems. In addition, some drugs including therapeutic enzymes (e.g., proteases), have specific inhibitors in the blood. Also, drugs can be eliminated through a number of mechanisms, including clearance from the bloodstream by non-specific targets (e.g., red blood cells and hepatocytes) and specific clearance systems (e.g., reticuloendothelial system and renal filtration). This often dictates that administration of large doses is required for efficacy, also increasing potentially dangerous side effects.

Elimination and inactivation of pharmacological agents is decreased when a therapeutic "cargo" is loaded into or conjugated with natural or artificial carriers increasing bioavailability of a drug (e.g., liposomes, polymer nanoparticles, lipoproteins, blood cells or proteins) [27, 29-37]. Coating of drugs or their carriers by activated polyethylene glycol, PEG, forms an aqueous shell masking against natural protective mechanisms including macrophages, complement and immune cells, a strategy sometimes referred to as "stealth" technology [38-40]. PEG-coating markedly prolongs circulation of drugs and reduces side effects associated with the immune response and systemic activation of host defense including complement and leukocytes.

In addition, many delivery systems such as liposomes or conjugation with carrier lipoproteins, facilitate intracellular uptake of drugs [41]. The mechanisms of this phenomenon are complex and depend on specific cell type and carrier (see below). However, there are several mechanisms employed by currently available drug carriers to facilitate intracellular uptake.

First, drugs conjugated with ligands of cellular receptors can be internalized *via* vesicle-mediated pathways. Endocytosed carriers usually follow the natural itinerary their receptors would normally traverse to the point of dissociation or degradation in intracellular compartments such as lysosomes. For example, cells expressing transferrin receptor internalize drugs conjugated or genetically fused with transferrin *via* clathrin-mediated endocytosis [42]. Second, fusion-competent liposomes can be designed to enter the cells *via* endocytic pathways, leading to delivery and fusion with intracellular membrane organelles, or to fuse with lipids in the plasma membrane, thus injecting their content directly into the cytosol. In an attempt to control the extent and specificity of cytosolic delivery, liposome carriers have been designed that are destabilized after internalization at acidic pH in endocytic compartments prior to release of a drug or fusion with cell membranes [43]. Third, antibodies and their derivatives with multivalent binding sites facilitate cellular entry of liposomes [44-48]. Fourth, a more recent approach to cytosol delivery has been to couple proteins and sub-micron particles with the TAT-peptide from HIV virus, which in some instances can enter cells in an energy independent manner, although they may require endocytosis in other cases [49, 50]. This and some other charged peptides enriched with lysine and/or arginine promiscuously permeate cell membranes and enable cytosolic delivery to diverse cell types *in vitro* and *in vivo* [51, 52].

Therefore, diverse natural carriers (e.g., lipoproteins or transferrin) or synthetic carriers (e.g., liposomes) can facilitate vascular drug delivery and intracellular uptake. In the next section we consider how these means can be employed in the context of specific drug targeting to EC.

3. ENDOTHELIAL SURFACE DETERMINANTS: POTENTIAL TARGETS FOR DRUG DELIVERY

Stealth liposomes, protein carriers and other delivery systems prolong the circulation time of drugs and may enhance their cellular uptake, but do not confer an affinity to

EC. Unless drugs are coupled to high-affinity carriers, the circulation removes drugs and their derivatives rapidly, even after local infusion *via* vascular catheters. In these instances, the major fraction of injected materials ends up in the liver and not in EC. Devices allowing a transient cessation of blood flow in the site of catheter placement have been designed in order to attain a high local concentration and a more effective prolonged interaction of the infused material with endothelium, but blood flow interruption may lead to ischemia and vascular injury.

Viable means for effective, rapid, and safe targeting of therapeutic molecules to EC are beginning to emerge to address this important and persisting biomedical problem. In order to facilitate targeting, cargoes or their carriers can be conjugated (chemically or genetically) with affinity moieties that bind to EC. Antibodies directed against endothelial surface determinants and small antigen-binding fragments of these antibodies represent one of the most useful classes of affinity carriers for targeted drug delivery to EC. Indeed, coupling drugs with carrier antibodies permits targeted delivery to EC (vascular immunotargeting) [19, 53].

Immunostaining of tissues, *in vivo* selection of peptide ligands using phage display and tracing labeled antibodies in animals have been used to identify several EC antigens that potentially can be used as targets [14, 15, 20, 21, 54-57]. However, no universal or ideal carrier suits all therapeutic needs. Specific therapeutic goals require different secondary effects mediated by binding to EC, drug targeting to different sub-populations of EC (e.g., resting *vs.* inflammation-engaged EC), and to diverse cellular compartments. Also, targeted delivery of antioxidants or NO-donors to normal or resting EC can be useful for either prophylaxis or therapies. On the other hand, specific recognition and drug delivery to abnormally activated or pathologically altered EC might permit more specific means for treatment of such maladies as localized tumor growth and inflammation. Table **1** shows some endothelial determinants useful for experimental vascular targeting to EC, which may have therapeutic potential.

Several surface determinants are potentially useful for targeting either normal and/or pathologically altered EC. For example, antibodies to thrombomodulin (TM), a constitutively expressed EC antigen, can be used for targeting of diverse cargoes to the endothelium [58]. Unfortunately, TM is functionally "untouchable" for therapies, because its inhibition by anti-TM may cause thrombosis [59]. However, TM antibodies are being successfully utilized for delivery of reporter or toxic compounds to the pulmonary EC in animal models [60].

Angiotensin-converting enzyme (ACE) is a transmembrane glycoprotein expressed on the endothelial luminal surface, which converts Ang I into Ang II to induce vasoconstricting, pro-oxidant and pro-inflammatory activities [61-63]. Pulmonary vasculature is enriched in

Table 1. Endothelial Determinants: Selected Candidate Targets for Drug Delivery

Target	Function and Localization	Targeting Advantages	Potential Problems
ACE	Peptidase, converts Ang I into Ang II and cleaves bradykinin. ACE enriched in the lung capillaries.	Selective targeting to lung EC. Intracellular delivery. Vasodilating and anti-inflammatory effects of ACE inhibition.	Inflammation suppresses targeting. ACE inhibition may be dangerous.
TM	Binds thrombin and converts it into an anti-coagulant enzyme. Enriched in the lungs.	Intracellular delivery to EC useful for modeling of lung injury in animals.	Inflammation suppresses targeting. Thrombosis due to TM inhibition.
PECAM	Facilitates transmigration of leukocytes. Stably expressed in EC borders.	Intracellular delivery of anti-PECAM conjugate may also suppress inflammation	PECAM-signaling and side effects are not understood
ICAM	Mediates leukocyte adhesion to EC. Stably expressed by EC, and up-regulated by pathological agents.	Similar to PECAM, but inflammation enhances targeting.	Similar to PECAM
E-selectin	Supports leukocytes adhesion. Expressed only on altered EC.	Intracellular targeting to EC in inflammation	Targeting is not robust. Transient expression.
P-selectin	Similar to E-selectin	Similar to E-selectin	Similar to above. Targeting platelets
gp90	Function unknown. Localized in EC cavoli.	Transendothelial targeting.	Human analogue and side effects are not known.
gp85	Function unknown. EC avesicular zone in alveolar capillaries.	Targeting to the EC surface	Similar to above
gp60	Albumin-binding protein in EC caveoli	Transendothelial targeting	Side effects and specificity of targeting are not known

EC – endothelial cells, ACE – angiotensin-converting enzyme, TM - thrombomodulin, PECAM - platelet-endothelial adhesion molecule, ICAM - intercellular adhesion molecule; gp – glycoproteins.

ACE: nearly 100% of EC in the alveolar capillaries are ACE-positive *vs* <15% ACE-positive EC in the extra-pulmonary capillaries [64]. Radiolabeled anti-ACE accumulates in the pulmonary vasculature after intravascular and intraperitoneal injections in rats, cats, primates and humans [14, 17]. Diverse reporter compounds and drugs conjugated with anti-ACE accumulate selectively in the lungs after intravenous injection in rats [14, 17, 65]. Recently, anti-ACE has been used successfully for re-targeting of viruses to pulmonary EC in rats [25, 26].

ACE also inactivates bradykinin, a peptide stimulating NO production, although Ang II may stimulate NO production by EC [66]. Some anti-ACE antibodies block its active site and/or facilitate ACE shedding from the endothelium by specific secretases regulated by metalloproteases [67-69]. However, other ACE antibodies enable ACE to retain its function. Therefore, using ACE antibodies directed to different epitopes enables targeting strategies to be developed that either retain or inhibit ACE activity, enhancing flexibility and therapeutic applicability of the strategy. ACE inhibition may be beneficial in conditions associated with vascular oxidant stress, ischemia and inflammation.

Pro-inflammatory agents (e.g., ROS) suppress endothelial expression of ACE [70, 71] which may inhibit therapeutic targeting. However, anti-ACE is a good candidate for targeting to the pulmonary endothelium for a prophylactic use; it does not cause acute harmful reactions in animals and humans [17]. EC internalize anti-ACE that may deliver drugs intracellularly [65]. Anti-ACE-conjugated antioxidant enzymes such as catalase, accumulates in rat lungs *in vivo* [72] and protect perfused rat lungs against H_2O_2 [73].

Platelet-Endothelial Cell Adhesion Molecule-1 (PECAM, CD31) is a pan-endothelial transmembrane Ig superfamily glycoprotein (m.w. 130 kD), predominantly localized in the sites of cellular contacts in the endothelial monolayer [74]. Platelets and WBC also express PECAM, but at levels that are orders of magnitude lower than EC. PECAM is abundant in EC, which express millions of anti-PECAM binding sites [75]. In addition, PECAM is a stable EC antigen: cytokines and ROS do not down regulate its expression and surface density on the endothelium. This promises a robust PECAM-targeted drug delivery to either normal or pathologically altered vasculature, for either prophylaxis or therapies.

PECAM is involved in the cellular recognition, adhesion, signaling, and trans-endothelial migration of leukocytes [74]. Adhesion and transmigration of leukocytes is involved in pathogenesis of many disease conditions including inflammation, sepsis, atherosclerosis, acute lung injury and diabetes [76-78]. Animal studies showed that blocking PECAM by administration of anti-PECAM suppresses inflammation and protects organs against leukocyte-mediated oxidant stress [77, 79]. Therefore, anti-PECAM targeting may provide secondary benefits for management of inflammation, perhaps by attenuation of leukocyte transmigration.

EC bind anti-PECAM without internalization, but anti-PECAM conjugation (e.g., by streptavidin) provides multimeric anti-PECAM complexes that are readily internalized by endothelium and accumulate in animal lungs in perfusion or after IV administration [64, 75]. An active reporter enzyme, beta-galactosidase, conjugated to anti-PECAM has been shown to accumulate intracellularly in the pulmonary endothelium as soon as 10 min after IV injection in mice and pigs [80, 81].

InterCellular Adhesion Molecule-1 (ICAM-1, CD54) is another Ig superfamily surface glycoprotein with a short cytoplasmic domain, transmembrane domain and large extracellular domain [6, 82-84]. It is normally expressed by EC at relatively high surface density ($2x10^4$-$2x10^5$ surface copies per cell). Some other cell types also express ICAM-1 (e.g., alveolar epithelial cells, macrophages). However, the major fraction of blood-accessible ICAM-1 is exposed on the luminal surface of EC. Several laboratories demonstrated robust and specific binding of radiolabeled ICAM antibodies and anti-ICAM conjugates to vascular endothelium after intravenous administration in diverse laboratory animals [64, 73, 85-87].

Pathological stimuli, such as ROS, cytokines, abnormal shear stress and hypoxia stimulate surface expression of ICAM-1 by EC *via* signaling mechanisms involving activation of MAP kinases and nuclear translocation of NF-kappaB [88, 89]. ROS and cytokines elevate the ICAM-1 surface density in pulmonary EC [90, 91]. Therefore, in contrast with some other constitutive endothelial determinants (e.g., TM and ACE), immunotargeting to ICAM-1 is not suppressed, but instead is markedly facilitated in inflammation and other pathological conditions [85-87, 92-96].

ICAM-1, a counter-receptor for integrins on WBC, supports their firm adhesion to EC and thus contributes to inflammation [97-100]. In addition, ICAM-1 serves as a natural ligand for certain viruses [101]. ICAM-1 may also serve as a signaling molecule, yet the exact mechanisms, specificity and significance of this signaling in different cell types remains to be more fully elucidated. Antibodies (including humanized murine mAbs) directed against ICAM-1 suppress leukocytes adhesion to EC, thus producing anti-inflammatory effects in animal models and clinical pathological settings associated with vascular injury, such as acute inflammation, ischemia/reperfusion and oxidant stress [102-106]. Blocking of endothelial ICAM-1 by targeting may inhibit leukocyte adhesion to EC and thus suppress inflammation, a benefit for treatment of vascular oxidant and thrombotic stress. The anti-inflammatory effect of anti-ICAM conjugates may be even more potent due to their potentially higher affinity/valency and down regulation of surface ICAM-1 *via* internalization (see below).

Antibodies directed against constitutive cell adhesion molecules PECAM and ICAM described above do not discriminate between EC in different vascular areas, thus providing "pan-endothelial targeting". Anti-PECAM and anti-ICAM directed conjugates accumulate preferentially in the lungs after intravenous administration (due to the fact that pulmonary vasculature represents about 30% of the total vascular surface in the body and receives 100% cardiac first pass venous blood output), whereas injecting *via* catheters inserted in a conduit artery facilitates local delivery in the downstream vascular area [64, 81]. Local delivery may also

be enhanced by surface endothelial determinants enriched in particular vascular areas or in focal pathological processes.

For example, glycoprotein gp85 identified by Ghitescu [107] is predominantly localized in the thin part of EC body that separates alveolar and vascular compartments and lacks main organelles ("avesicular zone"); gp85 monoclonal antibodies accumulate in rat pulmonary vasculature without internalization [108]. On the other hand, animal studies showed that the pulmonary endothelium in rats contains surface determinants localized to cholesterol-enriched plasma membrane microdomains, including caveoli. Ligands of determinants localized to caveoli such as gp60 and gp90 also accumulate in the pulmonary vasculature after intravenous injection in rats, enter EC and traverse endothelial barrier [57]. The functions and human counterparts of these endothelial determinants are not known and, thus their potential utility as targets for drug delivery is not clear. However, caveoli-localized determinants might provide an exciting opportunity for trans-endothelial drug delivery (see Section 6).

Endothelium in the cerebral vasculature represents a specially important and difficult target. Recent animal studies showed that carrier antibodies and peptides directed to several surface determinants relatively enriched in EC in the brain, including receptors for transferrin, insulin, putrescin and some growth factors, permit delivery of the reporter compounds and genes into the brain [109-111]. Importantly, some of these endothelial receptors apparently permit transendothelial drug delivery into the brain tissue and neurons (see in Section 6).

EC exposed to inflammatory mediators and abnormal shear stress show cell surface expression of P-selectin, normally stored intracellularly and mobilized rapidly to the surface, and E-selectin, which is newly synthesized by activated EC [7]. Therefore, selectins are transiently exposed on the surface of stressed EC [112, 113]. Experiments in cell cultures and limited animal studies show that selectins may permit targeting of drugs to cytokine-activated endothelium [16, 114-118].

EC in solid tumors also represent a specially important and challenging target for delivery of agents designed to visualize tumors, inhibit angiogenesis, or eradicate malignant cells [119-121]. Tumor vasculature is characterized by numerous morphological abnormalities [122, 123]. EC in tumor vessels expose abnormal determinants including selectins (see above), integrins, apoptosis markers and receptors for growth factors [124-128]. Targeting these determinants in tumors might be useful to accomplish two goals: i) inflict damage in the tumor vasculature leading to thrombosis, infarction and starvation of malignant cells [18, 129] and, ii) delivery of anti-tumor agents to the proper malignant cells using, for example, PEG-immunoliposomes or polymers loaded with taxol or doxorubicin [130, 131]. The latter approach involves permeation of the endothelial barrier, mostly *via* paracellular pathways (see Section 6). EC seem to internalize protein carriers modified with peptides containing RGD sequence to provide recognition of integrins over-expressed on tumor endothelium [132].

In summary, affinity carriers directed to diverse determinants presented on surface of normal or pathologically altered EC, permit targeted delivery of reporters and, perhaps, therapeutic cargoes to the vascular endothelium. In addition to this delivery function, affinity carriers may provide additional means to control rate of internalization and sub-cellular or trans-cellular traffic. This subject will be considered in more detail in the following sections.

4. MECHANISMS OF ENDOTHELIAL ENDOCYTOSIS

Endocytosis is a complex and delicately coordinated process, which involves an extensive cellular machinery to mediate the formation of membrane transport vesicles to enable the internalization of extracellular material (reviewed in [133-135]). In endothelium, which is strategically positioned at the interface between blood vessels and interstitial milieu, endocytosis has a prime role in the maintenance of body homeostasis by regulating transendothelial gradients and the transport of macromolecules (reviewed by [136, 137]). Depending upon the ultimate fate of the internalized vesicles, endocytic events in EC have been categorized as either endocytosis, i.e., the uptake of fluids, biomolecules and other ligands that sort to endothelial processing pathways, or transcytosis that reflects transport across the cells to the subendothelial space [138-140]. EC employ multiple mechanisms for vesicle-mediated membrane transport (see Fig. **1** and Table **2**). The mechanism of endocytosis is frequently dictated by membrane receptors used by extracellular ligands to bind to the plasma membrane as a prerequisite to internalization.

Caveolar-mediated uptake plays an important role in endothelial transport functions (reviewed by [141-144]). Caveolar-mediated endocytosis is preferentially inhibited by chelators of cholesterol (e.g., filipin or cyclodextrin) and is mediated by interactions of the coat protein caveolin with cell signaling and cytoskeletal molecules. Internalization *via* caveoli is involved in the uptake of glycolipids, GPI-anchored proteins, and chemokines [145-148], dynamic recycling of brain microvascular EC membranes [149], constitutive turnover of TM [150], potocytosis of folate and other solutes [151], and can participate in the regulation of the vascular permeability [152]. Importantly, caveolar-mediated endocytosis serves as an entry point for transcytosis of many compounds through the endothelial monolayer from the bloodstream to sub-endothelial tissues (see Section 6).

Clathrin-mediated endocytosis, which is the predominant form of receptor-mediated endocytosis in most cell types, is less prominent in EC than caveolar-mediated endocytosis. Nonetheless, numerous cases of clathrin-mediated endocytosis have been reported among EC, particularly, in EC in hepatic sinusoids, which participate in clathrin-mediated internalization of IgG immune complexes *via* Fc receptors [153]. Mannose-terminated glycoproteins or lactosilated albumin particles are internalized through mannose or galactose-specific receptors [154, 155]. Also, colloidal gold coated with mannan, albumin, or thrombospondin aggregates on coated pits and is taken up by EC in sinusoids in liver [156-159]. This is also the case for chondroitin sulphate proteoglycan attached to gold particles,

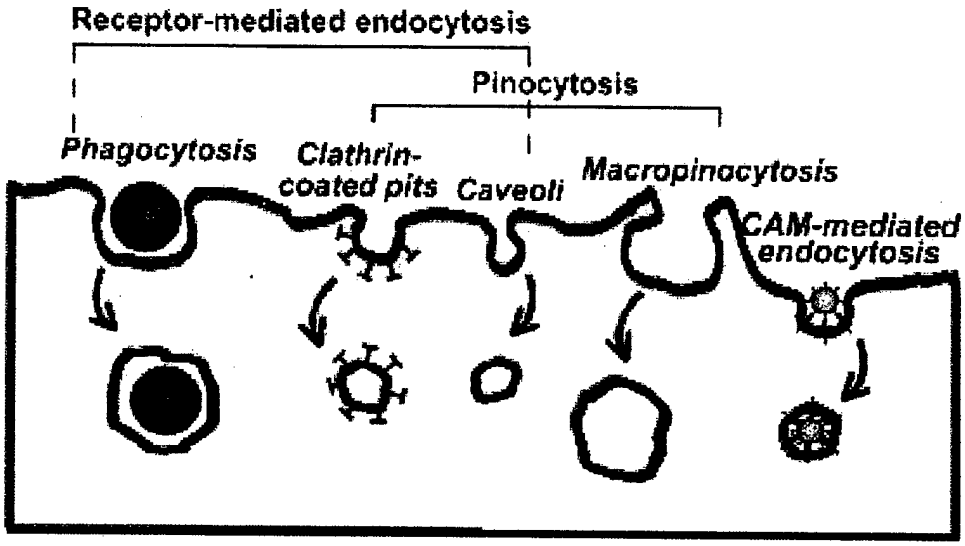

Fig. (1). *Endocytic pathways.* Endocytosis accounts for the internalization of extracellular material into cells, mediated by formation of transport vesicles derived from the plasma membrane. The terms "phagocytosis" and "pinocytosis" refer to the uptake of large particulate ligands and extracellular medium, respectively. In addition, macromolecular ligands can bind to specific receptors at the plasma membrane, triggering their internalization by what is known as "receptor-mediated endocytosis". This term contrasts with "macropinocytosis", which consists in the non-adsorptive bulk uptake of extracellular fluids. Cell adhesion molecule (CAM)-mediated endocytosis is stimulated by clustering Ig superfamily CAMs. "Clathrin-" and "caveoli"-mediated pathways are ubiquitous endocytic mechanisms, whereas "phagocytosis" and "macropinocytosis" are most typically presented by specialized cells (e.g., macrophages, dendritic cells). The five different pathways depicted have been found to some extent in EC, yet "caveoli"-mediated endocytosis seems to be the most active process.

Table 2. Endocytic Pathways and Inhibitors

Internalization pathway	Inhibitor	Molecular target
Clathrin-mediated	Potasium depletion	Clathrin dissociation
Clathrin-mediated	MDC	Protein interaction at latices
Clathrin-mediated	Amantadine	Vesicle budding
Caveoli	Genistein	Tyrosine kinases
Caveoli	Filipin	Cholesterol sequestration
Caveoli	Cyclodextrin	Cholesterol extraction
Multiple	Dynamin K44A, PH*	Dynamin
Macropinocytosis/Phagocytosis	Cytochalasin	Actin filaments
Multiple	Latrunculin	Monomeric actin
Macropinocytosis	Amiloride	Na^+/H^+ exchanger
Macropinocytosis	BIM-1, H7, staurosporin	Protein kinase C
EGF/BCR receptor uptake	Radicicol	Src kinase
Rho dependent uptake	Y27632	ROCK
Macropinocytosis/Phagocytosis	Wortmannin	PI3 kinase

MDC – Monodansyl cadaverine. Dynamin K44A – dominant negative dynamin affected at the ATPase site. Dynamin PH* - dominant negative dynamin affected at the plecktrin homology domain. BIM-1 – Bisindolylmaleimide-1. H7 - 1-(5-Isoquinolinesulfonyl)-2-methylpiperazine. ROCK – Rho dependent kinase. PI 3 kinase – phosphatidyl inositol 3 kinase.

which bind to hyaluronic acid/chondroitin sulphate receptor at the plasma membrane and undergo internalization by coated pits in rat liver EC [160].

The endothelium in many organs (i.e. spleen, bone marrow, thymus, or brain) has been shown to internalize ligands through clathrin-mediated endocytosis, as is the case for acetoacetylated or acetylated LDL [161], gold-coated LDL or insulin/[162], and transferrin [163, 164]. Also, EC likely internalize lipoprotein lipase (LPL) by clathrin-related mechanisms. LPL synthesized and secreted by EC is retained on the abluminal side, being further transported across the cell to the apical space [165], where it provides intravascular hydrolysis of triacylglycerol-rich lipoproteins [166] and also contributes to LDL-holoparticle turnover and selective uptake of LDL-associated lipids [167]. Internalization of LPL within the cell might occur as a consequence of its interaction with heparan sulphate proteoglycans during turnover or recycling of the latter [168]. For instance, LPL stimulates endocytosis of LDL upon binding of membrane-associated heparan sulphate [169] and also enhances binding, uptake and degradation of glycated LDL in a manner independent of LDL receptor and LDL-receptor related protein [170]. Additionally, LPL has been found to bind with high affinity to the glycoprotein gp330 in microvascular EC [171, 172]. Although the localization of gp330 in EC remains unclear, this is typically concentrated to clathrin-coated areas in epithelial cells, indicating that LPL internalization might be mediated by a clathrin-related pathway [173]. However, lipoprotein interactions with the syndecan family of endothelial proteoglycans also can lead to internalization *via* a clusterization-induced pathway distinct from coated pits endocytosis [174].

Clathrin-coated pits also mediate constitutive internalization of plasma membrane proteins, as is the case for E- and P-selectins, two inducible endothelial adhesion molecules whose recycling and/or surface expression is regulated by clathrin-mediated uptake [112, 175]. The inducible expression of selectins has been used as a means to enable intracellular delivery to activated EC. For instance, anti-E-selectin targeted liposomes or conjugates have been found to internalize *via* clathrin-coated pits within EC, to enable intracellular delivery of anti-inflammatory drugs [176, 177].

Another membrane internalization process represented in EC, although to a low extent, is phagocytosis (reviewed in [178, 179]). Phagocytosis, which is typically displayed by macrophages and antigen presenting cells, accounts for the internalization of large (> 1μm) particulate ligands [180]. This requires initial binding of the particle to specific receptors (i.e. scavenger receptor, C3R, FcγR, etc), with subsequent activation of a battery of signaling cascades (i.e. phosphatidyl inositol 3 kinase and Rho family GTPases, among others) (reviewed by [181]). In many instances, these events drive a major redistribution of the actin cytoskeleton. As a consequence of the cortical actin polymerization, either pseudopods or large invaginations form at the cell surface, where the plasma membrane surrounds the particulate ligand in a zipper-like mechanism [182], finally resulting in a cup-shape invagination. This is the case of vascular EC, which have been reported to uptake aged red blood cells and apoptotic cells with phosphatidylserine exposed in the outer layer of the cell surface, upon binding of these to the lectin-like oxidized LDL receptor 1 (LOX-1) [183]. *Neisseria meningitidis* induces the formation of cellular protrusions *via* activation of Rho and Cdc42 and recruitment of ezrin and moesin to the cortical membrane, which mediate bacterial entrance in EC [184].

In contrast to caveoli-mediated, clathrin-mediated endocytosis and phagocytosis, macropinocytosis [185, 186] is generally considered a non-receptor mediated process, where cells uptake large volumes of extracellular fluids and solutes (classical macropinosomes are > 1μm in diameter), during a mechanism that involves active formation of membrane ruffles and protrusions at the plasma membrane [187-189]. This is reminiscent of phagocytosis, where macropinocytosis requires large re-arrangements of the actin cytoskeleton, with involvement of protein kinases C and Rho family small GTPases as central signal transduction players [190-194]. In general, however, macropinocytosis is constitutive in highly specialized cells (i.e. macrophages and dendritic cells) and can be induced by growth factors in epithelial cells [195-197], but does not seem to be a principal endocytic pathway in EC. Nevertheless, it has recently been found that human immunodeficiency virus (HIV) can access brain microvascular EC by a macropinocytic mechanism, apparently involving endothelial ICAM-1 [198].

However, neither phagocytosis, macropinocytosis nor classical clathrin-mediated endocytosis seem to be principal endocytic pathways in vascular endothelium. In fact, coated-pits are much less abundant than non-coated vesicles in capillary endothelium in lung [199]. For example, hormones like insulin or gonadotropin [200, 201], long chain fatty acids such as oleate [202], or ligands for TM [203, 204], have been described to enter vascular EC *via* coated pits as a minor fraction, whereas caveoli account for the internalization of the main pool.

Interestingly, two adhesion molecules constitutively expressed in EC, ICAM-1 and PECAM-1, present the capability to drive internalization of small multivalent ligands, although neither these molecules nor their monomeric ligands (i.e. antibodies) have been found to undergo endocytic uptake in endothelium [75, 87, 205, 206]. However, major group human rhinovirus and respiratory syncytial virus use ICAM-1 as a receptor during cell invasion, although the mechanism of cell uptake remains uncertain [207, 208]. Also, PECAM-1 is required for binding of malaria infected red blood cells to EC in culture [209] and homophilic PECAM-1 interaction displays a signaling role during recognition and phagocytic ingestion of apoptotic leukocytes by macrophages [210].

This offers a pathway for intracellular delivery of therapeutic cargoes, by using small multimeric conjugates of ICAM-1 and PECAM-1 antibodies. These have been recently shown to enter EC by a non-classical endocytic mechanism, CAM-mediated endocytosis, which is distinct from classical clathrin- or caveolar-mediated uptake as well as from phagocytic and macropinocytic processes [206]. In particular, internalization of anti-ICAM-1 or anti-PECAM-1 conjugates was dependent on antigen clustering, and a critical parameter for internalization was conjugate size (100

- 300 nm in diameter). CAM-mediated endocytosis also required Rho kinase- and protein kinase C- mediated rearrangements of the actin cytoskeleton [206].

Anti-PECAM/DNA conjugates provide specific transfection of EC in culture [205] and in mice [22]. Furthermore, anti-PECAM-conjugated glucose oxidase generates H_2O_2 in cultured EC intracellularly in cell culture [211] and induces acute oxidative endothelial injury in murine lungs after IV injection [212]. Recent studies indicate that anti-CAM/catalase conjugates bind to and enter EC, which protects endothelium against oxidant stress in cell cultures [75, 213] and in animals [214].

5. INTRACELLULAR TRAFFICKING AND FATE OF INTERNALIZED MATERIALS

The endocytic pathways reviewed above can be used for the intracellular or transcellular delivery of therapeutic cargoes in EC. Therefore, control of the cellular processes driving the internalization of site-specific therapeutics is important in order to achieve their optimal effects. Intracellular trafficking of a drug can be dictated by its entry pathway; hence determining its final destination and degradation rate. For instance, internalized membranes and/or contents can be selected for recycling to the cell surface, transported through the cell body and exocytosed by transcytosis, sorted to other sub-cellular destinations such as Golgi, trans-Golgi network (TGN) or endoplasmic reticulum (ER), or most typically processed for delivery to specialized intracellular compartments responsible for degradation of internalized materials (see Fig. **2** and Table **3**).

In this context, there are three main systems accounting for protein degradation in mammalian cells. Cytosolic proteins are degraded by proteosomes or calpains, whereas lysosomal proteases digest proteins within the lumen of endocytic vesicles. Calpains are cysteine proteases localized

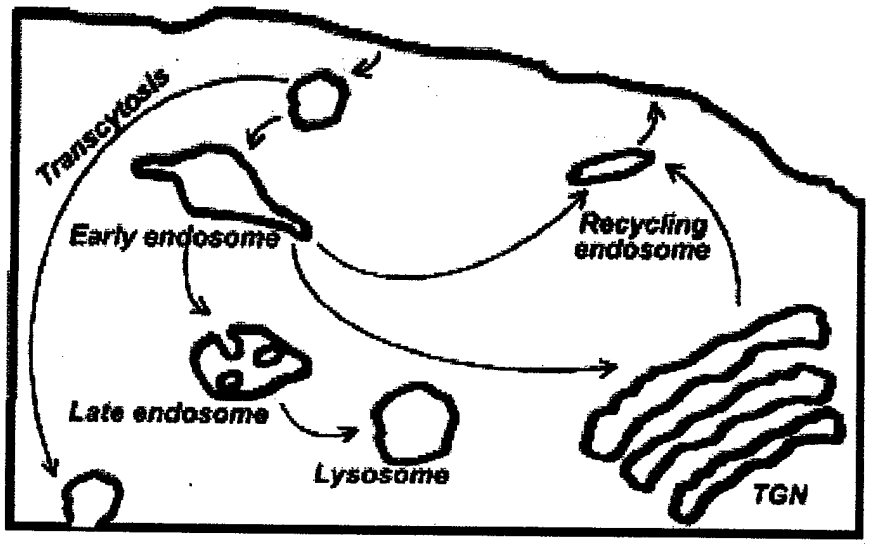

Fig. (2). *Intracellular trafficking.* Endocytic vesicles, containing membrane receptors and their respective ligands or other contents, can be selected for sorting to different sub-cellular compartments. For instance, these can recycle to the cell surface by "recycling endosomes" (e.g., directly or through Trans Golgi Network (TGN) compartments) or transported through the cell body and exocytosed to the abluminal space by "transcytosis". Internalized material can also be processed for delivery to endocytic compartments for degradation (e.g., by trafficking through "early endosomes", "late endosomes" and "lysosomes"), or sorted to other sub-cellular destinations such as Golgi or the Endoplasmic Reticulum.

Table 3. Intracellular Trafficking and Inhibitors

Trafficking pathway	Inhibitor	Molecular target
Trans Golgi network (TGN) trafficking	Brefeldin	TGN/ER-Arf1
Receptor recycling	Chlorpromazine	Recycling
Trafficking to lysosomes and recycling	Monensin	Na^+/H^+ exchange at the endosome
Lysosomal degradation	Ammonium chloride, chloroquine	Vesicle acidification
Lysosomal degradation	Bafilomycin	Vacuolar H^+-ATPase
Endosome-lysosome trafficking	Nocodazole, colchicine	Microtubular network

to the cytoplasm and nucleus of all cell types studied (reviewed by [215]). They undergo activation by Ca^{2+} and phospholipids, which promote targeting of calpains to membranes. In this situation, calpains can exert proteolytic activity, resulting in modification of enzyme [216] and receptor function [217, 218]. Also, cytoskeleton-related proteins can undergo modification by calpain activity, as is the case for calpain-dependent disruption of integrin/ cytoskeleton interactions [216, 219-221].

Another cytosolic degradation system, the proteosome, is also primarily located in the cytosol of all eukaryotic cells. Proteosomes are multisubunit complexes (i.e., 20S, 26S, the immunoproteosome, and the hybrid proteosome), which contain a common core and different additional regulatory subunits (reviewed by [222]). For instance, cytokine-dependent immunoproteosome activation has been related to the production of peptides that will act as ligands of MHC-I [223]. On the other hand, activation of the hybrid proteosome (depending on ATP but not on ubiquitin) generates peptides that are targeted to ER lumen [224]. The function of the proteosome 26S containing subunits that confer this complex the ability to selectively recognize, bind and cleave ubiquitin-tagged proteins has been extensively studied [222]. The process of protein degradation by the ubiquitin system requires initial attachment of ubiquitin residues to the protein substrate by ubiquitin-protein ligases, which recognize particular post-translational modifications in the target proteins. Subsequently, the ubiquitin-tagged proteins will be degraded by the 26S proteosome complex, concomitantly with the release of reusable ubiquitin residues.

However, most typically lysosomes are responsible for proteolysis of internalized material, since most endocytic traffic merges with lysosomal compartments. The endolysosomal system contains a series of differentiated vesicles including early endosomes, late endosomes and lysosomes. Early endosomes are the first compartment where sorting of materials to recycling, degradation pathways or other subcellular organelles is decided [225-229]. In this context, H^+-ATPases and Na^+, K^+-ATPases favor acidification of the endosomal lumen, whereas Na^+/H^+-exchangers help to generate a positive potential that inhibits proton influx [230]. These combined actions regulate the pH at the early endosome lumen, which becomes to be around 6.3-6.5. This mildly acidic pH favors separation of some ligands from their receptors, being the latter typically recycled to the plasma membrane, whereas ligands tend to traffic to late endosomes, as is the case of LDL-R or transferrin-R (reviewed by [231]). Alternatively, the receptor/ligand complex can also be recycled as a unit, or the complex can be entirely targeted to degradation [232].

When sorted to lysosomal compartments, materials traffic to late endosomes. Here, the vacuolar-ATPase pumps H^+ to the vesicle lumen [233], being responsible for the further acidification of this compartment to a pH around 5-5.5 [234]. Regulation of pH also depends on Cl^- channels directed inwardly to counteract the positive membrane potential created by the vacuolar-ATPase activity [235]. The compartments continue to acidify to very low pH (pH 4.8) and materials traffic to lysosomes, the terminal compartment in the degradation pathway. Lysosomes appear as electron dense bodies, where the entrapped materials can be then rapidly degraded by lysosomal acidic proteases [236].

Lysosomal hydrolysis is regulated by proton ATPases and cysteine transporters, as mentioned above, and also by lysosome-associated membrane proteins, the main protein constituent of endolysosomal membranes (reviewed by [237]). The latter are heavily glycosylated transmembrane proteins, referred to as LAMPs, which protect lysosomes from the action of degradative enzymes [238]. Hydrolysis at lysosomal compartments is carried out by proteases (i.e. cathepsins), including both exopeptidases (cysteine and serine proteases) and endopeptidases (cystein and aspartic proteases) [237, 239]. These proteases are extensively glycosylated, which facilitates their trafficking to lysosomes and helps confer resistance to low pH [236].

An example of a typical endocytic pathway, which delivers the internalized materials to the endolysosomal system, is clathrin-mediated internalization, although this can also sort the internalized contents to recycling or transcytotic pathways, after rapid removal of the clathrin coat from the membrane of the vesicles. For instance, transferrin-R or P-selectin can transit from the cell surface to endosomes and TGN, following by trafficking back to the EC surface [163, 175]. However, rapid degradation of P-selectin in lysosomes can also occur as a consequence of its frequent passage through endosomal compartments [175].

Also, a variety of ligands such as IgG immune complexes, glycoproteins, ferritin, thrombospondin, or colloidal gold coated with albumin, insulin, LDL or chondroitin sulphate proteoglycans are transported within minutes to lysosomal compartments in hepatic endothelial sinusoids [153, 154, 157-160, 162, 240]. Moreover, site-specific delivery vehicles targeted to endothelium through E-selectin (i.e. anti-E-selectin liposomes and conjugates) traffic rapidly to multivesicular bodies and other acidic compartments [176, 177], which could considerably reduce the half-life of potential cargoes. In epithelial cells, IgA is internalized by clathrin-mediated endocytosis and subsequently transcytosed from the basolateral to the apical plasma membrane [241]. Whether this pathway also operates in EC remains to be determined, however, some ligands internalized by EC through caveolae are transcytosed (see Section 6).

Phagocytosis typically results in lysosomal delivery. Phagosomes rapidly undergo uncoating of the actin-based machinery after internalization, with recycling of the plasma membrane proteins and degradation of receptors and content by sequential fusion with endosomes and lysosomes [109, 242-244]. Similarly, during macropinocytosis, the internalized contents can be recycled to the cell surface, but more typically are processed by delivery to the endosome-lysosome system. The first case can occur by tubulation of macropinosomes with fission into small vesicular intermediates [245], whereas classically, macropinosomes mature to acidic degradation vesicles by sequential interactions with pre-existing compartments [185, 246].

Ligands internalized by caveolar-mediated endocytosis can be sorted to several intracellular compartments using a variety of sorting pathways, with an interesting capability of

avoiding lysosomal compartments. For instance, cholera toxin traffic through early and late endosomes [145, 146], and SV40 is sorted from early endosomes to Golgi and finally ER [247, 248]. Some ligands, such as folate, can be delivered to the cytoplasm during a process called potocytosis, where folate is transported across the plasma membrane while folate receptor remains associated with caveolae at the plasma membrane [249]. Others, such as alkaline phosphatase, bradykinin, acetylcholine and endothelin, are returned to the cell surface after their internalization [147, 250-252]. Therefore, internalization *via* caveoli tends to favor sorting to sub-cellular compartments other than lysosomes and thus may be useful to avoid rapid degradation pathways. Also caveolar-mediated uptake provides a rapid mechanism for membrane turnover in EC, where plasma membrane components traffic through tubular endosomes and TGN in a constant influx-efflux cycle [149].

As mentioned above, EC can also use a ligand-induced endocytic pathway known as CAM-mediated endocytosis [206]. This internalization pathway delivers materials to lysosomal compartments with unusually slow kinetics (around 3 h) [253]. Conjugation of catalase to anti-ICAM-1 or anti-PECAM-1 antibodies permits intracellular delivery of the active enzyme to EC, and provides anti-oxidant protection for a relatively prolonged window time due to the slow kinetics of delivery to lysosomes [214, 253].

The protective effect of anti-CAM delivered catalase can be further prolonged either in the presence of drugs acting on the microtubular-network (i.e. nocodazole) [253], which is involved in traffic to lysosomes [254], or using weak bases (i.e. chloroquine), which impair acid-dependent activation of degradation enzymes in these compartments [253].

6. TRAVERSING ENDOTHELIAL BARRIERS *VIA* TRANSCYTOSIS AND PARACELLULAR TRANSPORT

In cases when a drug must be delivered to malignant cells in tumors, across the Blood Brain Barrier (BBB) or cardiomyocytes in the heart and other extravascular targets, endothelium represents a barrier that must be traversed for the therapeutic effect. In theory, drugs and macromolecules can extravasate *via* two pathways: transcytosis (i.e., endocytosis on the apical surface followed by traffic through the EC body to the basolateral surface) or diffusion *via* intercellular junctions (paracellular transport). The role and contribution of these two pathways in migration of macromolecules from the bloodstream into tissues is a subject of intense research and ongoing discussions. The theoretical concept of endothelial transcytosis of macromolecules involving dynamic or stable trans-cellular vesicular channels has been postulated by Majno and Palade in the 1960s [255, 256]. However, even today the mechanisms, regulation, significance and therapeutic utility of this pathway remain very much elusive [257].

Numerous studies from several groups including experiments in perfused organs and intact animals strongly indicate that transcytosis represents a significant route across the vascular endothelial barrier [57, 258-263]. When considering transcytosis for the purposes of drug delivery, ligands are endocytosed by the apical (lumenal) aspect of the endothelial plasma membrane, followed by transport through a series of intracellular compartments and delivery to the basolateral (ablumenal) plasma membrane where they are secreted.

An alternate model for transcytosis is through the formation of an organelle, called the vesiculo-vacuolar organelle (VVO) that may form dynamic or stable channels through cells [264]. Both morphological and functional evidence including studies of transendothelial transfer of labeled compounds in animal models show the presence of a VVO in EC [57, 264]. However, relatively little is known about mechanisms of VVO formation and how it can be manipulated pharmacologically. For example, histamine and VEGF seem to stimulate transport *via* VVO formation [264], but the specificity of this functional modulation is difficult to interpret, because these vasoactive agents also facilitate pericellular transport (see below).

Endothelial transcytosis often originates from the caveolar endocytotic pathway, where plasma solutes and macromolecules are taken up from the bloodstream in bulk by fluid phase adsorption (glycogen, dextran, ferritin, etc) or by binding to specific receptors (LDL, ceruloplasmin, etc) and reach the abluminal space [138, 258, 260, 265-267]. Plasma proteins such as albumin, TM, chorionic gonadotropin, insulin and growth factors can be transported to the abluminal surface of the EC *via* caveoli-mediated transcytosis [200, 201, 266, 268]. The levels of plasma lipoproteins and cholesterol homeostasis are believed to be maintained largely by endothelium in arteries which, due to continuous caveolar uptake, serves to reconstitute the levels of cholesterol in the vessel wall and permits the transit and subsequent accessibility of cholesterol-carrying lipoproteins to sub-endothelial layers of the vessel wall and peripheral tissues [269, 270].

Several studies indicated that interaction of a protein ligand leading to receptor clustering in caveoli and activation of specific signaling pathways plays a critical role in initiation of transcytosis [260, 261]. For example, caveolar clustering of endothelial albumin binding protein gp60 has been shown to increase transendothelial permeability by mediation of phosphorylation events including signaling through the Src family of tyrosine kinases [271]. Interestingly, chemical modifications of caveolar ligands, such as albumin nitration (that may take place in oxidant stress and inflammation) even further stimulate transcytosis [272].

Caveolar transcytosis pathways are envisioned as means for transcellular delivery of therapeutics, which could be achieved by targeting caveolae-located receptors. For example, active reporter compounds conjugated with antibodies directed against specific antigen (gp90) localized in pulmonary endothelial caveolae undergo transendothelial and transepithelial transport through pulmonary endothelium from the blood stream to the alveolar space after injection *in vivo* [57]. Although the function of gp90 and potential effects of its inhibition by targeting are unknown, it is tempting to speculate that caveolar targeting will permit more effective extravascular drug delivery.

In this context, transcytosis through the BBB represents a specific interest. The paracellular pathways (see below) in

this vascular area are relatively restricted, yet the BBB endothelium is not all that impermeable and yet can be traversed *via* aplethora of agents (for reviews see [273, 274]). From a biological standpoint, this can be illustrated by the fact that *Escherichia coli* invades the central nervous system by transmigration through brain microvascular EC using an actin- and microtubule-dependent phagocytic mechanism, although this pathway was inactive in systemic EC [275]. From a drug delivery standpoint, it is important that ligands of insulin, putrescine and transferrin receptors are expressed on the BBB endothelium. Also, antibodies and high-affinity binding peptides defined using a BBB endothelial phage-display library show an encouraging ability to accumulate in the brain tissue [32, 276]. Moreover, proteins and genetic "drugs" or reporter compounds conjugated with these affinity carriers display their activities in the brain tissue after systemic administration, suggesting transmission across the BBB [110, 111, 277].

In addition to transcytosis mechanisms, the density and permeability between cells of the endothelial monolayer varies between different organs; in this respect, endothelium can be roughly categorized into three types. The first type is fenestrated endothelium, which is localized to organs of the reticuloendothelial system, including hepatic and spleenic sinuses and bone marrow. Fenestrae is Latin for "windows" and refers to the relatively large pores between the fenestrated EC. These pores can be up to several microns in diameter and thus permit the relatively unhindered extravasation of blood components, including red and WBC in these tissues. A second type is continuous endothelium, which is present in most of other organs such as cardiac, pulmonary and mesenterial blood vessels. Continuous endothelium is relatively tighter than fenestrated endothelium and has fewer pores with 100 nm diameters. Although this can permit passage of macromolecules to tissues, in most cases, filtration through the continuous endothelium is restricted to small molecules and solutes such as glucose and small hormones. The third type is microvascular endothelium, which is the most restricted in permeability. In particular, brain microvascular EC form an extremely dense monolayer, resulting in an extremely tight BBB, which lacks significant permeability for plasma proteins and possesses specific enzymatic systems (glycoprotein P, e.g.) to facilitate reverse transport of molecules from the brain tissue to the circulation [274]. Clearly, due to these differences in vascular permeability, BBB endothelium represents the most formidable biological barrier for the extravascular drug delivery, while fenestrated endothelium does not restrict extravasation of even large carriers such as liposomes, polymer particles and viruses [278].

However, in many organs (e.g., liver) and types of vasculature (e.g., venules) the mainstream of transendothelial transport for nano-scale drug delivery vehicles such as liposomes and polymer carriers follows paracellular pathways. Paracellular endothelial permeability is controlled by proteins which form the tight junction complex localized to contact sites between EC. Proteins in the claudin family form the basis for regulating paracellular permeability [279, 280]. Claudins are not a simple barrier, per se, since many claudins form paracellular channels that enable selective ion permeability. Also, different tissues express different claudins, suggesting at least some regulation at the level of transcription. Recently, a definitive role for claudin-5 in regulating the BBB was demonstrated since substrates less than 1 kD molecular mass were freely permeable across the BBB in claudin-5 deficient mice [281]. Moreover, claudin function and paracellular permeability is also regulated by associated transmembrane proteins (occludin, junction adhesion molecule (JAM), connexins, VE-cadherin) and peripheral proteins, which tether it to the actin cytoskeleton such as ZO-1, ZO-2, ZO-3 and PATJ [282-284]. For instance, HGF/SF treated vascular EC show increased permeability due to ZO-1 phosphorylation, with no effect on claudin expression levels, suggesting a change in barrier function due to disruption of the ZO-1/claudin-1 complex [285]. The ability of VEGF and thrombin to increase endothelial permeability may also be due to a comparable upstream effect on signaling cascades that alter tight junction organization. Hormone activation and cross talk between these different classes of junction proteins and the regulation of claudin function is just beginning to be elucidated and is an active area of research.

The array of different tight junction associated proteins suggests many avenues for pharmacological manipulations of vascular permeability (see [286]). Studies using clostridium toxin, which binds to the extracellular domains of claudin-3 and claudin-4 and disrupts intestinal epithelial barrier function provide a basis for the notion that tight junction interfaces can be disrupted by targeting claudins. Thus, it seems plausible that another class of small molecules or perhaps claudin antibodies might provide an alternative strategy for preferential and transient disruption of EC tight junctions. In particular, the selective change in BBB paracellular permeability exhibited by claudin-5 deficient mice suggests that specific modulation of claudin-5 may have potential as a method to temporarily alter BBB permeability [281]. Conversely, blockade of junction proteins may help increase endothelial barrier function, as indicated above, where anti-ICAM-1 conjugates appear to inhibit leukocyte transmigration.

Many pathological mediators and conditions including hypoxia, hyperoxia, histamine, VEGF, thrombin, hyperthermia, abnormal shear stress, cytokines and ROS elevate vascular permeability [287-291]. However, some compounds (e.g., adenosine) tend to restrict endothelial permeability in cell cultures [292]. Some permeability-enhancing agents (histamine, VEGF) apparently stimulate both transcytosis [122] and pericellular transport [291, 293]. Vasoactive agents inducing paracellular permea-bility cause elevation of cytosolic Ca^{2+} in EC [294], activation of kinases leading to myosin light chain phosphorylation and subsequent endothelial contraction and reorganization of adhesion contacts [77, 288, 295, 296].

Vascular cells, including the endothelium itself, can regulate vascular permeability *via* the action of diverse vasoactive substances, which regulate porosity of endothelial monolayer and blood pressure (the higher intravascular pressure, the more effective extravascular transport). Interestingly, one modality of a vasoactive agent (e.g., its effect on blood pressure) frequently is balanced by its other

modality (effect on permeability). For example, endothelial ACE converts Ang I into Ang II, which induces vasoconstriction, yet ACE also inactivates bradykinin and substance P [61], peptides that increase vascular permeability. EC produce a potent vasodilating agent NO that may reduce vascular permeability at low levels [297].

Due to activities of substance P, thrombin, ROS, VEGF, bradykinin and other kinins endothelial permeability is usually enhanced under pathological conditions including inflammation, which can exacerbate edema [257]. Both these factors and morphological alterations (fenestrations) enhance permeability of tumor vasculature and cause tumor vascular leakiness [123, 290, 298]. This phenomenon is being actively exploited in design of liposomal and polymer carrier-based strategies for drug delivery to tumors (enhanced permeability and retention effect, EPR) [299].

The role of transcytosis *vs* paracellular transport of particular compounds under normal and pathological conditions is controversial and is the subject of continuing discussions. For example, although liposomes can undergo endothelial transcytosis in cell cultures, they likely leave the vasculature *via* pericellular pathways in animals [278]. Experiments in perfused organs showed that albumin extravasation is independent on temperature, suggesting that this process represents a passive diffusion *via* intercellular pores rather than *via* energy-dependent endocytotic pathways [137]. Mice genetically deficient in caveolin, a critical component of caveolar endocytotic pathway, do not show overt abnormalities of tissue transport of plasma components [300, 301]. However, both transcellular and pericellular pathways can and should be employed for rational design of modern drug delivery systems. In theory, pericellular pathways may be more useful for extravasation of drugs in tumors and inflammation foci, whereas endothelial transcytosis might serve as a pathway for drug delivery through the BBB.

CONCLUSION AND PERSPECTIVES

Recent years have produced a wealth of knowledge of molecular mechanisms regulating pathways for endothelial entry, intracellular traffic, degradation or recycling and transcytosis of diverse materials, including therapeutic agents. Optimal endothelial and transendothelial drug delivery promises substantial improvements of effectiveness and safety of therapeutic strategies for treatment of cardiovascular (e.g., atherosclerosis, hypertension, ischemia-reperfusion syndrome), pulmonary (e.g., acute lung injury, hyperoxia, pulmonary hypertension), and metabolic diseases (e.g., diabetes), inflammation (e.g., sepsis and endotoxemia) and tumor growth. One key to effective treatment of these distinct pathologies is the ability to control the rates and precise destinations of endothelial drug delivery. There is a plethora of potential avenues for achieving this challenging and exciting goal.

Optimal selection of endothelial surface determinants and design of drug delivery system molecular characteristics such as valency of binding to endothelium, charge and size will be likely used to control the uptake and fate of drugs. Utilization of cross-linkers sensitive to minute changes in pH or specific cellular proteases (e.g., lysosomal cathepsin G) can be employed for the release of active drugs at selected stages of their intracellular traffic. Conjugation of drugs or drug vehicles with membrane fusion and chaperone peptides will help to achieve yet even more precise sub-cellular localization in organelles such as mitochondrion, nucleus or peroxysomes.

In some cases, therapeutic needs might require methods to decelerate or avoid endothelial internalization such as in case of delivery of anti-thrombotic and other agents, which need to exert their activity in the vascular lumen. Therefore, using non-internalizable determinants (e.g., monomeric anti-ICAM-1) or deceleration of natural endocytotic pathways (e.g., by using vehicles with diameter exceeding the limit of internalization) could be used for this goal. Transcytotic and pericellular transport mechanisms could be employed in the cases when a drug should be delivered beyond the EC.

In summary, binding, entry and traffic of drugs into and through EC represent central paradigms of many drug delivery strategies serving diverse therapeutic goals. Future progress in understanding the control of these processes will provide more effective and safe therapeutic means.

ACKNOWLEDGEMENTS

This work was supported by NIH SCOR in Acute Lung Injury (NHLBI HL 60290, Project 4), NHLBI RO1 (HL/GM 71175-01) and Department of Defense Grant (PR012262) to VRM. SM was supported in part by a fellowship from Fundación Ramón Areces (Spain). M.K. was supported by NIH grants GM61012 and P01 HL019737-26, Project 3.

ABBREVIATIONS

ACE	=	Angiotensin-Converting Enzyme
Ang I	=	Angiotensin 1
Ang II	=	Angiotensin 2
BBB	=	Blood Brain Barrier
CAM	=	Cellular Adhesion Molecule
EDHF	=	Endothelium-Derived Hyperpolarizing Factor
ER	=	Endoplasmic Reticulum
EGF	=	Epithelial Growth Factor
EC	=	Endothelial Cell(s)
GPI	=	Glycosyl Phosphatidyl Inositol
HGF	=	Human Growth Factor
ICAM-1	=	Intercellular Adhesion Molecule-1
JAM	=	Junction Adhesion Molecule
LOX-1	=	Lectin-like Oxidized LDL receptor-1
LPL	=	Lipoprotein Lipase
LAMP	=	Lysosomal Associated Membrane Protein 1
LDL	=	Low Density Lipoprotein
LDL-R	=	Low Density Lipoprotein Receptor
NO	=	Nitric Oxide

PEG	=	Polyethylene Glycol
PECAM	=	Platelet EC Adhesion Molecule-1
ROS	=	Reactive Oxygen Species
ROCK	=	Rho-dependent Kinase
RBC	=	Red Blood Cell
Transferrin-R	=	Transferrin Receptor
TM	=	Thrombomodulin
TGN	=	Trans-Golgi Network
VVO	=	Vesiculo-Vacuolar Organelle
VEGF	=	Vascular Endothelial Growth Factor
WBC	=	White Blood Cells

REFERENCES

[1] Cines DB, Pollak ES, Buck CA, Loscalzo J, Zimmerman GA, McEver RP, et al. Endothelial cells in physiology and in the pathophysiology of vascular disorders. Blood 1998; 91(10): 3527-61.

[2] Gimbrone MA, Jr. Vascular endothelium, hemodynamic forces, and atherogenesis. Am J Pathol 1999; 155(1): 1-5.

[3] Esmon CT. The roles of protein C and thrombomodulin in the regulation of blood coagulation. J Biol Chem 1989; 264(9): 4743-6.

[4] Carlos TM, Harlan JM. Leukocyte-endothelial adhesion molecules. Blood 1994; 84(7): 2068-101.

[5] Muller WA. Leukocyte- endothelial cell interactions in the inflammatory response. Lab Invest 2002; 82(5): 521-33.

[6] Springer TA. Adhesion receptors of the immune system. Nature 1990; 346(6283): 425-34.

[7] Bevilacqua MP, Nelson RM. Endothelial-leukocyte adhesion molecules in inflammation and metastasis. Thromb Haemost 1993; 70(1): 152-4.

[8] Ley K, Tedder TF. Leukocyte interactions with vascular endothelium. New insights into selectin-mediated attachment and rolling. J Immunol 1995; 155(2): 525-8.

[9] Zimmerman GA, McIntyre TM, Prescott SM. Adhesion and signaling in vascular cell-cell interactions. J Clin Invest 1996; 98(8): 1699-702.

[10] Vanhoutte PM. Endothelium-derived free radicals: for worse and for better. J Clin Invest 2001; 107(1): 23-5.

[11] Zulueta JJ, Sawhney R, Yu FS, Cote CC, Hassoun PM. Intracellular generation of reactive oxygen species in endothelial cells exposed to anoxia-reoxygenation. Am J Physiol 1997; 272(5 Pt 1): L897-902.

[12] Rubbo H, Tarpey M, Freeman BA. Nitric oxide and reactive oxygen species in vascular injury. Biochem Soc Symp 1995; 61: 33-45.

[13] Kennel SJ, Lee R, Bultman S, Kabalka G. Rat monoclonal antibody distribution in mice: an epitope inside the lung vascular space mediates very efficient localization. Int J Rad Appl Instrum B 1990; 17(2): 193-200.

[14] Danilov SM, Muzykantov VR, Martynov AV, Atochina EN, Sakharov I, Trakht IN, et al. Lung is the target organ for a monoclonal antibody to angiotensin-converting enzyme. Lab Invest 1991; 64(1): 118-24.

[15] Jacobson BS, Schnitzer JE, McCaffery M, Palade GE. Isolation and partial characterization of the luminal plasmalemma of microvascular endothelium from rat lungs. Eur J Cell Biol 1992; 58(2): 296-306.

[16] Keelan ET, Harrison AA, Chapman PT, Binns RM, Peters AM, Haskard DO. Imaging vascular endothelial activation: an approach using radiolabeled monoclonal antibodies against the endothelial cell adhesion molecule E-selectin. J Nucl Med 1994; 35(2): 276-81.

[17] Muzykantov VR, Danilov SM. Targeting of radiolabeled monoclonal antibody against ACE to the pulmonary endothelium. In: V. Torchilin, editor. Targeted Delivery of Imaging Agents. Roca Baton, Florida: CRC Press; 1995; p. 465-485.

[18] Huang X, Molema G, King S, Watkins L, Edgington TS, Thorpe PE. Tumor infarction in mice by antibody-directed targeting of tissue factor to tumor vasculature. Science 1997; 275(5299): 547-50.

[19] Schnitzer JE. Vascular targeting as a strategy for cancer therapy. N Engl J Med 1998; 339(7): 472-4.

[20] Rajotte D, Arap W, Hagedorn M, Koivunen E, Pasqualini R, Ruoslahti E. Molecular heterogeneity of the vascular endothelium revealed by *in vivo* phage display. J Clin Invest 1998; 102(2): 430-7.

[21] Stan RV, Ghitescu L, Jacobson BS, Palade GE. Isolation, cloning, and localization of rat PV-1, a novel endothelial caveolar protein. J Cell Biol 1999; 145(6): 1189-98.

[22] Li S, Tan Y, Viroonchatapan E, Pitt BR, Huang L. Targeted gene delivery to pulmonary endothelium by anti-PECAM antibody. Am J Physiol Lung Cell Mol Physiol 2000; 278(3): L504-11.

[23] Nicklin SA, White SJ, Watkins SJ, Hawkins RE, Baker AH. Selective targeting of gene transfer to vascular endothelial cell by use of peptides isolated by phage display. Circulation 2000; 102(2): 231-7.

[24] Ranney DF. Biomimetic transport and rational drug delivery. Biochem Pharmacol 2000; 59(2): 105-14.

[25] Reynolds PN, Zinn KR, Gavrilyuk VD, Balyasnikova IV, Rogers BE, Buchsbaum DJ, et al. A targetable, injectable adenoviral vector for selective gene delivery to pulmonary endothelium *in vivo*. Mol Ther 2000; 2(6): 562-78.

[26] Reynolds PN, Nicklin SA, Kaliberova L, Boatman BG, Grizzle WE, Balyasnikova IV, et al. Combined transductional and transcriptional targeting improves the specificity of transgene expression *in vivo*. Nat Biotechnol 2001; 19(9): 838-42.

[27] Poznansky MJ, Juliano RL. Biological approaches to the controlled delivery of drugs: a critical review. Pharmacol Rev 1984; 36(4): 277-336.

[28] Drexler H, Hornig B. Endothelial dysfunction in human disease. J Mol Cell Cardiol 1999; 31(1): 51-60.

[29] Semple G, Ashworth DM, Batt AR, Baxter AJ, Benzies DW, Elliot LH, et al. Peptidomimetic aminomethylene ketone inhibitors of interleukin-1 beta-converting enzyme (ICE). Bioorg Med Chem Lett 1998; 8(8): 959-64.

[30] Bangham AD. Surrogate cells or Trojan horses. The discovery of liposomes. Bioessays 1995; 17(12): 1081-8.

[31] Tamada JA, Langer R. Erosion kinetics of hydrolytically degradable polymers. Proc Natl Acad Sci USA 1993; 90(2): 552-6.

[32] Jeong B, Bae YH, Lee DS, Kim SW. Biodegradable block copolymers as injectable drug-delivery systems. Nature 1997; 388(6645): 860-2.

[33] Bartus RT, Tracy MA, Emerich DF, Zale SE. Sustained delivery of proteins for novel therapeutic agents. Science 1998; 281(5380): 1161-2.

[34] Luo D, Saltzman WM. Synthetic DNA delivery systems. Nat Biotechnol 2000; 18(1): 33-7.

[35] Shen ZR, Zhu JH, Ma Z, Wang F, Wang ZY. Preparation of biodegradable microspheres of testosterone with poly(D,L-lactide-co-glycolide) and test of drug release *in vitro*. Artif Cells Blood Substit Immobil Biotechnol 2000; 28(1): 57-64.

[36] Yang YY, Chung TS, Ng NP. Morphology, drug distribution, and *in vitro* release profiles of biodegradable polymeric microspheres containing protein fabricated by double-emulsion solvent extraction/evaporation method. Biomaterials 2001; 22(3): 231-41.

[37] Siepmann J, Gopferich A. Mathematical modeling of bioerodible, polymeric drug delivery systems. Adv Drug Deliv Rev 2001; 48(2-3): 229-47.

[38] Abuchowski A, McCoy JR, Palczuk NC, van Es T, Davis FF. Effect of covalent attachment of polyethylene glycol on immunogenicity and circulating life of bovine liver catalase. J Biol Chem 1977; 252(11): 3582-6.

[39] Phillips WT, Klipper RW, Awasthi VD, Rudolph AS, Cliff R, Kwasiborski V, et al. Polyethylene glycol-modified liposome-encapsulated hemoglobin: a long circulating red cell substitute. J Pharmacol Exp Ther 1999; 288(2): 665-70.

[40] Liu TH, Beckman JS, Freeman BA, Hogan EL, Hsu CY. Polyethylene glycol-conjugated superoxide dismutase and catalase reduce ischemic brain injury. Am J Physiol 1989; 256(2 Pt 2): H589-93.

[41] Freeman BA, Turrens JF, Mirza Z, Crapo JD, Young SL. Modulation of oxidant lung injury by using liposome-entrapped superoxide dismutase and catalase. Fed Proc 1985; 44(10): 2591-5.

[42] Lee HJ, Engelhardt B, Lesley J, Bickel U, Pardridge WM. Targeting rat anti-mouse transferrin receptor monoclonal antibodies through blood-brain barrier in mouse. J Pharmacol Exp Ther 2000; 292(3): 1048-52.

[43] Adlakha-Hutcheon G, Bally MB, Shew CR, Madden TD. Controlled destabilization of a liposomal drug delivery system enhances mitoxantrone antitumor activity. Nat Biotechnol 1999; 17(8): 775-9.

[44] Raso V. Immunotargeting intracellular compartments. Anal Biochem 1994; 222(2): 297-304.

[45] Caron PC, Laird W, Co MS, Avdalovic NM, Queen C, Scheinberg DA. Engineered humanized dimeric forms of IgG are more effective antibodies. J Exp Med 1992; 176(4): 1191-5.

[46] Pardridge WM, Buciak J, Yang J, Wu D. Enhanced endocytosis in cultured human breast carcinoma cells and *in vivo* biodistribution in rats of a humanized monoclonal antibody after cationization of the protein. J Pharmacol Exp Ther 1998; 286(1): 548-54.

[47] Becerril B, Poul MA, Marks JD. Toward selection of internalizing antibodies from phage libraries. Biochem Biophys Res Commun 1999; 255(2): 386-93.

[48] Nielsen UB, Marks JD. Internalizing antibodies and targeted cancer therapy: direct selection from phage display libraries. Pharm Sci Technol 2000; 3(8): 282-291.

[49] Schwartz JJ, Zhang S. Peptide-mediated cellular delivery. Curr Opin Mol Ther 2000; 2(2): 162-7.

[50] Jin LH, Bahn JH, Eum WS, Kwon HY, Jang SH, Han KH, et al. Transduction of human catalase mediated by an HIV-1 TAT protein basic domain and arginine-rich peptides into mammalian cells. Free Radic Biol Med 2001; 31(11): 1509-19.

[51] Lewin M, Carlesso N, Tung CH, Tang XW, Cory D, Scadden DT, et al. Tat peptide-derivatized magnetic nanoparticles allow *in vivo* tracking and recovery of progenitor cells. Nat Biotechnol 2000; 18(4): 410-4.

[52] Torchilin VP, Rammohan R, Weissig V, Levchenko TS. TAT peptide on the surface of liposomes affords their efficient intracellular delivery even at low temperature and in the presence of metabolic inhibitors. Proc Natl Acad Sci USA 2001; 98(15): 8786-91.

[53] Muzykantov V. Immunotargeting of drugs to the pulmonary vascular endothelium as a therapeutic strategy. Pathophysiology 1998; 5: 15-33.

[54] Greenwalt TJ, Steane EA. Evaluation of methods for quantitating erythrocyte antibodies and description of a new method using horseradish peroxidase-labelled antiglobulin. Haematologia (Budap) 1980; 13(1-4): 33-48.

[55] Vainio O, Dunon D, Aissi F, Dangy JP, McNagny KM, Imhof BA. HEMCAM, an adhesion molecule expressed by c-kit+ hemopoietic progenitors. J Cell Biol 1996; 135(6 Pt 1): 1655-68.

[56] Goetz DJ, el-Sabban ME, Hammer DA, Pauli BU. Lu-ECAM-1-mediated adhesion of melanoma cells to endothelium under conditions of flow. Int J Cancer 1996; 65(2): 192-9.

[57] McIntosh DP, Tan XY, Oh P, Schnitzer JE. Targeting endothelium and its dynamic caveolae for tissue-specific transcytosis *in vivo*: a pathway to overcome cell barriers to drug and gene delivery. Proc Natl Acad Sci USA 2002; 99(4): 1996-2001.

[58] Kennel SJ, Lankford TK, Foote LJ, Davis IA, Boll RA, Mirzadeh S. Combination vascular targeted and tumor targeted radioimmunotherapy. Cancer Biother Radiopharm 1999; 14(5): 371-9.

[59] Esmon CT. Thrombomodulin as a model of molecular mechanisms that modulate protease specificity and function at the vessel surface. Faseb J 1995; 9(10): 946-55.

[60] Christofidou-Solomidou M, Kennel S, Scherpereel A, Wiewrodt R, Solomides CC, Pietra GG, et al. Vascular immunotargeting of glucose oxidase to the endothelial antigens induces distinct forms of oxidant acute lung injury: targeting to thrombomodulin, but not to PECAM-1, causes pulmonary thrombosis and neutrophil transmigration. Am J Pathol 2002; 160(3): 1155-69.

[61] Erdos EG. Angiotensin I converting enzyme and the changes in our concepts through the years. Lewis K. Dahl memorial lecture. Hypertension 1990; 16(4): 363-70.

[62] Laursen JB, Rajagopalan S, Galis Z, Tarpey M, Freeman BA, Harrison DG. Role of superoxide in angiotensin II-induced but not catecholamine-induced hypertension. Circulation 1997; 95(3): 588-93.

[63] Heitsch H, Brovkovych S, Malinski T, Wiemer G. Angiotensin-(1-7)-Stimulated Nitric Oxide and Superoxide Release From Endothelial Cells. Hypertension 2001; 37(1): 72-76.

[64] Danilov SM, Gavrilyuk VD, Franke FE, Pauls K, Harshaw DW, McDonald TD, et al. Lung uptake of antibodies to endothelial antigens: key determinants of vascular immunotargeting. Am J Physiol Lung Cell Mol Physiol 2001; 280(6): L1335-47.

[65] Muzykantov VR, Atochina EN, Kuo A, Barnathan ES, Notarfrancesco K, Shuman H, et al. Endothelial cells internalize monoclonal antibody to angiotensin-converting enzyme. Am J Physiol 1996; 270(5 Pt 1): L704-13.

[66] Olson SC, Dowds TA, Pino PA, Barry MT, Burke-Wolin T. ANG II stimulates endothelial nitric oxide synthase expression in bovine pulmonary artery endothelium. Am J Physiol 1997; 273(2 Pt 1): L315-21.

[67] Danilov S, Jaspard E, Churakova T, Towbin H, Savoie F, Wei L, et al. Structure-function analysis of angiotensin I-converting enzyme using monoclonal antibodies. Selective inhibition of the amino-terminal active site. J Biol Chem 1994; 269(43): 26806-14.

[68] Sadhukhan R, Santhamma KR, Reddy P, Peschon JJ, Black RA, Sen I. Unaltered cleavage and secretion of angiotensin-converting enzyme in tumor necrosis factor-alpha-converting enzyme-deficient mice. J Biol Chem 1999; 274(15): 10511-6.

[69] Balyasnikova IV, Karran EH, Albrecht RF 2nd, Danilov SM. Epitope-specific antibody-induced cleavage of angiotensin-converting enzyme from the cell surface. Biochem J 2002; 362(Pt 3): 585-95.

[70] Muzykantov VR. Delivery of antioxidant enzyme proteins to the lung. Antioxid Redox Signal 2001; 3(1): 39-62.

[71] Atochina EN, Hiemisch HH, Muzykantov VR, Danilov SM. Systemic administration of platelet-activating factor in rat reduces specific pulmonary uptake of circulating monoclonal antibody to angiotensin-converting enzyme. Lung 1992; 170(6): 349-58.

[72] Muzykantov VR, Atochina EN, Ischiropoulos H, Danilov SM, Fisher AB. Immunotargeting of antioxidant enzyme to the pulmonary endothelium. Proc Natl Acad Sci USA 1996; 93(11): 5213-8.

[73] Atochina EN, Balyasnikova IV, Danilov SM, Granger DN, Fisher AB, Muzykantov VR. Immunotargeting of catalase to ACE or ICAM-1 protects perfused rat lungs against oxidative stress. Am J Physiol 1998; 275(4 Pt 1): L806-17.

[74] Newman PJ. The biology of PECAM-1. J Clin Invest 1997; 99(1): 3-8.

[75] Muzykantov VR, Christofidou-Solomidou M, Balyasnikova I, Harshaw DW, Schultz L, Fisher AB, et al. Streptavidin facilitates internalization and pulmonary targeting of an anti- endothelial cell antibody (platelet- endothelial cell adhesion molecule 1): a strategy for vascular immunotargeting of drugs. Proc Natl Acad Sci USA 1999; 96(5): 2379-84.

[76] Rinaldo J, Christman, J. ARDS: pathogenesis. In: Fishman A, editor. Fishman's Pulmonary Diseases and Disorders. New York: McGraw and Hill; 1998. p. 2537-2548.

[77] Mulligan MS, Miyasaka M, Tamatani T, Jones ML, Ward PA. Requirements for L-selectin in neutrophil-mediated lung injury in rats. J Immunol 1994; 152(2): 832-40.

[78] Meyrick BO. Endotoxin-mediated pulmonary endothelial cell injury. Fed Proc 1986; 45(1): 19-24.

[79] Vaporciyan AA, DeLisser HM, Yan HC, Mendiguren, II, Thom SR, Jones ML, et al. Involvement of platelet- endothelial cell adhesion molecule-1 in neutrophil recruitment *in vivo*. Science 1993; 262(5139): 1580-2.

[80] Scherpereel A, Wiewrodt R, Christofidou-Solomidou M, Gervais R, Murciano JC, Albelda SM, et al. Cell-selective intracellular delivery of a foreign enzyme to endothelium *in vivo* using vascular immunotargeting. FASEB J 2001; 15(2): 416-26.

[81] Scherpereel A, Rome JJ, Wiewrodt R, Watkins SC, Harshaw DW, Alder S, et al. Platelet- endothelial cell adhesion molecule-1-directed immunotargeting to cardiopulmonary vasculature. J Pharmacol Exp Ther 2002; 300(3): 777-86.

[82] Bevilacqua MP, Stengelin S, Gimbrone MA Jr, Seed B. Endothelial leukocyte adhesion molecule 1: an inducible receptor for neutrophils related to complement regulatory proteins and lectins. Science 1989; 243(4895): 1160-5.

[83] Albelda SM. Endothelial and epithelial cell adhesion molecules. Am J Respir Cell Mol Biol 1991; 4(3): 195-203.

[84] Kishimoto TK, Rothlein R. Integrins, ICAMs, and selectins: role and regulation of adhesion molecules in neutrophil recruitment to inflammatory sites. Adv Pharmacol 1994; 25: 117-69.

[85] Panes J, Perry MA, Anderson DC, Muzykantov VR, Carden DL, Miyasaka M, et al. Portal hypertension enhances endotoxin-induced intercellular adhesion molecule 1 up-regulation in the rat. Gastroenterology 1996; 110(3): 866-74.

[86] Komatsu S, Panes J, Russell JM, Anderson DC, Muzykantov VR, Miyasaka M, et al. Effects of chronic arterial hypertension on constitutive and induced intercellular adhesion molecule-1 expression *in vivo*. Hypertension 1997; 29(2): 683-9.

[87] Murciano JC, Muro S, Koniaris L, Christofidou-Solomidou M, Harshaw DW, Albelda SM, et al. ICAM-directed vascular immunotargeting of anti-thrombotic agents to the endothelial surface. Blood 2003; 101(10): 3977-84.

[88] Dustin ML, Rothlein R, Bhan AK, Dinarello CA, Springer TA. Induction by IL 1 and interferon-gamma: tissue distribution, biochemistry, and function of a natural adherence molecule (ICAM-1). J Immunol 1986; 137(1): 245-54.

[89] Hubbard AK, Rothlein R. Intercellular adhesion molecule-1 (ICAM-1) expression and cell signaling cascades. Free Radic Biol Med 2000; 28(9): 1379-86.

[90] Mulligan MS, Vaporciyan AA, Miyasaka M, Tamatani T, Ward PA. Tumor necrosis factor alpha regulates *in vivo* intrapulmonary expression of ICAM-1. Am J Pathol 1993; 142(6): 1739-49.

[91] Doerschuk CM, Quinlan WM, Doyle NA, Bullard DC, Vestweber D, Jones ML, et al. The role of P-selectin and ICAM-1 in acute lung injury as determined using blocking antibodies and mutant mice. J Immunol 1996; 157(10): 4609-14.

[92] Amano J, Hiroe M, Ohta Y, Ishiyama S, Nishikawa T, Tanaka H, et al. Uptake of indium-111-anti-intercellular adhesion molecule-1 monoclonal antibody in the allografted rat lung during acute rejection. J Heart Lung Transplant 1996; 15(10): 1027-33.

[93] Sasso DE, Gionfriddo MA, Thrall RS, Syrbu SI, Smilowitz HM, Weiner RE. Biodistribution of indium-111-labeled antibody directed against intercellular adhesion molecule-1. J Nucl Med 1996; 37(4): 656-61.

[94] Villanueva FS, Jankowski RJ, Klibanov S, Pina ML, Alber SM, Watkins SC, et al. Microbubbles targeted to intercellular adhesion molecule-1 bind to activated coronary artery endothelial cells. Circulation 1998; 98(1): 1-5.

[95] Weiner RE, Sasso DE, Gionfriddo MA, Syrbu SI, Smilowitz HM, Vento J, et al. Early detection of bleomycin-induced lung injury in rat using indium-111-labeled antibody directed against intercellular adhesion molecule-1. J Nucl Med 1998; 39(4): 723-8.

[96] Klibanov AL, Hughes MS, Villanueva FS, Jankowski RJ, Wagner WR, Wojdyla JK, et al. Targeting and ultrasound imaging of microbubble-based contrast agents. Magma 1999; 8(3): 177-84.

[97] Diamond MS, Staunton DE, Marlin SD, Springer TA. Binding of the integrin Mac-1 (CD11b/CD18) to the third immunoglobulin-like domain of ICAM-1 (CD54) and its regulation by glycosylation. Cell 1991; 65(6): 961-71.

[98] Kunkel EJ, Jung U, Bullard DC, Norman KE, Wolitzky BA, Vestweber D, et al. Absence of trauma-induced leukocyte rolling in mice deficient in both P-selectin and intercellular adhesion molecule 1. J Exp Med 1996; 183(1): 57-65.

[99] Steeber DA, Campbell MA, Basit A, Ley K, Tedder TF. Optimal selectin-mediated rolling of leukocytes during inflammation *in vivo* requires intercellular adhesion molecule-1 expression. Proc Natl Acad Sci USA 1998; 95(13): 7562-7.

[100] Jun CD, Shimaoka M, Carman CV, Takagi J, Springer TA. Dimerization and the effectiveness of ICAM-1 in mediating LFA-1-dependent adhesion. Proc Natl Acad Sci USA 2001; 98(12): 6830-5.

[101] Staunton DE, Merluzzi VJ, Rothlein R, Barton R, Marlin SD, Springer TA. A cell adhesion molecule, ICAM-1, is the major surface receptor for rhinoviruses. Cell 1989; 56(5): 849-53.

[102] Rothlein R, Mainolfi EA, Kishimoto TK. Treatment of inflammation with anti-ICAM-1. Res Immunol 1993; 144(9): 735-9; discussion 754-62.

[103] DeMeester SR, Molinari MA, Shiraishi T, Okabayashi K, Manchester JK, Wick MR, et al. Attenuation of rat lung isograft reperfusion injury with a combination of anti-ICAM-1 and anti-beta2 integrin monoclonal antibodies. Transplantation 1996; 62(10): 1477-85.

[104] Lefer DJ, Flynn DM, Anderson DC, Buda AJ. Combined inhibition of P-selectin and ICAM-1 reduces myocardial injury following ischemia and reperfusion. Am J Physiol 1996; 271(6 Pt 2): H2421-9.

[105] Murohara T, Delyani JA, Albelda SM, Lefer AM. Blockade of platelet endothelial cells adhesion molecule-1 protects against myocardial ischemia and reperfusion injury in cats. J Immunol 1996; 156(9): 3550-7.

[106] Kumasaka T, Quinlan WM, Doyle NA, Condon TP, Sligh J, Takei F, et al. Role of the intercellular adhesion molecule-1(ICAM-1) in endotoxin-induced pneumonia evaluated using ICAM-1 antisense oligonucleotides, anti-ICAM-1 monoclonal antibodies, and ICAM-1 mutant mice. J Clin Invest 1996; 97(10): 2362-9.

[107] Ghitescu L, Jacobson BS, Crine P. A novel, 85 kDa endothelial antigen differentiates plasma membrane macrodomains in lung alveolar capillaries. Endothelium 1999; 6(3): 241-50.

[108] Murciano JC, Harshaw DW, Ghitescu L, Danilov SM, Muzykantov VR. Vascular immunotargeting to endothelial surface in a specific macrodomain in alveolar capillaries. Am J Respir Crit Care Med 2001; 164(7): 1295-302.

[109] Muller WA, Steinman RM, Cohn ZA. The membrane proteins of the vacuolar system. II. Bidirectional flow between secondary lysosomes and plasma membrane. J Cell Biol 1980; 86(1): 304-14.

[110] Song BW, Vinters HV, Wu D, Pardridge WM. Enhanced neuroprotective effects of basic fibroblast growth factor in regional brain ischemia after conjugation to a blood-brain barrier delivery vector. J Pharmacol Exp Ther 2002; 301(2): 605-10.

[111] Zhang Y, Schlachetzki F, Pardridge WM. Global non-viral gene transfer to the primate brain following intravenous administration. Mol Ther 2003; 7(1): 11-8.

[112] von Asmuth EJ, Smeets EF, Ginsel LA, Onderwater JJ, Leeuwenberg JF, Buurman WA. Evidence for endocytosis of E-selectin in human endothelial cells. Eur J Immunol 1992; 22(10): 2519-26.

[113] Kuijpers TW, Raleigh M, Kavanagh T, Janssen H, Calafat J, Roos D, et al. Cytokine-activated endothelial cells internalize E-selectin into a lysosomal compartment of vesiculotubular shape. A tubulin-driven process. J Immunol 1994; 152(10): 5060-9.

[114] Kiely JM, Cybulsky MI, Luscinskas FW, Gimbrone MA, Jr. Immunoselective targeting of an anti-thrombin agent to the surface of cytokine-activated vascular endothelial cells. Arterioscler Thromb Vasc Biol 1995; 15(8): 1211-8.

[115] Spragg DD, Alford DR, Greferath R, Larsen CE, Lee KD, Gurtner GC, et al. Immunotargeting of liposomes to activated vascular endothelial cells: a strategy for site-selective delivery in the cardiovascular system. Proc Natl Acad Sci USA 1997; 94(16): 8795-800.

[116] Fujise K, Revelle BM, Stacy L, Madison EL, Yeh ET, Willerson JT, et al. A tissue plasminogen activator/P-selectin fusion protein is an effective thrombolytic agent. Circulation 1997; 95(3): 715-22.

[117] Harari OA, Wickham TJ, Stocker CJ, Kovesdi I, Segal DM, Huehns TY, et al. Targeting an adenoviral gene vector to cytokine-activated vascular endothelium via E-selectin. Gene Ther 1999; 6(5): 801-7.

[118] Lindner JR, Song J, Christiansen J, Klibanov AL, Xu F, Ley K. Ultrasound assessment of inflammation and renal tissue injury with microbubbles targeted to P-selectin. Circulation 2001; 104(17): 2107-12.

[119] McDevitt MR, Ma D, Lai LT, Simon J, Borchardt P, Frank RK, et al. Tumor therapy with targeted atomic nanogenerators. Science 2001; 294(5546): 1537-40.

[120] Folkman J. Angiogenesis inhibitors generated by tumors. Mol Med 1995; 1(2): 120-2.

[121] Jain RK. Delivery of molecular and cellular medicine to solid tumors. Adv Drug Deliv Rev 2001; 46(1-3): 149-68.

[122] Dvorak HF, Nagy JA, Dvorak AM. Structure of solid tumors and their vasculature: implications for therapy with monoclonal antibodies. Cancer Cells 1991; 3(3): 77-85.

[123] Hashizume H, Baluk P, Morikawa S, McLean JW, Thurston G, Roberge S, et al. Openings between defective endothelial cells explain tumor vessel leakiness. Am J Pathol 2000; 156(4): 1363-80.

[124] Brooks PC, Clark RA, Cheresh DA. Requirement of vascular integrin alpha v beta 3 for angiogenesis. Science 1994; 264(5158): 569-71.

[125] Burrows FJ, Derbyshire EJ, Tazzari PL, Amlot P, Gazdar AF, King SW, et al. Up-regulation of endoglin on vascular endothelial cells in human solid tumors: implications for diagnosis and therapy. Clin Cancer Res 1995; 1(12): 1623-34.

[126] St Croix B, Rago C, Velculescu V, Traverso G, Romans KE, Montgomery E, et al. Genes expressed in human tumor endothelium. Science 2000; 289(5482): 1197-202.

[127] Molema G. Tumor vasculature directed drug targeting: applying new technologies and knowledge to the development of clinically relevant therapies. Pharm Res 2002; 19(9): 1251-8.

[128] Arap W, Pasqualini R, Ruoslahti E. Cancer treatment by targeted drug delivery to tumor vasculature in a mouse model. Science 1998; 279(5349): 377-80.

[129] Ran S, Gao B, Duffy S, Watkins L, Rote N, Thorpe PE. Infarction of solid Hodgkin's tumors in mice by antibody-directed targeting of tissue factor to tumor vasculature. Cancer Res 1998; 58(20): 4646-53.

[130] Duncan R. Polymer-drug conjugates: targeting cancer. In: Muzykantov V and Torchilin V, editors. Biomedical aspects of drug targeting. Boston/Dodrecht/London.: Kluwer Academic Publishers; 2003; p. 193-209.

[131] Sugano M, Egilmez NK, Yokota SJ, Chen FA, Harding J, Huang SK, et al. Antibody targeting of doxorubicin-loaded liposomes suppresses the growth and metastatic spread of established human lung tumor xenografts in severe combined immunodeficient mice. Cancer Res 2000; 60(24): 6942-9.

[132] Schraa AJ, Kok RJ, Berendsen AD, Moorlag HE, Bos EJ, Meijer DK, et al. Endothelial cells internalize and degrade RGD-modified proteins developed for tumor vasculature targeting. J Control Release 2002; 83(2): 241-51.

[133] Riezman H, Woodman PG, van Meer G, Marsh M. Molecular mechanisms of endocytosis. Cell 1997; 91(6): 731-8.

[134] Conner SD, Schmid SL. Regulated portals of entry into the cell. Nature 2003; 422(6927): 37-44.

[135] Mukherjee S, Ghosh RN, Maxfield FR. Endocytosis. Physiol Rev 1997; 77(3): 759-803.

[136] Simionescu M, Gafencu A, Antohe F. Transcytosis of plasma macromolecules in endothelial cells: a cell biological survey. Microsc Res Tech 2002; 57(5): 269-88.

[137] Rippe B, Rosengren BI, Carlsson O, Venturoli D. Transendothelial transport: the vesicle controversy. J Vasc Res 2002; 39(5): 375-90.

[138] Simionescu M, Simionescu N. Endothelial transport of macromolecules: transcytosis and endocytosis. A look from cell biology. Cell Biol Rev 1991; 25(1): 5-78.

[139] Predescu D, Palade GE. Plasmalemmal vesicles represent the large pore system of continuous microvascular endothelium. Am J Physiol 1993; 265(2 Pt 2): H725-33.

[140] Minshall RD, Tiruppathi C, Vogel SM, Malik AB. Vesicle formation and trafficking in endothelial cells and regulation of endothelial barrier function. Histochem Cell Biol 2002; 117(2): 105-12.

[141] Stan RV. Structure and function of endothelial caveolae. Microsc Res Tech 2002; 57(5): 350-64.

[142] Schnitzer JE, Liu J, Oh P. Endothelial caveolae have the molecular transport machinery for vesicle budding, docking, and fusion including VAMP, NSF, SNAP, annexins, and GTPases. J Biol Chem 1995; 270(24): 14399-404.

[143] Schnitzer JE, McIntosh DP, Dvorak AM, Liu J, Oh P. Separation of caveolae from associated microdomains of GPI-anchored proteins. Science 1995; 269(5229): 1435-9.

[144] Schnitzer JE. Caveolae: from basic trafficking mechanisms to targeting transcytosis for tissue-specific drug and gene delivery *in vivo*. Adv Drug Deliv Rev 2001; 49(3): 265-80.

[145] Montesano R, Roth J, Robert A, Orci L. Non-coated membrane invaginations are involved in binding and internalization of cholera and tetanus toxins. Nature 1982; 296(5858): 651-3.

[146] Tran D, Carpentier JL, Sawano F, Gorden P, Orci L. Ligands internalized through coated or noncoated invaginations follow a common intracellular pathway. Proc Natl Acad Sci USA 1987; 84(22): 7957-61.

[147] Parton RG, Joggerst B, Simons K. Regulated internalization of caveolae. J Cell Biol 1994; 127(5): 1199-215.

[148] Vilhardt F, Nielsen M, Sandvig K, van Deurs B. Urokinase-type plasminogen activator receptor is internalized by different mechanisms in polarized and nonpolarized Madin-Darby canine kidney epithelial cells. Mol Biol Cell 1999; 10(1): 179-95.

[149] Raub TJ, Audus KL. Adsorptive endocytosis and membrane recycling by cultured primary bovine brain microvessel endothelial cell monolayers. J Cell Sci 1990; 97 (Pt 1): 127-38.

[150] Teasdale MS, Bird CH, Bird P. Internalization of the anticoagulant thrombomodulin is constitutive and does not require a signal in the cytoplasmic domain. Immunol Cell Biol 1994; 72(6): 480-8.

[151] Anderson RG, Kamen BA, Rothberg KG, Lacey SW. Potocytosis: sequestration and transport of small molecules by caveolae. Science 1992; 255(5043): 410-1.

[152] Hofman P, Blaauwgeers HG, Tolentino MJ, Adamis AP, Nunes Cardozo BJ, Vrensen GF, et al. VEGF-A induced hyperpermeability of blood-retinal barrier endothelium *in vivo* is predominantly associated with pinocytotic vesicular transport and not with formation of fenestrations. Vascular endothelial growth factor-A. Curr Eye Res 2000; 21(2): 637-45.

[153] Kosugi I, Muro H, Shirasawa H, Ito I. Endocytosis of soluble IgG immune complex and its transport to lysosomes in hepatic sinusoidal endothelial cells. J Hepatol 1992; 16(1-2): 106-14.

[154] Stang E, Kindberg GM, Berg T, Roos N. Endocytosis mediated by the mannose receptor in liver endothelial cells. An immunocytochemical study. Eur J Cell Biol 1990; 52(1): 67-76.

[155] Dini L, Kolb-Bachofen V. Preclustered receptor arrangement is a prerequisite for galactose-specific clearance of large particulate ligands in rat liver. Exp Cell Res 1989; 184(1): 235-40.

[156] Kempka G, Kolb-Bachofen V. Binding, uptake, and transcytosis of ligands for mannose-specific receptors in rat liver: an electron microscopic study. Exp Cell Res 1988; 176(1): 38-48.

[157] Geoffroy JS, Becker RP. Endocytosis by endothelial phagocytes: uptake of bovine serum albumin-gold conjugates in bone marrow. J Ultrastruct Res 1984; 89(3): 223-39.

[158] Volker W, Schon P, Vischer P. Binding and endocytosis of thrombospondin and thrombospondin fragments in endothelial cells cultures analyzed by cuprolinic blue staining, colloidal gold labeling, and silver enhancement techniques. J Histochem Cytochem 1991; 39(10): 1385-94.

[159] Yoshioka T, Yamamoto K, Kobashi H, Tomita M, Tsuji T. Receptor-mediated endocytosis of chemically modified albumins by sinusoidal endothelial cells and Kupffer cells in rat and human liver. Liver 1994; 14(3): 129-37.

[160] Smedsrod B, Malmgren M, Ericsson J, Laurent TC. Morphological studies on endocytosis of chondroitin sulphate proteoglycan by rat liver EC. Cell Tissue Res 1988; 253(1): 39-45.

[161] Pitas RE, Boyles J, Mahley RW, Bissell DM. Uptake of chemically modified low density lipoproteins *in vivo* is mediated by specific EC. J Cell Biol 1985; 100(1): 103-17.

[162] Stitt AW, Anderson HR, Gardiner TA, Bailie JR, Archer DB. Receptor-mediated endocytosis and intracellular trafficking of insulin and low-density lipoprotein by retinal vascular endothelial cells. Invest Ophthalmol Vis Sci 1994; 35(9): 3384-92.

[163] Roberts RL, Fine RE, Sandra A. Receptor-mediated endocytosis of transferrin at the blood-brain barrier. J Cell Sci 1993; 104 (Pt 2): 521-32.

[164] Roberts RL, Sandra A. Transport of transferrin across the blood-thymus barrier in young rats. Tissue Cell 1994; 26(5): 757-66.

[165] Stins MF, Maxfield FR, Goldberg IJ. Polarized binding of lipoprotein lipase to endothelial cells. Implications for its physiological actions. Arterioscler Thromb 1992; 12(12): 1437-46.

[166] Stein O, Halperin G, Leitersdorf E, Olivecrona T, Stein Y. Lipoprotein lipase mediated uptake of non-degradable ether analogues of phosphatidylcholine and cholesteryl ester by cultured cells. Biochim Biophys Acta 1984; 795(1): 47-59.

[167] Goti D, Balazs Z, Panzenboeck U, Hrzenjak A, Reicher H, Wagner E, et al. Effects of lipoprotein lipase on uptake and transcytosis of low density lipoprotein (LDL) and LDL-associated alpha-tocopherol in a porcine *in vitro* blood-brain barrier model. J Biol Chem 2002; 277(32): 28537-44.

[168] Stins MF, Sivaram P, Sasaki A, Goldberg IJ. Specificity of lipoprotein lipase binding to endothelial cells. J Lipid Res 1993; 34(11): 1853-61.

[169] Schonherr E, Zhao B, Hausser H, Muller M, Langer C, Wagner WD, et al. Lipoprotein lipase-mediated interactions of small proteoglycans and low-density lipoproteins. Eur J Cell Biol 2000; 79(10): 689-96.

[170] Zimmermann R, Panzenbock U, Wintersperger A, Levak-Frank S, Graier W, Glatter O, et al. Lipoprotein lipase mediates the uptake

of glycated LDL in fibroblasts, endothelial cells, and macrophages. Diabetes 2001; 50(7): 1643-53.

[171] Schnitzer JE, Shen CP, Palade GE. Lectin analysis of common glycoproteins detected on the surface of continuous microvascular endothelium in situ and in culture: identification of sialoglycoproteins. Eur J Cell Biol 1990; 52(2): 241-51.

[172] Kounnas MZ, Chappell DA, Strickland DK, Argraves WS. Glycoprotein 330, a member of the low density lipoprotein receptor family, binds lipoprotein lipase *in vitro*. J Biol Chem 1993; 268(19): 14176-81.

[173] Le Panse S, Galceran M, Pontillon F, Lelongt B, van de Putte M, Ronco PM, et al. Immunofunctional properties of a yolk sac epithelial cell line expressing two proteins gp280 and gp330 of the intermicrovillar area of proximal tubule cells: inhibition of endocytosis by the specific antibodies. Eur J Cell Biol 1995; 67(2): 120-9.

[174] Fuki IV, Kuhn KM, Lomazov IR, Rothman VL, Tuszynski GP, Iozzo RV, et al. The syndecan family of proteoglycans. Novel receptors mediating internalization of atherogenic lipoproteins *in vitro*. J Clin Invest 1997; 100(6): 1611-22.

[175] Straley KS, Green SA. Rapid transport of internalized P-selectin to late endosomes and the TGN: roles in regulating cell surface expression and recycling to secretory granules. J Cell Biol 2000; 151(1): 107-16.

[176] Kessner S, Krause A, Rothe U, Bendas G. Investigation of the cellular uptake of E-Selectin-targeted immunoliposomes by activated human EC. Biochim Biophys Acta 2001; 1514(2): 177-90.

[177] Everts M, Kok RJ, Asgeirsdottir SA, Melgert BN, Moolenaar TJ, Koning GA, et al. Selective intracellular delivery of dexamethasone into activated endothelial cells using an E-selectin-directed immunoconjugate. J Immunol 2002; 168(2): 883-9.

[178] Stossel TP. The early history of phagocytosis. In: Tartakoff AM, editor. In Advances in cell and molecular biology of membranes and organelles. Stamford. Connecticut: JAI Press Inc.; 1999; p. 3-18.

[179] Caron E, Hall A. Phagocytosis: Oxford University Press; 2001.

[180] Koval M, Preiter K, Adles C, Stahl PD, Steinberg TH. Size of IgG-opsonized particles determines macrophage response during internalization. Exp Cell Res 1998; 242(1): 265-73.

[181] Hall A. Phagocytosis. In: Marsh M, editor. Endocytosis. Oxford. UK: Oxford University Press; 2001; p. 58-77.

[182] Griffin FM Jr, Griffin JA, Leider JE, Silverstein SC. Studies on the mechanism of phagocytosis. I. Requirements for circumferential attachment of particle-bound ligands to specific receptors on the macrophage plasma membrane. J Exp Med 1975; 142(5): 1263-82.

[183] Oka K, Sawamura T, Kikuta K, Itokawa S, Kume N, Kita T, et al. Lectin-like oxidized low-density lipoprotein receptor 1 mediates phagocytosis of aged/apoptotic cells in EC. Proc Natl Acad Sci USA 1998; 95(16): 9535-40.

[184] Eugene E, Hoffmann I, Pujol C, Couraud PO, Bourdoulous S, Nassif X. Microvilli-like structures are associated with the internalization of virulent capsulated Neisseria meningitidis into vascular endothelial cells. J Cell Sci 2002; 115(Pt 6): 1231-41.

[185] Swanson JA, Watts C. Macropinocytosis. Trends Cell Biol 1995; 5: 424-81.

[186] Lewis. Pinocytosis. Johns Hopkins Hosp Bull 1931; 49: 17-36.

[187] Machesky LM, Reeves E, Wientjes F, Mattheyse FJ, Grogan A, Totty NF, et al. Mammalian actin-related protein 2/3 complex localizes to regions of lamellipodial protrusion and is composed of evolutionarily conserved proteins. Biochem J 1997; 328 (Pt 1): 105-12.

[188] Machesky LM, Mullins RD, Higgs HN, Kaiser DA, Blanchoin L, May RC, et al. Scar, a WASp-related protein, activates nucleation of actin filaments by the Arp2/3 complex. Proc Natl Acad Sci USA 1999; 96(7): 3739-44.

[189] Saito T, Lamy F, Roger PP, Lecocq R, Dumont JE. Characterization and identification as cofilin and destrin of two thyrotropin- and phorbol ester-regulated phosphoproteins in thyroid cells. Exp Cell Res 1994; 212(1): 49-61.

[190] Veithen A, Cupers P, Baudhuin P, Courtoy PJ. v-Src induces constitutive macropinocytosis in rat fibroblasts. J Cell Sci 1996; 109 (Pt 8): 2005-12.

[191] Ridley AJ, Hall A. The small GTP-binding protein rho regulates the assembly of focal adhesions and actin stress fibers in response to growth factors. Cell 1992; 70(3): 389-99.

[192] Bar-Sagi D, Feramisco JR. Induction of membrane ruffling and fluid-phase pinocytosis in quiescent fibroblasts by ras proteins. Science 1986; 233(4768): 1061-8.

[193] Swanson JA. Phorbol esters stimulate macropinocytosis and solute flow through macrophages. J Cell Sci 1989; 94 (Pt 1): 135-42.

[194] Wennstrom S, Siegbahn A, Yokote K, Arvidsson AK, Heldin CH, Mori S, et al. Membrane ruffling and chemotaxis transduced by the PDGF beta-receptor require the binding site for phosphatidylinositol 3' kinase. Oncogene 1994; 9(2): 651-60.

[195] Willingham MC, Haigler HT, Fitzgerald DJ, Gallo MG, Rutherford AV, Pastan IH. The morphologic pathway of binding and internalization of epidermal growth factor in cultured cells. Studies on A431, KB, and 3T3 cells, using multiple methods of labelling. Exp Cell Res 1983; 146(1): 163-75.

[196] Mellstrom K, Heldin CH, Westermark B. Induction of circular membrane ruffling on human fibroblasts by platelet-derived growth factor. Exp Cell Res 1988; 177(2): 347-59.

[197] Brunk U, Schellens J, Westermark B. Influence of epidermal growth factor (EGF) on ruffling activity, pinocytosis and proliferation of cultivated human glia cells. Exp Cell Res 1976; 103(2): 295-302.

[198] Liu NQ, Lossinsky AS, Popik W, Li X, Gujuluva C, Kriederman B, et al. Human immunodeficiency virus type 1 enters brain microvascular endothelia by macropinocytosis dependent on lipid rafts and the mitogen-activated protein kinase signaling pathway. J Virol 2002; 76(13): 6689-700.

[199] Gil J. Number and distribution of plasmalemmal vesicles in the lung. Fed Proc 1983; 42(8): 2414-8.

[200] Ghinea N, Mai TV, Groyer-Picard MT, Milgrom E. How protein hormones reach their target cells. Receptor-mediated transcytosis of hCG through endothelial cells. J Cell Biol 1994; 125(1): 87-97.

[201] Roberts RL, Sandra A. Receptor-mediated endocytosis of insulin by cultured endothelial cells. Tissue Cell 1992; 24(5): 603-11.

[202] Ring A, Pohl J, Volkl A, Stremmel W. Evidence for vesicles that mediate long-chain fatty acid uptake by human microvascular endothelial cells. J Lipid Res 2002; 43(12): 2095-104.

[203] Conway EM, Nowakowski B, Steiner-Mosonyi M. Thrombomodulin lacking the cytoplasmic domain efficiently internalizes thrombin via nonclathrin-coated, pit-mediated endocytosis. J Cell Physiol 1994; 158(2): 285-98.

[204] Conway EM, Boffa MC, Nowakowski B, Steiner-Mosonyi M. An ultrastructural study of thrombomodulin endocytosis: internalization occurs via clathrin-coated and non-coated pits. J Cell Physiol 1992; 151(3): 604-12.

[205] Wiewrodt R, Thomas AP, Cipelletti L, Christofidou-Solomidou M, Weitz DA, Feinstein SI, et al. Size-dependent intracellular immunotargeting of therapeutic cargoes into endothelial cells. Blood 2002; 99(3): 912-22.

[206] Muro S, Wiewrodt R, Thomas A, Koniaris L, Albelda SM, Muzykantov VR, et al. A novel endocytic pathway induced by clustering endothelial ICAM-1 or PECAM-1. J Cell Sci 2003; 116(Pt 8): 1599-1609.

[207] Behera AK, Matsuse H, Kumar M, Kong X, Lockey RF, Mohapatra SS. Blocking intercellular adhesion molecule-1 on human epithelial cells decreases respiratory syncytial virus infection. Biochem Biophys Res Commun 2001; 280(1): 188-95.

[208] Schober D, Kronenberger P, Prchla E, Blaas D, Fuchs R. Major and minor receptor group human rhinoviruses penetrate from endosomes by different mechanisms. J Virol 1998; 72(2): 1354-64.

[209] Treutiger CJ, Heddini A, Fernandez V, Muller WA, Wahlgren M. PECAM-1/CD31, an endothelial receptor for binding Plasmodium falciparum-infected erythrocytes. Nat Med 1997; 3(12): 1405-8.

[210] Brown S, Heinisch I, Ross E, Shaw K, Buckley CD, Savill J. Apoptosis disables CD31-mediated cell detachment from phagocytes promoting binding and engulfment. Nature 2002; 418(6894): 200-3.

[211] Gow AJ, Branco F, Christofidou-Solomidou M, Black-Schultz L, Albelda SM, Muzykantov VR. Immunotargeting of glucose oxidase: intracellular production of H_2O_2 and endothelial oxidative stress. Am J Physiol 1999; 277(2 Pt 1): L271-81.

[212] Christofidou-Solomidou M, Pietra GG, Solomides CC, Arguiris E, Harshaw D, Fitzgerald GA, et al. Immunotargeting of glucose oxidase to endothelium *in vivo* causes oxidative vascular injury in the lungs. Am J Physiol Lung Cell Mol Physiol 2000; 278(4): L794-805.

[213] Sweitzer TD, Thomas AP, Wiewrodt R, Nakada MT, Branco F, Muzykantov VR. Pecam-directed immunotargeting of catalase: specific, rapid and transient protection against hydrogen peroxide. Free Radic Biol Med 2003; 34(8): 1035-46.

[214] Kozower BD, Christofidou-Solomidou M, Sweitzer TD, Muro S, Buerk DG, Solomides CC, et al. Immunotargeting of catalase to the pulmonary endothelium alleviates oxidant stressand reduces acute lung transplantation injury. Nat Biotechnol 2003; 21(4): 392-8.

[215] Yajima Y, Kawashima S. Calpain function in the differentiation of mesenchymal stem cells. Biol Chem 2002; 383(5): 757-64.

[216] Gil-Parrado S, Popp O, Knoch TA, Zahler S, Bestvater F, Felgentrager M, et al. Subcellular localization and *in vivo* subunit interactions of ubiquitous mu -calpain. J Biol Chem 2003; 278: 1636-46.

[217] Gregoriou M, Willis AC, Pearson MA, Crawford C. The calpain cleavage sites in the epidermal growth factor receptor kinase domain. Eur J Biochem 1994; 223(2): 455-64.

[218] Guttmann RP, Baker DL, Seifert KM, Cohen AS, Coulter DA, Lynch DR. Specific proteolysis of the NR2 subunit at multiple sites by calpain. J Neurochem 2001; 78(5): 1083-93.

[219] Fox JE. Cytoskeletal proteins and platelet signaling. Thromb Haemost 2001; 86(1): 198-213.

[220] Huttenlocher A, Palecek SP, Lu Q, Zhang W, Mellgren RL, Lauffenburger DA, et al. Regulation of cell migration by the calcium-dependent protease calpain. J Biol Chem 1997; 272(52): 32719-22.

[221] Potter DA, Tirnauer JS, Janssen R, Croall DE, Hughes CN, Fiacco KA, et al. Calpain regulates actin remodeling during cell spreading. J Cell Biol 1998; 141(3): 647-62.

[222] Dunlop RA, Rodgers KJ, Dean RT. Recent developments in the intracellular degradation of oxidized proteins. Free Radic Biol Med 2002; 33(7): 894-906.

[223] Tanaka K, Kasahara M. The MHC class I ligand-generating system: roles of immunoproteasomes and the interferon-gamma-inducible proteasome activator PA28. Immunol Rev 1998; 163: 161-76.

[224] Groettrup M, Khan S, Schwarz K, Schmidtke G. Interferon-gamma inducible exchanges of 20S proteasome active site subunits: why? Biochimie 2001; 83(3-4): 367-72.

[225] Gruenberg J. The endocytic pathway: a mosaic of domains. Nat Rev Mol Cell Biol 2001; 2(10): 721-30.

[226] Stoorvogel W, Strous GJ, Geuze HJ, Oorschot V, Schwartz AL. Late endosomes derive from early endosomes by maturation. Cell 1991; 65(3): 417-27.

[227] Reaves BJ, Banting G, Luzio JP. Lumenal and transmembrane domains play a role in sorting type I membrane proteins on endocytic pathways. Mol Biol Cell 1998; 9(5): 1107-22.

[228] Mellman I. Endocytosis and molecular sorting. Annu Rev Cell Dev Biol 1996; 12: 575-625.

[229] Knight A, Hughson E, Hopkins CR, Cutler DF. Membrane protein trafficking through the common apical endosome compartment of polarized Caco-2 cells. Mol Biol Cell 1995; 6(5): 597-610.

[230] Fuchs R, Male P, Mellman I. Acidification and ion permeabilities of highly purified rat liver endosomes. J Biol Chem 1989; 264(4): 2212-20.

[231] Mellman I. The importance of being acid: the role of acidification in intracellular membrane traffic. J Exp Biol 1992; 172: 39-45.

[232] Warnock DG. Regulation of endosomal acidification via Gi-type protein. Kidney Int 1999; 55(6): 2524-5.

[233] Gille L, Nohl H. The existence of a lysosomal redox chain and the role of ubiquinone. Arch Biochem Biophys 2000; 375(2): 347-54.

[234] Killisch I, Steinlein P, Romisch K, Hollinshead R, Beug H, Griffiths G. Characterization of early and late endocytic compartments of the transferrin cycle. Transferrin receptor antibody blocks erythroid differentiation by trapping the receptor in the early endosome. J Cell Sci 1992; 103 (Pt 1): 211-32.

[235] Futai M, Oka T, Moriyama Y, Wada Y. Diverse roles of single membrane organelles: factors establishing the acid lumenal pH. J Biochem (Tokyo) 1998; 124(2): 259-67.

[236] Kornfeld S, Mellman I. The biogenesis of lysosomes. Annu Rev Cell Biol 1989; 5: 483-525.

[237] Pillay CS, Elliott E, Dennison C. Endolysosomal proteolysis and its regulation. Biochem J 2002; 363(Pt 3): 417-29.

[238] Fukuda M. Lysosomal membrane glycoproteins. Structure, biosynthesis, and intracellular trafficking. J Biol Chem 1991; 266(32): 21327-30.

[239] Storer AC, Menard R. Catalytic mechanism in papain family of cysteine peptidases. Methods Enzymol 1994; 244: 486-500

[240] de Bruyn PP, Cho Y, Michelson S. *In vivo* endocytosis by bristle coated pits of protein tracers and their intracellular transport in the endothelial cells lining the sinuses of the liver. II. The endosomal-lysosomal transformation. J Ultrastruct Res 1983; 85(3): 290-9.

[241] Sheff DR, Daro EA, Hull M, Mellman I. The receptor recycling pathway contains two distinct populations of early endosomes with different sorting functions. J Cell Biol 1999; 145(1): 123-39.

[242] Mellman IS, Plutner H, Steinman RM, Unkeless JC, Cohn ZA. Internalization and degradation of macrophage Fc receptors during receptor-mediated phagocytosis. J Cell Biol 1983; 96(3): 887-95.

[243] Pitt A, Mayorga LS, Schwartz AL, Stahl PD. Transport of phagosomal components to an endosomal compartment. J Biol Chem 1992; 267(1): 126-32.

[244] Mayorga LS, Bertini F, Stahl PD. Fusion of newly formed phagosomes with endosomes in intact cells and in a cell-free system. J Biol Chem 1991; 266(10): 6511-7.

[245] Hewlett LJ, Prescott AR, Watts C. The coated pit and macropinocytic pathways serve distinct endosome populations. J Cell Biol 1994; 124(5): 689-703.

[246] Desjardins M, Huber LA, Parton RG, Griffiths G. Biogenesis of phagolysosomes proceeds through a sequential series of interactions with the endocytic apparatus. J Cell Biol 1994; 124(5): 677-88.

[247] Parton RG, Lindsay M. Exploitation of major histocompatibility complex class I molecules and caveolae by simian virus 40. Immunol Rev 1999; 168: 23-31.

[248] Norkin LC. Simian virus 40 infection via MHC class I molecules and caveolae. Immunol Rev 1999; 168: 13-22.

[249] Kamen BA, Johnson CA, Wang MT, Anderson RG. Regulation of the cytoplasmic accumulation of 5-methyltetrahydrofolate in MA104 cells is independent of folate receptor regulation. J Clin Invest 1989; 84(5): 1379-86.

[250] Haasemann M, Cartaud J, Muller-Esterl W, Dunia I. Agonist-induced redistribution of bradykinin B2 receptor in caveolae. J Cell Sci 1998; 111 (Pt 7): 917-28.

[251] Chun M, Liyanage UK, Lisanti MP, Lodish HF. Signal transduction of a G protein-coupled receptor in caveolae: colocalization of endothelin and its receptor with caveolin. Proc Natl Acad Sci USA 1994; 91(24): 11728-32.

[252] Dessy C, Kelly RA, Balligand JL, Feron O. Dynamin mediates caveolar sequestration of muscarinic cholinergic receptors and alteration in NO signaling. EMBO J 2000; 19(16): 4272-80.

[253] Muro S, Cui X, Gajewski C, Muzykantov VR, Koval M. Slow intracellular trafficking of catalase nanoparticles targeted to endothelial ICAM-1 protects endothelial cells from oxidative stress. Am J Physiol Cell 2003; 285(5): 1339-4.

[254] Bomsel M, Parton R, Kuznetsov SA, Schroer TA, Gruenberg J. Microtubule- and motor-dependent fusion *in vitro* between apical and basolateral endocytic vesicles from MDCK cells. Cell 1990; 62(4): 719-31.

[255] Palade GE, Simionescu M, Simionescu N. Structural aspects of the permeability of the microvascular endothelium. Acta Physiol Scand Suppl 1979; 463: 11-32.

[256] Majno G. Maude Abbott Lecture--1991. The capillary then and now: an overview of capillary pathology. Mod Pathol 1992; 5(1): 9-22.

[257] McDonald DM, Thurston G, Baluk P. Endothelial gaps as sites for plasma leakage in inflammation. Microcirculation 1999; 6(1): 7-22.

[258] Schnitzer JE, Oh P, McIntosh DP. Role of GTP hydrolysis in fission of caveolae directly from plasma membranes. Science 1996; 274(5285): 239-42.

[259] Niles WD, Malik AB. Endocytosis and exocytosis events regulate vesicle traffic in EC. J Membr Biol 1999; 167(1): 85-101.

[260] Minshall RD, Tiruppathi C, Vogel SM, Niles WD, Gilchrist A, Hamm HE, et al. Endothelial cell-surface gp60 activates vesicle formation and trafficking via G(i)-coupled Src kinase signaling pathway. J Cell Biol 2000; 150(5): 1057-70.

[261] Vogel SM, Easington CR, Minshall RD, Niles WD, Tiruppathi C, Hollenberg SM, et al. Evidence of transcellular permeability pathway in microvessels. Microvasc Res 2001; 61(1): 87-101.

[262] Volker W, Hess S, Vischer P, Preissner KT. Binding and processing of multimeric vitronectin by vascular endothelial cells. J Histochem Cytochem 1993; 41(12): 1823-32.

[263] John TA, Vogel SM, Tiruppathi C, Malik AB, Minshall RD. Quantitative analysis of albumin uptake and transport in the rat microvessel endothelial monolayer. Am J Physiol Lung Cell Mol Physiol 2003; 284(1): L187-96.

[264] Dvorak AM, Feng D. The vesiculo-vacuolar organelle (VVO). A new endothelial cell permeability organelle. J Histochem Cytochem 2001; 49(4): 419-32.

[265] Simionescu N, Siminoescu M, Palade GE. Permeability of muscle capillaries to small heme-peptides. Evidence for the existence of patent transendothelial channels. J Cell Biol 1975; 64(3): 586-607.

[266] Schnitzer JE, Oh P, Pinney E, Allard J. Filipin-sensitive caveolae-mediated transport in endothelium: reduced transcytosis, scavenger endocytosis, and capillary permeability of select macromolecules. J Cell Biol 1994; 127(5): 1217-32.

[267] Predescu D, Predescu S, McQuistan T, Palade GE. Transcytosis of alpha1-acidic glycoprotein in the continuous microvascular endothelium. Proc Natl Acad Sci USA 1998; 95(11): 6175-80.

[268] Horvat R, Palade GE. Thrombomodulin and thrombin localization on the vascular endothelium; their internalization and transcytosis by plasmalemmal vesicles. Eur J Cell Biol 1993; 61(2): 299-313.

[269] Vasile E, Simionescu M, Simionescu N. Visualization of the binding, endocytosis, and transcytosis of low-density lipoprotein in the arterial endothelium in situ. J Cell Biol 1983; 96(6): 1677-89.

[270] Robinson CS, Wagner RC. Differential endocytosis of lipoproteins by capillary endothelial vesicles. Microcirc Endothelium Lymphatics 1985; 2(3): 313-29.

[271] Tiruppathi C, Song W, Bergenfeldt M, Sass P, Malik AB. Gp60 activation mediates albumin transcytosis in endothelial cells by tyrosine kinase-dependent pathway. J Biol Chem 1997; 272(41): 25968-75.

[272] Predescu D, Predescu S, Malik AB. Transport of nitrated albumin across continuous vascular endothelium. Proc Natl Acad Sci USA 2002; 99(21): 13932-7.

[273] Terasaki T, Pardridge WM. Targeted drug delivery to the brain; (blood-brain barrier, efflux, endothelium, biological transport). J Drug Target 2000; 8(6): 353-5.

[274] Prokai-Tatrai K, Nguyen V, Zharikova AD, Braddy AC, Stevens SM, Prokai L. Prodrugs to enhance central nervous system effects of the TRH-like peptide pGlu-Glu-Pro-NH(2). Bioorg Med Chem Lett 2003; 13(6): 1011-4.

[275] Stins MF, Nemani PV, Wass C, Kim KS. Escherichia coli binding to and invasion of brain microvascular endothelial cell derived from humans and rats of different ages. Infect Immun 1999; 67(10): 5522-5.

[276] Muruganandam A, Tanha J, Narang S, Stanimirovic D. Selection of phage-displayed llama single-domain antibodies that transmigrate across human blood-brain barrier endothelium. FASEB J 2002; 16(2): 240-2

[277] Wengenack TM, Curran GL, Olson EE, Poduslo JF. Putrescine-modified catalase with preserved enzymatic activity exhibits increased permeability at the blood-nerve and blood-brain barriers. Brain Res 1997; 767(1): 128-35.

[278] Scherphof GL, Romero EL, Velinova MJ, Kamps JAAM, Koning GA, Meijer DKF, Swart P, Daemen T, editor. Endothelial and transendothelial delivery of pharmaceutically active agents; potential of liposomes. Leiden. The Netherlands.: Kupffer Cell Foundation; 1999.

[279] Tsukita S, Furuse M, Itoh M. Multifunctional strands in tight junctions. Nat Rev Mol Cell Biol 2001; 2(4): 285-93.

[280] Fanning AS, Mitic LL, Anderson JM. Transmembrane proteins in the tight junction barrier. J Am Soc Nephrol 1999; 10(6): 1337-45.

[281] Nitta T, Hata M, Gotoh S, Seo Y, Sasaki H, Hashimoto N, et al. Size-selective loosening of the blood-brain barrier in claudin-5-deficient mice. J Cell Biol 2003; 161(3): 653-60.

[282] Hopkins AM, Li D, Mrsny RJ, Walsh SV, Nusrat A. Modulation of tight junction function by G protein-coupled events. Adv Drug Deliv Rev 2000; 41(3): 329-40.

[283] Nourry C, Grant SG, Borg JP. PDZ domain proteins: plug and play! Sci STKE 2003; 2003(179): RE7.

[284] Pawson T, Nash P. Assembly of cell regulatory systems through protein interaction domains. Science 2003; 300(5618): 445-52.

[285] Martin TA, Mansel RE, Jiang WG. Antagonistic effect of NK4 on HGF/SF induced changes in the transendothelial resistance (TER) and paracellular permeability of human vascular endothelial cells. J Cell Physiol 2002; 192(3): 268-75.

[286] Stevens T, Garcia JG, Shasby DM, Bhattacharya J, Malik AB. Mechanisms regulating endothelial cell barrier function. Am J Physiol Lung Cell Mol Physiol 2000; 279(3): L419-22.

[287] Lum H, Malik AB. Regulation of vascular endothelial barrier function. Am J Physiol 1994; 267(3 Pt 1): L223-41.

[288] McDonald DM, Thurston G, Baluk P. Endothelial gaps as sites for plasma leakage in inflammation. Microcirculation 1999; 6(1): 7-22.

[289] Hashizume H, Baluk P, Morikawa S, McLean JW, Thurston G, Roberge S, et al. Openings between defective endothelial cells explain tumor vessel leakiness. Am J Pathol 2000; 156(4): 1363-80.

[290] Hobbs SK, Monsky WL, Yuan F, Roberts WG, Griffith L, Torchilin VP, et al. Regulation of transport pathways in tumor vessels: role of tumor type and microenvironment. Proc Natl Acad Sci USA 1998; 95(8): 4607-12.

[291] Feng D, Nagy JA, Pyne K, Hammel I, Dvorak HF, Dvorak AM. Pathways of macromolecular extravasation across microvascular endothelium in response to VPF/VEGF and other vasoactive mediators. Microcirculation 1999; 6(1): 23-44.

[292] Haselton FR, Alexander JS, Mueller SN. Adenosine decreases permeability of *in vitro* endothelial monolayers. J Appl Physiol 1993; 74(4): 1581-90.

[293] Dejana E. Endothelial adherens junctions: implications in the control of vascular permeability and angiogenesis. J Clin Invest 1996; 98(9): 1949-53.

[294] Moore TM, Norwood NR, Creighton JR, Babal P, Brough GH, Shasby DM, et al. Receptor-dependent activation of store-operated calcium entry increases endothelial cell permeability. Am J Physiol Lung Cell Mol Physiol 2000; 279(4): L691-8.

[295] Lum H, Malik AB. Regulation of vascular endothelial barrier function. Am J Physiol 1994; 267(3 Pt 1): L223-41.

[296] Verin AD, Csortos C, Durbin SD, Aydanyan A, Wang P, Patterson CE, et al. Characterization of the protein phosphatase 1 catalytic subunit in endothelium: involvement in contractile responses. J Cell Biochem 2000; 79(1): 113-25.

[297] Cho MM, Ziats NP, Pal D, Utian WH, Gorodeski GI. Estrogen modulates paracellular permeability of human endothelial cells by eNOS- and iNOS-related mechanisms. Am J Physiol 1999; 276(2 Pt 1): C337-49.

[298] Wu J, Akaike T, Maeda H. Modulation of enhanced vascular permeability in tumors by a bradykinin antagonist, a cyclooxygenase inhibitor, and a nitric oxide scavenger. Cancer Res 1998; 58(1): 159-65.

[299] Maeda H, Sawa T, Konno T. Mechanism of tumor-targeted delivery of macromolecular drugs, including the EPR effect in solid tumor and clinical overview of the prototype polymeric drug SMANCS. J Control Release 2001; 74(1-3): 47-61.

[300] Drab M, Verkade P, Elger M, Kasper M, Lohn M, Lauterbach B, et al. Loss of Caveolae, Vascular Dysfunction, and Pulmonary Defects in Caveolin-1 Gene-Disrupted Mice. Science 2000; 293: 2449-2452.

[301] Schlegel A, Pestell RG, Lisanti MP. Caveolins in cholesterol trafficking and signal transduction: implications for human disease. Front Biosci 2000; 5: D929-37.

Abstracts of papers presented
at the 2003 meeting on

VECTOR TARGETING STRATEGIES FOR GENE THERAPY

March 20–March 23, 2003

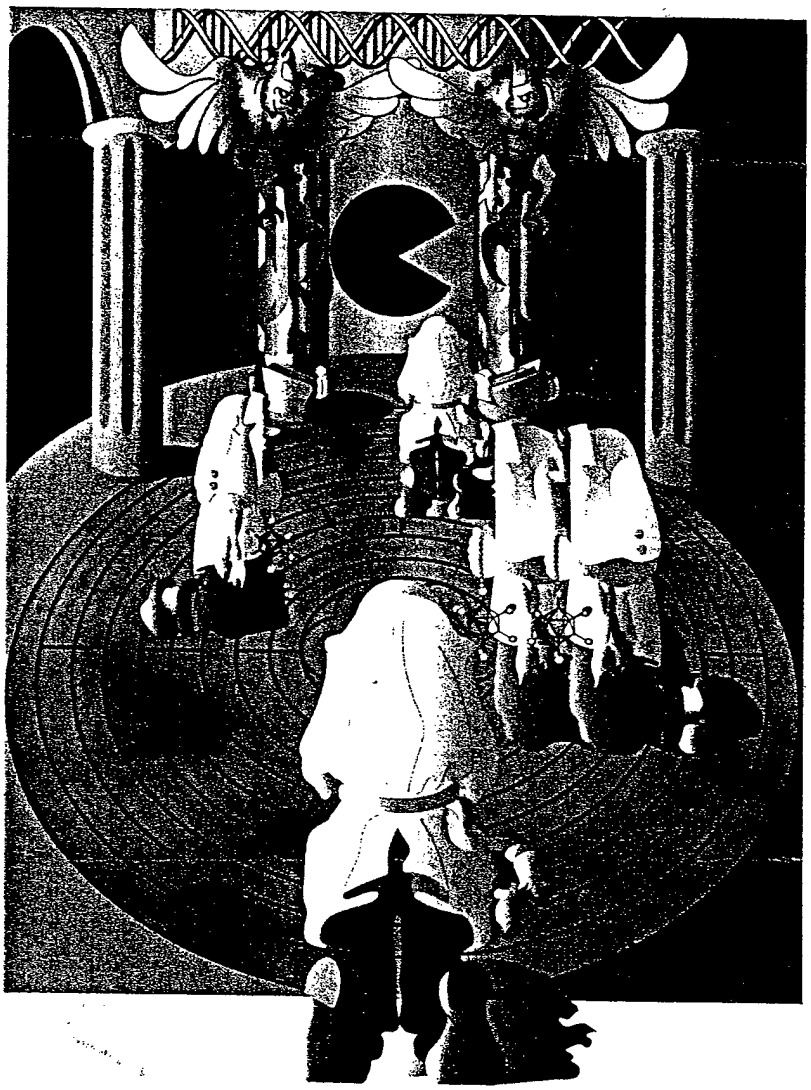

Cold Spring Harbor Laboratory
Cold Spring Harbor, New York

METABOLICALLY BIOTINYLATED GENE THERAPY VECTORS FOR VECTOR TARGETING AND PURIFICATION

Samuel K. Campos[1,5], M. Brandon Parrott[1], Kristen E. Adams[1,4], Jeremy S. Blum[1,4], Hoyin Mok[1,4], Vladimir Muzykantov[7], and Michael A. Barry[1,2,3,4]
Center for Cell and Gene Therapy[1], Baylor College of Medicine, Houston, TX Department of Bioengineering[4], Department of Biochemistry and Cell Biology[5], Rice University, Houston, TX. Institute for Environmental Medicine[7], University of Pennsylvania

One method of altering viral vector specificity is to genetically introduce cell-targeting ligands directly into the viral capsid proteins of the vector. While this approach can work, in many cases inserted ligands fail to function or destroy the function of the virus making targeting impossible. To provide an alternate vector targeting approach, we have developed metabolically biotinylated vectors in which viruses are genetically engineered to display a biotin acceptor peptide (BAP). When these viruses are encapsidated in helper mammalian cells, the tagged viral protein can be metabolically biotinylated by the endogenous biotin ligase, holocarboxylase synthetase, or by co-expression of an exogenous ligase such as the bacterial enzyme BirA. BAP-modification of the fiber protein of adenovirus allowed virions to be produced directly from 293 helper cells with biotinylated fibers incorporated into the viral particles. When applied for vector targeting, biotinylated adenoviral particles could be re-targeted to new receptors in vitro and in vivo by conjugation to biotinylated antibodies using tetrameric avidin (K_d = 10^{-15} M). Re-targeting has been demonstrated using antibodies against CD40, CD59, CD71, CD86, and PECAM on a variety of cells including CML, endothelial, dendritic, and mucosal epithelial cells. Subsequent work has demonstrated the ability to target other cells by direct biotinylation of their surface or by use of non-conventional ligands including biotinylated lectins and avidin-coated magnetic beads. Metabolically biotinylated adenovirus could also be purified by biotin-reversible binding on monomeric avidin (K_d = 10^{-7} M). Our recent production of metabolically biotinylated AAV vectors demonstrates this technology has potential for a number of viral vectors systems. This work demonstrates proof of principle for the use of metabolically biotinylated viruses for targeting and purification applications without the need to re-engineer a new virus for each new ligand. Further this technology allows the use of large high affinity antibodies that will be difficult to genetically engineer into capsid proteins. This technology may therefore have utility for rapid screening of ligand libraries, for vector re-targeting *in vitro* and *in vivo* and for vector and vaccine purification applications.

TARGETING ENDOTHELIAL CELL ADHESION MOLECULES

M.Christofidou-Solomidou, S.Muro, J-C.Murciano, M.Barry*, A.Thomas, V.Shuvaev, S.Albelda, D.Cines and V.R.Muzykantov
University of Pennsylvania Medical School, Philadelphia, PA, USA and *Rice University, Houston, TX

Endothelial determinants functionally involved in and stably expressed (or up-regulated) on the cell surface at inflammatory sites would be good candidate targets for delivery of drugs to manage vascular oxidative or thrombotic stress. Experiments in cell cultures and in animal models show that antibodies directed against constitutively expressed Ig-family cell adhesion molecules ICAM-1 and PECAM-1 can be utilized for targeted delivery of reporter and therapeutic cargoes to either resting or pathologically altered endothelium. Endothelial cells do not internalize monomeric anti-ICAM and anti-PECAM, but immunoconjugates smaller than 0.5 um diameter enter the cells via a novel previously unrecognized endocytotic pathway distinct from clathrin- and caveoli-mediated endocytosis. Enzymatically active catalase (that degrades H_2O_2) conjugated with anti-ICAM or anti-PECAM, specifically binds to endothelial cells, resides in a pre-lysosomal compartment for several hours and protects cells against oxidative stress. Experiments in intact mice showed that anti-PECAM/catalase accumulates in the pulmonary endothelium, protects animals against acute oxidative pulmonary injury and markedly improves survival. Anti-ICAM and anti-PECAM conjugates larger than 0.5 um do not enter target cells efficiently and thus can be used to deliver anti-thrombotic agents. Anti-ICAM conjugated tissue-type plasminogen activator (tPA) binds to the pulmonary endothelium in mice and rats, enhances the fibrinolytic capacity of the lung vasculature and facilitates dissolution of pulmonary fibrin emboli. Preliminary data indicate that anti-PECAM can also be used to re-direct viral vectors to endothelial cells. In addition to therapeutic effects of the delivered drugs, blockade of PECAM-1 and/or ICAM-1 by immunoconjugates may provide a secondary therapeutic benefit by suppressing tissue infiltration of leukocytes.

Funded by: National AHA Research Grant-0030192N (MC), Fundación Ramón Areces (SM), DOD PR 012262, NIH HL71175 and HL60290 (VM)

An Annual Meeting of Professional Research Scientists

Experimental Biology 2003®
San Diego, California

April 11 – April 15, 2003

ABSTRACTS 13.1 – 455.10

PART I

The American Physiological Society
American Society for Biochemistry and Molecular Biology
American Society for Pharmacology and Experimental Therapeutics
American Society for Investigative Pathology
American Society for Nutritional Sciences
American Association of Anatomists

American Federation for Medical Research
The American Society for Clinical Nutrition
Latin-American Association of Physiological Sciences
The Biomedical Engineering Society
Cajal Club
The Histochemical Society
International Society for Stereology
The Microcirculatory Society
North American Vascular Biology Organization
Society for Experimental Biology and Medicine
Society for International Nutrition Research

p=0.06). These data suggest that scavenging peroxynitrite can be beneficial in protecting against lung damage in ARDS.

161.9

Hyperoxia Potentiates Oxidative Injury In Murine Lungs Induced By Glucose Oxidase Targeted To Thrombomodulin

Melpo Christofidou-Solomidou[1], Arnaud Scherpereel[1], Alyssa Bohen[1], Evguenia Arguiri[1], Vladmimir Shuvaev[1], Stephen Kennel[2], Vladimir Muzykantov[1]. [1]Medicine, University of Pennsylvania, 421 Curie Boulevard, Philadelphia, PA 19403-6160, [2]Medicine, Oak Ridge National Labs, Oak Ridge, TN

Hyperoxia induces oxidative lung injury by mechanisms including overproduction of reactive oxygen species (ROS) in mitochondrial respiratory chain in lung cells, release of ROS from activated leukocytes and modulating activity of pro-oxidant enzymes in the lung that utilize O_2 as a substrate (NADPH-oxidase, LOX, NOS, XO, etc). To test directly whether pulmonary level of O_2 modulates generation of ROS in endothelium, we injected mice with glucose oxidase (GOX), coupled to a thrombomodulin antibody (anti-TM). Immediately after iv injection, anti-TM/GOX binds to pulmonary endothelium, generates H_2O_2 from O_2 and glucose, and causes edematous oxidative lung injury. Mice were injected with a low dose (35 μg) anti-TM/GOX and exposed to hyperoxia (PO_2>95%) for 6 h prior to sacrifice. Lung injury was characterized by BAL protein, WBC counts, lipid peroxidation by malondialdehyde (MDA) levels and Acute Lung Injury Score, ALIS. BAL proteins for untreated control, anti-TM/GOX (35μg), saline +O_2 and anti-TM/GOX +O_2 were 0.1, 0.4±0.03, 0.1, and 4.8±2.10 respectively. BAL WBC (x10^3) for the same groups were 44.0±4.9, 48.2±4.8, 43.0±5.2, 44.2±1.3 respectively. MDA levels/g lung were 2.5±0.1, 3.58±0.16, 4.7±0.4 and 7.8±1.1 and ALIS was 1, 2.5, 2.3 and 8.8 respectively. Therefore, hyperoxia alone did not cause noticeable injury, yet markedly augmented edematous injury induced by low doses anti-TM/GOX which cannot be explained by WBC influx. These data indicate that tissue-level O_2 directly modulates the activity an exogenous pro-oxidant enzyme bound to endothelium, thus augmenting ROS-mediated tissue injury.

161.10

Reovirus 1/L and 3/D induce protection against reovirus 1/L induced Acute Respiratory Distress Syndrome

Elsie Hill Long[1], Elizabeth Majeski[1], Jimmell Felder[2], Steve D London[1], Lucille London[1]. [1]Microbiology and Immunology, Medical University of South Carolina, 173 Ashley Avenue, BSB 215, Charleston, South Carolina 29403, [2]College of Medicine, Medical University of South Carolina, Charleston, SC

Intranasal inoculation of 10^7 pfu of reovirus 1/L results in acute respiratory distress syndrome (ARDS) in CBA/J mice, whereas a similar inoculation with reovirus 3/D only results in a mild viral pneumonia. Viral reassortant studies have suggested that this difference in pathology is correlated to differences in the small 1 (S1) gene product which is the hemagglutanin responsible for viral attachment.

We hypothesize that intranasal priming with low doses of reovirus 1/L will induce protection against development of reovirus 1/L induced ARDS, while intranasal priming with reovirus 3/D will not induce such protection. Female, 4-5 week old, CBA/J mice were inoculated with 10^4 pfu of reovirus 1/L, reovirus 3/D or saline. Seven days later mice in each group were then boosted with 10^7 pfu of reovirus 1/L or saline. Control and experimental mice from each group were sacrificed over a 21 day time course and lung pathology was evaluated by Hematoxylin and Eosin (H/E) staining.

Preliminary evaluation of H/E stained lungs suggests that low dose priming with reovirus 1/L produces protection against reovirus 1/L induced ARDS, while priming with reovirus 3/D also demonstrated such protection. The mechanisms of this viral strain cross-reactive protection are being investigated.

161.11

Attenuation of lung inflammation and fibrosis in reovirus 1/L-induced ARDS by the caspase inhibitor, ZVAD

Andrea Del Pilar Lopez, Catherine Kalyn Brown, Steve D London, Lucille London. Microbiology and Immunology, Medical University of South Carolina, 173 Ashley Avenue BSB Rm 215, Charleston, South Carolina 29403

The Fas/FasL apoptotic pathway and the effect of the caspase inhibitor, ZVAD, on the acute inflammatory and later fibrotic phases of reovirus 1/L-induced Acute Respiratory Distress Syndrome (ARDS) was investigated.

CBA/J mice were i.n. inoculated with 10^7 pfu reovirus 1/L and sacrificed over 21 days. Daily administration of the caspase inhibitor, ZVAD, (1 mg/kg i.p.) was begun on day 3-post infection. Lungs were collected for immunohistochemical studies, RT-PCR analysis, collagen content, and in situ apoptosis detection.

Positive staining for Fas and FasL was observed in alveolar epithelium on days 9 & 12 post infection. FasL was also expressed on the infiltrating cells. RT-PCR confirmed Fas/FasL RNA expression. Detection of apoptosis via DNA fragmentation (Tunel) was observed on days 3 to 12 after infection with more evident expression at earlier time points. Treatment of mice with ZVAD reduced both the reovirus 1/L-induced inflammatory response and lung fibrosis as shown by histopathological examination and by a decrease in lung collagen content.

These results demonstrate the Fas/FasL pathway is expressed in reovirus 1/L-induced ARDS and may play a role in the pathophysiology of ARDS. In addition, the caspase inhibitor, ZVAD, may be useful in the prevention of experimental acute lung injury and fibrosis raising the possibility of a therapeutic approach to human ARDS.

161.12

Pathogenetic role of xanthine oxidase in a murine model of acute lung injury

Jon G Mabley, Alex Nivorozhkin, Garry J. Southan, Csaba Szabo, Andrew L Salzman. Inotek Pharmaceuticals Corporation, Suite 419E, 100 Cummings Center, Beverly, MA 01915

This study evaluated the effects of a novel xanthine oxidase inhibitor, AN-01-24, on lung inflammation induced by intratracheal LPS (50μg) in vivo. LPS treatment increased the total leukocyte count (11 x104±1 x104 to 7.6 x105±8 x104 cells/ml), MPO activity (19±1 to 353±54mU/ml), protein concentration (282±37 to 576±27μg/ml), chemokine level (MIP-1 6±2 to 905±142pg/ml; MIP-2 13±8 to 955±215pg/ml) and inflammatory cytokine level (TNF 168±85 to 5840±858pg/ml) of the bronchiolar lavage fluid following 24h. AN-01-24 dose dependently (30 or 60mg/kg) significantly reduced the leukocyte count (42±6; 37±5), MPO levels (203±49; 84±39), protein concentration (431±22; 368±31), MIP-1 (475±78; 442±74), MIP-2 (504±93; 394±63) and TNF (3685±502; 1913±554). In addition LPS increased the measurable xanthine oxidase activity in lung tissue from undetectable levels to 37±8mU/mg protein, which AN-01-24 (30mg/kg) reduced to 11±4mU/mg protein ($p<0.01$). These data support the proposal that inhibition of xanthine oxidase might represent a useful adjunct in the therapy of ARDS.

161.13

Tachykininergic mechanisms of Acute Respiratory Distress Syndrome following fire smoke inhalation

Simon S. Wong, Nina N. Sun, Mark L. Witten. Department of Pediatrics, University of Arizona, 1501 N. Campbell Avenue, Tucson, Arizona 85724

To characterize the molecular nature of substance P (SP) signaling underlying fire smoke (FS)-induced neurogenic inflammation, we initiated dose-/time-effect studies in a rat model of Acute Respiratory Distress Syndrome (ARDS). Fire smoke inhalation dose-dependently induced significant increases in bronchoalveolar lavage concentrations of SP, increasing approximately 60% from one to 24 hours. However, FS did not induce a significant change of β-preprotachykinin (PPT)-I gene encoding SP in lung tissues, by real-time quantitative RT-PCR. The rats subjected to a low level of FS had an upregulation, whereas

Transactions

Abstracts

Acknowledgements

Membership

Copyright

Help

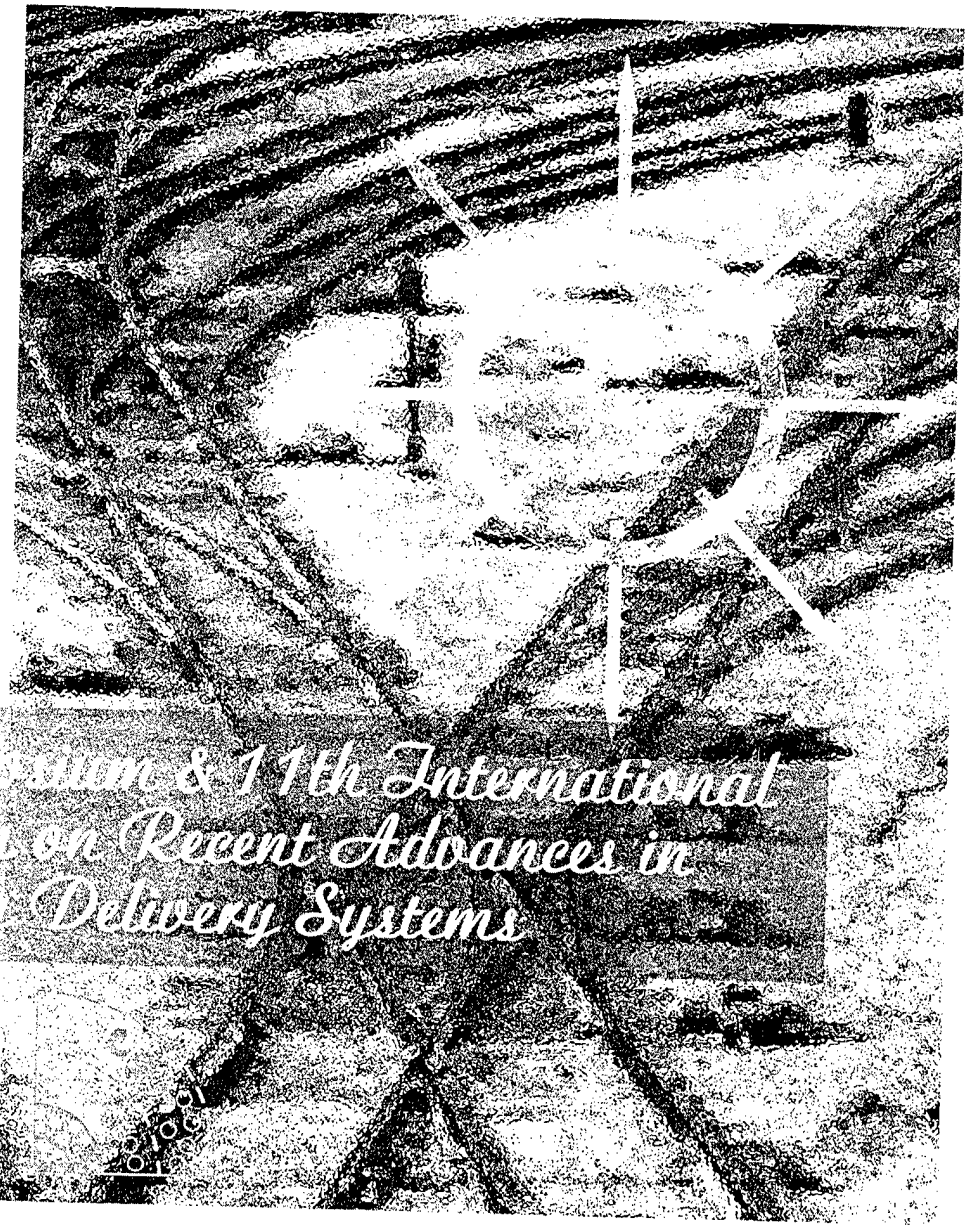

Winter Symposium & 11th International Symposium on Recent Advances in Drug Delivery Systems

March 3-6, 2003
Grand America Hotel
Salt Lake City, Utah
United States of America

#014

Pharmacological Modulation of Intracellular Trafficking and Lysosomal Degradation Prolongs the Anti-oxidant Effect of Catalase Conjugates Delivered into Endothelial Cells via ICAM-1

Silvia Muro, Xiumin Cui, Christine M. Gajewski, Michael Koval, Vladimir R. Muzykantov
University of Pennsylvania School of Medicine. Philadelphia. PA. 19104
silvia@mail.med.upenn.edu

ABSTRACT SUMMARY:

Conjugates of the antioxidant enzyme catalase with antibodies to the surface adhesion molecule ICAM-1 could provide a therapeutic means for pathologies associated with oxidative stress. Human umbilical vein endothelial cells were incubated in the presence of conjugates prepared by coating both anti-ICAM and catalase onto the surface of latex beads, and the results were analyzed by fluorescence microscopy. The conjugates showed rapid intracellular delivery, followed by slow trafficking to lysosomes and degradation (2 h -3 h). The cells were protected from H_2O_2 injury during a period of time <3 h after the internalization of the conjugates. Pharmacological agents, nocodazole and chloroquine, prolonged the stability of anti-ICAM-1 conjugates by either inhibiting microtululi-dependent trafficking to lysosomes or preventing lysosomal acidification and degradation, respectively. Consequently, nocodazole and chloroquine also prolonged the anti-oxidant effect of anti-ICAM/catalase conjugates.

INTRODUCTION:

Monoclonal antibodies to a surface adhesion molecule up-regulated in altered endothelium, InterCellular Adhesion Molecule-1 (ICAM-1), may serve as affinity carriers for targeting of therapeutic products to endothelial cells (EC). We have previously shown that anti-ICAM antibodies accumulate in pulmonary endothelium both in isolated lungs in perfusion and *in vivo* (1,2). We also found that monomeric antibodies to ICAM-1 bind to, but do not internalize into EC in culture (3). Modification of anti-ICAM to form multimeric conjugates of a diameter ranging between 100 nm to 300 nm (i.e. by coating onto latex beads), leads to an active (37°C *vs.* 4°C), rapid (t½=5 min) and efficient (85%) cellular uptake, indicating the similarity of this process to a typical receptor mediated endocytosis. However, using pharmacological inhibitors, dominant-negative constructs and immuno-colocalization studies we demonstrated that anti-ICAM conjugates are internalized in EC by a mechanism distinct from caveolae- or clathrin-mediated endocytosis. The pathway of anti-ICAM uptake conjugates is similar, but not equal to classical macropinocytosis and phagocytosis (4). Briefly, the internalization of anti-ICAM conjugates into EC was dependent on ICAM-1 clustering (monomeric antibodies vs. multimeric conjugates), the size of the conjugates (conjugates >300 nm in diameter were poorly internalized), it was affected by amiloride and required the re-organization of the actin cytoskeleton, dynamin, Ca^{2+} signaling, protein kinase C (but not PI3K or PLC), Src kinases, and Rho dependent kinase (4). Additionally, the intracellular trafficking of anti-ICAM conjugates was unusually slow, where conjugates traffic via early endosomes to lysosomes, localizing within these compartments 3 h after their internalization into the cells. Since our goal is to use anti-ICAM conjugates as carriers to deliver therapeutic cargoes into EC, in this work we have tested internalization, trafficking, degradation, and anti-oxidant activity of beads coated with both anti-ICAM-1 and catalase.

EXPERIMENTAL METHODS:

Control anti-ICAM conjugates or anti-ICAM/catalase conjugates were prepared by coating the corresponding IgG and enzyme onto the surface of 100 nm FITC-fluorescent latex beads. The effective diameter of the resulting conjugates was determined by dynamic light scattering (5). HUVEC were maintained to passage 4 to 5 in M199 medium supplemented with FBS, glutamine, heparin, ECGS and antibiotics. The internalization of the conjugates was tested by incubation with HUVEC at 37°C, either in control medium or medium containing the inhibitors amiloride, monodansyl-cadaverine (MDC), or filipin. Surface-bound conjugates were visualized by co-staining with a secondary antibody to anti-ICAM IgG and/or anti-catalase, without cell permeabilization. For trafficking studies, the cells were incubated following pulse (4°C-binding) and chase (37°C-internalization) techniques and the intracellular compartments were detected by immunostaining. Anti-oxidant protection of anti-ICAM/catalase conjugates was tested in cells treated with 5 mM H_2O_2 for 15min.

RESULTS AND DISCUSSION:

As in the case of control anti-ICAM conjugates, latex beads coated with both anti-ICAM and catalase specifically bind to EC and are subsequently internalized by an active endocytic process. This internalization was not affected by MDC or filipin, but was sensitive to amiloride, indicating that neither clathrin- nor caveolae-mediated endocytosis (6) are responsible for the uptake of anti-ICAM/catalase conjugates, but is likely mediated by the macropinocytosis-related pathway.

Internalized anti-ICAM/catalase conjugates trafficked to lysosomal compartments with a unusual slow kinetics, i.e. even 2 h after internalization in HUVEC the conjugate co-localized only partially with lysosomal markers, whereas 3 h incubation were necessary before the entire conjugate population was visualized within lysosomes.

Consistent with their localization within these compartments, both catalase and anti-ICAM IgG were degraded 3 h after their uptake by HUVEC. Therefore, the kinetics and mechanisms of endocytosis, intracellular trafficking and degradation of the anti-ICAM/catalase conjugates are equivalent to those previously observed in the case of control anti-ICAM/beads (4). This result validates the use of the later as an appropriate general model to study the cellular processing of these anti-ICAM-based delivery systems.

To determine the potential therapeutic activity of the anti-ICAM/catalase conjugates, HUVEC were exposed for 15 min to 5mM H_2O_2 at different time points after the internalization of the conjugates. The cells treated with catalase-carrying anti-ICAM/beads, but not with control conjugates, were protected from H_2O_2 injury. This indicates that anti-ICAM/beads deliver active catalase intracellularly, conferring anti-oxidant protection.

However, consistent with the kinetics of lysosomal degradation, this protection was lost between 2 h to 3 h after internalization of the conjugates. Therefore, we studied the effect of two compounds that typically affect intracellular trafficking and/or degradation, i.e. nocodazole (which disrupts microtubuli) and chloroquine (an alkalinizing agent). Both pharmacological agents prolonged the stability of anti-ICAM-1 conjugates by either inhibiting their traffic to lysosomes (nocodazole) or preventing lysosomal acidification and most likely activation of lysosomal degrading enzymes (chloroquine). Furthermore, chloroquine or nocodazole prolonged the protective effect of anti-ICAM-1/catalase conjugates against H_2O_2, injury at least to 3h and 5h, respectively. Therefore, the combined application of anti-ICAM-driven conjugates together with these or other pharmacological agent of similar action, which can be used in animal or human subjects (7,8), could help to improve the capabilities of this therapeutic system.

CONCLUSIONS:

In general, these results highlight the importance that lies beneath the mechanism of cellular uptake and subsequent processing of therapeutics delivered into cells, which may help to determine their suitability for therapeutic interventions, and can be pharmacologically modified to improve their therapeutic capacity. These studies, applied to our system, indicate that catalase can be delivered specifically into endothelial cells via a surface adhesion molecule up-regulated in altered endothelium, ICAM-1. This represents a potentially effective strategy for vascular-specific anti-oxidant therapies. Finally, pharmacological modulation of the intracellular processing of anti-ICAM conjugates prolongs their therapeutic effect, which may suffice the time requirements in some pathological settings.

REFERENCES:

1 Atochina E., Balyasnikova I., Danilov S., Granger D., Fisher A., Muzykantov V. (1998) Immunotargeting of catalase to ACE and ICAM-1 protects perfused rat lungs against oxidative stress. *Am J Physiol (Lung)* 19:L806-L817.

2 Danilov S., Gavriljuk V., Franke F., Pauls K., Harshaw D., McDonald T., Miletich D., Muzykantov V. (2001) Pulmonary uptake and tissue selectivity of antibodies to surface endothelial antigens:key determinants of vascular immunotargeting. *Am J Physiol* (Lung) 280(6):L1335-L1347.

3 Murciano J.C., Muro S., Koniaris L., Christofidou-Solomidou M., Harshaw D., Albelda S.M., Granger D.N., Cines D.B., Muzykantov V.R. ICAM-directed vascular immunotargeting of plasminogen activators to the endothelial luminal surface. *Blood*, under revision.

4 Muro S., Wiewrodt R., Thomas A., Koniaris L., Albelda S.M., Muzykantov V, Koval M. A novel endocytic pathway induced by clustering endothelial ICAM-1 and PECAM-1. (Submitted)

5 Wiewrodt R., Thomas A.P. Cipelleti L. Christofidou-Solomidou M., Weitz D.A., Feinstein S.I., Schaffer D., Albelda S.M. Kival M., Muzykantov V.R. (2002) Size-dependent intracellular immunotargeting of therapeutic cargoes into endothelial cells. *Blood*. 1;99(3):912-922.

6 Marsh M. Ed. (2001) Endocytosis. Frontiers in Molecular Biology Series. *Oxford University Press*.

7 Mahboobi S., Pongratz H., Hufsky H., Hoeckemeyer J., Frieser M., Lyssenko A., Paper
D.H., Burgermeister J., Bohmer F.D., Fiebig H.H., Burger A.M., Baasner S., Beckers T. (2001) Synthetic 2-aroylindole derivatives as a new class of potent tubulin-inhibitory, antimitotic agents. *J Med Chem* 20;44(26):4535-4553.

8 Boelaert J.R., Piette J., Sperber K. (2001) The potential place of chloroquine in the treatment of HIV-infected patients. *J Clin Virol* 20(3):137-140.

ACKNOWLEDGEMENTS:

This work was supported by Fundación Ramón Areces (SM), Department of Defense Research Grant and NIH RO1 from HLBI (VRM).

6th World Congress on Inflammation

2 – 6 August 2003

Vancouver Conference and Exhibition Centre
Canada

The Abstracts

INTERNATIONAL ASSOCIATION OF
IAIS
INFLAMMATION SOCIETIES

Congress President: A Robin Poole (Canada)

Congress Organising Committee: Lisa Marshall (USA) (Chair), Richard Dyer (USA), Richard Carlson (USA), Gordon Letts (USA) and Steven Stimpson (USA)

Abstract Committee: J Winkler (USA), J Chapdelaine (USA), Elizabeth Capper (USA) and John Sommerville (USA)

Young Investigator Award Committee:
David Howat (UK) (Co-chair), Richard Carlson (USA) (Co-chair), Vincent Lagente (France), Eric Morand (Australia), Richard Griffiths (USA), Timothy Williams (UK), Kiyoshi Takatsu (Japan), John Schrader (Canada), Hugo Castro (Brazil)

Inflammation Research

Supplement 2
Vol. 52
pp. S 79 – S 209
July 2003
ISSN 1023-3830

Contents

Sunday 3 August 2003

***Please note**: No abstracts have been received for some sessions and the session titles are therefore not included in this supplement. All abstracts, including those selected for oral presentation, will appear as posters – with the exception of the Young Investigator Finalists (Focus Session 18), the Lunch Time Session abstracts) and the Invited Speakers (IS). Abstract numbers are identical to poster board numbers.*

Posters will be on the boards from Sunday August 3 to Tuesday pm, August 5

IS/09
ENDOGENOUS CONTROL OF ACUTE INFLAMMATION - THE ROLE OF PROSTAGLANDINS IN MEDIATING INFLAMMATORY RESOLUTION

DW Gilroy
Department of Experimental Pathology, William Harvey Research Institute, St. Bartholomew's & The Royal London School of Medicine & Dentistry, Charterhouse Square, London, EC1M 6BQ, United Kingdom

Inflammation is increasingly regarded as a series of checkpoints controlling the influx and clearance of leukocytes. These checkpoints are managed by endogenous mediators that act as go or stop signals, with some mediators that drive inflammation also acting as suppressers of the response. We have shown that eicosanoids behave in this manner, with onset of an acute pleurisy, for instance, being dependent on prostaglandin (PG) E2 and resolution reliant on a switch to PGD2. Therefore, in acute inflammation there are two waves of PG synthesis, one at onset for pro-inflammatory PGs and a second at resolution for pro-resolving PGs. Here, I provide an insight into changes within the PG biosynthetic pathway that facilitates eicosanoid class switching necessary for resolution. I will also discuss the mechanisms by which pro-resolving PGD2 and its metabolites bring about resolution as well as reveal new data on the inflammatory response of mice knocked out for prostaglandin D2 synthase, the enzyme responsible for PGD2 synthesis.

IS/10
INTERLEUKIN-1 AS A THERAPEUTIC TARGET: OPPORTUNITIES FOR INFLAMMATORY DISEASE

MARTIN BRADDOCK, ASSOCIATE DIRECTOR, RESPIRATORY AND INFLAMMATION RESEARCH AREA
M Braddock
AstraZeneca R&D Charnwood, Bakewell Road, Loughborough, LE11 5RH, United Kingdom

Interleukin-I (IL-1) is a pivotal mediator of inflammation and tissue damage in multiple organs in both animal models and in man. The pro-inflammatory nature of IL-1 may make it an attractive target for therapeutic intervention in a number of diseases in man which include rheumatoid and osteoarthritis, inflammatory bowel disease and inflammatory diseases of the lung and central nervous system.
In this presentation, the role of IL-1, the IL-1 pathway and possible therapeutic antagonist approaches directed against IL-1 will be discussed, together with an appraisal of the efficacy of the IL-1 receptor antagonist, Anakinra in rheumatoid arthritis in man.

Focus Session 1: Targeted Drug Delivery

IS/11
TARGETING OF ANTIOXIDANTS TO ADHESION MOLECULES

M Christofidou-Solomidou[1], B Kozower[2], A Sherpereel[1], T Sweitzer[1], S Muro[1], R Wiewrodt[1], V Shuvaev[1], A Thomas[1], M Koval[1], A Patterson[2], S Albelda[1] and VR Muzykantov[1]
[1]IFEM, U.Pennsylvania Med.Center, 1 John Morgan Building, 3620 Hamilton Walk, Philadelphia, PA 19104, USA and [2]Washington University Medical Center, Department of Cardiothoracic Surgery, St.Louis, MO 63110, USA

Endothelial oxidative stress is common in inflammation, sepsis and acute lung injury. Antibodies to endothelal cell adhesion mocelule PECAM-1 can deliver therapeutics to either resting or inflammation-engaged endothelium. Enzymatically active reporter enzymes and antioxidant enzyme, catalase, conjugated with anti-PECAM, bind to endothelium after intravascular administration. Endothelial cells do not internalize monomeric anti-PECAM, but anti-PECAM/catalase immunoconjugates smaller than 0.5 um diameter enter the cells via a pathway distinct from clathrin- and caveoli-mediated endocytosis. Anti-PECAM/catalase resides in a pre-lysosomal compartment for several hours and protects endothelial cells against oxidative stress. Animal studies showed that anti-PECAM/catalase accumulates in the pulmonary endothelium, protects against acute pulmonary oxidative stress, including rat model of lung transplantation, and improves survival. In addition to therapeutic effects of the delivered drugs, blockade of PECAM-1 may suppress inflammation.
Grants: DOD PR 012262, NIH HL71175 and HL60290

IS/12
TARGETING AND VISUALIZING INFLAMMATION

JR Lindner
Cardiovascular Division, University of Virginia, Charlottesville, VA, 22902, USA

Methods for assessing tissue inflammatory responses non-invasivley with ultrasound have recently been developed. For this purpose, microbubble ultrasound contrast agents have been targeted to either activated leukocytes or endothelial cell adhesion molecules. For leukocyte targeting, lipid-shelled microbubbles containing phosphatidylserine as a shell constituent have been created that bind to activated leukocytes in venules of inflamed tissue via opsonization. Imaging of this agent has been used to assess leukocyte recruitment following ischemic injury of the kidney and heart. A more direct method of targeting has been achieved by conjugating monoclonal antibodies or other peptide ligands to the surface of lipid microbubbles. Microbubbles targeted against p-selectin, VCAM-1, and ICAM-1, have been developed to assess cardiac, vascular, and renal inflammatory phenotype in models of ischemia, atherosclerotic disease, and transplant rejection. Microbubbles targeted against MAdCAM-1 have also been developed to assess inflammatory bowel disease.

IS/13
TARGETING OF DRUGS TO CANCEROUS AND INFLAMED TISSUES

J Kopecek and P Kopeckova
[1]Department of Pharmaceutics and Pharmaceutical Chemistry, University of Utah, 30S 2000E Rm. 301, Salt Lake City, 84112, USA

The design, synthesis and properties of N-(2-hydroxypropyl(methacryl-amide) (HPMA) copolymers as carriers of anticancer and anti-inflammatory drugs will be discussed. Macromolecular anticancer therapeutics have the potential to overcome drug efflux pumps, induce apoptosis, and inhibit DNA repair and biosynthesis when compared to low molecular weight drugs. In addition, increasing the intravascular half-life of conjugates results in enhanced tumor accumulation with concomitant augmentation of therapeutic efficacy.
Cell transformation in inflammatory bowel diseases such as ulcerative colitis results in altered carbohydrate compositions of glycoproteins. In diseased tissue, the Thomsen-Friedenreich (TF) antigen (galactose-b 1,3-N-acetylgalactosamine) is often manifested. In mature, healthy tissue, the antigen is hidden by glycosylation or sialylation. The potential of peanut agglutinin (PNA) to distinguish between normal and diseased cells serves as a rationale for the design of site-specific HPMA copolymer-drug conjugates biorecognizable by inflamed tissue in the GI tract.

IS/14
DEVELOPMENT OF POTENT MONOCLONAL ANTIBODY AURISTATIN CONJUGATES FOR THE TREATMENT OF CANCER

PD Senter, S. Doronina, D. Meyer, J. Francisco and A. Wahl
Seattle Genetics, 21823 30th Dr. SE, Bothell, WA, 98021, USA

We describe the properties of monoclonal antibody-drug conjugates consisting of the potent synthetic dolastatin 10 analogues auristatin E (AE) and monomethyl-AE (MMAE), linked to the chimeric mAbs cBR96 (anti-Lewis Y on carcinomas) and cAC-10 (anti-CD30 on hematologic malignancies). The linkers included an acid-labile hydrazone, and protease-sensitive dipeptides, leading to uniformly-substituted conjugates that efficiently released active drug in the lysosomes of antigen positive tumor cells. The mAb-peptide-MMAE conjugates exhibited greater in vitro specificity and lower in vivo toxicity, compared to corresponding hydrazone conjugates. mAb-valine-citrulline-MMAE conjugates led to immunologically-specific cures and regressions of established anaplastic large cell lymphoma (ALCL) and breast carcinoma xenografts at 1/30th to 1/10th the MTDs, respectively. These new conjugates illustrate the importance of linker technology, drug potency, and conjugation methodology in developing safe and efficacious mAb-drug conjugates for cancer therapy.

Penn

University of Pennsylvania 9th Annual Respiration Research Retreat

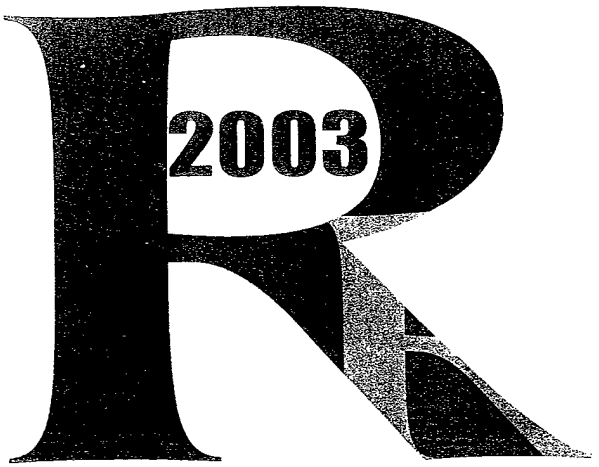

June 20, 2003

Program and Abstracts

Sugarloaf Conference Center • Philadelphia, PA

ABSTRACTS

Binding and uptake of anti-ICAM-1 coated nanoparticles by flow adapted endothelial cells

Erik Berk, Vladimir R. Muzykantov and Silvia Muro

Institute for Environmental Medicine. University of Pennsylvania School of Medicine. Philadelphia. PA.

9

A major focus in the treatment of diseases is the delivery of drugs, enzymes or DNA to the endothelial cells that line blood vessels. This can be done by immunotargeting antigens on the surface of the cells, e.g. ICAM-1. The mechanism by which HUVEC bind and internalize anti-ICAM-1 conjugates or nanoparticles in static cultures is known as CAM-mediated endocytosis, however little is known about the internalization of these particles by cells adapted to flow conditions. Since endothelial cells subjected to flow for a sustained period of time experience substantial changes concerning their morphology, protein expression and actin cytoskeleton, cell adaptation to flow may have an effect on the endocytic uptake of anti-ICAM-1 nanoparticles. This study shows that TNFα stimulated HUVEC that are exposed for 24 hours to a shear stress of ~4 $^{dynes}/_{cm^2}$ adapt to flow, as deducted by morphological cell alignment following the flow direction and the appearance of actin stress fibers. The flow did not have any significant effect on the efficiency of binding of anti-ICAM-1 nanoparticles to HUVEC. The kinetics for the uptake of FITC labeled anti-ICAM-1 particles under flow was slower than their uptake under static conditions, although maximal internalization values were similar after 2 h incubation. Furthermore, HUVEC that were adapted to flow and then incubated with anti-ICAM-1 nanoparticles in the absence of flow showed similar rate of internalization than non-flow adapted cells. Also, the internalization of the particles under flow was not affected by MDC (inhibitor of clathrin mediated endocytosis), but it was markedly inhibited by amiloride, consistent with CAM-mediated endocytosis. Preliminary data suggest that filipin (inhibitor of caveolar uptake) may inhibit the internalization of anti-ICAM-1 nanoparticles under flow, although at a considerably lower extent. Altogether, these results seem to indicate that immunotargeting to ICAM-1 may represent an effective mean for site-specific and intracellular delivery of therapeutics to endothelial cells subjected to flow.

10

INTERLEUKIN (IL)-4 INDUCES AND CYCLOHEXAMIDE INHIBITS INTRACELLULAR EXPRESSION OF SURFACTANT PROTEIN (SP)-D BUT NOT SP-A IN PULMONARY EPITHELIAL CELLS. Y. Cao[1], J. Tao[2], G. Vass[1], S. R. Bates[2], M. F Beers[1], A. Haczku[1]. [1]*Pulmonary, Allergy and Critical Care Div., Dept. of Medicine, Univ. of PA;* [2]*The Institute for Environmental Medicine, Univ. of Pa, Philadelphia, PA.*

Allergic airway inflammation induces significant increases in production of SP-D, an innate immune mediator with potent modulatory effects on adaptive immune responses. The mechanisms involved in regulation of this lung collectin are unknown. The effects of IL-4 and the protein synthesis inhibitor, cyclohexamide were investigated *in vitro* on intracellular SP-D in comparison with SP-A expression. Type II alveolar epithelial cells were isolated from postnatal rats and cultured with dexamethasone and cAMP, in order to maintain their ability to generate surfactant proteins. IL-4 had a dose-dependent stimulatory effect on intracellular SP-D but it did not affect SP-A production. Cyclohexamide significantly inhibited intracellular SP-D protein expression when cells were treated for as short as a 6 h period before harvest while SP-A levels did not change over 24 h cyclohexamide treatment. The inhibitory effect on SP-D was dose dependent and significant at 0.5 μg/ml but SP-A was not affected even at 1 μg/ml of cyclohexamide concentrations. Inhibition of intracellular SP-D was not rescued by the addition of 20ng/ml IL-4 into the cell culture. These indicate that IL-4 induced upregulation of SP-D protein expression is not due to a decreased metabolism or prolonged half-life of the produced protein. Our results suggest that intracellular SP-D production requires constitutive protein synthesis and is upregulated by the presence of extracellular stimuli such as the Th2 cytokine IL-4.

PBF (AH); Centocor Inc. (AH); NIH # HL64520 (MFB); NIH # HL19737 (SRB)

Penn

University of Pennsylvania 9th Annual Respiration Research Retreat

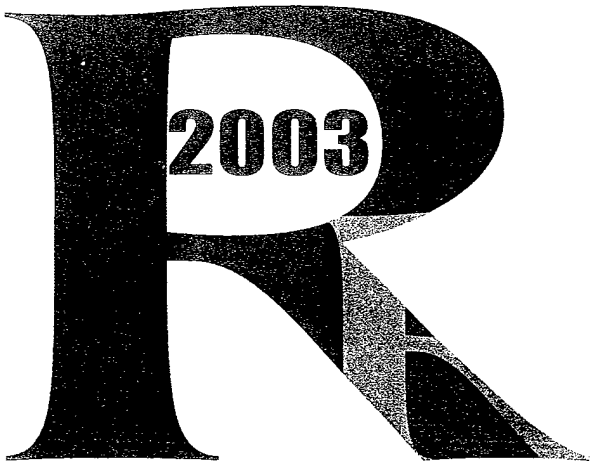

June 20, 2003

Program and Abstracts

Sugarloaf Conference Center • Philadelphia, PA

ABSTRACTS

15 **HUMANIZED LUNG SURFACTANT (KL4-SURFACTANT) PREVENTS HYPEROXIC LUNG INJURY IN MICE.** M Christofidou-Solomidou, E Argyris, A Bohen, S Stephens, R Niven and R Segal. University of Pennsylvania, Philadelphia PA, and Discovery Laboratories, Inc., Doylestown, PA, USA.

KL4-surfactant lavage of LPS-treated rabbit lungs markedly reduces the inflammatory exudate and inflammation. KL4-surfacant consists of the human surfactant protein B mimic, sinapultide (KL4), with phospholipids (DPPC, POPG, PA). We evaluated the anti-inflammatory properties of KL4-surfactant in a mouse model of hyperoxic lung injury (80% O_2) which is associated with increased permeability, leukocyte (WBC) recruitment to the lungs, and death. Survanta® was also studied. Mice were placed in 80% O_2 for 7 days. Intranasal bolus of vehicle (100µl Tris buffer), KL4-surfactant (100µl; 20mg/ml) and Survanta® (100µl; 25mg/ml) was given on days 3–6, and mice sacrificed on day 7. Lung injury assessment was by morphology (Acute Lung Injury Score [ALIS]), histopathology, and WBCs, PMNs, and protein in BAL.

Treatment Group	N	BAL			ALIS
		WBC Cells/ml	PMN %	Protein mg/ml	
Room Air	10	65,563	1.6	0.12	1.6
None + 80% O_2	20	118,947*	24.8*	2.33*	5.56*
Vehicle + 80% O_2	20	107,790*	23.9*	1.29*	4.56*
Survanta® + 80% O_2	10	79,627	19.8*	1.07	5.81*
KL4-surfactant + 80%	20	60,653**	1.1** #	0.49** #	3.13* #

** - $p<0.05$ vs. Room Air **- $p<0.05$ vs. None + 80% O2 # - $p<0.05$ vs. Survanta®*

Our data show that KL4-surfactant, unlike vehicle or Survanta®, blocked neutrophil influx into alveoli, and significantly suppressed lung injury in hyperoxic mice.

Funding: Discovery Labs, Inc., Doylestown, PA

16 **HYPEROXIA POTENTIATES OXIDATIVE INJURY IN MURINE LUNGS INDUCED BY GLUCOSE OXIDASE TARGETED TO THROMBOMODULIN.** Melpo Christofidou-Solomidou[1], Arnaud Scherpereel[1], Alyssa Bohen[1], Evguenia Arguiri[1], Vladimir Shuvaev[2], Stephen Kennel[3] and Vladimir Muzykantov[2]. University of Pennsylvania, Departments of Medicine[1] and Pharmacology[2], Philadelphia PA 19104-6160 and Oak Ridge National Labs[3], Oak Ridge, TN.

Hyperoxia induces oxidative lung injury by mechanisms including overproduction of reactive oxygen species (ROS) in mitochondrial respiratory chain in lung cells, release of ROS from activated leukocytes and modulating activity of pro-oxidant enzymes in the lung that utilize O_2 as a substrate (NADPH-oxidase, LOX, NOS, XO, etc). To test directly whether pulmonary level of O_2 modulates generation of ROS in endothelium, we injected mice with glucose oxidase (GOX), coupled to a thrombomodulin antibody (anti-TM). Immediately after iv injection, anti-TM/GOX binds to pulmonary endothelium, generates H_2O_2 from O_2 and glucose, and causes edematous oxidative lung injury. Mice were injected with a low dose (35 µg) anti-TM/GOX and exposed to hyperoxia (PO_2>95%) for 6 h prior to sacrifice. Lung injury was characterized by BAL protein, WBC counts, lipid peroxidation by malondialdehyde (MDA) levels and Acute Lung Injury Score, ALIS. BAL proteins for untreated control, anti-TM/GOX (35mg), saline +O_2 and anti-TM/GOX +O_2 were 0.1, 0.4±0.03, 0.1, and 4.8±2.10 respectively. BAL WBC (x10^3) for the same groups were 44.0±4.9, 48.2±4.8, 43.0±5.2, 44.2±1.3 respectively. MDA levels/g lung were 2.5±0.1, 3.58±0.16, 4.7±0.4 and 7.8±1.1 and ALIS was 1, 2.5, 2.3 and 8.8 respectively. Therefore, hyperoxia alone did not cause noticeable injury, yet markedly augmented edematous injury induced by low doses anti-TM/GOX which cannot be explained by WBC influx. These data indicate that tissue-level O_2 directly modulates the activity an exogenous pro-oxidant enzyme bound to endothelium, thus augmenting ROS-mediated tissue injury.

Supported by: AHA (MCS) SCOR NIH (VM)

Penn

University of Pennsylvania 9th Annual Respiration Research Retreat

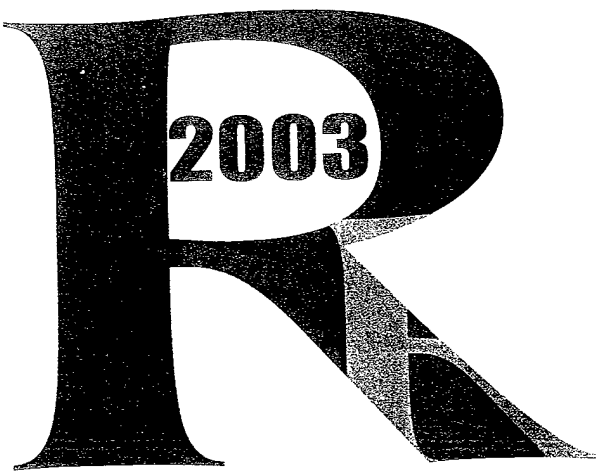

June 20, 2003

Program and Abstracts

Sugarloaf Conference Center • Philadelphia, PA

ABSTRACTS

Slow intracellular degradation of ICAM-1 or PECAM-1 targeted catalase nanoparticles protects endothelial cells from oxidative stress.

Silvia Muro, Christine Gajewski, Michael Koval and Vladimir R. Muzykantov. **Institute for Environmental Medicine. University of Pennsylvania School of Medicine. Philadelphia, PA.**

49

Novel carrier systems based on nanotechnologies offer the opportunity for the design of more effective, specific and safe drug delivery. InterCellular Adhesion Molecule 1 (ICAM-1) and Platelet Endothelial Cell Adhesion Molecule 1 (PECAM-1) represent particularly attractive molecules to target nanocarriers to pathologically altered endothelium, as they are expressed by stressed endothelial cells and are functionally involved in vascular oxidative stress, ischemia-reperfusion injury and inflammation. Although endothelial cells do not internalize monomeric antibodies to ICAM-1 or PECAM-1, coupling these antibodies to nanoparticles creates site-specific, multivalent ligands that enter cells via a novel endocytic pathway (e.g., CAM-mediated endocytosis). This feature suggests that anti-CAM nanoparticles may represent a suitable means for intracellular delivery of therapeutics. Fluorescence microscopy, radiotracing and immunoblot data revealed that addition of catalase to anti-ICAM or anti-PECAM nanoparticles, to provide these with anti-oxidant activity, did not affect the binding efficiency or the mechanism of nanoparticle uptake by human umbilical vein endothelial cells (HUVEC). Neither catalase cargo affected intracellular trafficking to lysosomes and degradation rate of anti-CAM nanoparticles, which was unusually slow (3 h). Intracellularly delivered nanoparticles were functionally active, since HUVEC were resistant to H_2O_2-induced oxidative injury for 2 h following anti-CAM/catalase particle uptake. Moreover, the pharmacological agents nocodazole and chloroquine, which are known to inhibit lysosomal trafficking and acidification respectively, increased the duration of the anti-oxidant protection by decreasing the extent of anti-CAM/catalase degradation. Therefore, the slow trafficking pathway followed by internalized anti-CAM nanoparticles seems well suited for targeted delivery of therapeutic enzymes to endothelial cells and may provide a basis for treatment of pathological conditions associated with vascular oxidative stress.

DOES SLEEP DEPRIVATION LEAD TO ER STRESS? Naidoo, N., Mackiewicz, M., Giang, W., and Pack, A.I. Division of Sleep Medicine and Center for Sleep and Respiratory Neurobiology, University of Pennsylvania.

50

The homeostatic regulation of sleep proposes that with increasing durations of wakefulness there are progressive physiological, biochemical and/or molecular changes in the brain. Understanding these alterations will provide clues as to the functions and mechanisms of sleep. We recently performed a large transcript profiling study in mouse brain following different durations of prolonged wakefulness. Of the classes of genes that changed, we found that the heat shock protein or stress genes were among the most responsive to sleep deprivation. Glucose regulated protein (GRP78 also known as BiP) is a heat shock family gene whose expression is significantly and progressively elevated in the cortex with increasing durations of sleep deprivation. GRP78/BiP is a chaperone that plays a key role in de novo protein folding (Ellis, 1987), in the refolding of misfolded proteins and in the unfolded protein response (UPR) during stress of the endoplasmic reticulum (ER) (Kozutsumi et al, 1988; Kohno et al, 1993). The response to ER stress has 2 distinct components: the first is the transcriptional induction of genes that encode ER resident proteins such as GRP78/ BiP that prevent polypeptide aggregation and participate in protein folding; the second component consists of a profound and rapid repression of protein synthesis. Both responses minimize the accumulation of, and aggregation of, misfolded proteins, the first by increasing the capacity of the machinery for folding and degradation and the second by reducing the burden placed on them. Attenuation of protein synthesis in ER stress is caused by phosphorylation of the translation initiation factor eIF2α by the kinase PERK. PERK is a transmembrane protein resident in the ER membrane whose activity is repressed by GRP78/BiP (Bertolotti et al, 2000). During the unfolded protein response, GRP78/BiP dissociates from PERK, resulting in phosphorylated, activated PERK, which then phosphorylates eIF2α. Phosphorylation of eIF2α interferes with the formation of an active 43S translation-initiation complex resulting in the inhibition of global protein synthesis.

We have data in mice that suggests that a response similar to that in ER stress occurs, at least in some brain regions (cortex), during sleep deprivation. GRP78/BiP gene expression is progressively induced following 3, 6, 9 and 12 hours of sleep deprivation. We have also observed a 30% increase in GRP78/BiP protein expression in mouse cortex following 3 hours of sleep deprivation. Further studies determining the temporal expression of GRP78/BiP and PERK proteins and the PERK phosphorylation profile during sleep deprivation are currently in progress. Additionally, we have seen in our microarray studies that the expression of key protein synthesis factors and ribosomal proteins is decreased with increasing durations of prior wakefulness suggesting an attenuation of protein synthesis. Three hours of sleep deprivation resulted in a large (approximately 4 fold change) - downregulation of elongation factor1α and 16 ribosomal protein transcripts in the cerebral cortex. We propose that sleep deprivation produces a stress response in brain that is similar to that produced by ER stress and the mechanism of action involves the same key molecules. We suggest that GRP78/BiP and PERK are those key molecules.

Penn

University of Pennsylvania 9th Annual Respiration Research Retreat

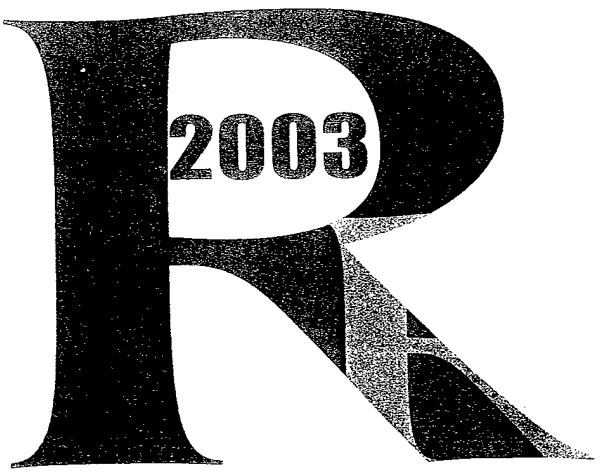

June 20, 2003

Program and Abstracts

Sugarloaf Conference Center • Philadelphia, PA

ABSTRACTS

EVALUATION OF HEART RATE RECOVERY FOR PREDICTING EXTUBATION OUTCOME. C. SEYMOUR, B. FUCHS. UNIVERSITY OF PENNSYLVANIA.

55 PURPOSE. Recent data measuring mixed venous oxygen saturation suggests that limitations of the cardiovascular system may be important in determining weaning outcome. Two recent studies found an association between anemia and reintubation. This suggests the possibility that limitations in cardiovascular reserve may have a role in determining extubation outcome. Based on the use of peak heart rate (HR) response during exercise stress testing as an index of cardiovascular reserve, and the value of HR recovery in predicting patient mortality, we evaluated the HR response and it's recovery following the "stress" of a spontaneous breathing trial (SBT) to determine whether these have any value in predicting extubation outcome. METHODS. Patients receiving mechanical ventilation for >24h in the trauma and cardio thoracic ICUs were evaluated for inclusion in this prospective cohort study. If patients were enrolled in the ventilator liberation pathway, peak HR was recorded at the end of the SBT and the degree of recovery at 1 and 5 min to a pre-determined baseline was measured following the final SBT prior to extubation, after returning to pre-SBT settings. Baseline HR was defined as the final recording pre-SBT while on their resting mode of ventilation. RESULTS. 22 successful extubations (SE) and 9 failed extubations (FE) after 3.0±2.5 days were studied in 30 patients. No significant differences in age, co-morbid status, or APACHE II score were present between groups (P>0.05). Baseline HR prior to SBT (91±17 vs. 93± 19 B/min, P>0.01) was similar. ΔHR during the SBT was higher in failed extubations (5.4±5.5 vs. -0.86±7.5 B/min, P=0.04) and a larger proportion of SE had HR at or below baseline at the end of the SBT (45 vs. 0.0%, P<0.01). Comparing those SE with elevated HR during the SBT to FE, HR and HR recovery at 1 and 5 min post-SBT were similar (P>0.01). HR recovery to baseline at 1 and 5 min post-SBT did not predict extubation outcome (unadjusted OR_1=5.05, [0.8-30.1], OR_5= 5.6 [1.0-30.9], P>0.01). At 10 min. post-SBT, 13.6% of SE and 44.4% of FE had not returned to baseline HR (P>0.01). CONCLUSIONS. In this pilot study, differences in cardiovascular stress may be apparent during the weaning trial of patients who subsequently fail extubation. However, neither HR response nor HR recovery at 1 and 5 min following the stress of a SBT predicted extubation outcome. CLINICAL IMPLICATIONS. Recovery of respiratory parameters such as V_E, in the post-SBT recovery period, may be a more fruitful area of investigation in the search for factors that predict extubation outcome.

Combined immunoconjugate delivery of Cu,Zn superoxide dismutase and catalase to human endothelial cells and their protection against oxidative stress.

56 Vladimir V.Shuvaev[a], Samira Tliba[a], Thomas Dziubla[a], and Vladimir R.Muzykantov[a,b]

Institute for Environmental Medicine[a], Department of Pharmacology[b], University of Pennsylvania School of Medicine, Philadelphia, PA.

Cu,Zn superoxide dismutase (SOD) and catalase form primary enzymatic antioxidative defense line in cells acting in tandem to eliminate superoxide anion and H_2O_2. Thus, the specific endothelial delivery of the enzymes may be important in the treatment of the vascular oxidative stress. In order to achieve such combined treatment, enzymes and anti-PECAM antibody were biotinylated and tandem SOD/catalase/anti-PECAM conjugate was prepared using a streptavidin cross-linking one-step procedure. We found that biotinylation did not affect the activity of catalase and decreased SOD activity by 30%. Streptavidin conjugation slightly reduced activities of both enzymes. However, catalase and SOD retained 80% and 70% of their initial activity in conjugate, respectively. This is probably due to diffusion limitations in the core of the conjugate. Human umbilical vein endothelial cells (HUVEC) were exposed to superoxide radical-producing system, xanthine/xanthine oxidase (X/XO), and cell protection by SOD/catalase conjugate against the oxidative stress was analyzed by ^{51}Cr release assay. We demonstrated that the conjugates protected HUVEC against moderate X/XO-induced oxidative stress in a dose-dependent manner. The combined immunoconjugates could be useful in endothelial cell protection in conditions where superoxide radical and/or H_2O_2 are the major damaging reactive oxygen species.